Rates and mechanisms of chemical processes affecting the treatment of ferruginous mine water

A thesis submitted for the Degree of Doctor of Philosophy

By

Jennifer Nia Geroni, MChem(Hons)*Oxon*. MSc.

School of Engineering, Cardiff University

October 2011

DECLARATION

This work has not been previously accepted in substance for any degree and is not concurrently submitted in candidature for any degree

Signed……(candidate) Date……

STATEMENT 1

This thesis is being submitted in partial fulfilment of the requirements for the degree of ……(insert MCh, MD, MPhil, PhD etc, as appropriate)

Signed……(candidate) Date……

STATEMENT 2

This thesis is the result of my own independent work/investigation, except where otherwise stated. Other sources are acknowledged by explicit references.

Signed……(candidate) Date……

STATEMENT 3

I hereby give consent for my thesis, if accepted, to be available for photocopying and for interlibrary loan, and for the title and summary to be made available to outside organisations.

Signed……(candidate) Date……

STATEMENT 4: PREVIOUSLY APPROVED BAR ON ACCESS

I hereby give consent for my thesis, if accepted, to be available for photocopying and for interlibrary loans after expiry of a bar on access previously approved by the Graduate Development Committee.

Signed……(candidate) Date……..

Acknowledgements

I would like to thank Dr Devin Sapsford, Prof Keith Williams and Dr Ian Watson for their advice, guidance and support throughout the production of this thesis. I would also like to thank Jeffery Rowlands and Ravi Mitha whose assistance with aspects of both laboratory and field work has been greatly appreciated. In addition to colleagues at Cardiff School of Engineering I am very grateful to Charles Cravotta III of the United States Geological Survey who was immensely helpful in providing me with a starting point for much of the geochemical modeling presented here. I have also had assistance from numerous people in carrying out my field work including Dave and Keith, Joe and Matt of IWS, Gwendolin Bitter, Kate James, Kay Florence and Dan Pugh. Finally I would like to thank my husband Gilles for everything that he has done to support me over the last 3 years both in the field and at home.

Abstract

This thesis presents the results of research undertaken into the rates of Fe(II) oxidation and CO_2 stripping from ferruginous mine drainage. It also provides new insight into the applicability of Vertical Flow Reactors (VFRs) to the treatment circumneutral waters.

Batch-wise experiments were used to determine Fe(II) oxidation rates in the field. The data collected were used to show that values for the rate constant k_1 were up to 3 orders of magnitude greater at the field sites than would be predicted from previously published laboratory studies. A methodology was also developed for determining k_2 (the heterogenous oxidation rate constant) in the field.

The results of field based monitoring of aeration cascades as well as batchwise CO_2 stripping experiments conducted using waters of varying chemistry were combined with geochemical modelling to demonstrate the evolution of the chemistry in these systems over time. The aeration cascades were shown to remove approximately 50% of the dissolved CO_2 initially present but this was not shown to have an appreciable effect on mine water treatability. Continued removal of the residual CO_2 fraction by mechanical aeration resulted in the elevation of pH by up to 2 units.

Trials of pilot scale Vertical Flow Reactors (VFR) at two sites in South Wales showed that rapid decreases in bed permeability over time make these systems unsuitable for deployment in the treatment highly net alkaline waters. As a result of adverse weather conditions and other technical difficulties there was insufficient data collected to determine the performance of these systems under net acid conditions. Qualitative observations suggest however that Fe removal was taking place at a significantly higher rate than would be seen in settling lagoons under the same conditions.

Contents

List of Figures

List of Tables

1 Introduction and Aims

The mining industry underpins all aspects of modern life from the extraction of coal for large scale energy production to gold and rare earth metals used in hi-tech industry. The extraction and processing of billions of tonnes of metal ores generates waste materials both above and below ground that without careful management can have a serious and long term impact on the environment. One of the major challenges for the mining industry is the remediation of water arising from underground workings and waste rock piles that have been contaminated as a result of the oxidation and dissolution of sulphide minerals exposed by the excavation of mine shafts. Anoxic conditions below ground allow the mobilisation of Fe (iron) (and other elements) as soluble Fe(II) which rapidly oxidises to Fe(III) on mixing with atmospheric oxygen and then precipitates to form voluminous (hydroxy)oxides. Where these mine waters discharge above ground, water courses become smothered with Fe(III) precipitates damaging the ecosystems contained within them.

In the UK the historic legacy of coal mining has lead to numerous Fe bearing mine water discharges appearing across the country. At the time of writing the Coal Authority, part of the Department of Energy and Climate Change is responsible for the management of these polluting discharges. They have built and trialled a large number of mine water treatment schemes successfully remediating more than 50 of the most polluting mine waters. The main driver for the continued development of new treatment schemes is the EU Water Framework Directive which requires that waterways within the EU attain “good ecological status” by 2015.

The Coal Authority is continually looking at ways to increase the efficiency of their treatment schemes in order to reduce the amount of land required and long term

operating costs. Partially funded by the Coal Authority this thesis describes and investigates several aspects of Fe bearing mine water chemistry in an attempt to increase knowledge and understanding in the field so that treatment scheme design might be improved in the future, especially with regard to reducing the land requirement (footprint) for passive treatment schemes. The perceived need for this for this work was derived from the following factors;

- Whilst in recent years there has been a great deal of work published regarding iron oxidation in circumneutral mine drainage a methodology for determining values for k_1 and k_2 (the rate constant for homogeneous and heterogeneous Fe oxidation respectively) in the field has yet to be published.
- Determination of values for k_1 and k_2 in the field where the conditions are very different to those in laboratory studies would allow a greater understanding of the behaviour of iron within the Coal Authority's (and other) treatment systems allowing for optimisation beyond the current sizing guidelines.
- One low footprint passive treatment option known as the Vertical Flow Reactor (VFR) has thus far only been trialled at a single site (Taff Merthyr) and so its applicability to mine waters with different chemistries is unknown.
- Despite the publication of numerous studies on CO_2 stripping for the water and process industries there has been relatively little published with specific reference to circumneutral mine drainage scenarios. High concentrations of dissolved CO_2 can greatly influence the pH of mine waters and as a result the oxidation rates of Fe.

1.1 Thesis aims

The study is split into three main sections that can be read independently or as a whole to make best use of the cross-referencing of information between them. The three sections are as follows:

1. *The Vertical Flow Reactor (VFR)*
2. *Iron(II) oxidation rates*
3. *Carbon dioxide degassing*

For this reason the methods chapter deals with these three sets of experiments separately and the results and discussion chapters are separated into three parts. The aims of each set of experiments are described as follows:

1.1.1 Vertical Flow Reactor (VFR)

i. To determine whether the VFR at Taff Merthyr be run so that the predominant Fe removal mechanism is via HFO (hydroxy ferric oxide) accretion rather than filtration of precipitates formed within the water column.
ii. To determine the maximum Fe removal rate that can be achieved by running the VFR at Taff Merthyr at high flow rates and how long high Fe removal rates can be sustained.
iii. To confirm that Mn removal within the VFR is only occurring within the Fe(III)(hydroxy)oxide bed and not within the water column.
iv. To determine whether the VFR can be used to treat net-acid waters.

1.1.2 Fe(II) oxidation rates

i. To develop new methodology for the measurement of rates of Fe(II) oxidation in the field and to allow values of k_1 the rate constant for homogenous Fe(II) oxidation to be calculated independent of pH temperature and dissolved O_2.
ii. To determine whether the rates of homogenous oxidation of Fe(II) as measured in the laboratory are applicable to mine waters in the field.
iii. To further develop the methodology from (i) to determine a value for k_2 the rate constant for heterogeneous oxidation of Fe(II) in the field.

1.1.3 Carbon dioxide degassing

i. To determine whether aeration cascades are a more appropriate means of removing dissolved CO_2 from mine water than mechanical forced aeration.
ii. To determine whether aeration cascade design affects the quantity of CO_2 degassed from a mine water over a given drop in height.

iii. To determine whether aeration cascade design has an influence on the Fe removal efficiency of a treatment system.

iv. To determine whether the pH changes occurring in mine water over time can be adequately accounted for by the rate of CO_2 degassing and the rate of Fe(II) oxidation alone.

1.2 Organisation of the thesis

Chapter 2 – Background: This chapter describes the mine water problem in more detail focussing on the chemical processes involved in both its formation and remediation. It also discusses various treatment processes that have been used in the treatment of mine waters and are relevant to the sites visited during the production of this thesis.

Chapter 3 – Site descriptions: This chapter gives an overview of the history, design and chemistry of the treatment schemes employed at each of the mine water discharges visited during this study.

Chapter 4 – Methods: This chapter describes all of the experimental and modelling methods and techniques used throughout the work presented here.

Chapter 5 – Results and Discussion: *The Vertical Flow Reactor*: This chapter presents the results collected during the VFR trials at two different sites. Data for Fe and Mn removal are included and discussed.

Chapter 6 – Results and Discussion: Iron Oxidation Rates: The results of the iron(II) oxidation experiments conducted in the field are presented and discussed along with the outcomes of computer modelling to determine values for the oxidation rate constants k_1 and k_2.

Chapter 7 – Results and Discussion: CO_2 degassing: The data from several sets of field experiments are presented along with the results of geochemical modelling for the calculation of dissolved CO_2 concentrations. These results are discussed in light of the implications for the design of mine water treatment schemes.

Chapter 8 – Conclusions and Further Work: This chapter provides a summary of the main findings of this thesis and makes suggestions as to where additional investigations could further increase understanding of mine water chemistry.

2 Background

This chapter describes the history and origins of acid mine drainage (AMD) and its impact on the natural environment. It also provides a detailed discussion of the rates and mechanisms of Fe(II) oxidation with particular emphasis on abiotic oxidation rates. Both homogeneous and heterogeneous oxidation pathways are discussed as well as the sorption of Fe(II) on Fe(III)(hydroxy)oxide (HFO) precipitates.

The pH of mine drainage is a critical controlling factor for rates of Fe(II) oxidation. The roles of carbonate alkalinity and high dissolved CO_2 concentrations in influencing the pH of mine drainage are described. Rates of gas transfer and mechanisms for degassing CO_2 are also discussed as a means to reduce the acidity of mine drainage prior to further treatment.

Finally options for passive treatment of mine drainage most relevant to the work carried out are discussed. These include aeration cascades, as well as performance and sizing criteria for settling lagoons and wetlands. In addition to passive methods active treatment options used at the sites investigated in this study are presented and include a variety of techniques from hydrogen peroxide dosing to sludge recirculation.

2.1 What is acid mine drainage?

The term Acid Mine Drainage (AMD) (also referred to as acid rock drainage (ARD)) is used to describe waters that have been acidified and polluted by the oxidation of sulphide minerals (e.g. pyrite and arsenopyrite) resulting in high concentrations of dissolved metals (and metalloids) such as Fe, As (UNEP report. 1991). The term is used to describe acidic waters with widely varying chemistries with pH starting as low as -3.6 (Nordstrom et al. 1999). The acidic medium formed by the AMD can result in the solubilisation of other metals including Zn, Pb and Au from surrounding minerals (Spotts et al. 1992). In some areas mine drainage is buffered by carbonate rocks resulting in a pH at discharge can be within the circumneutral range and in this case it can be referred to as neutral mine drainage (Hindmarsh et al. 1992; Cravotta et al. 1999). AMD occurs when pyrite is exposed to oxidising conditions as a result of the mining of a wide range of metals as well as coal. The generation of these acidic and metal rich waters are not however limited to anthropogenic activities and can be observed wherever sulphide minerals are exposed to the effects of oxidation and weathering. Indeed, in the early days of exploration it was often these natural ARD discharges that led to the discovery of new mineral deposits.

Metals such as lead and zinc have been mined since pre-Roman times (Li and Thornton 1993), though the relatively small number and scale of these operations meant that environmental consequences were minimal. The rapid growth in mining during the industrial revolution however, led to the appearance of streams and rivers stained with ferric(hydroxy)oxide (HFO) precipitates in communities throughout the UK and elsewhere.

The long term environmental impact of a mine may not be fully recognised for a number of years after decommissioning. Problems with mine drainage generally arise after the closure of a mine as a result of flooding of the workings (a process which can take decades) which are kept relatively dry by pumping during operation. Infiltration by ground water mobilises the contaminants within the mine and carries them to the surface. In some cases ground water flows can carry the mine drainage underground resulting in the pollution of nearby aquifers.

Despite the ever increasing number and size of AMD discharges legislation aimed at charging mining companies with responsibility for the long term pollution arising from their activities only came into play in Europe in 2001. Since the majority of British mines had already closed by this time and the “polluter pays” legislation could not be enforced retrospectively many mine drainage discharges were left requiring remediation with very little public funding available to cover the cost. The situation is similar across North America as well as the rest of Europe and so there has been much interest in the development of “passive” (very low or zero energy and no chemical dosing) treatment systems which have supposed minimal start up and long term operating costs.

The main legislative driver for the remediation of mine drainage discharges in Europe at the time of writing is the EU Water Framework Directive (CEC 2000). It requires that all inland and coastal waters be of a “good ecological status” by 2015. The Directive provides a range of demanding objectives set out in a framework for the protection, improvement and sustainable use of water resources.

2.1.1 Impact of acid mine drainage

One of the most immediate visual impacts of mine drainage is the coating of river and stream beds with an orange brown layer of ferric(hydroxy)oxide HFO precipitates. Figure 2-1 shows a distribution channel at the Ynysarwed treatment site fouled with HFO. Regular cleaning is required in order to prevent build up of thick layers of the sludge that might reduce the capacity of the channel.

2-1 Distribution channel fouled with HFO precipitates

Similar deposits of HFO in natural water courses can result in the smothering of algal communities on stream and river beds preventing new growth and disrupting the bottom of the food chain (Dudeney et al. 1994). This smothering can also have an adverse effect on invertebrate communities by burying the hard substratum on which they live as well as coating the invertebrates themselves (Dills and Rogers 1974, DeNicola and Stapleton 2002). Though Fe is generally not considered to be toxic, in the worst cases a combination of low pH and high metal concentrations can also decimate fish populations leaving rivers affected by AMD with dramatically reduced biodiversity (Gray 1998).

2.1.2 Generation of acid waters

Sulphide minerals deposited underground away from air or oxygenated water are chemically stable on a geological timescale. When these minerals are exposed to atmospheric oxygen and water however (as is the case when abandoned mine workings are allowed to flood) the sulphide component of the mineral is oxidised. This results in the dissolution of the mineral into the surrounding water. The important steps in the chemical reactions occurring under these circumstances are shown in Equations 2-1 to 2-3 (Moses et al. 1987; Stumm and Morgan 1996).

Initially sulphide is oxidised to sulphate. Upon further exposure to oxygen (either underground or after having discharged into the open air) Fe(II) is oxidised to Fe(III), and where pH is above approximately 3 Fe(III) precipitates as HFO. The overall reaction is described by Equation 2-4 and can be seen to produce 4 moles of H^+ ions for every mol of Fe sulphide consumed resulting in the overall acidification of the system.

Equation 2-1 $$\mathbf{FeS_2 + 3\tfrac{1}{2}O_2 + H_2O \rightarrow Fe^{2+} + 2\,SO_4^{2-} + 2\,H^+}$$

Equation 2-2 $$\mathbf{2\,Fe^{2+} + \tfrac{1}{2}O_2 + 2\,H^+ \rightarrow 2\,Fe^{3+} + H_2O}$$

Equation 2-3 $$\mathbf{Fe^{3+} + 2\,H_2O \rightarrow FeOOH_{(s)} + 3\,H^+}$$

Equation 2-4 $$\mathbf{2\,FeS_2 + 7\tfrac{1}{2}O_2 + 5\,H_2O \rightarrow 2\,FeOOH_{(s)} + 4\,SO_4^{2-} + 8\,H^+}$$

A second acid generating pathway for sulphide oxidation is also present in these systems and relies on the Fe(II)/(III) redox system with surface complexation of Fe(III) onto pyrite, resulting in sulphide oxidation as described by Equation 2-5 (Stumm and Morgan 1996, Langmuir 1997). It can be seen that this oxidation pathway produces much greater quantities of acid that oxidation by molecular oxygen giving 16 moles of H^+ for every 1 mole of FeS_2. Where oxygen levels have been depleted Fe(III) can become the main oxidising agent for the remaining pyrite increasing the rate of acid generation.

Equation 2-5 $$\mathbf{FeS_2 + 14\,Fe^{3+} + 8\,H_2O \rightarrow 15\,Fe^{2+} + 2\,SO_4^{2-} + 16\,H^+}$$

The kinetics of the abiotic homogeneous oxidation of Fe(II) to Fe(III) are slow in the acidic pH range with Fe(II) half life of the order of several years. This would suggest that once started the overall process would rapidly slow as the pH dropped. Under low pH conditions however bacterial oxidation becomes the dominant pathway regenerating Fe(III) 10^5-10^6 times faster than would abiotic oxidation (Kirby et al. 1999) and allowing the dissolution of the sulphide minerals to continue.

Once ferruginous mine drainage reaches the surface the ease and methods with which it can be remediated are determined by the rate of oxidation of Fe(II) to Fe(III) and where settling lagoons or wetlands are used the rate of precipitation and settling of the HFO solids produced. More detail about the rates and mechanisms for these processes are given in the following sections along with a discussion of other factors that influence the chemistry of mine drainage and a range of available treatment options.

2.2 Fe (II) oxidation chemistry

Fe occurs in numerous ores and minerals including haematite (Fe_2O_3), magnetite (Fe_3O_4) and pyrite (FeS_2). The oxidation and dissolution of pyrite can result in acid rock drainage (ARD) also known as acid mine drainage (AMD) (Spotts et al. 1992) as discussed in Section 2.1. Once released into solution the Fe(II) from pyrite is oxidised to Fe(III) (Stumm and Lee 1961) which rapidly precipitates to form ferric(hydroxy)oxide HFO solids at circumneutral pH (Pham et al. 2006). This section discusses the rates and mechanisms involved in these chemical transformations of iron in the context of mine drainage.

There are two possible chemical (abiotic) pathways for oxidation of Fe(II); homogeneous and heterogeneous (Tamura et al. 1976, Sung and Morgan 1980). Homogeneous oxidation occurs in aqueous solution in the absence of HFO precipitates, where all species involved in the oxidation reaction are in the same phase (i.e. are all in aqueous solution). Heterogeneous oxidation most commonly occurs where dissolved Fe(II) contacts suspended HFO particles, though it can occur anywhere that dissolved Fe(II) and O_2 become adsorbed onto solid HFO (or a number of other metal oxide) surfaces (Tamura et al. 1976, Tamura et al. 1980). When heterogeneous oxidation occurs the dissolved Fe(II) ions are in contact with the solid phase oxide. Above pH 7 heterogenous Fe oxidation has been observed to be autocatalytic with dissolved Fe(II) being adsorbed onto freshly formed HFO particulates where it undergoes rapid oxidation (Sung and Morgan 1980).

Abiotic rates of Fe(II) oxidation are highly pH dependent with Fe(II) having a half life of seconds at pH 8 and years at pH 2 (Singer and Stumm 1970, Ghosh 1974). At low pH or low pO_2 the rate of Fe(II) oxidation by lithotrophic bacteria can exceed of the abiotic oxidation rate whereas at circumneutral pH abiotic oxidation outcompetes the bacterially mediated pathway (Noike et al. 1983, Hallberg and Johnson 2003).

Sections 2.2.1 and 2.2.2 provide a review of the literature of the last few decades in the field of Fe(II) oxidation rates and mechanisms. Consideration is given not just to

the effects of pH, temperature and dissolved oxygen, but also to the effect of background chemistry on rates of Fe(II) oxidation.

2.2.1 Homogeneous oxidation

Proposals for the mechanism of Fe(II) oxidation in aqueous solution date back as far as the 1930s. In addition to O_2 both $O_2^{-\bullet}$ and H_2O_2 were identified as two of the species responsible for the Fe(II) to Fe(III) oxidation step (Weiss 1935). More recently King et al (1995) have developed a detailed model of Fe(II) oxidation shown in Table 2-1 with reactions 2 and 4 being much faster than the rate determining reactions 1 and 3. Both O_2 and H_2O_2 are well known oxidants. The radical species $O_2^{-\bullet}$ and $OH^{\bullet}$ may be less well known, but are highly unstable and as noted by King et al (1995) react rapidly with oxidisable species such as Fe(II) (much more rapidly than O_2 and H_2O_2).

Table 2-1 Model for Fe(II) oxidation

Reaction	No.
$Fe^{2+} + O_2 \rightarrow Fe^{3+} + O_2^{-\bullet}$	1
$Fe^{2+} + O_2^{-\bullet} + 2H^+ \rightarrow Fe^{3+} + H_2O_2$	2
$Fe^{2+} + H_2O_2 \rightarrow Fe^{3+} + OH^{\bullet} + OH^-$	3
$Fe^{2+} + OH^{\bullet} \rightarrow Fe^{3+} + OH^-$	4

At circumneutral pH the overall rate of oxidation of Fe(II) can be described by Equation 2-6 (Stumm 1992), though it has also often been quoted in the form as described by Stumm and Lee (1961) (Equation 2-7), where k_1 is the rate constant for homogeneous Fe(II) oxidation and Po_2 is the partial pressure of O_2 in atm.

Equation 2-6
$$-\mathbf{d}[\mathbf{Fe(II)}]/\mathbf{dt} = \boldsymbol{k_1}[\mathbf{Fe(II)}]\mathbf{P_{O_2}}/[\mathbf{H^+}]^2$$

Equation 2-7
$$-\mathbf{d}[\mathbf{Fe(II)}]/\mathbf{dt} = \boldsymbol{k_1}[\mathbf{Fe(II)}]\mathbf{P_{O_2}}(\mathbf{a_{OH^-}})^2$$

The two equations are linked by the temperature dependent dissociation constant for water K_w (Stumm and Morgan 1996) which is given by Equation 2-8 (concentrations in M).

Equation 2-8 $$[\mathbf{OH^-}][\mathbf{H^+}] = \mathbf{K_w} = \mathbf{10^{-14}}$$

The rate of Fe(II) oxidation has been found to be highly temperature dependent with activation energy in the range 29 $\pm$ 2 kJ mol^{-1} (Millero et al. 1987) to 96 kJ mol^{-1} (Stumm and Lee 1961). At 13^{o}C (a typical temperature for emerging mine water) this would give a range of calculated k_1 values that differ by a factor of 3.5.

It is clear that the rate of oxidation is highly pH dependent in the pH region relevant to Equation 2-6 with the reaction being 2nd order with respect to [H$^+$]. In fact this 2nd order dependence results in a 100 fold increase in rate of Fe(II) oxidation every time pH increases by 1 point over the circumneutral range. The pH dependence varies considerably in acidic solution changing from a 2nd to a 1st order dependence on [H$^+$] with increasing acidity (from pH 5 to 3), becoming independent of pH below pH 3 as illustrated in Figure 2-2.

Equations 2-6 and 2-7 provide the most simplified version of the rate equation for Fe(II) oxidation at circumneutral pH. Numerous authors (e.g. Millero and Sotolongo 1989, Emmeneger et al. 1998, King 1998, Rose and Waite 2002, Santana-Casiano et al. 2004, 2005, Trapp and Millero 2007, Pham and Waite 2008,) have further developed models to describe Fe(II) oxidation rate that describe not only individual Fe(II) species and ion pairs, but also differentiate between the rates of Fe(II) oxidation by each of the oxidising species shown in Table 2-1, O_2, H_2O_2, $O_2^{-\bullet}$, and $OH^{\bullet}$. In addition to the refinements that can be made to the rate equation by detailed chemical analyses there are several other factors that are also known to influence the rate of Fe(II) oxidation in natural systems; namely bacterial oxidation and the rate of precipitation of HFO. The relative importance of each of these factors is considered and discussed in more detail throughout the remainder of this section.

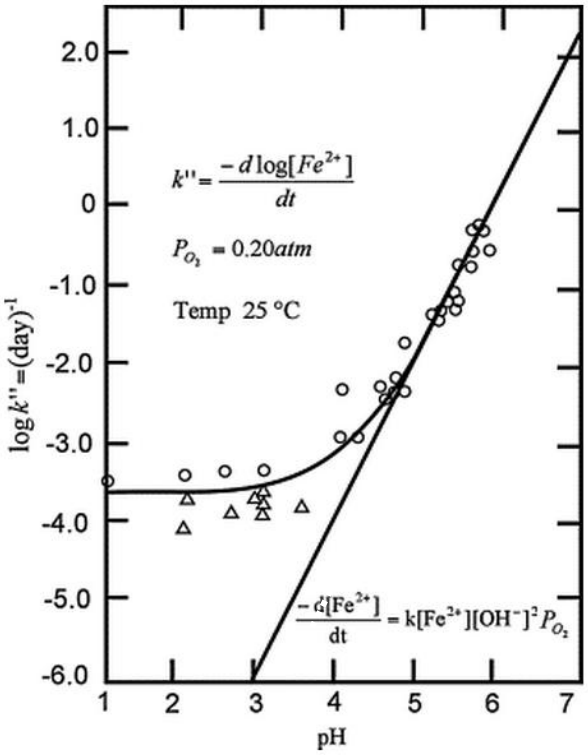

Figure 2-2 Effect of pH on rate of homogeneous Fe(II) oxidation

Reproduced from Singer and Stumm (1970)

2.2.1.1 Relative contributions of H_2O_2 and oxidising radicals to the overall Fe(II) oxidation rate

The relative contributions of the oxidising species H_2O_2, $O_2^{-\bullet}$, and $OH^{\bullet}$ compared to O_2 in the oxidation of Fe(II) in natural waters have been studied and commented on by a number of authors including Millero and Sotolongo (1989), Emmenegger et al (1998), Rose and Waite (2002) and Pham and Waite (2008). Millero and Sotolongo (1989) found that the realtive importance of O_2 and H_2O_2 as oxidants with respect to Fe(II) in natural waters varied considerably with pH, temperature and ionic strength of solution. They showed that the ratio $t_{\frac{1}{2}}(O_2)/t_{\frac{1}{2}}(H_2O_2)$ increased with decreasing pH from 8 to 7, decreased with decreasing ionic strength and showed an inverse relationship with temperature changing from 4 at 25°C to 84 at 5°C. Where $t_{\frac{1}{2}}$ is the half-life of the concentration of the species in the reaction mixture and increasing $t_{\frac{1}{2}}$

indicates decreasing rate of reaction. What this means is that as as pH and temperature decrease, oxidation of Fe(II) by O_2 becomes increasingly important with respect to oxidation by H_2O_2. In mine water scenarios where pH is typically <7 and temperature ≅ 10 -15 ^{o}C, O_2 is therefore likely to be the dominant oxidising species.

Emmenegger et al (1998) recast the rate equation at constant pH in the form given by Equation 2-9 where rate constants k'_{O_2} and $k'_{H_2O_2}$ include the concentrations of O_2 and H_2O_2 respectively. They also include a stoichiometric factor of 2 to account for the fast oxidation of a second Fe(II) which reacts with one of the highly oxidising species produced during the oxidation of the first Fe(II). This can be explained by the reactions in Table 2-1 where the oxidation of Fe(II) by O_2 and H_2O_2 results in the production of the unstable $O_2^{-\bullet}$ and $OH^{\bullet}$ radical species which rapidly react with additional Fe(II).

Equation 2-9

$$-\mathbf{d[Fe(II)]}/\mathbf{dt} = \mathbf{k'_{O_2}[Fe(II)]} + \mathbf{k'_{H_2O_2}[Fe(II)]}$$

They measured H_2O_2 concentrations generated naturally as a result of the reactions occurring within the samples and controlled DO levels by bubbling O_2 through the reaction mixture. In line with the findings of Millero and Sotolongo (1989) they found that the dominant oxidising species was O_2 over the range of conditions in their experiments.

2.2.1.2 Background chemistry and Fe(II) ion pair formation

The influence of background chemistry on the rate on Fe(II) oxidation has been the subject of numerous studies (e.g. Shenk and Webber 1968; Kester et al. 1975; Millero and Sotolongo 1989; Wolthoorn et al. 2004; Trapp and Millero 2007) . In recent years several of these studies have preferred to modify the mixed rate expression, Equation 2-6, to one which considers individually the major reactive Fe(II) species known to have the greatest effect on measured oxidation rates. Detailed studies of the oxidation rate of different ion pairs have been used to develop composite rate laws where each individual species can be given its own rate constant (e.g. King 1998; Santana-Casiano et al. 2004). The overall Fe(II) oxidation rate can then be explained as a weighted sum of the oxidation rates of individual Fe(II) species, with the rate constants for fast reacting species being greater than for slow reacting species. From this interpretation

it can be seen that low concentrations of fast reacting species will have a much greater effect on the overall rate than correspondingly low concentrations of slow reacting species.

Sung and Morgan (1980) were the first to investigate the effect of ionic strength on the kinetics of Fe(II) oxidation. They observed that increasing ionic strength with respect to Cl^- and SO_4^{2-} corresponded to decreasing oxidation rate. In addition to this organic acids such as humic acid which tend to form complexes with dissolved Fe species have also been shown to impact on the overall oxidation rate (Theis and Singer 1974; Miles and Brezonik 1981). Some organic complexes increase Fe(II) oxidation rate, while others have been shown to significantly retard the rate of oxidation with others promoting the cycling of Fe(III) back to Fe(II) particularly in the presence of UV light (Rose and Waite 2002). As with organic species the overall effect of dissolved silica on the oxidation rate of Fe(II) is unclear. Shenk and Webber (1968) found that silica enhanced the rate of Fe(II) oxidation whereas more recently Wolthoorn et al. (2004) showed that dissolved silica has very little effect on the homogeneous oxidation rate and actually retards heterogenous oxidation resulting in an overall decrease in oxidation rate.

Equation 2-10 and Equation 2-11 give one example of the speciated form of the rate equation as discussed by Trapp and Millero (2007) where α_i is the mole fraction and k_i is the rate constant for species *i*. Since the mole fractions of the Fe(II) hydroxyl species are highly pH dependent, the $[H^+]$ term is no longer included in the rate equation as it is accounted for in the calculation of k_{app}. It can be seen that despite using increasing concentrations of NaCl to influence the rate of Fe(II) oxidation only the fast reacting species are required in the rate equation. The effect of increasing ionic strength and hence increasing formation of $FeCl^+$, ion pairs is reflected by decreasing mole fractions of the fast reacting species in Equation 2-11.

Equation 2-10

$$\mathbf{d[Fe(II)]/dt} = -\mathbf{k_{app}[Fe(II)][O_2]}$$

Equation 2-11

$$\boldsymbol{k_{app}} = \boldsymbol{\alpha_{Fe^{2+}} k_{Fe^{2+}}} + \boldsymbol{\alpha_{FeOH^+} k_{FeOH^+}} + \boldsymbol{\alpha_{Fe(OH)_2} k_{Fe(OH)_2}} + \boldsymbol{\alpha_{Fe(CO_3)_2^{2-}} k_{Fe(CO_3)_2^{2-}}}$$

Whitney-King (1998) found that where natural waters contain greater than 1mM carbonate alkalinity, carbonate complexes [$FeCO_3$, $Fe(CO_3)_2^{2-}$, $FeCO_3OH^-$] dominate the Fe(II) speciation. Whitney-King also showed that below pH 6 Fe^{2+} and $FeOH^+$ can be used to describe the oxidation rate whereas above pH 6 the $Fe(CO_3)_2^{2-}$ complex dominates the reaction kinetics.

Much of the work carried out with respect to ionic strength and the effect of Fe(II) ion pair formation on overall oxidation rate has been carried out on sea waters and brines (e.g. Rose and Waite 2002; Santana-Casiano et al. 2004, 2005). As noted by Santana-Casiano et al (2010) the speciation based models for Fe(II) oxidation developed in these investigations "work very well for sea water and concentrated electrolyte solutions". They have not however often been used in the interpretation of Fe(II) oxidation rates in freshwater or mine drainage scenarios.

2.2.1.3 Differences in Fe stability constants in thermodynamic and geochemical data sets

One of the most common ways to calculate the speciation of Fe(II)/(III) in aqueous solution is to use geochemical models which perform speciation calculations such as PHREEQC (Parkhurst and Appelo 1999), Minteq (Felmy et al. 1984) or WateQ4F (Nordstrom and Ball 2001) in conjunction with a suitable thermodynamic database of stability constants. These models rely on mathematical equations to represent the chemical processes within a system and may be used to calculate the equilibrium concentrations of aqueous species or to describe kinetic processes such as Fe(II) oxidation (Gonçalves 2005). To date there is no universally agreed thermodynamic data set incorporating all of the available data for Fe(II) speciation and thus discrepancies can arise between studies using different speciation codes and thermodynamic data sets. Geochemical modelling has been used in this thesis the basis for Fe(II) speciation and ion pair formation in the mine waters under investigation. All modelling work has been conducted using the PHREEQCi software (Parkhurst and Appelo 1999) with Phreeqc.dat database.

2.2.1.4 Bacterial Fe(II) oxidation

Several types of Fe oxidising bacteria are commonly associated with mine drainage and include acidophiles such as *Leptospirillum ferrooxidans* and neutrophiles such as *Gallionella ferruginea* and *Leptothrix ochracea* (Hallberg and Johnson 2003). The contribution of these bacteria to the oxidation of Fe(II) in mine drainage is most important at low pH (Noike et al. 1983). Even neutrophillic bacteria have been shown not to greatly influence the overall rate of Fe(II) oxidation above pH 4 (Hallberg and Johnson 2003) with oxidation being primarily abiotic above pH 5 (Kirby et al. 1999). In a well oxygenated system, the relative contributions of biotic and abiotic Fe(II) oxidation pathways are clearly illustrated in Figure 2-3 (from Kirby and Brady 1998).

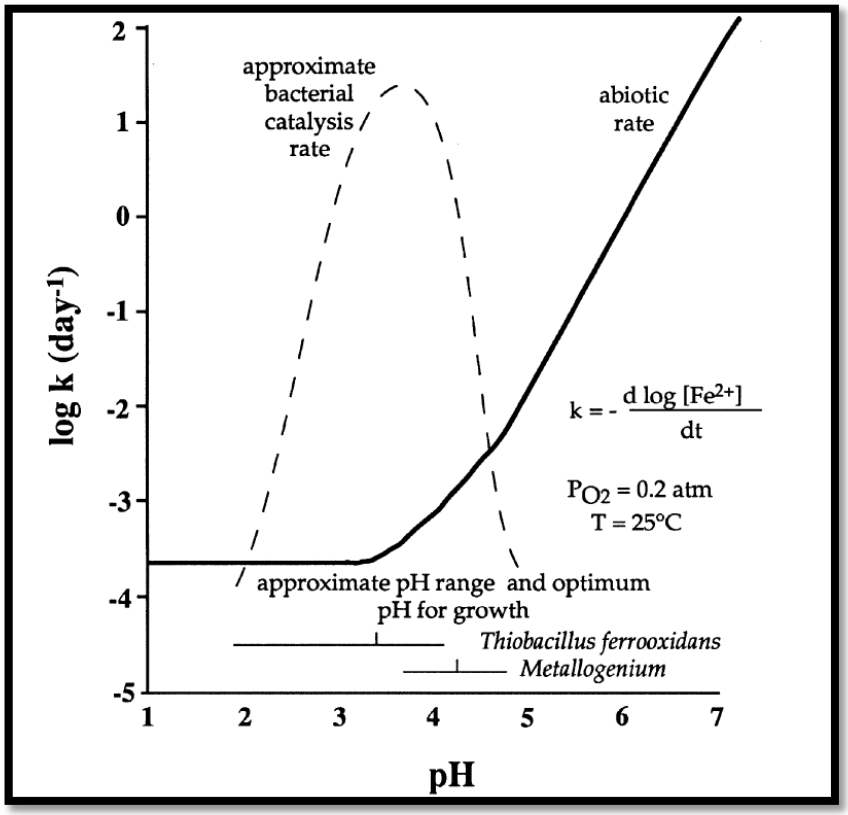

Figure 2-3 Schematic plot showing abiotic and biotic pseudo first order rate constants for Fe(II) oxidation by O_2, against pH

From Kirby and Brady (1998), using data from Singer and Stumm (1970) and Waddell (1978)

It can be seen that the abiotic oxidation rate decreases sharply between pH 7 to 3 with bacterial oxidation rates dominating between pH 4.5 and 2.5. Below pH 2 the

reduction in bacterial oxidation rate oxidation rate means that the abiotic oxidation process again begins to dominate.

Several other studies have concluded that at very low O_2 concentrations, bacterial oxidation can make a major contribution to the overall oxidation rate even at circumnutral pH. Sogaard et al (2000) conducted a survey of Fe(II) removal rates at a number of water treatment facilities in Denmark using sand filters for Fe removal. They noted Fe removal rates up to 60 times higher than would be expected from abiotic oxidation alone, and attributed this (at least partially) to the ability of the bacterial exopolymers of *G. ferruginea* to stabilise Fe(III) precipitates and prevent re-dissolution despite borderline anoxic conditions. Sobolev and Roden (2001) also showed elevated Fe(II) oxidation rates by lithotrophic Fe(II) oxidising bacteria at low partial pressures of dissolved O_2. What should be noted however, is that even at very low partial pressures of O_2 (<0.0096 atm) heterogeneous autocatalysis in the absence of Fe oxidising bacteria has been shown to result in rates of Fe(II) oxidation at least 2 orders of magnitude higher than that which would be predicted by homogeneous oxidation alone (Park and Dempsey 2005).

2.2.1.5 Precipitation of Fe(III)

Le Chatellier's principle dictates that one of the factors determining the rate of oxidation of Fe(II) is the concentration of Fe(III) in solution. Within the circumneutral pH range, once formed, Fe(III) is rapidly hydrolysed to form a number of species ($Fe(OH)^{2+}$, $Fe(OH)_2^{+}$, $Fe(HO)_3^{0}$ and $Fe(OH)_4^{-}$) (Pham 2006). It is suggested that precipitate formation then occurs via aggregation of these species in several identifiable stages; "formation of small precursor polymers, growth of these polymers to colloidal particles and subsequent condensation to settleable precipitates", with each stage having a different rate constant (Grundle and Delwiche 1993). Whilst this is likely the most accurate description of the formation of settleable Fe(III) precipitates for practical purposes Sapsford and Watson (2011) reduce the removal of Fe from mine drainage to a simple 2 step process as shown in Equation 2-12. Within the circumneutral pH range the first stage of the reaction is rapid. Dissolved Fe(III) is known to be stable at low pH with the rate of precipitation increasing with pH up to a

maximum at around pH 8 (Pham 2006) and becoming increasingly soluble again at high pH. Thus in the circumneutral pH range rapid precipitation of Fe(III) will provide a strong driving force for the oxidation reaction.

Equation 2-12 $$\mathbf{Fe(II)_{(aq)} \overset{k_1}{\rightarrow} Fe(III)_{(s)} \overset{k_s}{\rightarrow} Settled\ Fe(III)}$$

2.2.1.6 Fe(II) oxidation rates and k_1

As has been discussed previously in Sections 2.2.1.1 and 2.2.1.2 a number of authors have recently preferred to describe the rate equation for Fe(II) oxidation in terms of individual Fe(II) species or ion pairs and/or oxidising species. Such detailed analysis of the reacting species present may give a fuller picture of Fe(II) reaction kinetics, but it also adds a greater degree of complexity to calculations relating to Fe(II) oxidation rates. The general form of the rate law as described by Equation 2-6 and 2-7 (though less detailed) might therefore be more useful in the determination of Fe(II) oxidation rates in mine drainage in the field, where conditions cannot be controlled and monitored as they would be in a laboratory setting. This section therefore includes a brief discussion of oxidation kinetics with respect to these simple forms of the rate equation.

Numerous studies have been conducted to investigate the kinetics of Fe(II) oxidation at circumneutral pH. These have involved both natural and synthetic Fe(II) solutions and have sought to deduce values for d[Fe(II)]/dt and k_1. Several of the studies have found values for k_1 of the order of 1 to 3 x 10^{13} M^{-2} atm^{-1} min^{-1} (using Equation 2-7) for well oxygenated waters at pH 6.5 to 7 with µM concentrations of Fe(II) (Stumm and Lee 1961; Shenk and Webber 1968; Millero 1985; Liang 1993). The close agreement of all of these studies gives confidence in the k_1 values for this range of experimental conditions.

For mine drainage scenarios in the field, investigations have focused on reporting Fe(II) oxidation rates for a given set of conditions. As would be expected these vary widely with pH and many studies have focused on acidic rather than circumneutral mine drainage (e.g. Nordstrom 1985). Kirby and Brady (1998) collected oxidation rate data

about a number of mine discharges using a continuously stirred tank reactor and found values ranging from 1.0 x 10^{-9} Mol/L/s at pH 3.6 and Fe(II) ≅ 3.5 mg/L to 2.6 x 10^{-7} Mol/L/s at pH 7.2 and ≅ 29 mg/L.

2.2.2 Heterogeneous oxidation

Chemisorption, also known as surface coordination occurs when coordinate bonds form between reactive functional groups on the surface of a material and metals or other ligands in solution (Stumm and Morgan 1996). In the case of mine water discharges the HFO precipitates that form in the water column and coat the sides of distribution pipes and channels provide a significant surface area with sites suitable for adsorption of Fe(II) ions. In the case of these HFO solids the reactive surface species is the hydroxyl group. Equation 2-13 taken from Stumm and Morgan (1996) gives an example of the kind of surface complexation reaction that can occur in the case of the HFO/Fe(II) system where S represents the bulk solid attached to a terminal hydroxyl group. The symbol ≡ denotes a bond attached to the bulk solid with a single line – denoting a single covalent bond involving one of the species involved in chemical reactions on the surface of the solid. Once adsorbed onto the HFO surface the Fe(II) can then be oxidised to Fe(III). This pathway for Fe oxidation is considered to be catalytic as rates of Fe oxidation are greatly increased in the presence of HFO solids compared to situations where the predominant pathway for oxidation is the homogeneous mechanism alone (Tufekci and Sarikaya 1996).

Equation 2-13 $$\equiv \mathbf{S} - \mathbf{OH} + \mathbf{Fe^{2+}} \rightarrow \equiv \mathbf{S} - \mathbf{O} - \mathbf{Fe^{+}} + \mathbf{H^{+}}$$

2.2.2.1 Mechanisms for heterogeneous Fe oxidation

Several mechanisms have been proposed for the heterogeneous oxidation of Fe(II), the counter ion mechanism (Tufekci and Sarikaya 1996), reactive surface species mechanism (Wherli 1990) and semiconductor mechanism (Park and Dempsey 2005) as summarised in Barnes et al (2009).

The counter ion mechanism as proposed by Tufekci and Sarikaya (1996) is explained in terms of the concentration of OH^- ions in the diffuse layer immediately next to the

surface of the HFO precipitates. The point of zero charge (PZC) (the pH at which the surface charge of a mineral is zero) for HFO in a carbonate buffered system is around 8.5, below which the surface carries a positive charge. It was suggested that this positive charge caused an increase in the concentration of OH^- ions next to the surface that results in a localised increase in pH relative to the bulk solution. Thus adsorbed Fe(II) is oxidised faster than free Fe(II) since oxidation rate is proportional to $[OH^-]^2$. This mechanism is however disputed by Barnes et al (2009) who suggest that OH^- is not concentrated in the diffuse layer around HFO in mine drainage scenarios as a result of adsorption of counter ions such as CO_3^{2-} and SO_4^{2-} which lower the pH of the PZC.

The reactive surface species mechanism suggests that adsorption of Fe(II) enhances the rate of electron transfer during the oxidation reaction, similar to the mechanism by which hydrolysis enhances Fe(II) oxidation rate in solution (Wherli 1990). Liger (1999) suggested that there were two types of surface sites involved in the oxidation reaction $(\equiv \mathrm{Fe^{III}} - \mathrm{O} - \mathrm{Fe^{II}})^+$ and $(\equiv \mathrm{Fe^{III}} - \mathrm{O} - \mathrm{Fe^{II}} - \mathrm{OH})$. Of these two species they found that the rate of U(VI) reduction had a linear dependency on the concentration of the latter on a goethite surface indicating that it is the more redox active of the two species.

The semi-conductor mechanism also suggests that there are two distinct types of surface bound Fe(II) in these systems. Park and Dempsey (2005) showed that the rate of Fe oxidation was dependent on both the concentration of adsorbed and dissolved Fe(II) according to Equation 2-14 (where k_2 is the rate constant for heterogeneous oxidation). They found that the concentration of adsorbed Fe(II) remained constant during the oxidation reaction while the concentration of dissolved Fe(II) decreased. They explained this in terms of an anode/cathode type situation where O_2 is reduced at electron rich sites by strongly sorbed Fe(II) and Fe(II) oxidised at electron poor sites without sorbed Fe(II).

Equation 2-14 $$-\mathbf{d[Fe(II)]/dt} = \boldsymbol{k_2}\mathbf{[Fe(II)_{diss}][Fe(II)_{sorbed}][DO]}$$

2.2.2.2 Oxidation in mine water scenarios

The majority of the studies carried out in natural systems (e.g. Rose and Waite 2002) have investigated Fe redox chemistry in ocean and lake water where the concentrations of Fe(II) are several orders of magnitude lower than that found in acid mine drainage. Thus the kinetic models built to describe these systems may well not be applicable to the waters investigated in this study where Fe(II) concentrations are on the mM rather than the µM scale (Pham and Waite 2008; Santana-Casiano et al. 2010). In addition to this, the kinetic models developed in lake and sea water are often only tested over the pH range 6.5-8 and may not describe accurately the rates of reaction occurring below pH 6.

The overall rate of Fe(II) oxidation in mine water type scenarios can be summarised by Equation 2-15 from Tufekci and Sarikaya (1996) where ($k_1[\mathrm{OH}^-]^2\mathrm{P}_{\mathrm{O}_2}$) describes the contribution of homogeneous oxidation and ($k_2\left[\mathrm{Fe(III)}_{(\mathrm{s})}\right][\mathrm{OH}^-]\mathrm{P}_{\mathrm{O}_2}$) describes the contribution of heterogeneous oxidation to the overall rate. It can be seen that whereas the homogeneous pathway has a 2nd order dependence on [OH$^-$], the heterogeneous mechanism has a 1st order dependence.

Equation 2-15

$$-\mathbf{d}[\mathbf{Fe(II)}]/\mathbf{dt} = (\boldsymbol{k_1}[\mathbf{OH}^-]^2\mathbf{P_{O_2}} + \boldsymbol{k_2}\left[\mathbf{Fe(III)}_{(\mathbf{s})}\right][\mathbf{OH}^-]\mathbf{P_{O_2}})[\mathbf{Fe(II)}]$$

Below pH 7 the rapid reduction in the homogeneous oxidation rate, 10,000 times slower at pH 5.5 than at pH 7.5, means that where HFO solids are present heterogeneous oxidation increasingly becomes the dominant pathway.

Under certain conditions the oxidation of Fe(II) can be autocatalytic with dissolved Fe(II) sorbing onto the surface of freshly formed HFO precipitates in the water column. Work carried out by Sung and Morgan (1980) suggests that this only occurs above pH 7. The increased importance of autocatalysis above pH 7 can at least in part be explained by the pH dependence of the sorption of Fe(II) onto the surface of Fe(III) solids given by Equation 2-16. Thus as pH decreases increasing amounts of Fe(III) solids are required to produce the same catalytic effect.

Equation 2-16 $$[\mathbf{Fe(II)_{sorb}}]/[\mathbf{Fe(II)}] = \mathbf{K}\left[\mathbf{Fe(III)_{(s)}}\right]/[\mathbf{H^+}]$$

By their nature, the majority of mine drainage discharges have pH below 7, and so aside from systems where HFO solids are either added to the waters to catalyse oxidation, or allowed to build up on top of a vertical flow system (see Section 2.4.4), heterogeneous oxidation would not be expected to have a major influence on the overall oxidation rate.

2.2.3 Common errors incurred during kinetic experiments

Davison and Seed (1983) gave a critical review of the literature reporting homogeneous oxidation rate constants at circumneutral pH in light of common errors that might occur during the experimental procedure. They concluded that errors relating to the measurement of Fe(II) concentration and Po_2 could be minimised by careful measurement since they are directly related to d[Fe(II)]/dt (i.e a 10 % error in measurement produces a 10 % error in calculated oxidation rates and k_1 values). At circumneutral pH where the oxidation rate is dependent on $[OH^-]^2$ however the errors from pH measurement would have a much greater effect. With an accuracy of pH measurement of $\pm$ 0.1 points a calculated value of k_1 could vary from 7.8×10^{14} to 1.9×10^{15} $M^{-2}atm^{-1}s^{-1}$ based on a mean experimental value of 1.2×10^{15} $M^{-2}atm^{-1}s^{-1}$ giving an error of +/- 35 %.

2.3 pH control in acid mine drainage

It is well known that where ground waters are in contact with carbonate minerals they are likely to contain elevated levels of dissolved CO_2 with respect to surface waters which are in equilibrium with atmospheric CO_2. They also contain elevated levels of dissolved bicarbonates, referred to in this context as alkalinity because of their acid neutralising capacity (Stumm and Morgan 1996). It is the balance between alkalinity, dissolved CO_2 and Fe concentration that determines the pH of many mine waters including those in this study (Kirby and Cravotta 2005a, 2005b) . Since pH is the most important factor in determining the rate of Fe(II) oxidation (as discussed in Section 2.2) it is important to have a full understanding of the processes that affect pH in these systems. The importance and effects of alkalinity on mine waters will be discussed in more detail in the following sections.

2.3.1 Gas transfer

The basic concept and equations governing gas transfer between air and water can be described using the example of O_2. The instantaneous rate of change in DO concentration can be related to the oxygen mass transfer between air and water by Equation 2-17, where C_t is the DO concentration (ppm) at time t; C_s is the saturation concentration (ppm); k_L (m) is the liquid film coefficient for oxygen and A (m^2) is the surface area associated with volume V (m^3) over which gas transfer occurs. The equation does not take into account sources and sinks of oxygen within the body of the water as their rates of transfer are slow relative to the oxygen transfer occurs at most hydraulic structures such as stepped chutes (Emiroglu and Baylar 2006).

Equation 2-17

$$\frac{dC}{dt} = k_L \frac{A}{V}(C_s - C_t)$$

2.3.2 Dissolved CO_2 and atmospheric equilibration

The relationship between gaseous and dissolved carbon dioxide is not as straightforward as the case for oxygen. The solubility of CO_2 is linked to a number of other carbonate species by the reaction scheme shown by Equations 2-18 and 2-19.

The term H_2CO_3* is used to account for both dissolved CO_2 and H_2CO_3, though the concentration of $CO_{2(aq)}$ is almost identical to the concentration of H_2CO_3* when determined analytically by titration with alkali (i.e. the position of the equilibrium in Equation 2-18 lies far to the left hand side). The predominant carbonate species at lower pH is H_2CO_3*and CO_3^{2-} the predominant species at higher pH (Stumm and Morgan 1996).

Equation 2-18 $$[\mathbf{CO_{2\,(aq)}}] + [\mathbf{H_2CO_3}] = [\mathbf{H_2CO_3^*}]$$

Equation 2-19 $$[\mathbf{H_2CO_3^*}] \leftrightarrow [\mathbf{HCO_3^-}] \leftrightarrow [\mathbf{CO_3^{2-}}]$$

A detailed discussion of carbonate chemistry is given in Stumm and Morgan (1996). Table 2-2 summarises the carbonate equilibrium reactions occurring in aqueous solution.

Table 2-2 Equilibrium reactions and equilibrium constants for the aqueous carbonate system*

Equilibrium type	Reaction	Equilibrium constant
Gas/liquid	$CO_{2(g)} \leftrightarrow CO_{2(aq)}$	$K_H = P_{CO_2}/x_{CO_2}$
Hydration	$CO_{2(aq)} + H_2O \leftrightarrow H_2CO_3$	$K_0 = [H_2CO_3]/[CO_{2(aq)}]$
Acid-base	$H_2CO_3^* \leftrightarrow HCO_3^- + H^+$	$K_1 = [H^+][HCO_3^-]/[H_2CO_3^*]$
Acid-base	$HCO_3^- \leftrightarrow CO_3^{2-} + H^+$	$K_2 = [H^+][CO_3^{2-}]/[HCO_3^-]$
Acid-base	$H_2O \leftrightarrow H^+ + OH^-$	$K_w = [H^+][OH^-]$
Solubility	$CaCO_3 \leftrightarrow Ca^{2+}\ CO_3^{2-}$	$K_{sp} = [Ca^{2+}][CO_3^{2-}]$

* Reproduced from Stumm and Morgan (1996)
Proton exchange equilibria (acid/base reactions) are among the fastest known reactions. The hydration reaction however is slower taking place on a time scale of several tenths of a second (Lower, 2011).

It can be seen that the positions of the carbonate equilibria and hence the concentrations of the various carbonate species in solution are pH dependent. As pH decreases and H^+ concentration increases the carbonate and bicarbonate acid base equilibria shift in favour of H_2CO_3 which in turn favours an increase in the concentration of $CO_{2(aq)}$. Conversely it can be seen that a reduction in concentration of dissolved CO_2 will cause a shift in the position of the carbonate and bicarbonate acid-

base equilibria that results in a decrease in H^+ concentration and hence an increase in pH.

These equilibrium relationships allow the concentration of dissolved CO_2 (or $[H_2CO_3^*]$) to be calculated as long as both alkalinity and pH are known and can be used to relate dissolved CO_2 concentrations to total dissolved inorganic carbon (TDIC) (see Equation 2-20, where C_T = total concentration of all carbonic species present in solution, TDIC). They also form the basis for carbonate speciation calculations performed by the geochemical modelling software PHREEQCi used throughout the experimental and modelling sections of this thesis.

Equation 2-20

$$[\mathbf{H_2CO_3^*}] = \mathbf{C_T}\left(\mathbf{1} + \frac{\boldsymbol{K_1}}{[\boldsymbol{H^+}]} + \frac{\boldsymbol{K_1K_2}}{[\boldsymbol{H^+}]^{\mathbf{2}}}\right)^{\mathbf{-1}}$$

For the purposes of determining rates of CO_2 degassing Howe and Lawler (1989) described the carbonate system in terms of Equation 2-21 where the term α_g is used to account for the effect of pH on the proportion of total dissolved inorganic carbonate (TDIC) present as dissolved CO_2, where TDIC (C_T) = $[\mathrm{H_2CO_3^*}] + [\mathrm{HCO_3^-}] + [\mathrm{CO_3^{2-}}]$. Instead of basing calculations on dissolved CO_2 alone the equation makes use of TDIC and calculates dissolved CO_2 as a proportion of this.

Equation 2-21

$$\frac{\mathbf{d[C_T]}}{\mathbf{dt}} = \boldsymbol{\alpha_g}\,\mathbf{k_L a}\,(\mathbf{C_{T,eq}} - \mathbf{C_T})$$

Where:

C_T = total concentration of all carbonic species present in solution (TDIC)

$C_{T,eq}$ = equilibrium total carbonic species concentration

α_g = the pH dependent ratio $[H_2CO_3^*]/[C_T]$

k_La = mass transfer coefficient

This equation is valid over the range of pH values for which CO_2 is found in solution. In its simplest form the equation can be used to determine rates of CO_2 degassing in well buffered solutions at constant pH. The changes in pH that occur in the solutions considered in this study however mean that the equation could not be solved simply in the integrated form of Equation 2-22 as both $C_{T,eq}$ and α_g will change over time.

Equation 2-22 $$\mathbf{ln(C_{T,eq} - C_T) = ln(C_{T,eq} - C_{To}) - \alpha_g k_L a t}$$

In order to calculate k_La it would therefore be necessary to calculate incrementally the changes in $C_{T,eq}$ and α_g over time.

2.3.3 Acidity and Alkalinity

Alkalinity and acidity are important parameters in the analysis of AMD as it is often the balance between these two quantities that determines the methods used in the treatment of the water (Kirby and Cravotta 2005a, 2005b). Alkalinity is most often reported as mg/L $CaCO_3$ equivalent required to neutralise a certain quantity of acid. In reality the alkalinity in a water is largely present as both HCO_3^-. Acidity is also reported in mg/L $CaCO_3$ equivalent, but in this instance it is the quantity of $CaCO_3$ that would be required to neutralise the acidic species in the water. The parameters of acidity and alkalinity are most often determined by means of titration with NaOH or H_2SO_4 respectively to a predetermined end point. Where the acidity measured in a sample is greater than the alkalinity it would be described as net-acid, and where alkalinity is greater than acidity, net-alkaline (Kirby and Cravotta 2005a, 2005b). The mine drainage waters at all of the sites investigated in this study (see Chapter 3) are sufficiently well buffered by bicarbonate alkalinity that that they have circumneutral pH. In the following chapters they will be referred to as ferruginous mine drainage rather than AMD as despite the fact that they were formed by the same chemical processes as AMD, carbonate buffering means that at the point of discharge they are not acidic.

There are several factors related to the chemistry of mine drainage that can result in changes to both acidity and alkalinity over time. One of the most important factors is the acid generated by the combined processes of oxidation and hydrolysis of metals such as $Fe(II)_{aq}$ to $Fe(OH)_3$ solids as described by Equation 2-23. It can be seen that for every mole of Fe(II) oxidised and precipitated 1 mole of carbonate (alkalinity) is consumed.

Equation 2-23 $$\mathbf{Fe^{2+} + CO_3^{2-} + 2\tfrac{1}{2}H_2O + \tfrac{1}{4}O_2 \rightarrow Fe(OH)_3 + H_2CO_3}$$

Conversely, acidity can be lost from the system by CO_2 degassing. The loss of CO_2 does not affect alkalinity, but does result in a decrease in the concentration of dissolved carbonic acid. Thus in order to determine whether a water is net-acid or net-alkaline it is important to consider the acidity and alkalinity consuming/generating reactions that might occur as the water reaches equilibrium with the atmosphere.

One consequence of alkalinity consumption during the formation of HFO precipitates is that neutralisation of the acidity generated by HCO_3^- and CO_3^{2-} produces H_2CO_3 which can then be lost from the solution as CO_2. This adds further complexity with regards to calculating rates of CO_2 degassing as a solution initially containing 400mg/L CO_2, and 150mg/L HCO_3^- may end up losing 518mg/L CO_2 if all of the alkalinity is consumed during the production of $Fe(OH)_3$.

2.4 Options for passive treatment

2.4.1 Aeration cascades

It is widely known that hydraulic structures can be used to create turbulent conditions in flowing water that result in the entrainment of small air bubbles into the bulk flow. This in turn increases the surface area at the gas-liquid interface encouraging gas transfer both into and out of water (Tebbutt 1972; Novak and Avery 1978; Matter-Müller et al. 1981). In mine drainage treatment schemes aeration cascades have often been included to increase the concentration of DO in the water in an attempt to accelerate the Fe(II) oxidation process.

One of the more common types of hydraulic structure used in water treatment is the chute. A chute is characterised by a sloping bed which can be either smooth or stepped and is usually associated with torrential flow. These chutes also known as cascades are commonly used in water treatment processes to increase levels of DO or remove substances such as volatile organic compounds (VOCs) and chlorine (Matter-Müller 1981).

Studies by Toombes and Chanson (2000) and Emiroglu and Baylar (2006) and other have shown significantly greater gas transfer in stepped chutes compared to smooth chutes. The enhanced performance of the stepped chutes is a result of strong turbulent mixing and associated air entrainment brought about by macro-roughness. Both studies recognise the greater efficiency of the nappe flow regime where water spills from one step to the next compared to the skimming or transition flow as shown in Figure 2-4. Skimming flow is associated with narrow steps or high flow rates. Where this occurs the flowing water skims over a pseudo bottom created by recirulation zones on the faces of the steps. This serves to reduce turbulence and air entrainment resulting in less efficient gas transfer. Figure 2.4 give a diagrammatic representation of all three types of flow.

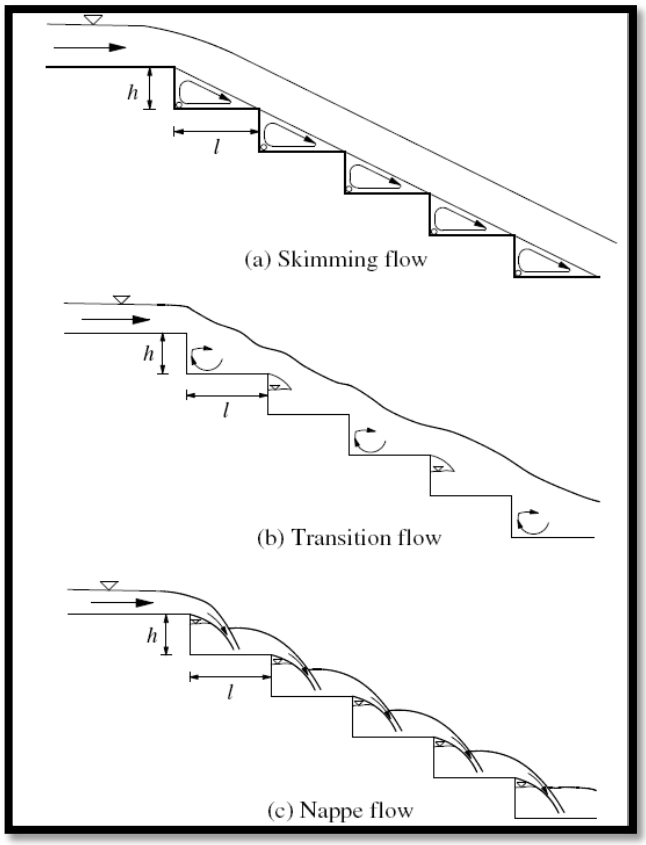

Figure 2-4 Comparison of different flow regimes over stepped chutes

Toombes and Chanson (2000) showed that gas transfer over a stepped chute is 10 times more efficient than a smooth chute for the same flow rate and bed slope, with "maximum air-water intersurface area observed in the spray region downstream of the nappe impact". The cascade designs highlighted in the PIRAMID (2003) guidelines differ from those investigated by Baylar et al (2007). They include a plunge pool between cascades which allows entrained air bubbles to fully dissipate into the water column before the water flows down over the next step (Figure 2-5). Experimental observations indicate that the depth and width of the plunge pool should be at least as large as the preceding fall of water is high (Novak 1994).

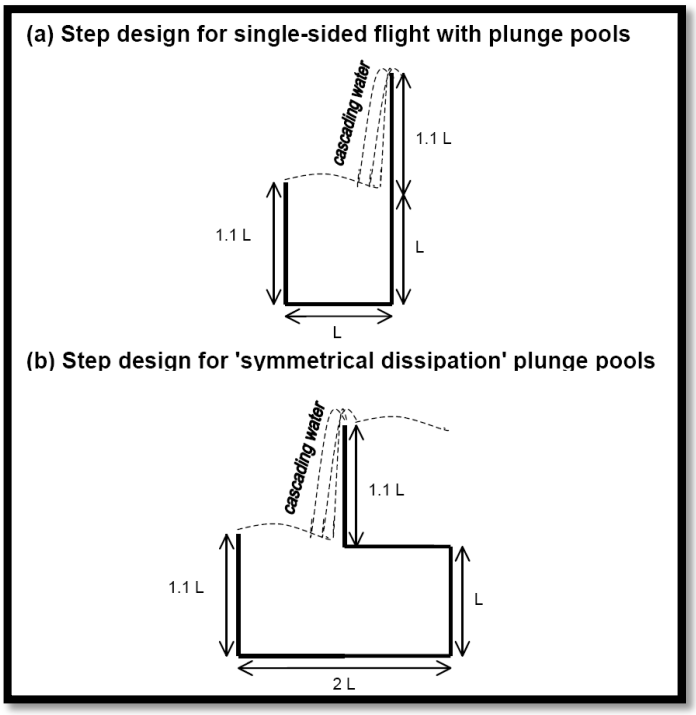

Figure 2-5 Plunge pool designs as described in the PIRAMID (2003) guidelines

2.4.2 Wetlands and lagoons

Wetlands and lagoons are commonly used in passive mine water treatment systems to provide the required residence time for Fe(II) oxidation and settling of precipitates (PIRAMID 2003). They can also be used as a final stage in the treatment of water by active means such as dosing with alkali and flocculants. Lagoons are commonly included in passive treatment systems ahead of wetlands with the function of removing a large proportion of the particulate Fe so that the main function of the wetlands is a final "polishing" of the last few mg/L of Fe(II) from the water (Younger et al. 2002).

2.4.2.1 Aerobic wetlands

Aerobic wetlands are one of the most widely used forms of passive treatment for mine waters. Removal of metals occurs via a number of mechanisms including sedimentation and filtration of suspended flocs, precipitation of metal hydroxides on plant stems and sediment surface, and adsorption of aqueous metal species. Batty and Younger (2002) have shown that at low Fe concentrations (<1mg/L) uptake by the

plants themselves is an important contributing factor in 'polishing' the remaining dissolved Fe to achieve low residual concentrations post treatment.

Whilst aerobic wetlands are generally included in passive systems for the purposes of polishing effluents after the majority of dissolved Fe has been removed in settlement lagoons, it is however possible to use wetlands to treat waters containing tens of mg/L of dissolved Fe (Watzlaf et al. 2003). The major drawback of this approach comes in the maintenance of the wetland which will accumulate significant volumes of HFO sludge at higher dissolved Fe concentrations. The closure and de-sludging of a wetland is both more complex and expensive than for a simple settling lagoon.

2.4.2.2 Compost (anaerobic) wetlands

Unlike aerobic wetlands, compost wetlands are generally employed in situations where the influent water is net-acidic and requires alkalinity generation for successful treatment. These wetlands have a thick anoxic substrate of saturated organic material which serves both to generate alkalinity and remove metals by precipitating them as sulphides. The organic 'compost' can come from many sources including amongst others sewage sludge cake and paper waste pulp (Laine and Jarvis 2002). Bacterial sulphate reduction occurs within the compost layer which serves to consume acidity by generating bicarbonate alkalinity as shown in Equation 2-24. This alkalinity generation helps to raise pH increasing the rate of Fe(II) oxidation.

Equation 2-24 $$\mathbf{SO_4^{2-} + 2CH_2O \rightarrow H_2S + 2HCO_3^-}$$

The production of sulphide results in the removal of some of the Fe(II) present as its sulphide according to Equation 2-25.

Equation 2-25 $$\mathbf{Fe^{2+} + HS^- \rightarrow FeS + H^+}$$

Since much of the flow through compost wetlands is surfacial the chemical reactions rely on the substrate exchanging solutes with the surface water via diffusion processes (unlike in the case of RAPS and PRBs discussed in Section 2.4.3). The (bio)chemistry involved is complex with the root systems of wetland plants such as *Typha* and

Phragmites maintaining locally oxic conditions via leakage of oxygen from the roots. While this inhibits the action of the surrounding anaerobic bacteria the roots of these plants often contain the organic compounds (notably acetate) which ultimately provide the substrates required by these same sulphate reducing bacteria. The interface zone may therefore be anoxic with micro-aerobic zones, resulting in both simultaneous oxidation and reduction of metal and sulphur species (Younger et al. 2000).

2.4.2.3 Settling lagoons

Settling lagoons have long been used in industrial settings as a low intensity method of water treatment. They encourage clarification of water by allowing the settlement of solids such as coal fines or in the case of mine waters HFO. In the case of treating mine drainage settlement lagoons offer the advantage over wetlands that routine maintenance and the removal of sediments is much easier. Hence including a settlement lagoon to trap a large portion of the HFO sediments as a first step in treatment can greatly extend the lifetime of a passive system. Settlement lagoons are routinely used in the UK by The Coal Authority with the aim of removing at least 50% of the Fe present in this first treatment step (PIRAMID 2003). In the case of net-acidic waters settlement lagoons may also be deployed as the second stage of treatment after an alkali producing step such as Reducing Alkalinity Producing Systems (RAPS) or Permeable Reactive Barriers (PRB) which will be discussed in more detail in Section 2.4.3.

In order for settlement lagoons to be effective, the water entering them is preferentially net-alkaline otherwise oxidation and precipitation rates for Fe(II)/(III) will be too low for its effective removal. In addition to this it is desirable to include an aeration cascade feeding into the lagoon in order to increase dissolved oxygen (see Section 2.4.1.).

Guidelines have been developed in relation to lagoon sizing for removal of Fe precipitates with a view to reducing dissolved Fe by at least 50% at this stage of the treatment process.

Sizing criteria have previously included (PIRAMID 2003)

- A nominal hydraulic retention time of 48 hours.
- 100m^2 of lagoon area per L/s of mine water to be treated.
- Application of the aerobic wetland sizing criterion which assumes a removal rate of 10g/m^2/d.

These three criteria can give widely differing values for the size of a settlement lagoon as shown in Table 2-3 and can result in lagoons being significantly over or under sized.

Table 2-3 Sizing criteria for lagoons and wetlands

Design criterion	Area (m^2)	Illustrative dimensions (L x W x D) (m^3)	Volume (m^3)	Retention time (days)	Sludge removal frequency (Years)
50 L/s; 50 mg/L Fe(II)					
48h retention time	3600	90x40x3	8680	2	1.8
100m^2 per L/s flow	5000	100x50x3	12520	2.9	2.6
Fe removal at 10g/m^2/day	21600	216x100x1	21600	4.9	4.6
10 L/s; 50 mg/L Fe(II)					
48h retention time	800	42x21x3	1730	2	1.5
100m^2 per L/s flow	1000	50x20x3	1960	2.3	1.7
Fe removal at 10g/m^2/day	4320	100x43x1	4020	4.7	4.3

The information contained within Table 2-3 is taken from the PIRAMID guidelines. Dimensions, volumes and areas were calculated on the basis that a trapezoidal basin is used (internal slopes 2:1). Water depth is 3 m for the first two formulae but only 1 for the third formula as it is intended for wetland sizing. The main problem with these criteria is that they take no account of the chemistry of the water being treated.

As shown in Section 2.2 a pH difference of 1 unit results in a 100 fold increase in Fe oxidation rate thus in some systems Fe removal will be limited by oxidation rate and in others by the settling velocity of the precipitates formed. In the case where settling velocity is the rate limiting step, hydraulics become increasingly important with

treatment efficiency decreasing as flow through the lagoon or wetland deviates from ideal (plug flow) conditions (Sapsford and Watson 2011).

2.4.3 Limestone drains, Reducing Alkalinity Producing Systems and Permeable Reactive Barriers

These systems are employed in the treatment of net-acid waters where the low pH and alkalinity results in low Fe(II) oxidation rates and hence low total Fe removal rates. The main principle of treatment by each of these systems is to increase the alkalinity in the system by passing the AMD over/through limestone or some other basic material such as Basic Oxygen Steel (BOS) slag (Kleinmann et al. 1998).

2.4.3.1 Limestone drains

Limestone drains can be further divided into anoxic and oxic systems. As the name suggests they both use calcium carbonate ($CaCO_3$) to generate alkalinity. The use of limestone is advantageous for large scale water treatment in that it is relatively low cost, non-hazardous and easy to handle when compared to other potential sources of alkalinity such as sodium hydroxide or quick lime. Unfortunately its dissolution rate is low compared to these other chemicals and it can quickly become coated ("armoured") with precipitates if environmental conditions are not carefully controlled.

The purpose of Anoxic Limestone Drains (ALDs) is to increase alkalinity prior to oxygenation of the mine water so that rapid precipitation of Fe will take place in subsequent treatment stages such as settlement lagoons or wetlands. In order to maintain anoxic conditions so that dissolved Fe remains in the ferrous form, ALDs comprise buried trenches filled with limestone ($CaCO_3$ >80%).

The application of ALDs is limited, as in order to avoid the problem of armouring with HFO and/or aluminium oxide precipitates concentrations of the dissolved metals must be less than 2 mg/L and dissolved oxygen less than 1mg/L (PIRAMID 2003). Since acidic mine waters in Europe rarely meet these conditions, with dissolved metal concentrations often being in double figures the PIRAMID guidelines recommend a cautious approach to the implementation of these systems.

Oxic limestone drains (OLDs) are often simple open channels lined with a limestone bed. As with ALDs alkalinity is provided by the limestone with flow rates kept high enough that the majority of particulate ferric Fe formed in the channel remains in suspension until it reaches wetlands or settling lagoons. The oxic nature of the system inevitably results in armouring of the limestone bed, though this does not result in the clogging of channels as is seen with ALDs. Ziemkiewicz et al (1997) have shown that armoured limestone can continue to produce a surprising amount of alkalinity making OLDs a viable option in, for example, very remote locations where more sophisticated treatment methods may not be practicable.

2.4.3.2 Reducing Alkalinity Producing Systems (RAPS)

The first RAPS systems were developed as a result of the shortcomings of ALDs as they are not restricted to waters containing <2mg/L Fe(II) and <1mg/L O_2. The RAPS system comprises a compost layer which generates anoxic reducing conditions as seen in the compost wetlands and a limestone layer like that of the ALD (see Figure 2-6). Water first passes down through the compost layer where Fe(III) is converted to Fe(II) which then passes down through the anoxic limestone layer where alkalinity is generated. Dissolved oxygen is consumed in the compost layer greatly reducing the tendency for armouring of the underlying limestone compared to the case of the ALD. The combination of these two elements allows the RAPS greater flexibility in the range of acidic waters that it can treat compared to either the ALD or compost wetland alone. Younger et al (2002) suggest that it should be the preferred option wherever there is sufficient driving head of water and suitable topographical relief across a site. RAPS force all water that passes through them to contact both the compost and the limestone resulting in a smaller required footprint (potentially as little as 20% of the size) for water treatment than for compost wetlands (PIRAMID 2003).

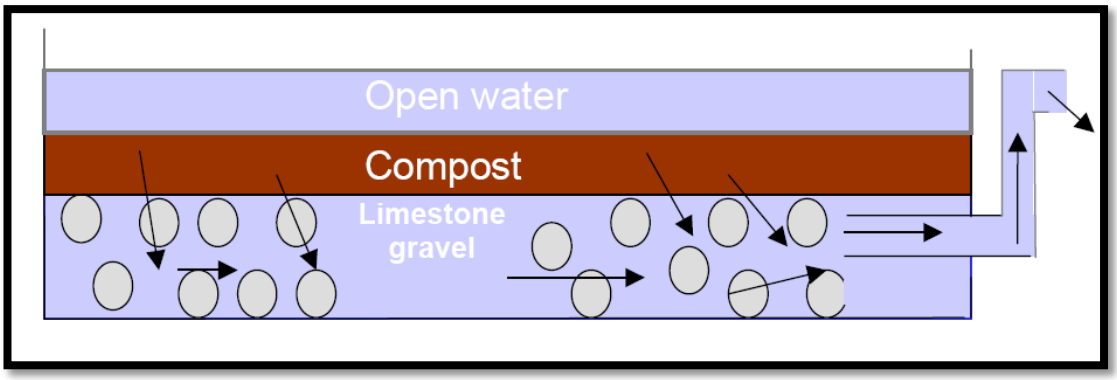

Figure 2-6 Simplified basic design concept for RAPS from Younger et al (2002)

Figure 2-7 Reducing Alkalinity Producing System (RAPS) at Tan-y-Garn, South Wales

2.4.3.3 Permeable reactive barriers (PRBs)

All of the systems discussed previously in this section deal with above ground point source discharges of polluted water. There are cases however where contaminated water may migrate via subsurface flow through aquifers resulting in diffuse pollution. Whether or not these aquifers are used to supply drinking water there can be serious ecological impacts just as for point source releases and *in situ* remediation techniques may be required. This can mean implementing a 'pump and treat' scheme whereby water is brought to the surface via a well or borehole for treatment. This option can be expensive to operate and does not fall within the criteria for passive treatment (Parker 2003). Permeable reactive barriers (PRBs) are simple in concept and offer a passive

alternative to 'pump and treat' schemes. A permeable barrier of geochemically suitable reactive material is placed across the flow path of the polluted water as illustrated in Figure 2-8.

In a similar way to RAPS the barrier serves to reduce acidity and remove dissolved metals from the water as it passes through. PRBs have been used worldwide to treat a number of different pollutants including uranium, chromium and organic substances. In these instances zero valent Fe (ZVI) has been successfully used to reduce pollutant concentrations by precipitating the metals or degrading the organic molecules (PIRAMID 2003). Whilst ZVI has proven effective in these niche applications, for the majority of acidic mine waters it would actually worsen the situation by liberating Fe into the surrounding water. Various PRB compositions have been investigated including that developed by Amos and Younger (2003) incorporating pea gravel, calcite chips, green waste compost and cattle slurry. Having passed though the PRB water should be net-alkaline and circumneutral pH allowing further treatment by one or more of the passive technologies described in (PIRAMID 2003).

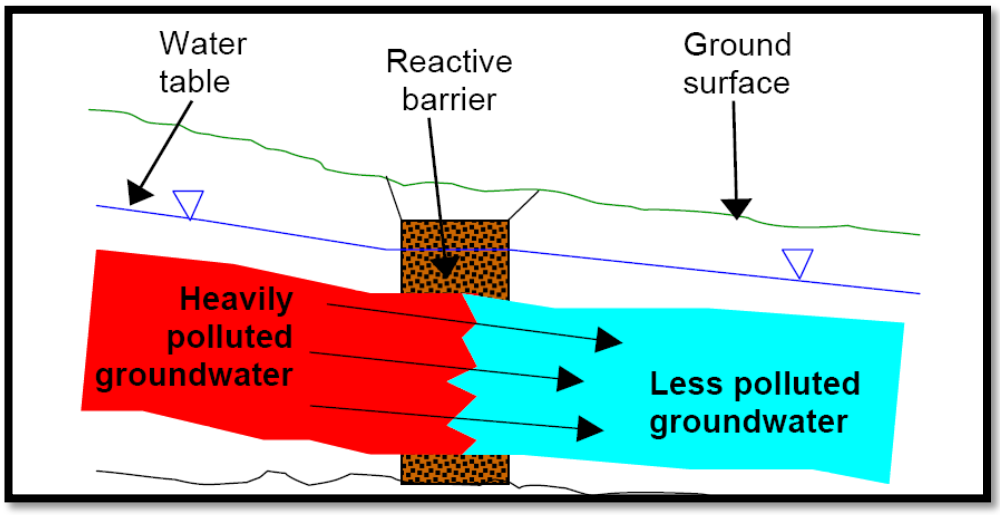

Figure 2-8 Simplified cross section of the basic concept design of a PRB (PIRAMID 2003)

2.4.4 Vertical flow systems

Vertical flow systems for the treatment of mine drainage have an advantage over horizontal flow systems such as settling lagoons in that their overall metal removal

rates are not limited by the settling velocity of HFO particulates. In addition to this, the build up of a layer of HFO solids on the bed of a vertical flow system can in itself act as a catalyst for further contaminant removal. Their major disadvantage however is blocking and significant reductions in flow rate over time (Barnes 2008)

2.4.4.1 Sand filters

Sand filtration has been used as a method of water purification since the beginning of the 19th century, and has been shown to be effective against numerous pollutants under widely differing circumstances**.** Slow sand filtration (see Figure 2-9) uses fine sand particles and can be described as an all-round treatment process incorporating "settlement, straining, filtration, organism removal….and to some extent [chemical] storage" (Huisman and Wood 1974). It is often used for treatment of drinking water due the fact that it effectively removes and/or destroys pathogenic bacteria as well as filtering particulate matter. The rate of downward flow of water is typically 0.1 - 0.4 m/h allowing the build up of a bacterial film known as the "schmutzdeke" which plays a crucial role in the water purification process.

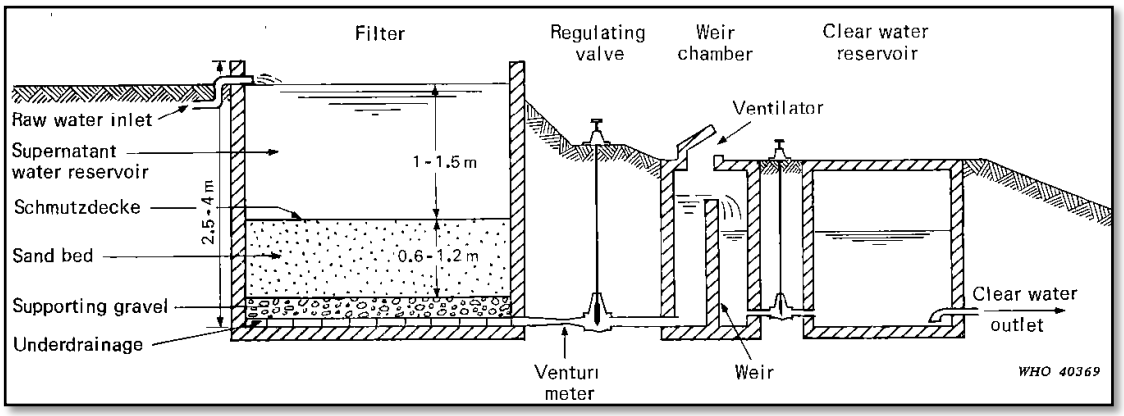

Figure 2-9 schematic diagram of a slow sand filter (Huisman and Wood 1974)

Rapid sand or "roughing" filters use coarser sand with grains up to 2mm in diameter. The increased grain size results in faster downward flow (around 20 times faster) of water and causes deposition of impurities deeper within the bed than for slow sand filters. They are therefore not as effective in removing impurities as slow sand filters and may be better used as one in a series of steps in the water treatment process.

It has been shown that in the case of Fe and Mn, deposition of the metal oxides is autocatalytic within the bed of a rapid sand filter. There is also evidence that microbial action, principally by *Gallionella ferruginea* plays an important role in reducing Fe concentration with biotic oxidation and removal rates being around 60 times faster than those achieved via the abiotic route (Sogaard et al. 2000).

Despite their potential for efficient Fe and Mn removal the rapid clogging of sand filters and hence the need for regular servicing makes them unsuitable for the large scale mine water treatment application considered in this study.

2.4.4.2 Surface-Catalysed Oxidation Of Ferrous Fe (SCOOFI) reactors

Surface-Catalysed Oxidation Of Ferrous Fe (SCOOFI) reactors as described by Jarvis and Younger (2001) and Younger et al (2002) are based on the principle that passing oxygenated mine water over high surface area media will stimulate HFO accretion. Once an initial HFO layer has formed on the surface of the media, ferrous Fe is adsorbed and rapidly oxidised via the heterogeneous mechanism. This has the potential to greatly increase rates of Fe removal compared to settlement lagoons and wetlands. One of the early examples of this type of system is described by Best and Aikman (1983) and uses a tank packed with brushwood to provide aeration and a surface for HFO accretion.

SCOOFI reactors can be subdivided into two types; saturated flow and unsaturated flow.

In the case of saturated flow reactors the mine water must already be well oxygenated and with Fe concentration <50 mg/L (PIRAMID 2003). They can be oriented either horizontally or vertically and thus do not necessarily require a significant hydraulic head. The intimate nature of the contact between the water and media in saturated systems results in greater Fe removal rates than for unsaturated systems.

Unsaturated flow reactors such as those trialled by Jarvis and Younger (2001) and Best and Aikman (1983) do not need to be preceded by an oxygenation facility since the nature of the flow through the reactor provides sufficient aeration. Though less efficient than saturated flow reactors they can also provide significant reductions in

both Fe and Mn concentrations. The main drawback with this type of reactor is the need for vertical alignment which limits its size according to the available hydraulic head.

As with settlement lagoons and wetlands, SCOOFI reactors are best suited to net-alkaline waters where the main objective is Fe removal, and an alkalinity producing system is not required.

2.4.4.3 The Vertical Flow Reactor

The original idea for the VFR as trialled previously (Barnes 2008) was based on observations at RAPS sites that a significant proportion of the Fe is removed on top of the system resulting in a layer of HFO that increases in thickness over time (see Figure 2-7). Given that RAPS systems are usually implemented to treat net-acid waters, this Fe removal prior to the alkalinity generating stage was not expected.

The VFR as constructed and trialled by Barnes (2008) (see Chapter 4, Section 4.9 for details) was found to have significantly increased Fe(II) removal properties compared to settling lagoons and wetlands with an average Fe(II) removal rate of 16 $g/m^2/day$. As with several of the other systems described here the VFR was successful in removing Mn and other trace metals as well as Fe. At the end of the trial, the sludge on the VFR bed was analysed and mixed valence Mn (II)/(III) oxides were found to be concentrated in several layers as black bands in the sludge. The mechanism for Fe(II) removal in this system was thought likely to be a combination of oxidation in the water column in the VFR reactor tank as well as heterogeneous catalysis within the HFO sludge.

2.5 Options for active treatment

Where the chemistry of the water, or a lack of space rule out passive treatment as an option then the dosing of mine drainage with chemicals such as lime, H_2O_2 and flocculants becomes necessary to increase Fe oxidation and removal rates. Once dosed with chemicals AMD may then be fed into passive settling lagoons or wetlands or HFO sludge may be dewatered using technology such as centrifuges, clarifiers and filter presses.

2.5.1 Chemical dosing

As discussed by Sapsford and Watson (2011) Fe removal from AMD can be separated into two stages, oxidation/precipitation and precipitate settling. In terms of increasing the rate of Fe removal there are therefore several categories of chemicals that could be added to reduce treatment time.

As discussed in Section 2.2 the rate of Fe(II) oxidation is highly pH dependent and so addition of basic substances such as lime that raise pH will dramatically increase the oxidation rate. As an alternative, or in addition to alkali dosing H_2O_2 may be added to further increase the rate of Fe oxidation (Johnson and Hallberg 2005). One example of this is at the Six Bells site in South Wales where sizing constraints on settling lagoons resulted in the decision being taken to does with H_2O_2 to reduce the overall treatment time (Jarvis et al. 2003).

Once oxidised the rate of removal of HFO particulates can be increased by the use of flocculants which bind the finely dispersed particles together into denser flocs increasing settling rate and increasing the ease of dewatering. Flocculants are used at the Dawdon site (see chapter 3) and a sample of AMD taken post flocculant dosing can be seen in Figure 2-10. Upon sample collection the HFO flocs had been uniformly distributed throughout the measuring cylinder and had been left to settle for just less than 1 minute at the point at which the photograph was taken.

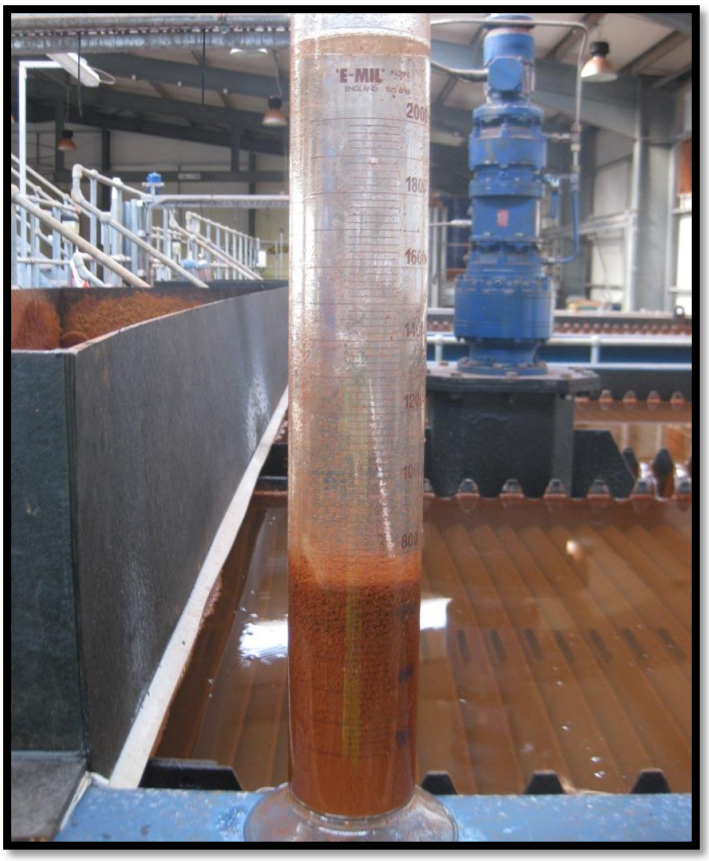

Figure 2-10 Settling of HFO particulates after flocculant dosing at Dawdon

2.5.2 Recirculation of HFO solids

A picture of one of the HFO recirculation tanks at the Dawdon mine water treatment scheme in the north of England can be seen in Figure 2-11. The recirculation of HFO particulates produces a final sludge that has a higher solids content than would be achieved simply by allowing HFO precipitates formed in the water column to settle naturally. The sludge by this recirculation process therefore has improved settling and dewatering properties (Dey et al. 2009) make disposal easier and less costly.

Figure 2-11 Sludge recirculation at the Dawdon mine water treatment plant

2.5.3 Clarification and mechanical sludge dewatering

Where space for treatment is very limited even relatively small settling lagoons and wetlands may not be an option. In this case the use of clarifiers may be required initially to concentrate HFO flocs, followed by a further dewatering stage such as centrifugation or a belt press. At the Dawdon treatment site (and previously the Ynysarwed treatment site, see Chapter 3) lamellar plate clarifiers are used to increase the rate of solids settling (see Figure 2-12). Water flows upwards through the clarifiers, and particulates are trapped out by inclined plates and settle to the bottom where they can be collected for further dewatering (Perry 1997).

Sludge that has been collected from the clarifiers is then transferred to a filter press as shown in Figure 2-13 where the water is literally squeezed out of it leaving a much denser solid with a texture similar to that of clay (Figure 2-14). In some instances a

centrifuge may be chosen instead of a filter press for dewatering purposes as is the case at the Ynysarwed treatment scheme. The centrifuge uses the forces produced by rapid rotation to separate solids from water and tends to give a final product with higher moisture content than that from a filter press.

Figure 2-12 Clarifiers at Dawdon

Figure 2-13 Filter press for sludge dewatering at Dawdon

Figure 2-14 Dewatered sludge from filter press at Dawdon

2.6 Summary

This chapter has introduced the concept of acid mine drainage (AMD) and discussed both its formation and various passive and active options for its remediation. Ideas about acidity, alkalinity and carbonate chemistry have been discussed as well as the roles that these parameters have in defining the chemistry of an AMD discharge. Also included is a review of the literature concerning the oxidation of Fe(II) by dissolved oxygen giving consideration to both homogeneous and heterogeneous abiotic mechanisms as well as the contribution of microbial oxidation. The chapter can be summarised as follows

- Acid Mine Drainage is generated when sulphide bearing minerals are exposed to oxygen and water as a result of mining activities. When AMD is discharged from a mine it often results in the oxidation and precipitation of dissolved Fe smothering water courses. Where high metals concentrations are coupled with low pH aquatic ecosystems are often found to be significantly damaged.
- The rate of homogeneous Fe(II) oxidation is highly pH dependant. In the pH range 5-8 there is an inverse squared dependence on $[H^+]$, which drops to a linear dependence in the pH range 3-5 becoming pH independent below pH 3.
- The pH dependence of Fe(II) oxidation has been explained in terms of the concentrations of various hydrolysed and carbonate species which are rapidly oxidised with respect to free Fe(II).
- Fe(II) oxidation can be autocatalytic, with the reaction product Fe(III)(hydroxyl)oxide an effective catalyst for the heterogeneous oxidation pathway.
- Microbial oxidation of Fe(II) only dominates at low pH and or low O_2 availability.
- Carbonate chemistry dominates the pH of circumneutral AMD whether through carbonate alkalinity (or a lack thereof) or elevated levels of dissolved CO_2. The balance between carbonate alkalinity and the acidity generated during Fe(II) removal has a large role in determining the type of system used to treat a particular AMD discharge.

- High levels of dissolved CO_2 can depress the pH of AMD and thus retard the rate of Fe(II) oxidation. Aeration cascades that were initially installed to increase levels of dissolved O_2 are also likely to encourage CO_2 degassing.
- The remediation of circumneutral (primarily Fe bearing) AMD relies on systems that encourage the oxidation of Fe(II) and the subsequent precipitation of hydrated Fe(III) particulates. These systems may simply provide sufficient residence time for Fe removal processes to occur, or they may enhance the Fe(II) oxidation rate by (for example) dosing with alkali and raising pH.

3 Minewater treatment site descriptions

In total ten Coal Authority treatment sites were visited and investigated at various stages throughout this study. Four were located in England and six in Wales. There was a mixture of net acid and net alkaline as well as highly saline waters with widely varying flow rates and iron concentrations. As a result there was a variety of different treatment systems including wetlands, settling lagoons, chemicals dosing and mechanical sludge dewatering. The following chapter provides descriptions of the history, water chemistry and treatment schemes at each of the sites along with aerial photographs taken from Google Earth[1]. The chapter is divided into sections according to each of the sites visited as follows; Belnkinsopp, Cadley Hill, Dawdon, Lindsay, Morlais, Six Bells, Strafford, Taff Merthyr, Tan-y-Garn and Ynysarwed with a final section summarising the work carried out and important characteristics at each of the sites.

The sites in South Wales were chosen as they represented the range of chemistries of the iron bearing discharges arising from abandoned coal mines present in the region. Sites in England were chosen by the Coal Authority as being of particular interest with regards to assessing the potential for developing new passive treatment schemes or reducing the chemicals dosing at existing schemes.

[1] Blue arrows on photographs indicate direction of flow of water.

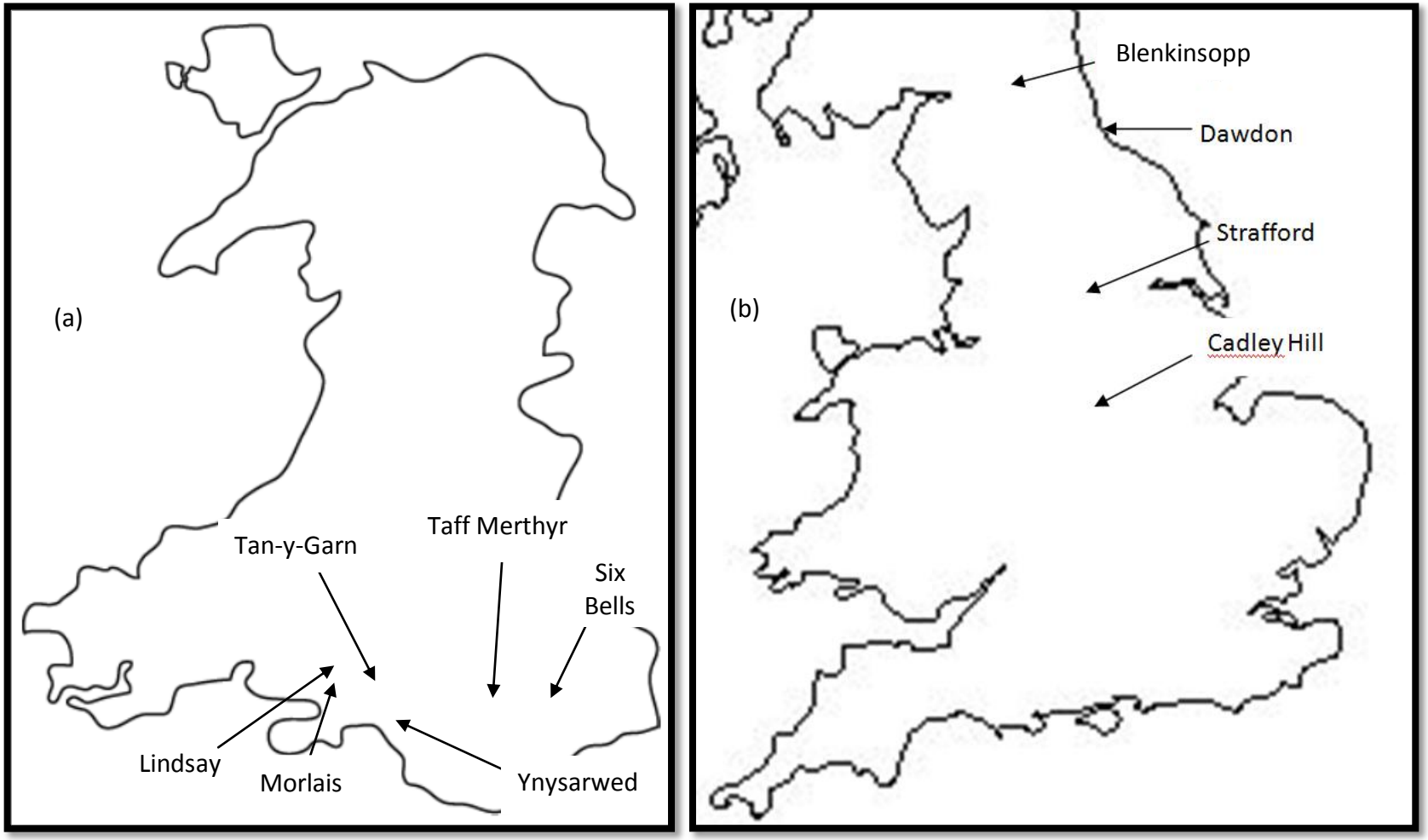

Figure 3-1: Location of mine water treatment sites visited during this study. (a) Wales, (b) England

3.1 Blenkinsopp

Site history: This site is situated approximately two miles from the town of Haltwhistle, half way between Newcastle and Carlisle in Northumberland (54°58'23 N, 2°31'07 W). The Blenkinsopp colliery was worked on and off from the early 1800's (and possibly before that) up until its final closure in 2002. Owing to the relatively recent planned closure of the site (8 years ago at the time of writing) a preventative treatment scheme was designed and commissioned in order to avoid pollution of nearby water courses. The concrete structures associated with the workings were demolished and the shaft treated with a grout curtain to ensure that the rising minewater reached the expected discharge point. Works were completed and the pump turned on in January 2005.

Water chemistry: Prior to the design and commissioning of the treatment scheme predictions of flow at Blenkinsop varied from 15 to 25 L/s with iron concentrations of around 100 mg/L expected for up to 11 years before settling down to 10-20 mg/L. In fact the first flush saw levels of 1000 mg/L of iron which to date have reduced to around 140mg/L. The water which was originally highly net acid is now borderline acid with mineral acidity and carbonate alkalinity almost perfectly balanced.

Site design: The scheme design included a pump in the shaft. This allowed a known constant flow of water through the system. The water is pumped at 15-25 L/s from 20m below the shaft top and passed initially through a Newton aerator which is a small metal box of roughly 2m x 1m x 1.2m that has been designed to naturally draw a maximum amount of oxygen into the water to begin the oxidation process. The construction work also included the refurbishment of two existing ponds and the creation of two reed beds. Additional works included the upgrading of a bridge to allow safe site access and the planting of a number of additional trees around the fenced settlement ponds.

During the ´first flush´ when the minewater water was expected to be at its most contaminated, a temporary dosing system was installed next to the distribution channel to kick start the treatment process. When the first flush settled down, the

temporary dosing kit was expected to be removed. Due to the higher levels of iron encountered, a more permanent dosing system has been employed to treat the minewater. A lime slurrey is added to the water up front of the distribution weir which results in the formation a bright blue $FeCO_3$ precipitate as can be see in Figure 3-2. As the alkali is diluted and the iron oxidises, precipitates and settles out and the blue colour fades leaving the water clear and colourless by the end of the reed beds.

Figure 3-2 Calcium carbonate dosing at Blenkinsopp showing blue $FeCO_3$

After aeration and chemical dosing the water flows into two parallel settling lagoons. Both lagoons then discharge into the first reed bed from where the water flows into a second reed bed and is then channelled into the neighbouring river. An aerial view of the site can be seen in Figure 3-3. Further details about the site can be found in Atkins (2006a and 2006b).

At the time of writing a temporary pilot scale high density sludge (HDS) plant was in operation on site which operated in several stages; aeration/CO_2 stripping, lime dosing, sludge recirculation, flocculent dosing and clarification.

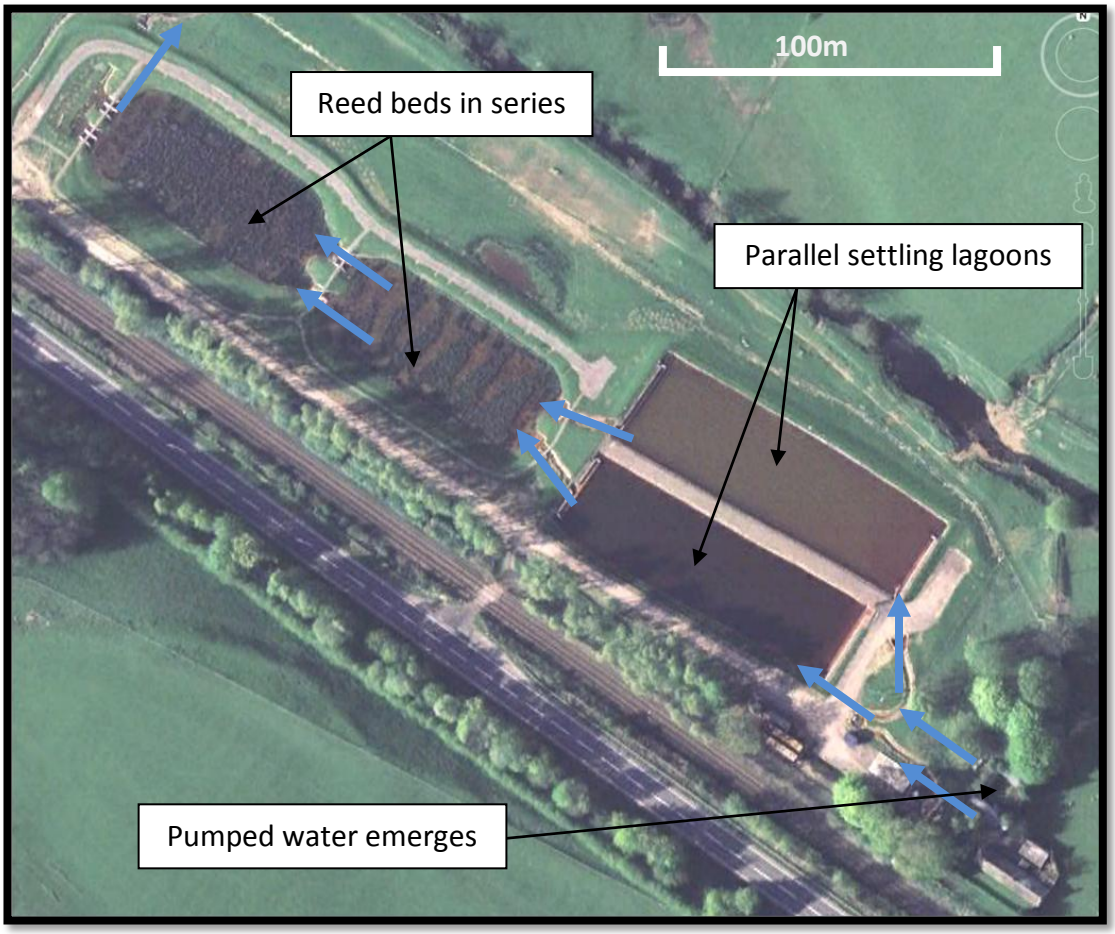

Figure 3-3 Aerial view of the Blenkinsopp mine water treatment scheme

3.2 Cadley Hill

Site history: The Cadley Hill mine situated near to the village of Swadlincote in South Derbyshire was one of a number of deep mines in the local area to be closed in the late 1980s. The site was connected to a number of other mines by various coal seams and being one of the lowest lying was predicted to be the site of an eventual outbreak of mine water. In recent years concerns have been raised about the infiltration of water from this site into an adjacent aquifer and as well as several surface discharges.

Water chemistry: The water is highly net alkaline and though levels of iron in the water are currently relatively low (≈ 20 mg/L) monitoring by the UK Coal Authority dating from 2009 suggests that water quality is worsening over time. As a result of local geology the water has a much higher salinity than would normally be expected for an inland mine water in the UK which means discharge of any effluent from a

treatment scheme for iron removal into the nearby Saltersford Brook is prohibited by the Environment Agency without prior salinity reduction.

Site Design: At the time of writing no permanent solution to the mine water problem has been found at the site. A pumping trial was carried out during the winter of 2009 where water was pumped to a temporary treatment scheme comprising dosing with H_2O_2 and flocculent to increase Fe(II) removal rates prior to discharge into a settling pond (see Figure 3-4 and Figure 3-5)

Figure 3-4: Premixing chamber for H_2O_2 and flocculent dosing at the Cadley Hill pumping trial

Figure 3-5: Settling pond at Cadley Hill pumping trial

3.3 Dawdon

Site history: The colliery at Dawdon, along with a number of others near the North East coast of England in County Durham was closed in the early 1990's. It became apparent shortly thereafter that flooding of the old workings would ultimately lead to contamination of the adjacent East Durham aquifer which provides around 20% of potable water supplies in the region. Figure 3-6 gives an outline of the area protected by pumping at Dawdon and a neighbouring mine water treatment site Horden. In total the aquifer covers 125km^2. A series of studies were conducted in order to determine the optimum combination of pumping sites that could house permanent treatment schemes and would not increase the risk of collapse in the old workings underground. Several abandoned mine sites in the area were considered and it was finally decided to set up the two pump and treat schemes at Horden and Dawdon. The treatment plant at Dawdon is now situated in an industrial park in the town of Seaham (54^{o}49'22 N 1^{o}19'54 W)

Figure 3-6: Area of East Durham aquifer protected by pumping at Dawdon and Horden[2]

[2] Blue area on the map shows the East Durham aquifer, red line marks out the area protected by pumping at Dawdon and Horden.

Water chemistry: The water is net alkaline at this site with initial Fe(II) concentration of around 66 mg/L. As a result of the local geology the water also has elevated salinity with respect to sodium chloride with recorded Cl^- concentrations up to 40,000 mg/L, approximately twice that of sea water. The water also contains high levels of dissolved CO_2 and can be seen to effervesce as it exits the pipe above ground.

Site design: Water at Dawdon is remediated via active treatment. The abstraction rate at the site is in the range 100 – 150 L/s. Water is transferred from the mine shaft to the treatment plant via an 850m pipeline. The heavy contamination and salinity of the mine water required a bespoke process design to be developed. The treatment occurs in a series of large reactor tanks (Figure 3-7 and Figure 3-8).

Figure 3-7: 1st stage reactor tanks for aeration at Dawdon

Initially there is an aeration stage followed by lime dosing. Recirculation of hydrated ferric oxide (HFO) solids between the treatment tanks results in the formation of high density sludge and further increases iron removal efficiency. Finally, the water is dosed with flocculent and passed through a lamellar plate clarifier with the overall process reducing the iron levels in the water to less than 1mg/L. The sludge from the clarifiers is then further dewatered with the use of a filter press and the treated effluent is discharged out to sea via twin outfalls. Further details about the treatment process can

be found in Chapter 2. Further information about the design and operation of the site can be found in Mott MacDonald (2009a and 2009b).

Figure 3-8: Sludge recirculation and lime dosing tank at Dawdon

3.4 Lindsay

Site history: The former Lindsay Drift mine site is situated at Capel Hendre near Ammanford, Carmarthenshire (51°46'41 N 4°02'36 W). The Lindsay Drift formed part of the Cwmgwili mine, which was abandoned in November 1996. Contractors on behalf of the Coal Authority subsequently sealed both the Cwmgwili and Lindsay mine entries in 1998. The emission of water was first observed at the Lindsay mine site in mid December 1999.

Water chemistry: The flow of water was reported as minimal and a sample taken at the time recorded total iron concentration of 2.5 mg/L. At that time no impact was observed on the Fferws Brook into which the water discharges via an underground pipe, which traverses the mine surface from the mine entrance. Further monitoring in January 2000 indicated that the flow of water from the mine had increased and a

water sample recorded a total iron of 98 mg/L. At the time of writing iron concentrations had reduced to around 16 mg/L and was highly net alkaline with pumped flows of around 20 L/s.

Site design: Water is pumped from a sump up to a distribution chamber elevated above two parallel settling lagoons. The water flows down aeration cascades to a distribution weir at the front of the lagoons. Water exits the lagoons and travels down a second aeration cascade before entering two parallel wetlands and finally passes through a third wetland before discharge to a nearby river. An aerial photograph of the site taken is shown in Figure 3-9. Further details about the site can be found in Parsons Brinkerhoff (2004a) and Scott Wilson (2004a).

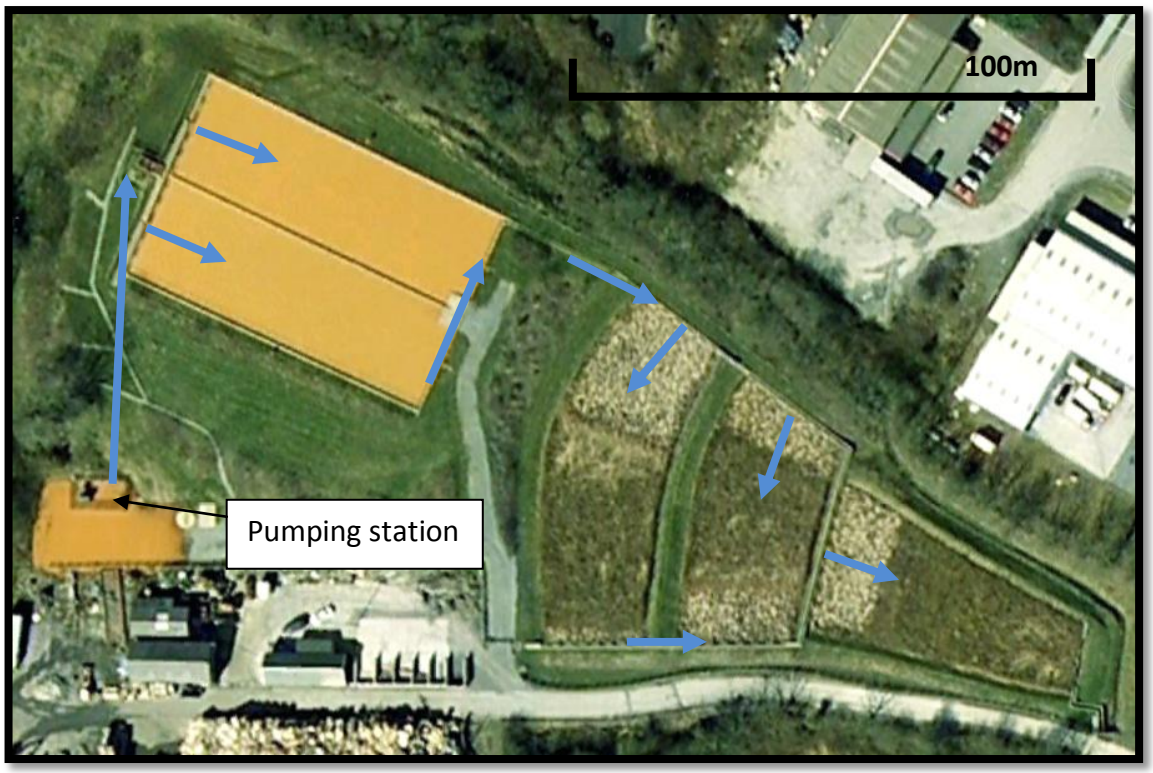

Figure 3-9: Aerial view of the Lindsay minewater treatment scheme[3]

[3] The orange staining around the pumping house in the photograph occurred as a result of damage to the pump and flooding of the surrounding low lying land.

3.5 Morlais

Site history: Since 1983, after the closure of the Morlais and Brynlliw Collieries minewater has been flowing from the Morlais shaft into the River Morlais, a watercourse which feeds the Loughor Estuary near Llanelli, South Wales (51°58'23 N 04°04'13 W). The Loughor Estuary which carries a SSSI (Site of Special Scientific Interest) status had been polluted by the high iron loadings of the minewater for many years. Since the minewater appeared at the Morlais Shaft, 400 tonnes of ochre (ferric hydroxide) had been deposited each year.

Water chemistry: The main problems at Morlais were the high flow rates (up to 298 L/s) coupled with high iron loadings (previously up to 53 mg/L) which varied seasonally. Aside from these two factors the water is net alkaline and would not be considered to have high salinity. At the time of writing the iron concentration at the site had decrease to around 10mg/L.

Site design: In summer 2002 work began on what was to be the biggest minewater treatment scheme the Authority had ever built. The scheme designed includes two settlement lagoons set in series which are 3.5m deep and have a combined area of 1.2 hectares and three large surface flow aerobic wetlands follow with a combined area of 3.1 hectares. This enables the scheme to have a combined retention time of 26 hours at average flows. The water initially flows over an aeration cascade into the lagoons, then through two parallel wetlands before finally recombining to flow through the third wetland (Figure 3-10). The land area acquired for the scheme was very flat and so the neck of the shaft from where the water was pumped was raised in order to provide sufficient head for an aeration cascade. The £1.2m civil engineering project was completed in early 2003, with the wetlands allowed to mature for 3 months before inundation with the minewater. The final landscaping of the scheme ensures that the site merges into the unique estuary setting. At the time of writing the first of the two settling lagoons was not in operation, but the site was still performing satisfactorily. Further details about the site can be found in Parsons Brinkerhoff (2004b) and Scott Wilson (2004b)

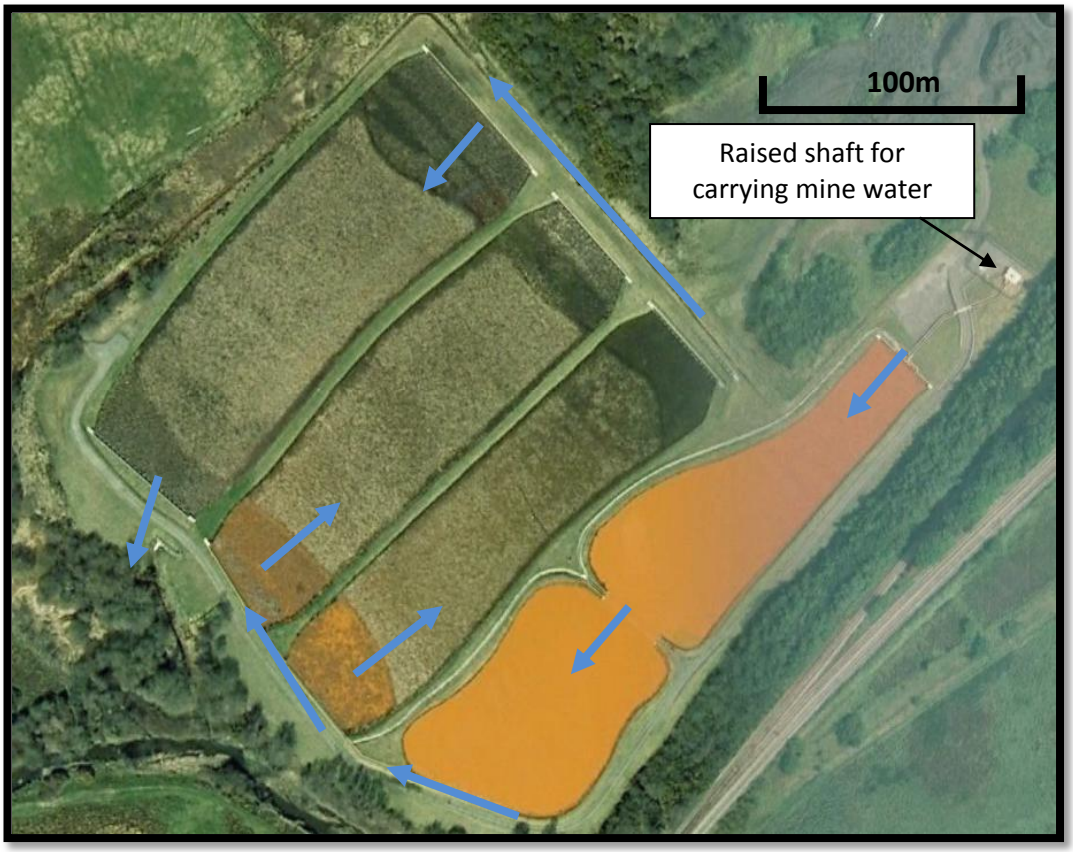

Figure 3-10: Aerial photograph of the Morlais mine water treatment scheme

3.6 Six Bells

Site History: During the 1970s all coal mined at Six Bells was brought to the surface via Marine colliery when the two pits were integrated. The pit was eventually closed in 1988. In 2001, the discharge at Six Bells was rated as a significant problem. The discharge first broke out in 1998 and the water was travelling into the Ebbw Fach, just to the south of Abertillery, South Wales near to where the treatment scheme is now situated (51°43'31 N 03°07'56 W). In 1999 IMC Consulting Engineers Ltd prepared a feasibility study to evaluate the situation at Six Bells. It was concluded that a borehole would need to be placed into the old workings to intercept the polluted minewater and pump it to the surface. The borehole was driven 216m into the workings at a point where an underground roadway intercepted the disused workings.

Water Chemistry: The minewater at Six Bells is highly net alkaline and is a deep discharge from the Vivian shaft. The water is pumped at a rate of approximately 40 L/s. The Iron concentration for the water at Six Bells is currently approximately 18 mg/L.

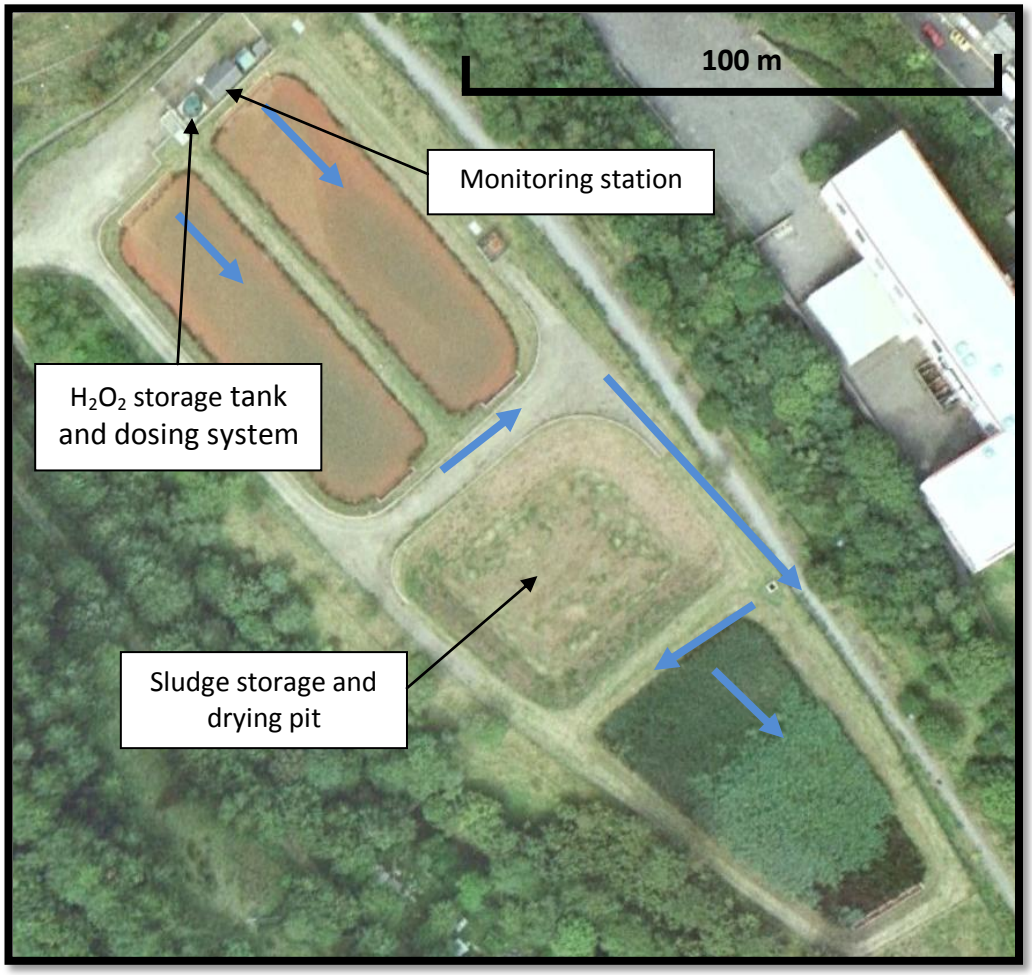

Figure 3-11: Aerial photograph of the Six Bells minewater treatment scheme

Site Design: Mine water is pumped via a borehole with flows of approximately 40 L/sec into a hydrogen peroxide aeration system, and then into two settlement lagoons measuring 1540m^2 each (see Figure 3-11). From here the water flows into a tertiary wetland area before being released into the Ebbw Fach (see Figure 3-11). Pumping commenced in January 2002, and initially the water was found to contain 250mg/L which was treated by caustic soda dosing. After a period of four months the Fe concentration in the water had reduced to the expected 45mg/L (at which point

caustic soda dosing was no longer required) though dosing with hydrogen peroxide continues. The original discharge has now dried up and pumping is ongoing to maintain the water levels in the workings.

3.7 Strafford

Site history: Historically the Strafford site was used as a pumping station operated by the National Coal Board (NCB)/British Coal used to protect deeper mines in the Barnsley area from flooding. Upon closure of those mines in the 1980's/1990's, pumping was no longer needed at Strafford and was discontinued. Subsequently, monitoring by the Coal Authority identified rising mine water levels which ultimately resulted in an uncontrolled AMD discharge that had a significant impact on the local Stainborough Dyke, and a continuing rise in water levels threatened to pollute the nearby Worsborough Reservoir. It was therefore decided to resume pumping and install a passive treatment scheme at the site.

Water chemistry: The water at the site is net alkaline with Fe(II) concentration <10mg/L and a flow rate of 20-30 L/s, thus the overall size of the scheme required is much smaller than for many of the other sites described in this chapter.

Site description: Water is pumped to a distribution chamber at the top of a set of aeration cascades. The water flows from here into a settling lagoon and finally into a constructed wetland. A phased approach has been taken to the construction of the treatment scheme and has made provision for future expansion, in the event that flow rates increase as water levels in surrounding mine workings recover. A landscaped area has also been constructed next to the reed-bed and provides a public space adjacent to the Trans Pennine Trail, as well as a new wildlife habitat. Figure 3-12 shows an aerial photograph of the scheme during the construction phase. The pond on the right of the photograph was subsequently planted with wetland plants.

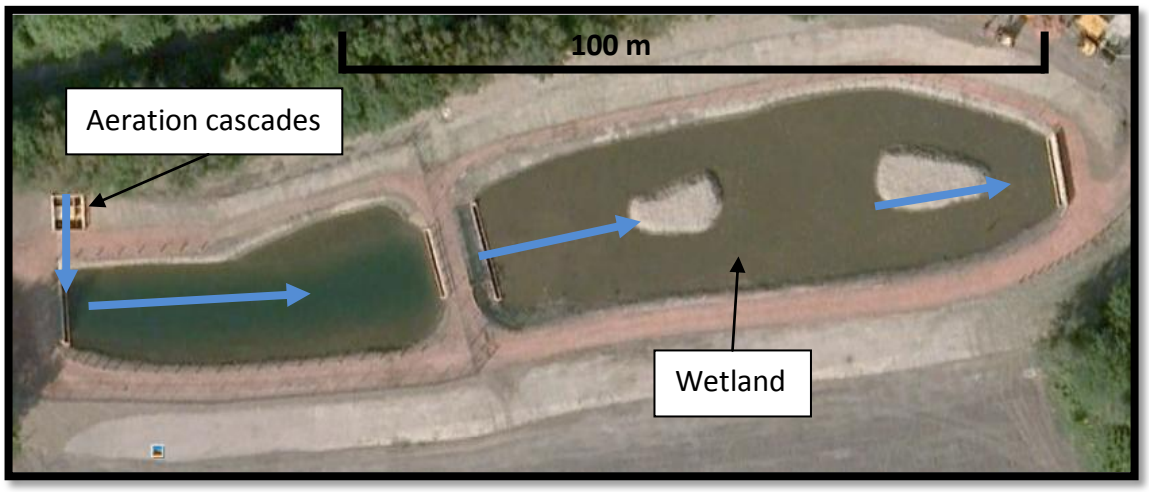

Figure 3-12: Aerial view of the mine water treatment scheme at Strafford

3.8 Taff Merthyr

Site History: The minewater scheme at Taff Merthyr (51°41'00 N 03°17'54 W) sits within the wider reclamation area of three former collieries: Taff Merthyr, Deep Navigation and Trelewis. All three mines were closed in 1990. Shortly afterwards a discharge appeared from the shaft of the Taff Merthyr Colliery resulting in pollution of a 3km stretch of the Bargoed Taff River. High flow rates placed the discharges high on the Environment Agency priority list, in light of the potential seriousness of the environmental impact. In addition to this it was thought that the remediation scheme could also bring major social and economic benefits to local communities.

Water chemistry: The minewater at Taff Merthyr is net alkaline and is arising from the Taff Merthyr colliery, which was the most recent deep mine closure in South Wales. The discharge has a total flow in the region of 60 L/sec which is a combination of flows from two different shafts. Sampling conducted in 2000 showed 2.2 mg/L Fe in the water discharging from the South shaft and 14 mg/L Fe from the North shaft. The combined raw minewater has total dissolved Fe in the region of 7.7 mg/L Fe.

Figure 3-13: Aerial view of the mine water treatment scheme at Taff Merthyr[4]

[4] Distribution chamber circled in red

Site Design: The treatment scheme designed and built at Taff Merthyr is one of the largest in the UK. It comprises aeration cascades and 4 settling lagoons as well as sixteen wetlands cells with a combined area of 1.8ha. The total area of the scheme is approximately 3ha. Water is pumped from an underground sump up to a distribution chamber (circled in red on Figure 3-13) where the flow is split between the 4 settling lagoons. At the end of the steeling lagoons the water then takes various pathways through the wetlands before discharge to the Bargoed Taff River. The scheme has been designed to form an integral part of a surrounding country park and contains a bridleway and cycle track connecting the north and south parts of the park. Further information about the treatment scheme can be found in Scott Wilson (2006a and 2006b).

3.9 Tan-y-Garn

Site history: Tan-y-Garn Colliery Ltd ceased trading in 1990. The mine was situated near to the village of Garnswllt in Carmarthenshire adjacent to the River Cathon. Work at the Tan-y-Garn treatment scheme (51^{o}46'10 N 03^{o}59'08 W) was begun in January 2006, in response to an AMD discharge polluting the nearby river.

Water chemistry: The water at the site is net acidic with low alkalinity compared to all other sites in this study of around 50-60 mg/L. Flow rates are low, around 3 L/s with Fe(II) concentration of the order of 50 mg/L, though this varies with periods of high and low rainfall.

Site design: Tan-y-Garn was an experimental site trialling the relatively new technology of a Reducing Alkalinity Producing System or RAPS which was the first of its kind commissioned by the Coal Authority. The RAPS is gravity fed and is arranged as a vertical flow system, where influent water percolates through a combined compost/limestone layer within a lagoon, followed by a series of 3 settling ponds and a wetland and finally into the River Cathon. Since the mine water is net acidic, the limestone in the RAPS serves to increase pH and alkalinity which in turn accelerates

iron oxidation and precipitation rates allowing treatment without the addition of chemicals. A more detailed description of the RAPS is given in Chapter 2. Further information about the treatment scheme can be found in Atkins (2006c and 2006d)

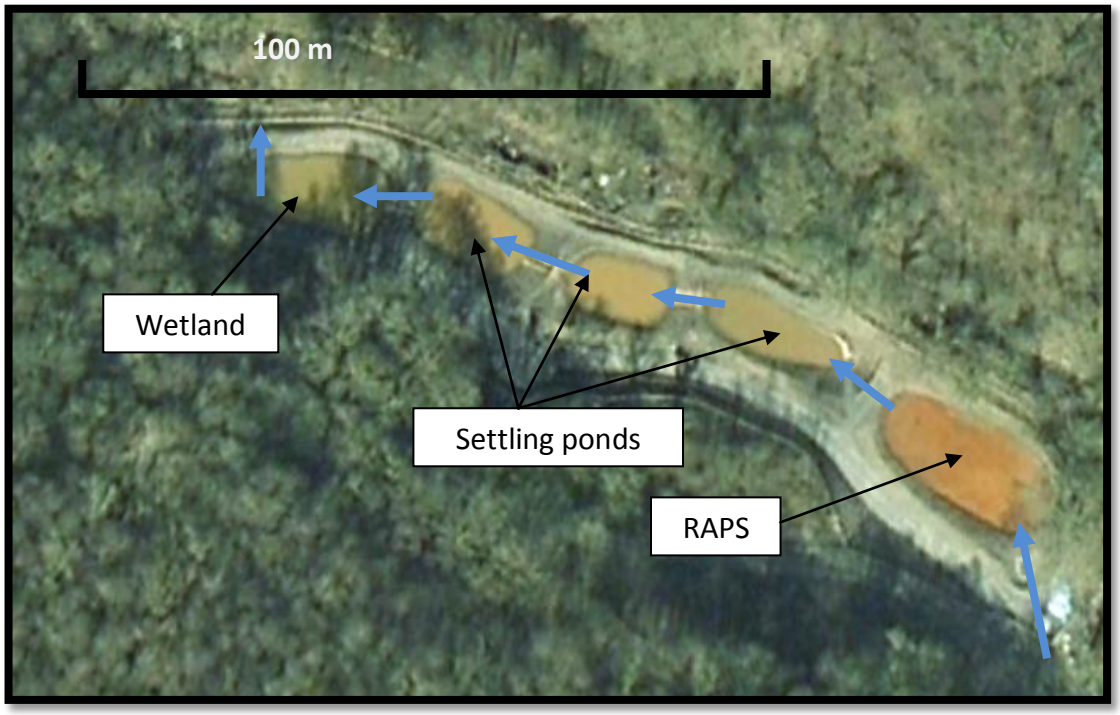

Figure 3-14: Aerial photograph of the mine water treatment site at Tan-y-Garn[5]

3.10 Ynysarwed

Site History: The polluting discharge at this site is associated with the Lower Ynysarwed Mine and flows from the Ynysarwed adit near Neath in South Wales (51°42'05 N 03°43'32 W). There has been an AMD discharge at this site for a number of years, but flow increased substantially and the quality worsened in spring 1993 requiring urgent remediation. The discharged affected a 12km length of the Neath Canal, a popular recreational waterway.

[5] Picture taken prior to planting of the reed bed.

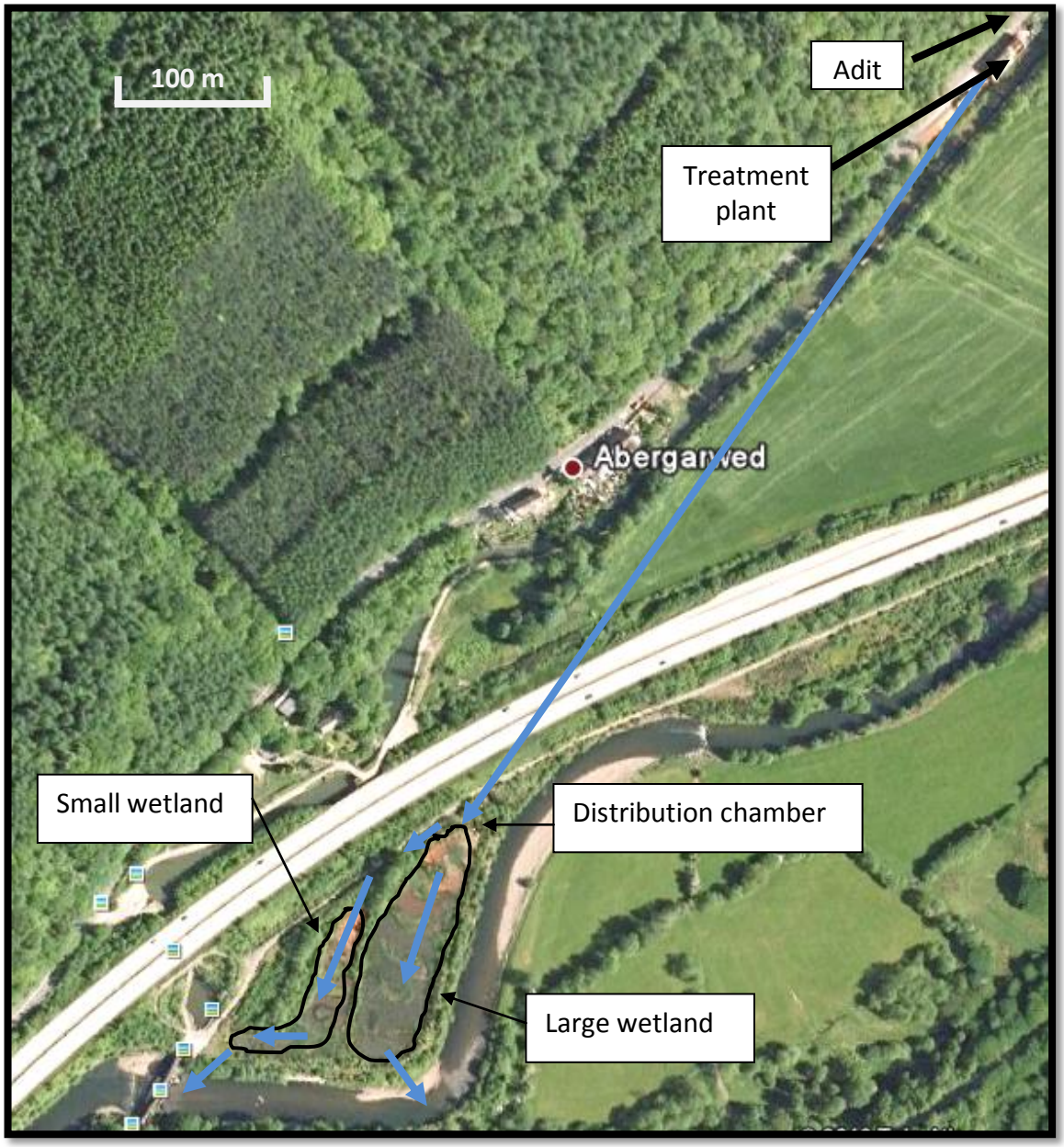

Figure 3-15: Arial photograph of the mine water treatment scheme at Ynysarwed

Water Chemistry: The flow from the Ynysarwed adit is net acidic. Historically this has resulted in pH levels as low as 3.5 following iron oxidation, though the relative acidity of the water is decreasing over time as iron concentrations decrease. Peak flows of 36 L/sec were discharged with over 400mg/L Fe in summer 1994. By early 2000 the Fe(II) concentrations had reduced to 150 mg/L with a further reduction to around 30 mg/L expected over the next 20 years.

Site Design : Given the initially high iron levels and associated acidity a combination of active and passive treatment was installed with lime and flocculent dosing as the first treatment stages. The water was then passed through lamellar plate clarifiers to remove any precipitates before flowing through parallel settling lagoons for final polishing and discharge to the River Neath. Due to the constraints involved with acquiring land the site is split with the active treatment plant approximately 0.5 km north east of the wetlands (see Figure 3-15).

The design of the treatment scheme took into account the long term predicted decline in Iron concentration in the minewater discharge from its peak of 400 mg/l to 30mg/l. At the time of writing dissolved Fe(II) levels had fallen to around 80 mg/L and lime dosing had ceased with the wetlands removing all of the iron by passive means.

3.11 Summary of site characteristics and work carried out

Table 3-1 provides a summary of the size, flow rate, total Fe and alkalinity data for each of the sites described in the previous sections. Values should be taken as indicative only as variations in all flow rate and water quality parameters can occur in response to weather events and the data only represent the conditions during the period of this study. Size and flow rate data have not been supplied for the Cadley Hill site as at the time of writing the pumping test is no longer in operation and a permanent treatment system has not been installed. It can be seen that all of the parameters differ by an order of magnitude or more across the sites studied reflecting the variation in both the contaminant loading and volumes of ferruginous mine water discharges through the UK. Methods used in the determination of Fe concentrations and Alkalinity are detailed in Chapter 4. Flow rate data was provided by the Coal Authority. Details about each of the sets of experiments conducted are contained within Chapter 4. Results and discussion for the Vertical Flow Reactor experiments, Fe(II) oxidation rates and CO_2 degassing are contained within Chapters 5, 6 and 7 respectively.

Table 3-1 Summary of key parameters for mine water treatment schemes

Site name	Size (m^2)	Flow rate (L/s)	Total Fe in (mg/L)	Alkalinity (mg/L $CaCO_3$ equivalent)	Experiments conducted
Blenkinsopp	9,100	15-25	140	264	CO_2 degassing
Cadley Hill	N/A	N/A	27	741	Fe(II) oxidation rates
Dawdon	Active	100-150	70	478	CO_2 degassing
Lindsay	6,000	20	16	251	Fe(II) oxidation rates
Morlais	31,000	≤298	10	283	Fe(II) oxidation rates
Six Bells	4300	40	18	215	CO_2 degassing
Strafford	1,200	20-30	5	520	Aeration cascade testing
Taff Merthyr	13,000	60	6	238	Fe(II) oxidation rates Vertical Flow Rector
Tan-y-Garn	830	3	40	73	CO_2 degassing Fe(II) oxidation rates
Ynysarwed	7,300	16	80	125	CO_2 degassing Fe(II) oxidation rates Vertical Flow Reactor

4 Methods

This chapter describes all of the methods used in the collection and generation of data for this thesis. It includes both experimental work and numerical and geochemical modelling. Experimental work for both rates of Fe(II) oxidation and CO_2 degassing was conducted in a batch reactor in the field. The resulting data were then processed and analysed using spreadsheet based and PHREEQCi (geochemical) models in order to determine the rate constants and other relevant parameters for the reactions under investigation. The work carried out on rates of Fe(II) oxidation was split into two main categories, homogeneous and heterogeneous oxidation. Similarly the investigations into CO_2 degassing were also separated into two categories based around aeration cascade testing and batch-wise degassing experiments. In addition to these experiments the work investigating the use of a Vertical Flow Reactor (VFR) (as developed by Barnes 2008) was repeated and extended to include mine waters with different chemistries. The chapter can therefore be divided into six main categories:

4.1 – 4.4 General techniques and equipment

These sections introduce the general experimental and numerical/geochemical modelling techniques that were used throughout this study. They include details of the analytical equipment and methods and tools for chemical analysis used in the

determination of various aqueous ionic species. They also provide a brief introduction to the geochemical modelling software PHREEQCi.

4.5 Homogeneous oxidation rates

This section covers all of the experimental procedures and experimental set up for the homogeneous oxidation experiments. It also gives details of the numerical model used for data analysis and the calculation of k_1 the rate constant for homogeneous Fe(II)oxidation.

4.6 Heterogeneous oxidation rates

The differences between the experimental procedures used in these experiments compared to the homogeneous oxidation experiments are explained. This section also explains how the model used to calculate k_1 was adapted and further developed for the calculation of k_2 the rate constant for heterogeneous oxidation.

4.7 Aeration cascade testing

A description together with schematic diagrams and photographs of the various aeration cascade designs that were tested are shown. In addition to this the sampling and monitoring regimes at the site are discussed.

4.8 CO_2 degassing

This section describes the experimental set up and procedures used in the batch-wise degassing experiment. It also discusses the various numerical and geochemical models that were used in the analysis of the data collected during the experiments.

4.9 The Vertical Flow Reactor (VFR)

This section describes the design and setup of the VFR at the Taff Merthyr site as well as the monitoring and testing regime that was implemented while it was running. Descriptions of the procedures used in the analysis of sludge samples from the VFR bed are also given. Additionally, work carried out in the development of a second VFR at the Ynysarwed treatment site is described.

4.1 Chemicals and equipment

All chemicals, 2'2-bipyridyl, acetic acid, ammonium acetate, HCl, H_2SO_4, HNO_3, $K_2Cr_2O_7$, $FeSO_4.7H_2O$, H_2O_2, 1,10-phenanthroline were analytical grade from Fisher Scientific and were used as received. High purity 18 MΩ deionised water was used for the preparation of solutions in the laboratory. All syringe filters used were 0.8/0.2µm Acrodisc PF syringe filters with Supor membrane. All field measurements of pH, dissolved oxygen and temperature were carried out using Hanna combination meters HI-9828 which were set to log data every 10 seconds during oxidation and degassing experiments. Specifications for each of the measurements are given in Table 4-1 as listed by the manufacturer. Both meters were calibrated according to manufacturer's instructions on site daily prior to experimentation. A 2 point calibration was carried out for pH using buffers at pH 4.01 and pH 7.01. DO was calibrated using the HI 9828-25 quick calibration solution designed for use in the field and air. The meter is factory calibrated for temperature. Since it is not possible to conduct accurate calibrations of temperature in the field the temperature was not calibrated prior to experimentation.

Table 4-1 Technical Specifications for Hanna combination meters HI-9828

	pH	Temperature	DO
Range	0.00 to 14.00	-5.00 to 55.00 °C	0.00 to 50.00 mg/L
Resolution	0.01	0.01 °C	0.01 mg/L
Accuracy	± 0.02	± 0.15 °C	0.00 to 30.00 mg/L ± 1.5 % of reading or 0.10 mg/L whichever is greater

In an attempt to better define the accuracy of pH measurement during the experiments the meters were always used in pairs and average values used in calculations. Despite regular calibration, the readings on the two meters could differ by as much as +/- 0.4 pH units (though a difference of +/- 0.04 to 0.1 was more usual). This was attributed to both the age of the pH probes and the build up of a film of HFO on the surface of the probes which interfered with accurate pH measurement. In order to reduce this effect to a minimum all probes were replaced at least once during the two year period over which experiments were conducted and probes were regularly

cleaned by standing in a solution of ammonium oxalate and oxalic acid which stripped HFO by complexing and re-dissolving Fe(III).

4.2 Geochemical modelling with PHREEQCi

All geochemical modelling was carried out using the PHREEQCi programme (Parkhurst and Appelo, 1999) with PHREEQC.dat database downloaded from the United States Geological Survey (2009). Various parameters were input for the different experiments which will be discussed in more detail in the following sections. PHREEQCi is a computer programme that can be used to simulate chemical reactions and transport processes in natural waters. It is based on the equilibrium chemistry between minerals, gases and sorption surfaces and the aqueous solutions in contact with them. The programme can be used to model kinetically controlled reactions. One of the major limitations of the programme is that it uses Debye Hückel expressions to account for the non-ideality of aqueous solutions. In practice this means that the model is adequate for solutions of low ionic strength, but becomes increasingly unreliable at ionic strengths approaching that of seawater. With the exception of Cadley Hill (see Chapter 3) all of the waters modelled using PHREEQCi in this study would be considered to have low ionic strength relative to sea water.

4.3 Determination of Fe concentration

Two separate methods were used in the determination of Fe concentration in the samples collected. The spectrophotometric method determined Fe(II) by complexation with 2,2' bipyridyl and the ICP-OES determined total Fe and dissolved (operationally defined) Fe passing through a through a 0.2 µM filter. Where possible all samples were analysed the same day as collection. Where this was not possible samples were stored in a fridge over night at 5^{o}C and analysed the following day. The main contributors to Fe(II) oxidation are chemical (homogeneous and heterogeneous)and bacterial (see Chapter 2). At pH<5 (true of acidified samples), and for the range of concentrations of Fe(II) in the waters studied here homogeneous oxidation rates are < 4 x 10^{-3} mg/L/day (based on values for k_1 from Davison and Seed (1983)). Filtration (0.2

µM) removes HFO and bacteria so the contribution from heterogeneous and bacterial oxidation should be negligible. Storing in the fridge (low temperature and dark) further reduces the rates of Fe(II) oxidation. It was therefore felt that the risk of sample degradation overnight (to the extent that it would influence the experimental outcome) was extremely low. Since ICP-OES does not speciate Fe, overnight storage should have no bearing on the outcome of this analysis in any case.

4.3.1 Spectrophotometric method

Fe(II) concentration in samples collected during oxidation experiments was measured spectrophotometrically using 2'2-bipyridyl as the complexing agent. A solution of 2'2-bipyridyl was prepared by dissolving 2 g of the solid in 100 mL of 0.2M HCl. 2 mL samples of aqueous Fe(II) (previously acidified with HNO_3 to quench the oxidation reaction[††]) were added to 5 mL of ammonium acetate buffer (prepared according AWWA et al (1999)) containing 2 drops of the 2'2-bipyridyl solution. A 2 mL portion of the buffer containing the sample was then transferred to a 1.5 mL semi-micro cuvette. The absorbance at 520 nm was measured using a Hitachi U1900 spectrophotometer and compared to a calibration curve (see Appendix 2) determined against a solution of $FeSO_4$ standardised using a method adapted from a chemical oxygen demand test (AWWA et al (1999)) as used by Park and Dempsey (2005). Beer's Law was obeyed with Fe(II) concentration in the range 0.93-46.5 mg/L (values determined from dilutions of Fe(II) secondary standard). Where initial concentrations of Fe(II) were found to be greater than 46.5 mg/L the samples were diluted by 50% and the procedure for analysis was repeated. Further details of the calibration and precision and accuracy of the method are given below.

[††] HNO_3 for sample quenching was initially used in error. However, later sampling comparing the effect of quenching with HCl vs HNO_3 showed no significant difference in measured Fe(II) concentration. Furthermore Kinetic studies of the oxidation of Fe(II) by HNO_3 show that at the concentrations of HNO_3 in the samples collected in this study the rate of reaction would be too low to affect the results presented in this thesis (Epstein, I. R. et al. 1980. A kinetics study of the oxidation of iron(II) by nitric acid. *Journal of the American Chemical Society* 102(11), pp. 3751-3758.)

4.3.1.1 Preparation of Fe(II) secondary standard

All glassware was washed with 10% nitric acid followed by 18mΩ deionised water prior to use. An approximately 10 mg/L (179mM) Fe(II) solution was prepared by dissolving 49.752 g of Fe(II)$SO_4.7H_2O$ in 2.6 N H_2SO_4. The stock was stored in a fridge at 5^oC in a tightly capped brown glass bottle. The exclusion of light (brown glass and darkness inside the fridge) prevents photo redox effects and the low pH retards aerial oxidation of the Fe(II) The stock solution was then calibrated using $K_2Cr_2O_7$ as described in AWWA et al (1999). The procedure is outlined below

1. 3 x 25 mL solutions of the $K_2Cr_2O_7$ primary standard (41.69 mM) were added to 250 mL conical flasks using a 25 mL class B volumetric pipette.
2. Approximately 75 mL of deionised water followed by 30 mL of conc H_2SO_4 (pipetted in 10 mL aliquots) was then added, swirled and left to cool to room temperature in a fume cupboard.
3. The Fe(II) solution was diluted to 50% using 2.6 N H_2SO_4 by pipetting 50 mL into a 100 mL class A volumetric flask and making up to the mark with the acid.
4. 3 drops of ferroin redox indicator were added to the cooled $K_2Cr_2O_7$ solutions (ferroin indicator was prepared according to AWWA et al (1999) by adding 1.485 g 1,10-phenanthroline monohydrate and 0.695 g Fe(II)$SO_4.7H_2O$ to 100 mL deionised water).
5. The $K_2Cr_2O_7$ solutions were then titrated with the 50% Fe(II) secondary standard through the orange/green transition ($Cr_2O_7^{2-}$ to Cr^{3+}) to the ferroin end point marked by a dark red colour.

4.3.1.2 Calibration of the spectrophotometer

The spectrophotometer was calibrated using a set of dilutions of the secondary Fe(II) standard. These were made from an initial 1 in 200 dilution which was then diluted by a further 10 %, 20 %, 30 %, 40%, 50 %, 70 %, 80 %, 95 %, 96 %, 97 % and 98 %. All dilutions were carried out using class A volumetric flasks and made up to the mark with 2.6 N H_2SO_4. All Fe(II) solutions were analysed by the method described at the beginning of Section 4.3.1. A calibration curve was produced and a linear relationship (R^2 = 0.9992) with absorbance was observed over the range 0.93-46.5 mg/L Fe(II). The

relationship is given in Equation 4-1 where [Fe(II)] is in mg/L and ABS_{520} is the absorbance of light at a 520 nm wavelength (using a 10 mm path length disposable polystyrene semi-micro cuvette). According to the manufacturer of the spectrophotometer, the photometric accuracy is +/- 0.002 ABS (0 – 0.5 ABS), +/- 0.004 ABS (0.5 – 1.0 ABS).

Equation 4-1

$$[\mathbf{Fe(II)}] = \mathbf{42.6} \times \mathbf{ABS_{520}}$$

The calibration procedure to obtain the relationship between [Fe(II)] and ABS_{520} was carried out once at the beginning of the experimental period (calibration data in Appendix 3). Calibration of the spectrophotometer against a blank was carried out immediately prior to the analysis of any mine water samples. The blank was prepared by adding several drops of 10 % HNO_3 to 10 mL of deionised water. The mixture was then treated in the same way as the mine water samples as described at the beginning of Section 4.3.1. The spectrophotometer was then calibrated such that the absorbance for the blank sample was taken to be zero.

The 2'2-bipyridyl indicator was chosen as it had been used for a number of years to distinguish between Fe(II) and Fe(III) in natural waters (Heaney and Davison 1977). It is also used in Iron Cell Tests for the Merck Spectroquant® Photometers and is advocated in the testing of ground and surface waters, industrial and waste waters and drinking waters containing up to 50 mg/L Fe(II) (www.merck-chemicals.com/photometry 2011).

Table 4-2 Concentrations of foreign substances in mg/L or % that interfere with 2,2' bipyridyl analysis

Al^{3+}	1000	**Cu^{2+}**	**10 (250[1])**	Ni^{2+}	250	**EDTA**	**2**
Ca^{2+}	1000	F^-	100	NO_2^-	100	Surfactants[2]	1 %
Cd^{2+}	1000	**Hg^{2+}**	**10**	Pb^{2+}	1000	NaCl	5 %
CN^-	50	Mg^{2+}	1000	PO_4^{3-}	50	$NaNO_3$	5 %
Co^{2+}	250	Mn^{2+}	1000	Polyphosphates	250	Na_2SO_4	5 %
Cr^{3+}	500	MoO_4^{2-}	1000	SiO_3^{2-}	1000		
$Cr_2O_7^{2-}$	250	NH_4^+	1000	Zn^{2+}	1000		

Table 4-2 is reproduced from the 2,2' bipyridyl Iron Cell Test (www.merck-chemicals.com/photometry 2011) instruction manual from Merck showing the levels at which other ions start to interfere with Fe(II) determination where Fe(II) is in the range 0-25 mg/L.

4.3.2 Inductively Coupled Plasma-Optical Emission Spectroscopy (ICP-OES)

10-15 mL samples of mine water were taken and acidified with 4 drops 20% HNO_3 to quench the oxidation reaction. Samples were normally taken in duplicate with one filtered through a 0.8/0.2 µm Supor syringe filter prior to acidification. Filtered samples were taken to be representative of Fe(II) concentration (i.e. colloidal Fe(III) was assumed to make a minimal contribution to total Fe concentration in filtered samples). Samples were then run on a Perkin Elmer Optima 2100DV ICP-OES with AS90 plus auto-sampler and a PC using WinLab 32 software. Prior to analysing each set of samples the ICP-OES was calibrated against a set of three standards prepared using commercially available 1000 mg/L standards. The three standards were chosen to cover the expected range of each sample e.g. [Fe] ≈ 40 mg/L, Standards chosen [Fe] = 0.5, 5, 50 mg/L. The standards were made by diluting by a factor of 10 from the highest standard. A blank containing 2% HNO_3 in deionised water was also used during the calibration. Standards were run during analysis between every 10 samples as unknowns to check calibration accuracy. The commercial standards used are certified as +/- 0.2 % of the stated concentration and dilutions are presumed to be accurate within +/- 10 %. There was some variation in the values of the standards run as unknowns during analysis, but the values were all within +/- 10% of the standard concentration, therefore this error should be used when interpreting results determined by ICP-OES analysis.

4.4 Determination of background chemistry

For the purposes of this thesis background chemistry is defined as any aspect of the chemistry of the water e.g. pH, acidity or dissolved species other than Fe(II)/(III) that may contribute to but is not necessarily directly involved in the rate of the Fe(II) oxidation reaction.

4.4.1 Alkalinity

Alkalinity was determined in the field using a Hach digital titrator with a 1.6N H_2SO_4 cartridge according to manufacturer's instructions. 100 mL samples of fresh mine water were taken and titrated using a bromocresol-green methyl-red indicator. The end point was determined as a colour change from green to pink. Titrations were carried out in duplicate and in triplicate where the first two readings differed by more than 5 mg/L $CaCO_3$ equivalent.

4.4.2 Acidity

A cold titration was carried out on freshly collected samples using a Hach digital titrator with a 1.6 N NaOH cartridge according to manufacturer's instructions. Samples were titrated to an end point of pH 8.4 measured using the pH module on a Hanna combination meter HI-9828. While phenolpthalene is the recommended indicator for this titration it was decided that the end point was impossible to determine visually due to interference from Fe(II) and Fe(III) precipitates. It should be noted that it was very difficult to get agreement between consecutive titrations as both CO_2 degassing and Fe(II) oxidation and precipitation occur on the same timescale as the titration.

4.4.3 Determination of net-acidity/alkalinity with "hot peroxide titration"

In order to overcome the difficulties encountered with the cold acidity titration an additional "hot titration" was carried out as described by AWWA (1999) to determine net-acidity/alkalinity. Initially 100 mL of fresh mine water was taken and titrated to pH

4 using a Hach digital titrator with a 1.6 N H_2SO_4 cartridge. Three drops of 30% H_2O_2 were then added. The sample was heated to boiling point and boiled for 2 minutes using a camping stove as shown in Figure 4-1. The sample was then allowed to cool before titration to pH 8.4 again using the Hach digital titrator, with a 1.6 N NaOH cartridge. Net-acidity or alkalinity was then determined according to the difference between the quantities of acid and alkali consumed during the procedure.

Figure 4-1 Experimental set up for hot peroxide titration

4.4.4 Chloride and Sulphate

Fresh mine water samples were collected for determination of chloride and sulphate. Samples were filtered using the 0.8/0.2 µm Supor syringe filters prior to analysis using a Dionex ICS-2000 Ion Chromatography System with Dionex Ionpac® AS11-HC column. Samples were loaded using a Dionex AS40 automated sampler and the system was controlled by a PC running Chromeleon software. After initially flushing the column with deionised water calibration was performed following the same procedure as for the ICP-OES using a set of three standards prepared using commercially available 1000 mg/L standards. Again the calibration standards were made by diluting by a factor of 10 from the highest standard and were chosen to cover the range of expected values

for the unknown samples. The column was flushed and calibrated immediately prior to analysis of each new set of samples.

4.4.5 Major cations

Fresh mine water samples were collected for determination of Ca, Na, K and Mg. Samples were filtered using the 0.8/0.2 µm Supor syringe filters and acidified with 4 drops 10% HNO_3. Samples were then run on a Perkin Elmer Optima 2100DV ICP-OES previously calibrated using standard solutions according to manufacturer's instructions. The calibration procedure followed for each of the different cations was the same as that described for Fe in Section 4.3.2.

4.5 Homogeneous Fe(II)oxidation rates

4.5.1 Experimental set up

Experiments were carried out at six mine water discharges; Lindsay, Morlais, Taff Merthyr, Tan-y-Garn and Ynysarwed in South Wales and Cadley Hill in England (see Chapter 3 for detailed site descriptions). At each site approximately 8 L of freshly emerged mine water was taken in a bucket and stirred and aerated using a Whale® Water Systems self venting submersible pump powered by a 12 V car battery as shown in Figure 4-2. The pH, temperature, and dissolved oxygen (DO) were measured using two hand held Hanna combination meters HI-9828 (see Section 4.2 for details). Measurements were logged every 10 seconds.

Figure 4-2 Experimental set up for homogeneous oxidation experiments

4.5.2 Sampling and Fe(II)analysis

15 mL samples of the mine water were taken at regular intervals during the field experiment and immediately filtered through syringe filters (Figure 4-3) and acidified

with 4 drops of 10% HNO_3 to quench the oxidation reaction. All samples were then analysed according the spectrophotometric procedure described in section 4.3.1.

Figure 4-3 Sampling during Fe(II) oxidation experiments

4.5.3 Numerical modelling

All of the logged data from the field experiments were input into Microsoft Excel along with the spectrophotometric measurements for dissolved Fe(II). Values for pH, DO and temperature were averaged over the readings from both of the logging Hanna combination meters HI-9828. A spreadsheet-based fourth-order Runge-Kutta (RK) method was employed in order to determine values for k_1 the rate constant for homogeneous Fe(II) oxidation based on the measured field data. This numerical method is often used to solve simple differential equations and is employed in its 5^{th} and 6^{th} order form to solve rate equations in PHREEQCi (Parkhurst and Appelo (1999)). All Runge-Kutta methods generate successive values for the concentration of the species under investigation over time. The ability of the method to accurately model the changes in a system depends on the length of the chosen time step between c_i and c_{i+1}. A more detailed discussion of the RK4 method and its application to chemical kinetics is given in Maeder and Neuhold (2007).

Incremental changes in Fe(II) concentration brought about by the homogeneous mechanism were calculated using Equation 4-2 , where c =concentration of Fe(II), h = time interval between t_i and t_{i+1} (in this case 10 seconds) and in the case of homogeneous oxidation x is calculated based on measurements of temperature, pH, DO and k_1 (Equation 4-3-Equation 4-6). ϑ is the temperature correction factor as described by Equation 4-7 where Tm = measured temperature, R = the gas constant and E_a = the activation energy for the oxidation reaction, in this case 96 kJ/mol (23kcal/mol) (Stumm and Morgan 1996) previously used by Kirby et al. (1999) and (2009).

Equation 4-2 $$c_{i+1} = c_i + \left[\frac{1}{6}(x_1 + 2x_2 + 2x_3 + x_4)\right] h$$

Equation 4-3 $$\boldsymbol{x_1 = (k_1/\vartheta)[Fe(II)]P_{O_2}[OH^-]^2}$$

Equation 4-4 $$x_2 = (k_1/\vartheta)([Fe(II)] + (5x_1))P_{O_2}[OH^-]^2$$

Equation 4-5 $$\boldsymbol{x_3 = (k_1/\vartheta)([Fe(II)] + (5x_2))P_{O_2}[OH^-]^2}$$

Equation 4-6 $$\boldsymbol{x_4 = (k_1/\vartheta)([Fe(II)] + (10x_3))P_{O_2}[OH^-]^2}$$

Equation 4-7 $$\vartheta = e^{[(1/Tm)-(1/298)](E_a/R)}$$

Once the spreadsheet had been set up an iterative least-squares method was employed using the Solver tool in Microsoft Excel to produce a value of k_1 that gave the best correlation between the changing concentration of Fe(II) measured during the experiments and the changes in concentration of Fe(II) predicted by the RK method (using initial Fe(II) concentration and logged values for temperature, pH and DO). All values for $[OH^-]$ were derived from pH measurements using a temperature corrected value for Kw (the dissociation constant for water).

4.5.4 Geochemical Modelling

Values for SO_4^{2-}, Cl^-, Fe^{2+}, Ca^{2+}, K^+, Mg^{2+}, Na^+, alkalinity, pH and temperature were input into PHREEQCi in order to determine the concentrations of the various ion pairs thought to affect the oxidation rate of Fe(II) in natural waters.

4.6 Heterogeneous oxidation rates

Experiments were carried out at the Tan-y-Garn mine water treatment site in South Wales. As with the homogeneous oxidation experiments approximately 8 L of freshly emerged mine water was taken in a bucket. The bucket had previously been calibrated in the laboratory using a 1 L measuring cylinder and the water level at 8 L marked on the inside of the bucket. HFO was collected from on top of the mine water treatment system (a Reducing Alkalinity Producing System) and partially dewatered by squeezing in a muslin cloth. The HFO on top of the treatment system is thought to have accumulated as a result of accretion via the heterogeneous oxidation mechanism. A more detailed explanation of this mechanism can be found in Chapter 2, a full description of RAPS and the Tan-y Garn site can be found in Chapters 2 and 3.

HFO solids were added to the freshly collected mine water in the bucket in order to commence the heterogeneous oxidation reaction. Owing to the fact that it was not possible to accurately determine the solids content of the HFO samples on site, a measured volume (one completely filled 30 mL sample pot) of the partially dewatered solid was added to the mine water in the bucket and an identical sample was taken for analysis in the lab. No attempt was made to determine the solids content of RAPS HFO. Only the partially dewatered HFO was used in the experiments and analysed in the lab. Solids concentration of the HFO was determined by weighing before and after drying in an oven at 120^{o}C for 48 hours. This was then used to calculate the HFO concentration in the mine water during the heterogeneous oxidation experiments.

Stirring and aeration using a hand whisk (to avoid clogging of the pump with HFO) were commenced immediately after addition of the HFO to the freshly emerged mine water. All parameters were logged as described in 4.5.1.

4.6.1 Sampling and Fe(II)analysis

1 mL samples of the mine water were taken at regular intervals and added directly to sample tubes containing 5 mL of the ammonium acetate buffer and 2 drops of 2’2-bipyridyl solution to quench the oxidation reaction. The Fe, 2’2-bipyridyl, buffer mixture was filtered using a 0.2 µM syringe filter. Samples were then analysed the

same day using the spectrophotometric analysis as described in Section 4.3.1. The Fe(II) 2'2-bipyridyl complex is highly stable. Studies have shown that over a 24 hour period no significant oxidation of Fe(II) occurs once complexed by 2'2-bipyridyl (Koenig and Johnson 1941) (the Merck Spectroquant® Iron Test Cells mentioned previously are also stated to be stable for at least 60 minutes once colour has developed showing the resistance of this form of complexed Fe(II) to oxidation). Thus it was decided that complexation with 2'2-bipyridyl was a suitable way to arrest the Fe(II) oxidation process.

There were several reasons for adopting the above method for quenching the oxidation reaction rather than using the same methodology as described for the homogeneous oxidation experiments (Section 4.5). Firstly, the increased solids concentration in these experiments resulted in the rapid build up of a filter cake on the syringe filters that slowed the rate at which the samples could be filtered. This meant that the time taken to filter the samples increased allowing for an increased time lag between sampling and quenching of the oxidation reaction. Perhaps more importantly however, the build up of a filter cake meant that the sample remaining in the syringe would be forced through a region of very high HFO concentration that might result in additional Fe(II) oxidation beyond that occurring in the bucket. Secondly, quenching of the chemical oxidation reaction by acidification but without filtration would still allow for bacterial oxidation of the sample. Since the time between sampling was short (30 s to 1 min) at the beginning of the reaction it was desired to keep the sampling procedure as simple as possible. Therefore it was finally decided to use the method of quenching with the 2'2-bipyridyl/buffer mixture with subsequent filtration.

4.6.2 Numerical modelling

Determination of k_2 was carried out by adapting the RK method used to calculate k_1. Equation 4-8 shows the new formula where x_{1a} to x_{4a} refer to the homogeneous reaction as described by Equations 4.2-4.7 and x_{1b} to x_{4b} refer to the heterogeneous reaction as described by Equation 4-9-Equation 4-12. The values for k_1 determined from the homogeneous oxidation runs were fed back into the equations to allow the calculation of k_2. The value used for the activation energy of the heterogeneous

reaction was 180 kJ/mol, as quoted by Dempsey et al (2002). As far as the author is aware at the time of writing this value for the activation energy has not been verified in the literature beyond its determination as part of a master's project (see Dempsey et al (2002)). Whilst there is then clearly a need for verification of the value for 180 kJ/mol it still provides a useful starting point for the determination of k_2.

Equation 4-8 $$c_{i+1} = c_i + \left[\frac{1}{6}(x_{1a} + 2x_{2a} + 2x_{3a} + x_{4a}) + \frac{1}{6}(x_{1b} + 2x_{2b} + 2x_{3b} + x_{4b})\right]h$$

Equation 4-9 $$x_{1b} = (k_2/T)[Fe(II)]P_{O_2}[OH^-][Fe(III)]$$

Equation 4-10 $$x_{2b} = (k_2/T)([Fe(II)] + (5x_{1b}))P_{O_2}[OH^-][Fe(III)]$$

Equation 4-11 $$x_{3b} = (k_2/T)([Fe(II)] + (5x_{2b}))P_{O_2}[OH^-][Fe(III)]$$

Equation 4-12 $$x_{4b} = (k_2/T)([Fe(II)] + (10x_{3b}))P_{O_2}[OH^-][Fe(III)]$$

4.7 Aeration cascade testing

Testing was carried out at the Strafford site (for a full site description see Chapter 3) where the aeration cascade is split into three sections. The two sections to the left were investigated in this study as they are of the same width and total height. The section to the right is narrower and used purely for gaining access to the top of the cascade. A picture of the aerations cascades is shown in Figure 4-4.

Figure 4-4 Aeration cascades at Strafford (full view)

Four Hanna combination meters HI-9828 were used to log pH, DO and temperature at the top and bottom of the aeration cascade. All of the meters were calibrated as described in Section 4.1 and were set to log readings every 10 seconds. The meters were used in pairs at the top and bottom of the cascade and swapped during the day so that each meter logged readings at both the top and bottom of the cascade for a minimum of two hours on each day. Readings for each of the logged parameters were then averaged over all four of the instruments to give the final results presented in

Chapter 5. Flow rates are continuously monitored and recorded at the pumping station on site. During the entire period studied the flow was within the range 29-30 L/s.

4.7.1 Aeration cascade configuration

At the beginning of each day wooden stop blocks were put in place so that the entire flow was diverted down one of the sections. Five configurations were tested in total. Each of the configurations are described and shown below. A schematic diagram showing the dimensions of each of the configurations tested is shown in Figure 4-4

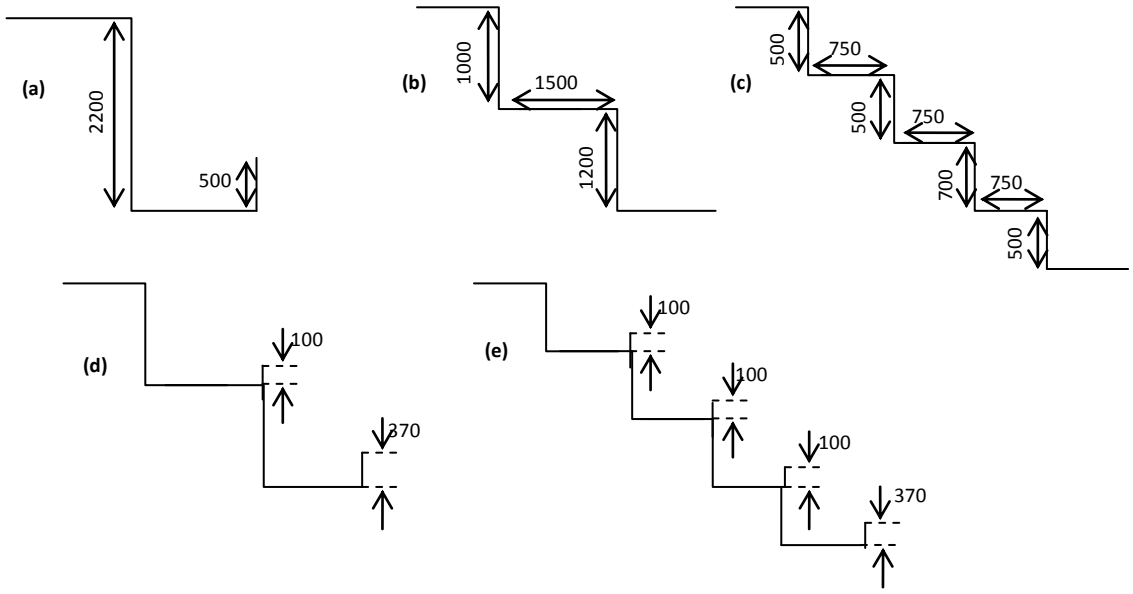

Figure 4-5 Schematic diagrams of aeration cascades at Strafford. Labels correspond to Figures 4-6 to 4-10

a. The central section was modified by placing a board across the entire width and length of the cascade resulting in one long drop into a plunge pool below. The plunge pool was created by placing stop blocks in the channel at the bottom of the cascade raising the water level. The volume of the plunge pool was calculated to be 2.34m^3, giving a residence time of approximately 1min 19s (flow rate recorded as 29-30 L/s throughout the experiment).

Figure 4-6 Configuration (a) single drop into plunge pool

b. All of the flow was diverted down the two steps in the central section. No weir boards were used. The collection channel at the bottom the cascade was unobstructed.

Figure 4-7 Configuration (b) two steps no weir boards

c. All of the water was directed down the three steps in the left hand section. No weir boards were used. The water flowed directly into the pipe connecting the cascade to the distribution channel at the front of the settling lagoon.

Figure 4-8 Configuration(c) three steps no weir boards

d. All water was diverted down the central section. A weir board was placed on the step to create a plunge pool 10 cm deep. As for configuration (d) the water in the channel at the bottom of the cascade was 37 cm deep.

Figure 4-9 Configuration (d) two steps, weir board, water level in channel 37cm

e. All flow was diverted down the left hand side of the cascade. Weir boards were put in place on the steps to create small plunge pools with a depth of 10 cm. Sand bags were put in front of the grille leading to the outflow pipe which raised the water in the collection channel to a height of 37 cm and allowed some mixing prior to discharge.

Figure 4-10 Configuration (e) three steps, weir boards, water level in channel 37cm

As a result of the difference in distance between the bottom step and the outflow pipe it is unlikely that the mean residence time and mixing of water in the bottom channel was the same for both configurations (d) and (e). It was not possible however to determine the exact residence time of the water in the channel at the bottom of the cascades.

4.7.2 Water quality monitoring

For clarity Figure 4-11 is reproduced from Chapter 3. The aeration cascades are situated to the left of the picture with sample points 1 and 2 being situated at the top and bottom of the cascades respectively. Samples were taken from each of the three points marked for each different cascade design. Samples were taken from point 3 after 24 hours of starting a new configuration to ensure that water coming over the cascade had had time to flow through the lagoon. The volume of the first lagoon is approximately 1700 m^3. With a flow rate of 30 L/s this gives a nominal retention time of around 16 hours. Samples were analysed for alkalinity and acidity as described in Section 4.4. Iron samples were collected and analysed by ICP-OES as described in Section 4.3.2

Figure 4-11 Aerial view of Strafford site showing sampling points (taken from Google Earth)

4.8 Batch-wise CO_2 degassing

The method employed for CO_2 degassing during these experiments was aeration and thorough mixing of the water using a submersible Whale® Water Systems self venting pump powered by a 12 V car battery (as in Figure 4-2). Approximately 10 L of fresh mine-water was collected and aerated with pH, temperature, and DO measured and logged throughout using two hand held Hanna combination meters HI-9828 (see Section 4.1). Measurements were logged every 10 seconds. Samples were collected and analysed by ICP-OES as described in Section 4.3.2. Alkalinity and Acidity were determined as described in sections 4.4.1 to 4.4.3.

4.8.1 Geochemical modelling

The relationship between dissolved and atmospheric CO_2 is not as straight forward as for other gases such as O_2 or N_2. An introduction to carbonate chemistry and a discussion about the complexities of CO_2 degassing, its relationship with pH and the effect of coupling to the Fe(II) oxidation process in given in Chapter 2.

Two different approaches were used to model the rates of CO_2 degassing with both approaches using k_1 the rate constant for homogeneous Fe(II) oxidation to account for the effect of alkalinity consumption on pH through the experiments. The values chosen for k_1 were based on those already determined from the Fe(II) oxidation experiments conducted previously. The numerical RK4 method for Fe(II) oxidation as described in section 4.5.3 was then used to verify that the predicted concentrations of Fe(II) at the end of the experiment (based on the chosen value of k_1) matched the values measured in the field.

The first model was based on the rate of Fe(II) oxidation, assuming that precipitation of HFO was instantaneous and that alkalinity was consumed stoichiometrically according to Equation 4-13. This method has been used previously as the basis for modelling CO_2 degassing by Kirby et al (2009).

Equation 4-13

$$\mathbf{Fe^{2+} + CO_3^{2-} + 2\tfrac{1}{2}H_2O + \tfrac{1}{4}O_2 \rightarrow Fe(OH)_3 + H_2CO_3}$$

Having chosen a suitable value for k_1, the changes in Fe(II) concentration over time were calculated (at 10 second intervals) using the RK4 method, followed by the corresponding changes in alkalinity according to the stoichiometry in Equation 4-13. Concentrations of Fe(II) and alkalinity, together with logged values for pH, temperature and DO were then input into PHREEQCi in spreadsheet mode. PHREEQCi was then used to produce corresponding values for dissolved CO_2 and other carbonate species as well as total dissolved inorganic carbon (TDIC) at 10 second intervals. PHREEQCi calculates concentrations of carbonate species using information about pH, alkalinity and the equilibrium constants that describe the relationships between the various carbonate species $CO_{2(aq)}$, H_2CO_3, HCO_3^-, CO_3^{2-}. Provided that pH and alkalinity are known, the concentrations of all other carbonate species can be calculated (Stumm and Morgan 1996). A more detailed discussion of aqueous carbonate chemistry is given in Chapter 2.

The changes in concentration for all of the carbonate species present (including dissolved CO_2) over time could then be plotted using the outputs from PHREEQCi. This way of modelling changes in carbonate speciation gave a useful indication of how the chemistry of the water was changing over the initial stages of the experiment. However, PHREEQCi assumes that when alkalinity is input as zero, TDIC is also zero. It was therefore not possible to show dissolved CO_2 reaching atmospheric equilibrium as in cases where the waters modelled were net-acid the method of calculation described above based on Equation 4-13 predicts consumption of all alkalinity. Since whenever alkalinity is zero PHREEQCi outputs TDIC as zero, then dissolved CO_2 must also be zero, which cannot be the case if it is in atmospheric equilibrium.

In order to overcome the problem of TDIC falling to zero it was decided to model the rate of CO_2 degassing independently of Fe(II) oxidation (and alkalinity consumption) and establish the form of the rate equation and values for the mass transfer coefficient k_La for the sites under investigation. A similar method was previously used by Cravotta (2007) in the evaluation of CO_2 degassing/Fe(II) oxidation rates in circumneutral ferruginous mine drainage in Pennsylvania, USA. By determining values for k_La and establishing the form of the rate equation, kinetic modelling could then be carried out in PHREEQCi such that dissolved CO_2 could be brought into atmospheric equilibrium.

Coupling of the rate equation for this process to the rate equation for Fe(II) oxidation in PHREEQCi would then allow changes in all of the species of interest to be modelled over time. The changes in pH output by PHREEQCi as a result if this coupling of the CO_2 degassing and Fe(II) oxidation rate equations could then be compared to empirical pH data as a way to check the validity of the model (since changes in pH are dependent on both rate of CO_2 degassing and rate of Fe(II) oxidation).

The decrease in concentration of dissolved CO_2 over the course of the degassing experiments is asymptotic with the final concentration of dissolved CO_2 in atmospheric equilibrium. Such kinetic relationships for asymptotic approach to steady-state values can be described according to Equation 4-14 (derived from Langmuir (1997)), where A_s is the equilibrium (asymptotic) concentration of a reactant, A is the concentration at time t and *n* is the order of the reaction with respect to A.

Equation 4-14 $$\mathbf{dC/dt} = \boldsymbol{k}\,(\mathbf{A_s} - \mathbf{A})^{\boldsymbol{n}}$$

Both first and second order forms of the rate equation for CO_2 degassing were investigated (as suggested by Cravotta (2011)). Values for k_La were determined by using the integrated forms of the equations for CO_2 degassing (Equation 4-15, 1st order and Equation 4-16, 2nd order), where C_s is the equilibrium concentration of CO_2, C_o is the initial concentration and C_t is the concentration at time t). For the 1st order rate equation $\ln(C_s\text{-}C_t)/(C_s\text{-}C_o)$ was plotted vs time and for the 2nd order rate equation $1/(C_s\text{-}C_t)+1/(C_s\text{-}C_o)$ was plotted vs time.

Equation 4-15 $$\mathbf{k_La} \times \mathbf{t} = \ln \frac{(\mathbf{C_s}-\mathbf{C_t})}{(\mathbf{C_s}-\mathbf{C_0})}$$

Equation 4-16 $$\mathbf{k_La} \times \mathbf{t} = \frac{1}{(\mathbf{C_s}-\mathbf{C_t})} + \frac{1}{(\mathbf{C_s}-\mathbf{C_0})}$$

Values for C_s, C_t and C_o were taken from the values calculated by PHREEQCi in spreadsheet mode based on measured pH and alkalinity consumption according to Equation 4-13. k_La was determined by taking the gradient of the $\ln(C_s\text{-}C_t)/(C_s\text{-}C_o)$ and $1/(C_s\text{-}C_t)+1/(C_s\text{-}C_o)$ vs t plots over the first 10 minutes of the experiments. The determination of k_La was limited to the first ten minutes because as the CO_2 degassing experiment proceeds calculations of alkalinity based on Equation 4-13 will show

increasing deviation from reality as [alkalinity] is reduced to zero. It was decided that this effect would be minimal over the first ten minutes of the reaction where alkalinity concentration remained relatively high.

Values for $logPco_2$ vs time were then calculated by plugging k_La back into the original forms of the rate equations. The values of $logPco_2$ calculated using the rate equation were then compared to $logPco_2$ output by PHREEQCi based on measured pH and values for alkalinity calculated using Equation 4-13 for each of the CO_2 degassing experiments.

It was decided to model CO_2 degassing in this way since if a robust model can be developed for coupling $d[CO_{2(aq)}]/dt$ and d[Fe(II)]/dt it could be a useful tool in informing the design of hydraulic structures/CO_2 stripping methods employed in the treatment of ferruginous mine drainage. If k_La for CO_2 is known for a particular system as well as the pH and $[Fe(II)]_0$ it should be possible to determine optimum residence times for achieving desired changes in pH or reduction in [Fe(II)]. Additionally, a model such as this could be further developed to contribute to the understanding of the mechanism of Fe(II) oxidation in these systems as a number of alternative rate equations could be included in the model for different Fe(II) oxidation pathways. With both of the major contributing factors to pH change included in the model output pH can be compared to field or laboratory measured pH to ascertain its validity.

Once values for k_1 (chosen based on values determined from homogeneous oxidation experiments, Section 4.5 and Chapter 6) and k_La for each site had been decided upon they were input into a PHRREQCi rate of reaction model adapted from Example 9 of the PHREEQCi manual (Parkhurst and Appelo 1999) by Cravotta (2011). The section of code relating to the rates of reaction is displayed below. The full code contains a description of the initial conditions in the solution, equilibrium phases and the possible Fe(II) and Fe(III) species that might be present. Outputs from this model for pH, as well as concentrations of dissolved carbonate species and Fe(II) were then compared to the experimental values and the values produced by the RK4 method.

```
TITLE Kinetically controlled exsolution of carbon dioxide coupled with
oxidation of ferrous iron. Decoupled valence states of iron.
Adapted from example 9 of PHREEQC.


RATES

CO2(g)
-start
10 REM Estimated pCO2 data for aeration experiments

## Second order model dC/dt = k2·(Cs-C)^2
20 Cs = -2.8 # Steady-state log[Pco2(atm)]
30 kLa = -0.000216 # Alk = 160, Co = -0.7, Cs = -2.8 [CO2(g)] taken
from PHREEQCi output by JNG
50 dco2dt = 2.303 * kLa * ((SI("CO2(g)") - Cs))^2 * MOL("CO2")
60 moles = dco2dt * TIME
100 save moles
-end

Fe_di_ox
-start
10  Fe_di = TOT("Fe_di")
20  if (Fe_di <= 0) then goto 200
30  p_o2 = 10^(SI("O2(g)"))
40  O2 = 10^(SI("O2(g)")) * 10^(-2.960)
50 k1 = 1.33e12
60 factor = 55 # change rate constant by factor selected
70 k1emp = k1 * factor # change multiplication factor
90  moles = (k1emp * p_o2 *(ACT("OH-"))^2) * Fe_di * TIME

200 SAVE moles
-end

INCREMENTAL_REACTIONS true

KINETICS 1
-steps 1000*10
```

4.9 The Vertical Flow Reactor (VFR)

4.9.1 VFR at Taff Merthyr

The VFR at Taff Merthyr had been previously conceived and constructed by a number of researchers and staff at Cardiff School of Engineering including Prof Keith Williams, Dr Devin Sapsford, Dr Matt Dey, Dr Andrew Barnes and Mr Jeff Rowlands. The design criteria for the VFR are covered briefly here. A more detailed discussion can be found in Barnes (2008). A schematic diagram of the reactor (Figure 4-12) as well as a cross sectional view (Figure 4-13) is shown.

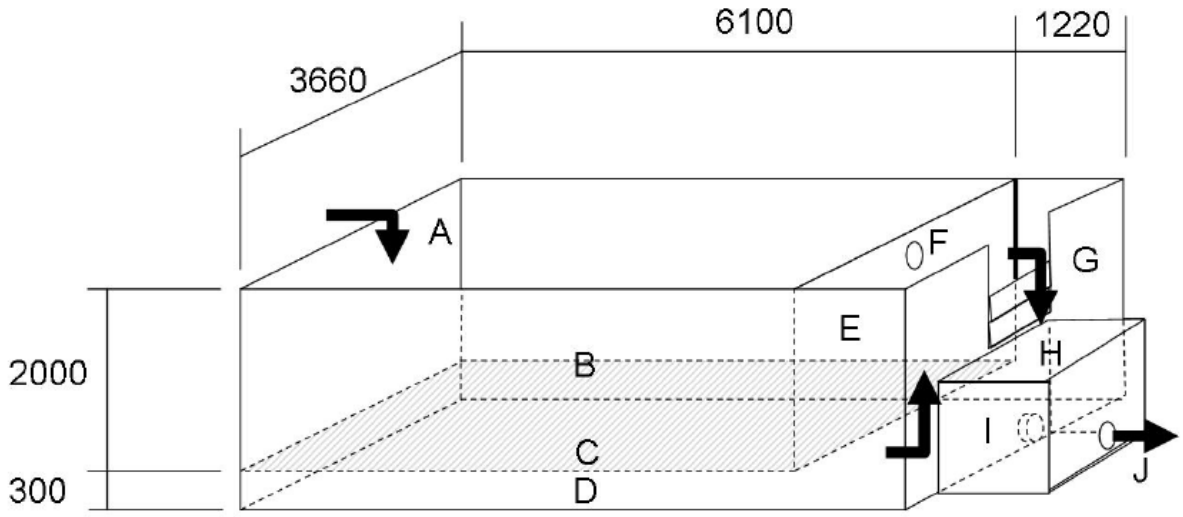

Figure 4-12 Schematic diagram of the VFR at Taff Merthyr (Barnes 2008)
Not to scale. Approximate measurements in mm. A = Raw mine water inlet, B = Down-flow treatment chamber, C = Gravel bed, D = Under-drain, E = Up-flow chamber, F = Treatment chamber overflow, G = Weir level control structure, H = Discharge collection chamber, I = Gate valve from up-flow chamber to discharge collection chamber, J = Outflow to stream

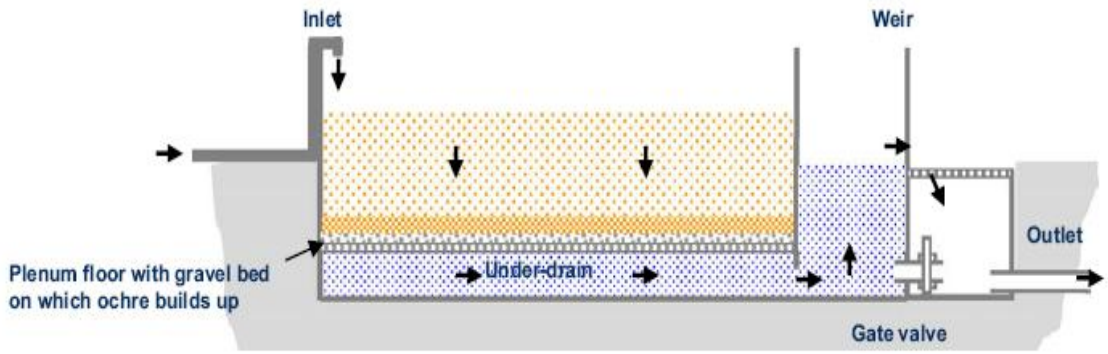

Figure 4-13 Cross sectional diagram of the VFR (Barnes 2008)

The gravel bed comprised two layers of gravel supported on a wire mesh with a fillet of builders' sand around the edge against the walls of the tank to prevent short cutting of flow (a problem in early operation). Both layers were approximately 100mm deep with the lower layer made up of 20mm gravel and the top layer made up of 6mm gravel.

4.9.1.1 Experimental set up

As a result of previous experimentation by Barnes (2008) the gravel bed of the VFR was covered by a layer of HFO approximately 7 cm thick. This was cleared from the bed by scouring with a pressure washer so that only traces of HFO remained (Figure 4-14). The gravel bed was raked flat and the tap at the inlet to the VFR was then opened fully to allow through the maximum flow of water approximately 4 L/s (taking into account the pumping cycles from the sump feeding the reactor tank). It was noted that HFO began to build up very quickly.

Figure 4-14 The VFR after cleaning, 7cm deep layer of sludge has been removed.

4.9.1.2 Flow rate measurement

Flow rate was initially measured at an outflow pipe that discharged from the VFR using a 10 L bucket previously calibrated in the laboratory and a stopwatch. Measurements of the time required to reach the 10 L mark on the bucket were taken in triplicate. Once the main tank of the VFR started to overflow the bucket and stopwatch was used to measure the flow rate from the overflow hole (Figure 4-15) as well as the outflow

pipe with the flow through the reactor bed taken to be the difference between the two measurements.

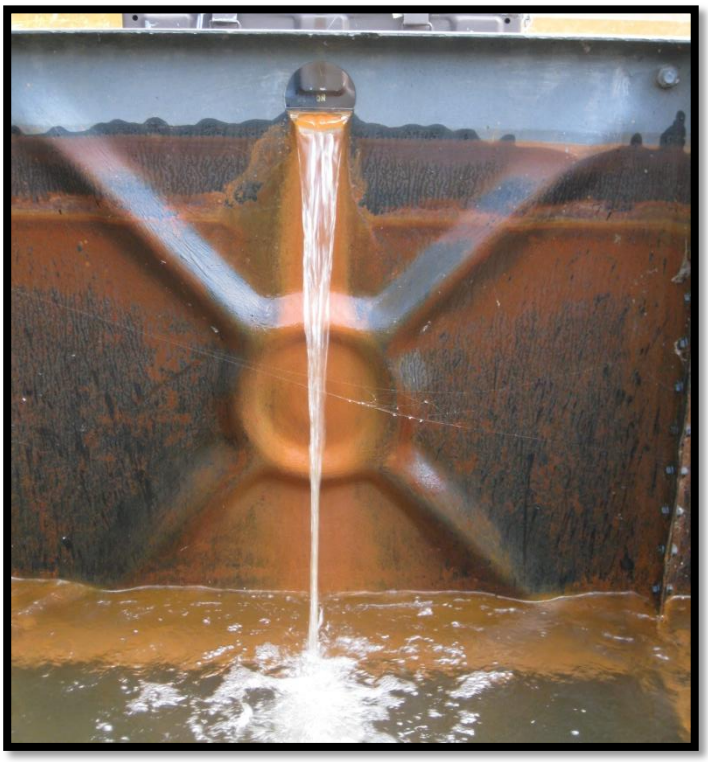

Figure 4-15 The overflow from the VFR

4.9.1.3 Water sampling

Samples were taken at the inflow, the overflow and the outflow of the VFR. Samples were analysed using ICP-OES as described in Section 4.3.2. The Fe concentrations together with flow rate measurements were then used to calculate Fe removal rates across the reactor bed. The VFR was allowed to run for nine months in total. For the first 3 months sampling was conducted once or twice a week with sampling approximately once a fortnight thereafter.

4.9.1.4 Analysis of old VFR sludge

Sludge samples were taken from the VFR bed and analysed for elemental composition. Samples were dried in an oven at 105^{o}C for 24 hours whereupon approximately 0.1 g of dry sample was weighed accurately to 3 figures using an analytical balance. 10 mL of aqua regia consisting 1 part HNO_3 to 3 parts concentrated HCl was then used to digest

the sample in a Perkin Elmer P1200 microwave. The digestate was subsequently analysed by ICP-OES to determine the concentrations of various metals in the samples.

4.9.2 The VFR at Ynysarwed

Two sets of VFR trial experiments were carried out at Ynysarwed from autumn 2010 to spring 2011. Schematic diagrams of both experimental set ups are shown in Figure 4-17 and Figure 4-21. From this point forward the first trial will be referred to as the bucket VFR and the second as the continuous flow VFR. The objective of both experiments was to find out how much Fe could be removed by a VFR that was not adding alkalinity to water that was net-acidic.

4.9.2.1 The bucket VFR

It was initially decided that the most useful point to set up the trial VFR would be next to the adit at Ynysarwed, as this would give the most accurate reflection of performance with raw water (Figure 4-16). Abstracting water from further along the treatment system might result in aeration and partial oxidation of the Fe(II) in the water prior to entering the VFR.

Figure 4-16 Adit from which water was taken for the bucket VFR

One of the major problems with setting up experimental trials at the Ynysarwed site is a lack of overnight security near the adit where the mine water emerges and the likelyhood of vandalism and theft. It was decided to run the experiment during the daytime only for periods of 6-8 hours and stop the flow over night so that pumping equipment could be stored securely. This pumping regime would reduce the total flow through the system to 1/3 or less of what would normally be expected over a 24 hour period compared to a continuous flow scenario. It was decided therefore to seed the bucket VFR with HFO from one of the distribution channels at the site so that results could be gathered without the long lag phase that might have occurred if HFO had been allowed to accumulate naturally. Figure 4-17 shows a schematic diagram of the bucket VFR.

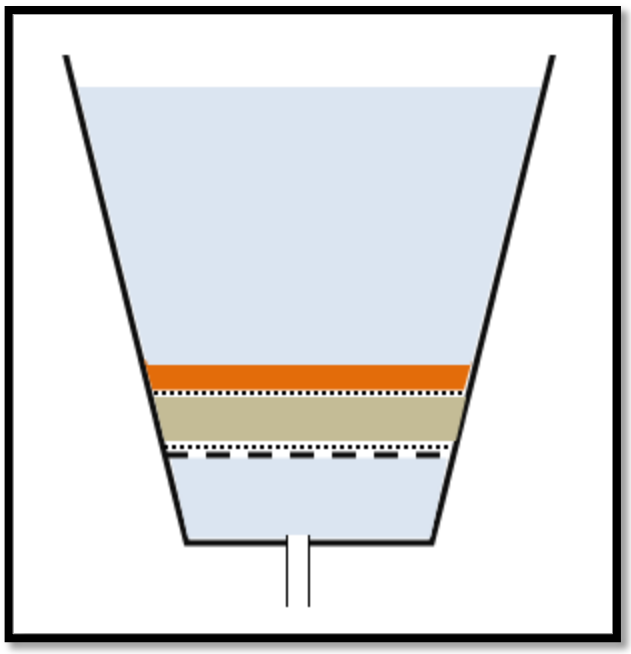

Figure 4-17 Schematic diagram of the bucket VFR pre-seeded with HFO
Dotted lines indicate a layer of muslin which helped to retain the sand (brown) and HFO (orange) layers, 80 mm and 50 mm deep respectively within the bucket VFR. The dashed line indicates the false bottom with 5 mm drainage holes

Water was drawn up as it exited the adit using a peristaltic pump (powered by a 12V car battery) and fed into the top of the bucket which had internal dimensions of 420 mm diameter at the top and a height of 500 mm. The bucket was fitted with a false bottom with drainage holes. This was then covered by a layer of muslin to prevent to prevent the sand layer on top from washing away. A second layer of muslin was then

added between the sand and the HFO collected from the distribution channel. A single drainage hole was drilled in the bottom of the bucket and a piece of 8 mm diameter rubbed hose attached for the outflow. A clip was placed over the hose that could be partially opened to control the flow of water during the initial stages of the experiment. Figure 4-18 shows the first muslin and sand layers in the bucket. Sand was chosen instead of gravel because of its lower permeability to help regulate the rate of flow down through the VFR bed during the initial stages of the experiment.

Figure 4-18 View of the bucket VFR with first muslin and sand layer

Once seeded with HFO the bucket VFR was placed near to the adit and slowly filled with water using a peristaltic pump powered by a 12 V car battery as shown in Figure 4-19. Initially the clip on the outflow hosing was closed as suspension of the HFO layer was a result of the disturbance by the inflowing water was causing much of it to be washed out of the VFR. This suspension of the solids can be seen in the dense orange colour of the water in Figure 8-4. Once the bucket had filled water it was allowed to drain out and the speed of the pump was regulated to keep pace with the rate of the water leaving the VFR. The flow rates were in the range 1 L every 16-20 minutes varying with the water level inside the bucket.

Figure 4-19 Bucket VFR being filled with peristaltic pump

Once water was allowed to flow down through the VFR bed the suspended solids started to settle and the water in the bucket became clearer (Figure 4-20). Flow rates were measured using a 500 mL measuring cylinder and a stopwatch. Acidity, alkalinity, pH and Fe concentrations were measured as described in Chapter 4 Sections 4.4 and 4.7.

Figure 4-20 Logging pH measurements in the bucket VFR showing how solids settled leaving clearer water over time.

4.9.2.2 The continuous flow VFR

The continuous flow VFR at Ynysarwed was designed in a similar manner to the larger scale reactor at Taff Merthyr (Chapter 5) as can be seen from the schematic diagram in Figure 4-21. A header tank was included at Ynysarwed to control flow rates. Each section of the VFR was constructed out of a plastic box as shown in Figure 4-22. Holes were drilled in the bottom of one box which was then placed on legs inside a second box to provide the under drained bed. The inner box was lined with gravel and a header tank was placed on top resting on two planks of wood for stability. The header tank was fed by water pumped up from the wet well beneath (Figure 4-23) (across the road from the adit) by an electric (120V) pump. Holes were drilled in the sides of header tank until equilibrium was reached so that the water level in the tank remained stable and the flow of water into the VFR was as constant as possible. Excess water drained away through holes in the back of the header tank.

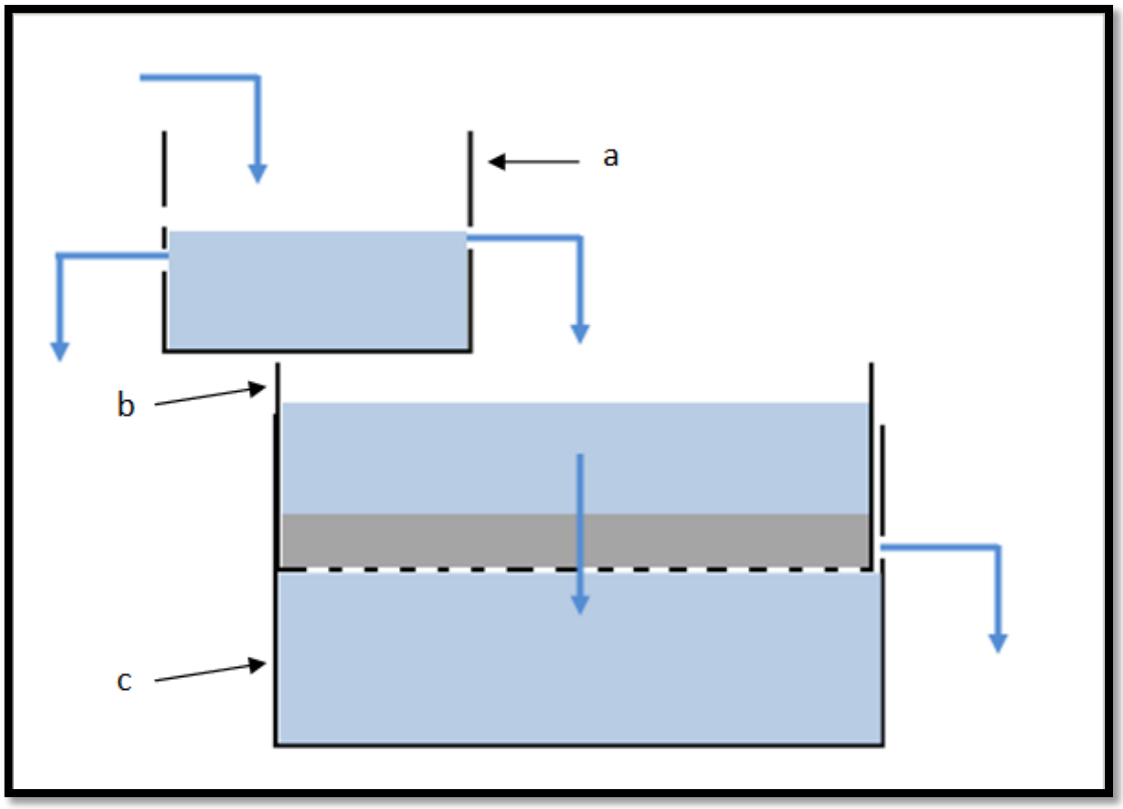

Figure 4-21 Schematic diagram of the continuous flow VFR
Flow of water indicated by blue arrows. Dimensions (l x d x h, mm) box a 570 x 390 x 420, box b 750 x 570 x 250, box c 790 x 570 x 420)

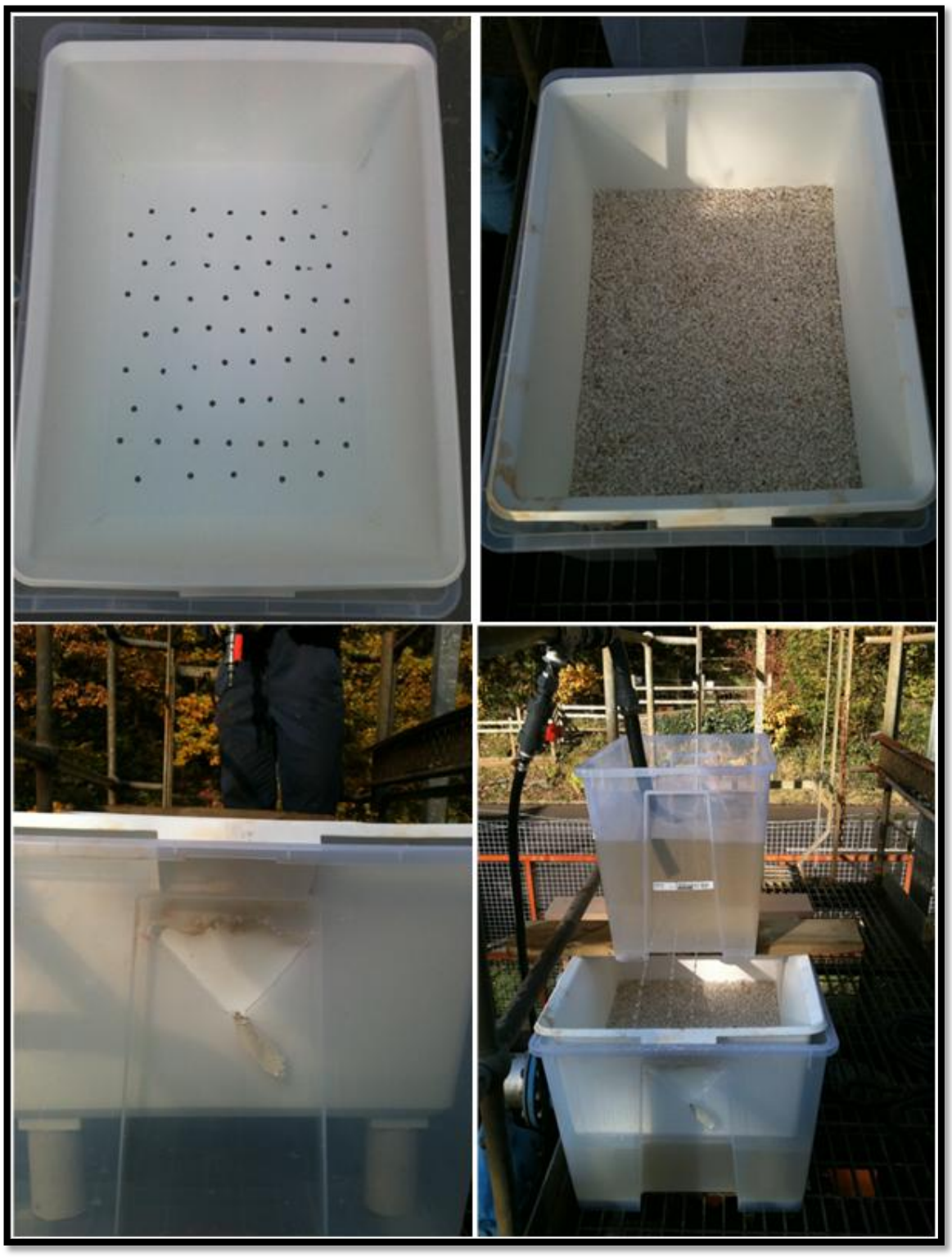

Figure 4-22 Continuous flow VFR trial at Ynysarwed.
Pictures clockwise from top left, drainage holes in inner box, gravel bed on top of drainage holes, inner and outer box together with v notch for outflow, water flowing from header tank into reactor tank

Figure 4-23 Position of continuous flow VFR on top of wet well

Again flow rates were measured using a 500 mL measuring cylinder and a stopwatch and acidity, alkalinity, pH and Fe concentrations were measured as described in Sections 4.4 and 4.7.

5 Results and Discussion: The Vertical Flow Reactors

This chapter presents the results of the Vertical Flow Reactor (VFR) experiments at the Taff Merthyr and Ynysarwed sites as described in Chapter 4 Section 4.9. Details about the treatment schemes are given in Chapter 3. The main aims of the experiments were (1) to see if the Taff Merthyr VFR could be run at a high flow rate that would favour HFO accretion/heterogenous catalysis over homogenous Fe(II) oxidation in the water column and (2) to investigate the efficacy of a VFR for treating net-acid ferruginous mine drainage at Ynysarwed.

Flow rate data and Fe and Mn removal data for the Taff Merthyr VFR are presented. Initially it was intended to run this VFR with a continuous flow rate of approximately 4 L/s. Unfortunately, due to fouling of the inflow pipe this was not possible and flow rates varied considerably over the course of the experimental period. The results of Barnes (2008) are confirmed by the data collected during this trial with respect to both Fe and Mn removal and chemical analysis of the VFR sludge. Since one of the secondary goals of this experiment was to confirm the results previously published in Barnes' PhD thesis detailed discussions and analyses are not presented unless new insight can be offered in addition to that contained within the previous study.

Unfortunately due to a number of unforeseen and unexpected problems only limited data were collected from the VFR trials at Ynysarwed.

This chapter is split into five main sections; set up of the VFR at Taff Merthyr, Flow rates and Fe and Mn removal, analysis of old VFR sludge, the VFR at Ynysarwed and Implications for the treatment of ferruginous mine water.

5.1 Set up of the VFR at Taff Merthyr

The VFR (as described in Chapter 4, Section 4.9) had previously been used by Barnes (2008) during his PhD and the suspended gravel bed had been left covered in a layer of HFO. This HFO layer was scoured using a pressure washer prior to commencing further experimentation. Having raked the gravel bed flat (as far as possible) the inlet pipe to the VRF was cleared of HFO and the valve opened fully to allow the maximum possible rate of flow into the VFR. In order to prevent short-circuiting down the side of the tank, splash boards and a fresh fillet of sand were added beneath the inlet pipe as shown in Figure 5-1.

Figure 5-1: Initial set up at inflow to VFR tank
Plastic sheet, sand fillet and splash boards were added to prevent scouring of the bed (and hence short cutting) by the inflowing water.

It was intended to run the VFR at the maximum possible flow rate (approximately 4 L/s) and to allow the HFO layer to build up naturally on the gravel bed by accretion rather than by settling of precipitates within the water column. It was initially thought that if the residence time within the VFR could be reduced by increasing the flow rate then there would be insufficient time for all of the Fe(II) to oxidise within the water column.

If this were the case then the remaining Fe(II) would be oxidised via heterogeneous catalysis by adsorbing onto the HFO solids on the reactor bed. To this end, no attempt was made to control the head within the VFR as had been done previously by Barnes (2008). It was hoped that allowing the HFO to build up via accretion rather than settling would produce a more granular sludge with better dewatering properties closer to those of high density sludge (HDS) (Coulton et al. 2003) that might also result in greater bed permeability. It was also hoped that by running the system with maximum flow rate and maximum potential head that the reduced retention time in the tank would continue to favour HFO accretion/heterogenous catalysis over homogenous oxidation.

Within 1 week of commencing the experiment a layer of fresh HFO had started to build up on top of the gravel bed at the inflow end of the tank and within two weeks this layer had extended across the entire gravel bed and the reactor tank had started to fill with water (Figure 5-2). Figure 5-2 (a) shows a dark red staining of the gravel at the edges of the pool of water that had formed. This is indicative of the initial stages of HFO accretion onto a surface and has been observed by the author at a number of mine water treatment sites. The dark red staining (as opposed to the orange brown colour of HFO particulates formed by homogenous oxidation) can also be seen in Figure 5-13 at Ynysarwed.

The rapid build up of the HFO layer and rapid reduction in permeability of the bed (less than 2 weeks), was initially surprising and suggested that the HFO bed may not maintain the high permeability that had been hoped for. It can be seen from Figure 5-2 (b) that even with a low water level and short retention time in the VFR reactor tank Fe(II) precipitation was already taking place within the water column (water has a cloudy orange/brown appearance). This indicated that despite every attempt to produce conditions that favoured heterogenous oxidation/HFO accretion of homogenous oxidation was also occurring. It appeared that Fe(II) oxidation was occurring more rapidly within the water column than had initially been anticipated.

(a)

(b)

Figure 5-2: The VFR after (a) one week and (b) two weeks of the experiment

Despite frequent attempts to maintain a high and consistent flow rate the pipe feeding the VFR with fresh ferruginous mine drainage quickly clogged with HFO deposits reducing flow rates between each monitoring visit. This meant that the head did not build up in the tank at a steady rate, and over the first few months went up and down depending on inflow rate, which was affected by both clogging of the pipe and levels of rainfall. Rainfall contributed to the water levels in the tank in two ways, both by directly filling, and by increasing the rate of inflow into the mine workings which altered the pumping cycle at the site causing the pumps to come on more frequently in order to maintain the water levels below ground. Since the VFR was fed directly from a distribution chamber leading to part of the main Taff Merthyr treatment system (see Figure 3-13) any increase in pumping caused an increase in flow into the reactor tank.

5.2 Flow rates, Fe and Mn removal

As a result of the factors described in the previous section (clogging of inflow pipe and inconsistent pumping cycles) it was impossible to control or maintain a consistent flow rate into the VFR. Notes were kept at each monitoring visit along with records of flow rates and dissolved Fe concentrations which are detailed in Table 5-1. Figures 5-3 to 5-6 are included to illustrate how the water levels in the tank changed over time. By 04/08/09 (Figure 5-5) the height of water in the main tank had reached the overflow level meaning that approximately 100,000 m^3 of mine water had been successfully treated with water exiting the VFR having < 1mg/L Fe(II). After this time an increasing proportion of the water overflowed and did not go down through the reactor bed.

Figure 5-3: The VFR 03/06/09

Table 5-1: Monitoring data from the Taff Merthyr VFR (flow rates L/s, Fe(II) concentration mg/L)

Date May 09 – Feb 10	Total flow[7]	Flow through bed[8]	Fe(II) in	Fe(II) out	Fe_{tot} in	Fe_{tot} out	Comments
29/05							Flow started
03/06	4.5			<1			Main chamber starting to back up slightly outflow water slightly cloudy
09/06	1.6	1.6	5.6	<1			Water level in main tank starting to fall back from maximum (tide mark) Water level almost the same on outflow and inflow side.
12/06	1.7	1.7	6.6	<1			
16/06	1.2	1.2	6.8	<1			
19/06	1.5	1.5	7.0	<1			
26/06			7.2	<1			Apparently "oily" film on surface of VFR water
30/06	1.1	1.1	7.1	<1			Water level had dropped in tank. Pipe was blocked. When agitated lumps of HFO sludge were discharged.
07/07			7.2	<1			Water level still very low in tank
16/07	1.5	1.5					Pipes cleared. Large increase in flow rate into VFR. Main tank starting to back up quite quickly
20/07			3.6	<1			Pipes cleared. Main tank level stabilised at about 1.2m water level above plenum floor
23/07	1.7	1.7					Pipes cleared. Higher level of tank maintained since last visit. Outflow side still very clear.
28/07	1.7	1.7	5.3	<1			No change in appearance
04/08							Level has increased in tank. Small flow through overflow channel. Most flow still out through bottom of bed. See photos. Outflow water still looks quite clear (very little suspended solids).
11/08			2.0	<1	7.1	1.4	After clearing the pipe flow rate in increased and VFR over flowed (see photos)
13/08	1.8	1.75					Flow rate in initial stages varies a great deal due to blockage of pipes and variation in inflow.

[7] Flow measured at outflow pipe into distribution channel.
[8] Difference between flow from outflow pipe and flow from overflow point on main reaction chamber.

18/08			2.9	< 1	4.3	1.4	VFR still overflowing, outlet side of chamber now much cloudier.
27/08	1.0	0.7					Initial overflow rate 0.3 l/s before pipe clearing, rising to 0.7 l/s after pipe clearing. Flow through bed has dropped from max 1.7 l/s to 0.7 l/s
07/09			5.3	0.9	5.8	1.6	Overflow chamber now acting as well aerated reactor. Removing significant proportion of Fe
12/10	1.0	0.5	6.5	1.0	6.5	3.2	Flow through bed dropped again, despite Fe(II) being close to discharge consent, more particulate Fe is being carried over.
28/10	1.1	0.4	5.7	N/A	7.2	N/A	Upon arrival v low flow. pipe cleared then flow measured. Flow through bed 0.45l/s
13/11	1.5	0.4			6.0*	4.9*	*Could not find syringe in tool kit. Only total Fe samples taken.
04/12	2.5	0.7	4.3	1.9	4.8	4.6	Very High flow rates due to recent heavy rain level in tank several cm higher than usual
18/12	0.9	0.5	5.0	<1	5.5	3.5	
06/02	0.3	0.3	4.8	<1	25.6	<1	Inflow decreased. Level dropped in the tank by approx 50 cm. After pipe clearing inflow increased to 1.1l/s. Decrease in flow through bed likely due to decrease in driving head.

Figure 5-4: The VFR 20/07/09

Figure 5-5: The VFR 04/08/2009

Figure 5-6 shows how clearing the inflow pipe changed the total flow rate through the reactor tank. Before clearing there was a slow trickle of water through the outflow

hole which made very little contribution to the total flow. After clearing the inflow pipe however the water level in the reactor tank quickly began to rise resulting in a large increase in overflow water (picture (b)).

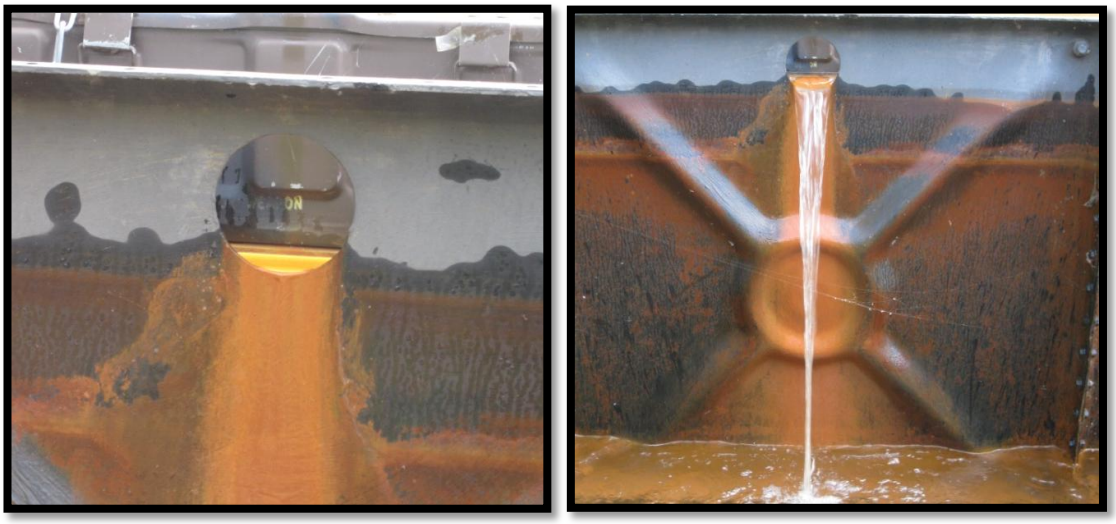

(a) (b)

Figure 5-6: The VFR overflow, 13/08/2009 (a) before clearing (b) after clearing inflow pipe

5.2.1 Fe removal and flow rates in the VFR

Using the data in Table 5-1 for flow rates and influent and effluent Fe(II) concentrations cumulative flows of ferruginous mine drainage through the VFR were estimated along with cumulative Fe removal (Figure 5-7). Given the variations in flow between visits the data presented in Figure 5-7 should be taken only as an estimate as to the performance of the VFR. Barnes (2008) used the formula $Fe_2O_30.5(H_2O)$ (formula weight = 169 g) to describe the HFO contained within the VFR sludge and found a solids content of 150 g/L. Using this information and taking the surface area of the VFR bed to be 22.33 m^2 (from dimensions given in Chapter 4, Section 4.9) the cumulative thickness of the bed over time was calculated and is shown in Figure 5-8. The final estimated be thickness was 99mm after 233 days.

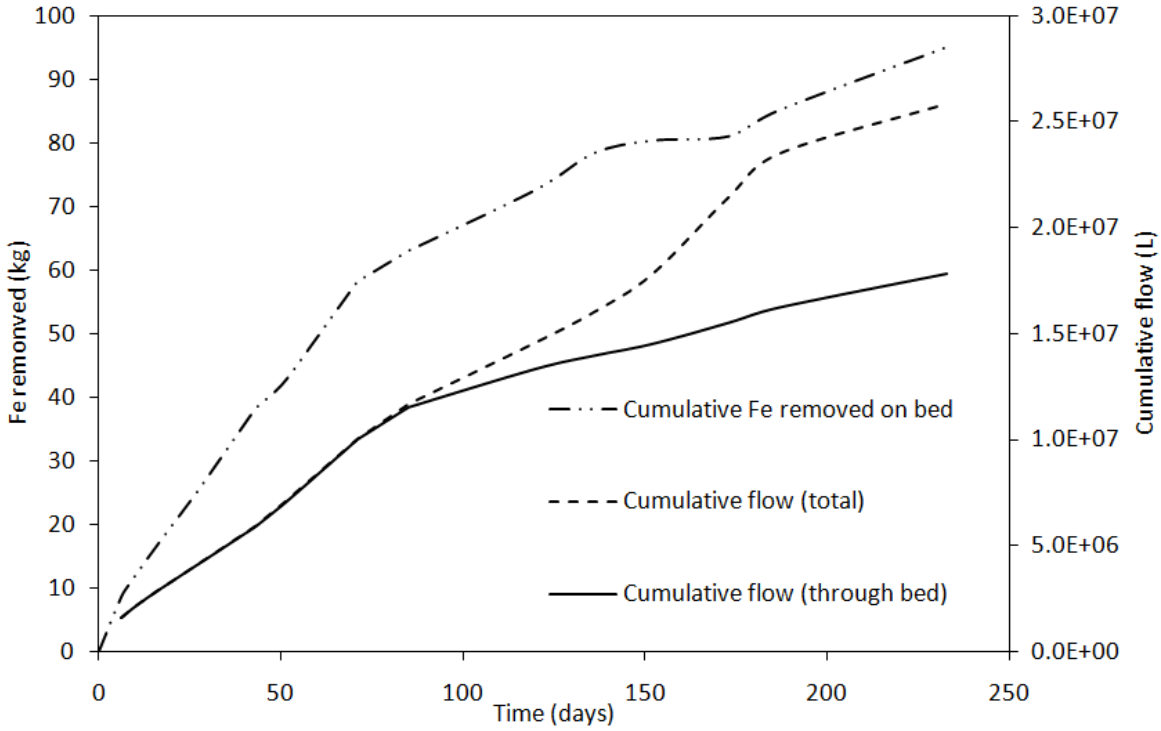

Figure 5-7: Estimated cumulative flows and Fe removal through the VFR

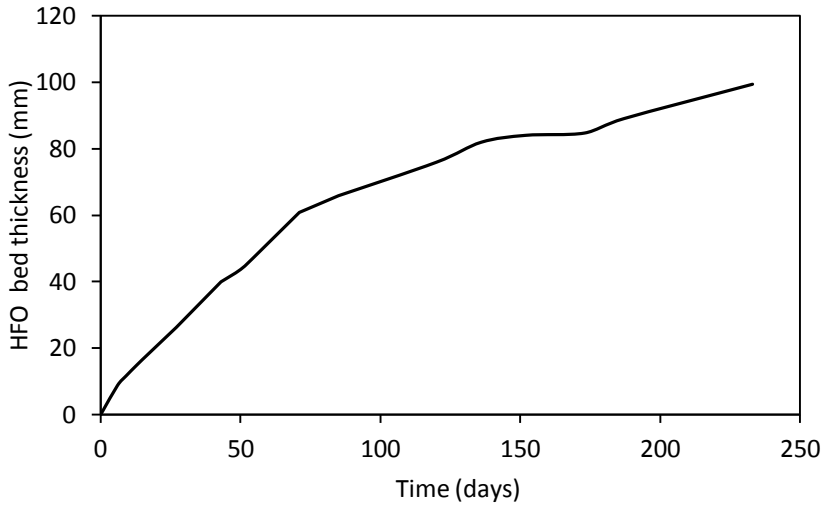

Figure 5-8: Estimated cumulative thickness of HFO bed in the VFR over time

Figure 5-9 compares the flow rates through the VFR bed to the measured Fe removal rates. It can be seen that there is a good correlation between the two parameters. Fe

removal rates were highest early on in the experimental period when the flow through bed was highest and as would be expected tailed off as flow through the bed reduced, with a greater proportion of dissolved Fe(II) and particulate HFO getting carried over in the overflow. The rates of Fe(II) removal can be separated into two groups as indicated in Figure 5-9 with higher removal rates corresponding to higher flow through bed. Comparison with Figure 5-7 shows that high Fe(II) removal rates correspond to the period when all flow was passing through the VFR bed at 0 to ~ 75 days. During this period the head in the main VFR reactor tank was increasing as the thickness of the HFO bed increased.

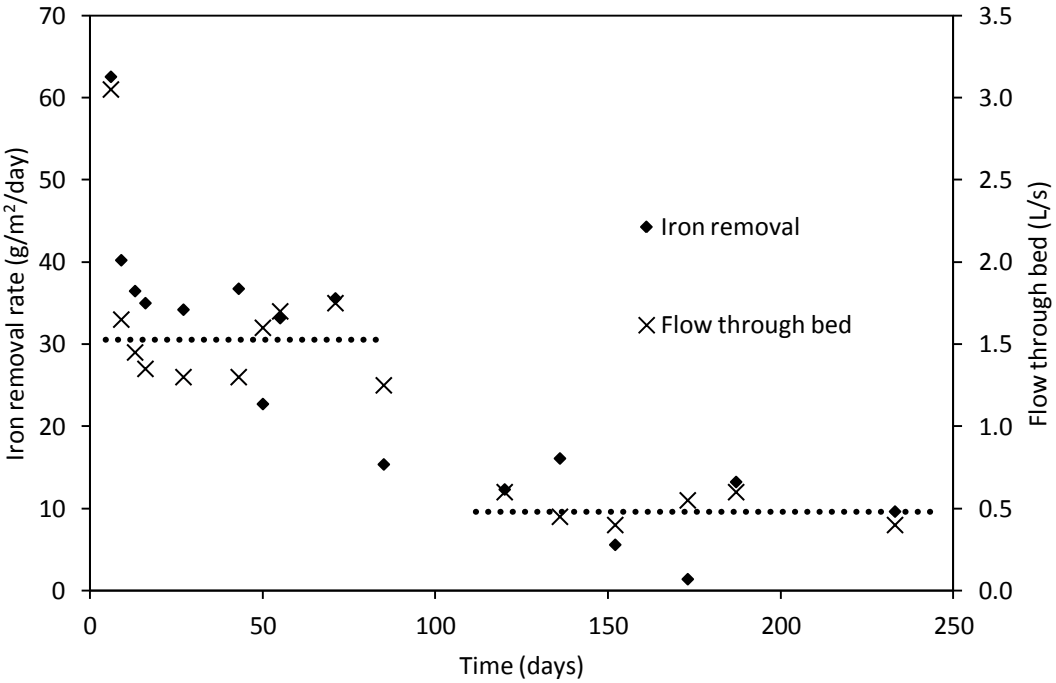

Figure 5-9: Fe removal rates and flow rates through the VFR bed
Dotted lines indicate regions of high flow through bed/high Fe(II) removal efficiency and low flow through bed/low Fe(II) removal efficiency

Barnes (2008) reported a mean total Fe removal rate of 16 g/m^2/day, which correlates well with the results obtained here given that total flow rates were in the range 0.5-1 L/s during his VFR trial. From Figure 5-9 it can be seen that average Fe(II) removal rate was approximately 35 g/m^2/day over the first 75 days of the experiment dropping to around 10 g/m^2/day as an increasing portion of Fe was carried out in the overflow

water. As discussed by Sapsford and Williams (2009) the rate of Fe removal over the first 75 days is significantly higher than that which would be expected in a settling lagoon treating water with similar chemistry. After 100 days of operation however, with an estimated bed thickness of 70 mm (see Figure 5-8) Fe removal rates in the VFR were no longer higher than those that could be achieved using a traditional wetland (often designed to have Fe removal rates of 10 g/m^2/day (PIRAMID 2003)). The rate of Fe removal was still higher however than the settling lagoons at the site which had an average total Fe removal of 5 g/m^2/day (Barnes, 2008). It would seem therefore that the initial goal of maintaining high bed permeability by encouraging HFO accretion/heterogenous catalysis rather than homogeneous oxidation was not achieved. The chemistry of the water naturally resulted in the oxidation of Fe(II) via the homogenous pathway as will be discussed further in the following section.

5.2.2 Fe removal mechanism in the VFR

When the VFR was designed it was thought that there would be two Fe removal mechanisms at work; filtration of particulates as they pass through the gravel bed and accretion of layers of HFO as a result of heterogeneous catalytic oxidation of Fe(II) adsorbed onto the HFO solids to Fe(III) (Sapsford and Williams 2009). A full discussion of the mechanisms of Fe(II) oxidation are given in Chapter 2, Section 2.2.

In the case of the VFR at Taff Merthyr, the dominant pathway for Fe(II) removal is homogeneous oxidation with particulate filtration of the resultant HFO. Fe oxidation experiments carried out at the site and discussed in detail in Chapter 6, Section 6.1 show that with mixing, Fe(II) concentrations in the Taff Merthyr ferruginous mine drainage can be reduced to <1 mg/L in under 30 minutes. Assuming a maximum flow rate of 4 L/s the residence time in the VFR main reactor tank would be close to 3 hours. Given this length of time the Fe(II) concentrations would almost certainly be <1 mg/L prior to passing through the VFR bed, which would be acting almost entirely as a filter in this case.

This is in contrast to the removal of Fe seen on top of the Reducing Alkalinity Producing System (RAPS) at the Tan-y-Garn treatment scheme described in Chapter 3.

In this case, given the lower pH (and hence lower Fe(II) oxidation rate) compared to the Taff Merthyr water, the build up of a layer of HFO solids on top of the RAPS is likely to be almost entirely due to heterogeneous catalysis by adsorption of Fe(II) onto the Fe(III) solids already present.

5.2.3 Mn removal

In line with the findings of Barnes (2008), the VFR was again found to remove Mn from solution as well as Fe. Unlike in the case of Fe however, Mn was not removed by precipitation within the water column, but was only removed within the HFO bed. It can be seen from Table 5-2 that where measurements were taken at the overflow, there was no significant reduction in Mn compared with the inflow water. On the final day of sampling where the flow rate had dropped off such that all water was flowing down through the HFO bed, 85% of total Mn was removed.

Table 5-2: Mn removal in the VFR[9]

	Mn concentration (mg/L)		
Date	**inflow**	**outflow**	**overflow**
28/07/2009	0.644	0.292	No overflow
11/08/2009	0.646	0.168	No overflow
18/08/2009	0.389	0.202	No overflow
07/09/2009	0.684	0.301	0.694
12/10/2009	0.747	0.436	0.735
13/11/2009	0.610	0.402	0.579
04/12/2009	0.604	0.497	0.603
18/12/2009	0.700	0.381	0.703
06/02/2010	0.791	0.116	No overflow

Barnes (2008) carried out XRD analysis on a black material found in the VFR sludge, which showed the presence of two Mn containing mineral phases, birnessite ($(Na,Ca)_{0.5}(Mn^{IV},Mn^{III})_2O_4.1.5H_2O$ and a Ba Mn oxide hydrate $Ba_2Mn_{14}O_{27}.xH_2O$ with mixed valence Mn 3+ and 4+. These results are consistent with catalysis of the

[9] Barnes (2008) previously showed that there was no significant difference between filtered and unfiltered samples with respect to Mn concentration. All values given are for unfiltered samples and can be taken as total dissolved Mn.

oxidation of the more soluble Mn(II) to Mn(III) and Mn(IV) by contact with HFO (Sung and Morgan 1981) or coupling to the Fe(II)-Fe(III) oxidation reaction (Hem 1977). Once an initial layer of insoluble Mn oxides have formed, the rate of precipitation is further increased by autocatalysis (Stumm and Morgan 1996) as shown in Equation 5-1. Studies have shown that the products of Mn(II) oxygenation are often non-stoichiometric with values ranging from approximately $MnO_{1.3}$ to $MnO_{1.9}$ (Stumm and Morgan 1996) so that not all of the Mn precipitated is actually in the +4 oxidation state.

Equation 5-1

$$-\mathbf{d}[\mathbf{Mn(II)}]/_{\mathbf{dt}} = \boldsymbol{k_0}\,[\mathbf{Mn(II)}] + \boldsymbol{k}\,[\mathbf{Mn(II)}][\mathbf{MnO_2}]$$

In addition to chemical oxidation and catalysis processes within the HFO sludge there is also the possibility of a contribution to Mn removal by bacterial oxidation. Given that abiotic oxidation rates for Mn(II) are low below pH 9 bacterial oxidation may be the dominant mechanism at circumneutral pH (Stumm and Morgan 1996). Zhang et al (2001) carried out laboratory studies on the bacterium *Leptothrix discophora* and found that it was an efficient oxidiser of Mn(II) in the pH range 6 to 8.5 with optimal oxidation rate at pH 7.5. Given the neutral pH of the water in the VFR an analysis of the sludge to investigate bacterial populations (that was beyond the scope of this study) would be required in order to determine the dominant pathway for Mn oxidation and precipitation.

5.3 Analysis of old VFR sludge

At the end of the experimental run previously conducted by Barnes (2008) the VFR was drained revealing the HFO sludge that had built up on the gravel bed of the reactor tank (Figure 5-10). The appearance of the black layers in the sludge was unexpected. A full chemical analysis of the sludge conducted by Barnes (2008) revealed that the black layers contained relatively high levels of Mn compared to the bulk of the sludge which as expected largely comprised hydrated Fe(III)oxide solids.

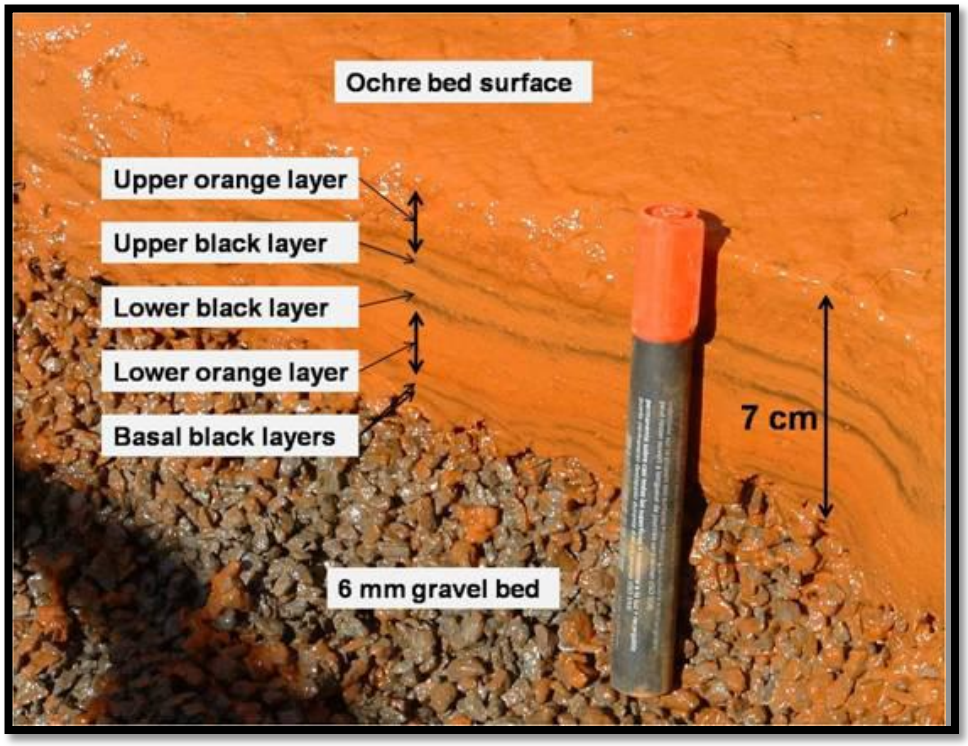

Figure 5-10: Picture of sludge deposited on the bed of the VFR (Barnes 2008)

Between the end of Barnes' experiments and the beginning of the current study the sludge on the VFR bed had had further time to consolidate and dry out making it easier to collect samples and cut into sections for analysis without disturbing the natural layering. Samples were taken back to the laboratory and cut into layers in order to determine more precisely how the chemical composition varied throughout the bed.

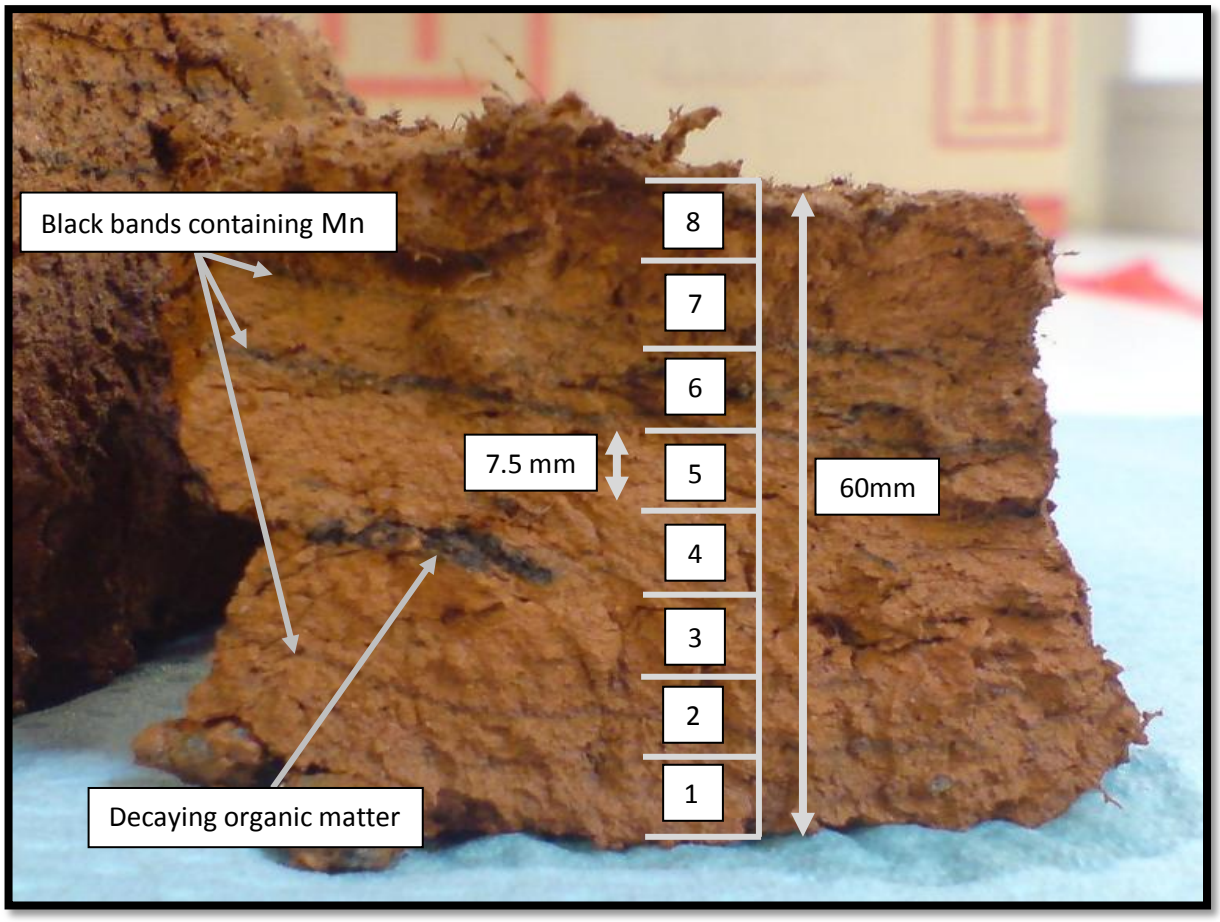

Figure 5-11: Cross section of consolidated VFR sludge with cross sectional layers marked

Figure 5-11 shows how the sample was divided into layers once it had been brought back to the laboratory. Once each layer had been cut it was prepared for analysis as described in Chapter 4, Section 4.9. In total 24 elements were analysed by ICP-OES. The concentrations of Ag, Be, Cd, Cu, Li, Mo, were < 30 µg/L in all samples. These values are so close to the detection limit of the ICP-OES that no reliable conclusions could be drawn from further analysis. The remainder of the results were converted from mg/L of the solutions prepared for analysis to mg/kg of solid and are shown in Table 5-3. It can be seen that Fe accounts for around 40% by mass of the solids, with Ca also making up a significant proportion of the total mass. It can also be seen that the concentration of Mn varied by more than a factor of 4 between the different layers in the cross section of sludge examined.

Table 5-3: Metals concentrations in samples from VFR sludge (mg/kg dry sludge)

Layer	Al	As	Ba	Bi	Ca	Co	Cr	Fe	K	Mg	Mn	Na	Ni	Pb	Sr	Ti	Tl	Zn
1	0.52	0.12	0.36	0.015	15	0.076	0.017	400	0.29	0.43	26	0.68	0.055	0.071	0.28	0.013	0.048	1.2
2	0.55	0.12	0.32	0.016	13	0.040	0.013	430	0.26	0.33	11	0.81	0.028	0.072	0.27	0.072	0.024	1.2
3	0.60	0.12	0.32	0.013	13	0.033	0.012	440	0.27	0.35	8.9	0.79	0.023	0.071	0.27	0.016	0.020	1.4
4	0.67	0.12	0.35	0.010	14	0.067	0.016	410	0.34	0.39	21	0.81	0.049	0.069	0.27	0.019	0.039	1.4
5	1.12	0.12	0.39	0.015	14	0.097	0.020	410	0.48	0.45	33	0.86	0.084	0.071	0.27	0.042	0.056	1.8
6	1.50	0.14	0.42	0.014	14	0.11	0.023	410	0.58	0.57	40	0.81	0.093	0.071	0.26	0.052	0.068	2.0
7	1.19	0.14	0.38	0.013	14	0.098	0.021	420	0.48	0.52	36	0.85	0.058	0.071	0.25	0.036	0.061	1.4
8	2.98	0.14	0.33	0.015	13	0.042	0.110	420	0.82	0.71	11	1.1	0.024	0.072	0.26	0.131	0.022	2.2

Values quoted to 2 significant figures and should be considered accurate to +/- 10% (error in ICP-OES results discussed in Chapter 4, Section 4.3.2)

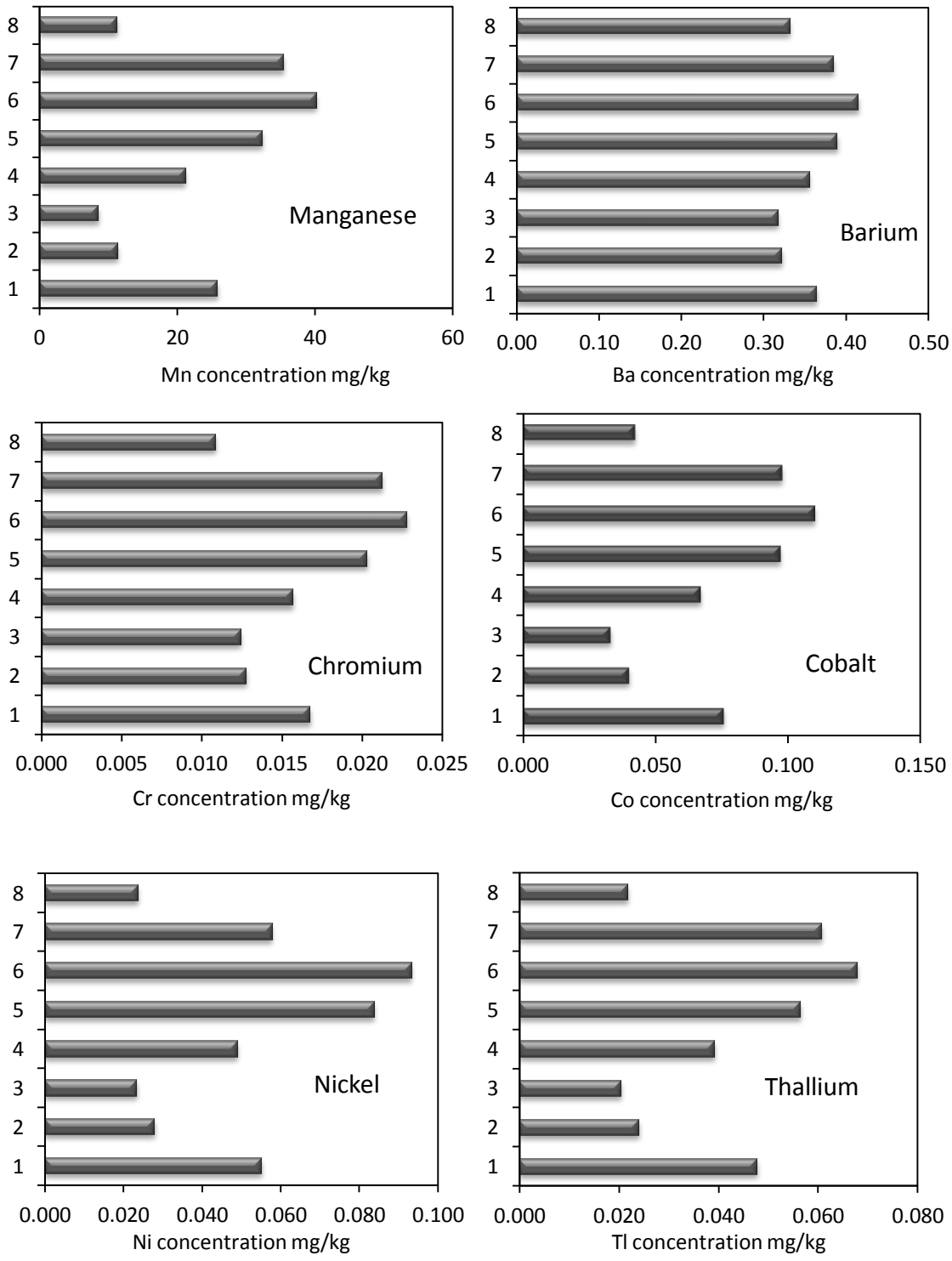

Figure 5-12: Comparison of variation in Mn concentrations with other metals throughout the VFR sludge

Numbers on y axes correspond to the layers shown in Figure 5-11

Figure 5-12 shows how the concentration of Mn, as well as a number of other trace metals varied with depth through the VFR sludge. Again these results are in line with those previously published by Barnes (2008). The appearance of peaks in the metal

concentrations suggests that redox conditions were not uniform throughout the sludge and that the precipitation of Mn oxides favoured the removal of the other metals either by adsorption, co-precipitation (in the case of Ba) or catalytic oxidation. Hem (1976) noted that in the presence of Fe oxides and Fe(II)/(III) redox reactions, mixed valence Mn (II)/(III) oxides can form which subsequently disproportionate to give Mn(IV). The disproportionation reaction results in strongly oxidising conditions that can increase the removal rates of some trace metals. In order to determine the precise removal mechanism for each of the metals quoted it would be necessary to determine in which oxidation states they exist within the sludge. As with the analysis for bacterial populations, this detailed speciation work was beyond the scope of this study.

5.4 The VFR at Ynysarwed

Problems were encountered with both versions of the VFR trialled at Ynysarwed and ultimately time constraints meant that no useful data about their performance was collected. In the case of the bucket VFR time was a problem because it could not be left to run continuously. In the case of the continuous flow VFR bad weather and technical problems at the site delayed experimentation for so long that it was eventually abandoned in favour of other work.

5.4.1 The bucket VFR

Flow rates in the bucket VFR were of the order of to 50 to 63 mL/min. If scaled up to the size of the VFR at Taff Merthyr (as described in Chapter 4, Section 4.9) the area of the VFR bed would be approximately 145 times larger. This would give a flow rate of approximately 0.14 L/s with a head height of 400 mm which is comparable to the actual flow rates measured at Taff Merthyr. In terms of assessing the overall performance of a VFR at Ynysarwed compared to the one at Taff Merthyr the flow rate was therefore within a suitable range. In terms of the constraints of only being able to run the experiment for a fixed period every day however the low flow rate was a problem.

Assuming an average diameter of the bucket of 440mm and a height of water above the bed of 400mm the total volume of water in the bucket VFR above the bed was approximately 67 L. At a flow rate of 63 mL/min that gave a residence time in the bucket of around 16 hours. Since the experiment was only run for 8 hours at a time this would only allow 50% of the water to exit the VFR each day meaning that the average residence time in the bucket would be more than 24h. This is sufficient time for a large portion of the Fe(II) in the mine water to oxidise in the water column and is therefore unlikely to give a realistic picture of what would happen in a continuous flow system.

Attempts were made to reduce the thickness of the HFO layer at the bottom of the bucket VFR in order to increase permeability and hence flow rate. This resulted in an increase in flow rate to 100 mL/min which reduced the residence time to around 8

hours. Even though this was a significant improvement it still meant a whole working day was required to allow the water left overnight to flush out of the bucket. Further attempts to increase flow rate resulted in short-circuiting and a high concentration of suspended solids in the outflow water. After several weeks of trying to obtain a consistent flow rate through the system it was eventually abandoned in favour of the continuous flow VFR.

5.4.2 The continuous flow VFR

Broadly speaking the continuous flow VFR was a great improvement on the bucket VFR in terms of experimental design. The only reason that it had not been trialled sooner was that water in the wet well feeding it had been aerated resulting in Fe(II) oxidation prior to pumping into the header tank. It may not therefore give an accurate picture of how the system would behave where water entered the VRF directly from the adit without additional aeration.

Figure 5-13: The continuous flow VFR after 10 days of operation showing ochreous deposits on all surfaces

Figure 5-14: Flow rate regulation in the continuous flow VFR showing water flowing out of the back of the header tank to prevent overspill

After the initial set up, the VFR was left to run for 10 days to allow the build up of an HFO layer on the reactor bed. Figures 5-13 and 5-14 show the condition of the VFR after 10 days. It can be seen that the entire system was coated in a dark red layer of HFO and that the water level had reached the top of the inner box. At this point samples were taken of total Fe in the influent and effluent water and analysed by ICP-OES giving 76 and 24.5 mg/L of Fe respectively. In an attempt to extend the life of the system the inner box was replaced with a larger one to increase the head that could be built up. The height of the v-notch on the outer box was also lowered.

At this point the VFR was left again for a week to allow the build up of HFO on the gravel bed. Unfortunately the experimentation coincided with a period of extreme cold weather which resulted in ice formation that interfered with the running of the VFR and made working conditions around the wet well dangerous. This meant that no results were collected during this time. There was subsequently significant flooding at the site as a result of snow melt and heavy rain again making it difficult to access the wet well area. These two events were unfortunately followed by a breakdown of one

of the main pumps at Ynysarwed which meant that the wet well had to be bypassed in order to prevent water backing up and overflowing. This caused the wet well to run dry meaning that there was no water supply to the VFR. The wet well remained dry for several more weeks whilst waiting for repairs to the broken pump and it was ultimately decided to abandon the experiment completely as there was insufficient time remaining to collect the required data.

5.5 Implications for the treatment of ferruginous mine water

As noted previously by Barnes (2008) the VFR can be used as an effective way to reduce the treatment footprint required for ferruginous mine drainage. The trials of the VFRs conducted in the production of this thesis showed that the VFR at Taff Merthyr can remove around 30 g/m^2/day of Fe, and providing that all water is passing through the VFR bed Fe concentrations in the outlet can be reduced to <1 mg/L. The application of this system to the treatment of net alkaline waters may however be limited. It was not possible to run the system at Taff Merthyr with a sufficiently high flow rate that the dominant Fe removal mechanism was via HFO accretion/heterogeneous catalysis on the VFR bed. The net-alkaline water encouraged the relatively rapid oxidation of Fe(II) in the water column prior to passing through the bed meaning that the major Fe removal mechanism was particulate filtration. The result was that the precipitate that built up on the bed of the reactor caused a rapid reduction in permeability meaning that it only had a useful lifetime of around 100 days before overtopping. Even with a low inlet Fe concentration of around 5 mg/L (and flow rate of 1-4 L/s) Fe removal rate dropped to 10 g/m^2/day the recommended design guideline for wetlands (PIRAMID 2003) within 3 months (though this was still higher than the Fe removal rate achieved in the settilng lagoons on site which averaged 5 g/m^2/day Barnes (2008)).

In circumneutral systems where inlet Fe(II) concetrations are higher than at Taff Merthyr it is likely that the lifespan of the system prior to overtopping would be reduced further due to a more rapid build-up of the sludge bed. Therefore the introduction of a VFR system of this type to such waters is unlikely to be economical since decomissioning for desludging would be required at far more frequent intervals than is currently the case for settling lagoons. Whilst a settling lagoon might remain maintenance free for a period of several years the results of this study sugest that a VFR system running under similar conditions might requre maintanance at least once a quarter. Therefore despite the relatively high Fe removal rates over the short to medium term considerable further work needs to be done in order to assess the potential for using this treament system for waters with higher inlet Fe concentrations.

One possible solution to the problems encountered with the short lifetime of the system at Taff Merthyr might be to run several VFR reactors in series with water flowing from one to the other. Even once it had started to overtop the first VFR in the series would still be removing a portion of the Fe from the system extending the lifespan of the reactors downstream. In this way it might be possible to run the whole series of reactors for a year or more before desludging was required. The results of the Taff Merthyr trial show that Fe removal rates in the VFR where twice that of the settling lagoons even at the end of the experimental period. This suggests it should be possible to design a VFR based system that could treat the same water with half the footprint of traditional settling lagoons.

Due to events beyond the control of the author attempts to quantitatively determine the effectiveness of the VFR system in net-acid water with Fe(II) concentration an order of magnitude higher than at Taff Merthyr were inconclusive. Differences in pH between the two sites mean that rates of Fe(II) oxidation would be expected to be several orders of magnitude lower at Ynysarwed than at Taff Merthyr. Therefore accretion of ochre by the heterogeneous oxidation mechanism would be expected to play a greater role in Fe removal at Ynysarwed since Fe(II) oxidation in the water column would be much slower. In fact visual inspection of the VFR reactors suggested that this was the case as the water within the reactor tank appeared much less cloudy than for the Taff Merthyr VFR. Another qualitative result is that the ochre within the Ynysarwed VFR was dark red in colour and had a similar appearance to the RAPS sludge from the Tan-y-Garn treatment scheme which is deposited via accretion. The appearance of the sludge produced under these conditions is readily distinguishable from sludge produced via settling of precipitates and the VFR sludge at Ynysarwed was a markedly different colour from that contained within the settling lagoons at the site.

Despite the lack of quantitative measurements for the Ynysarwed VFR it was observed qualitatively that a layer of HFO did start to build up in the VFR within a few days of operation. This suggests that the system would be effective in at least partially treating this type of water. On the only day that sampling was completed effectively Fe removal was 51.5 mg/L (68% removal). Whilst this still left around 25 mg/L Fe in the water it would vastly reduce the burden on any active treatment regime that was

required further down stream resulting a reductions in both the cost of chemicals dosing and sludge dewatering. Further trials are still required in order to determine the long term removal efficiencies and useful lifetime of a VFR in treating net acid waters. Whilts the set up at Ynysarwed did povide a useful starting point for this work and proof of principle in its ability to treat net acid waters a larger scale system fed directly from the adit and not using aerated water from the wet well would last longer without clogging and provide a more reliable set of conditions for future experimentation.

5.6 Summary

All of the results and analyses presented here confirm the work previously published by Barnes (2008). The conclusions that can be drawn from this chapter are summarized below. For a more detailed discussion of all aspects of the chemical and physical characteristics of Fe and Mn removal in the VFR at Taff Merthyr see Barnes (2008).

- The VFR at Taff Merthyr was shown to remove Fe at maximum rate of 60 $g/m^2/day$. The rate of Fe(II) removal tailed off (as a result of overflow) over a period of 100 days as the thickness of HFO sludge on the gravel bed increased causing a reduction in permeability and ultimately settled at approximately 10 $g/m^2/day$.
- The major mechanism for Fe removal in the VFR was almost certainly filtration of HFO particulates and not heterogeneous catalysis of Fe(II) oxidation in the HFO bed. A combination of high Fe(II) oxidation rates in the Taff Merthyr ferruginous mine drainage and sufficient residence time in the VFR reactor tank means that dissolved Fe(II) should fall below 1 mg/L in the water column prior to passing through the HFO layer.
- Removal of dissolved Mn(II) from the ferruginous mine drainage occurs within the HFO bed in the VFR and not within the water column. The variation in Mn concentration with depth through the HFO sludge suggests that removal is at least partially autocatalytic. Whether initial Mn oxide deposition is primarily bacterially catalysed or a result of interaction with Fe(II)/(III) redox processes is unclear and requires further investigation.
- The precipitation of Mn oxides appears to catalyse the removal of a number of other trace metals. There are several possible explanations for this including, adsorption, co-precipitation and catalytic oxidation processes. Careful speciation of the other trace metals present would be required in order to determine the dominant removal process in each case.

6 Results and Discussion: Iron (II) Oxidation Rates

This chapter presents the results of the iron (II) oxidation experiments and geochemical modelling described in Chapter 4, Sections 4.5 and 4.6. The sites investigated in these experiments were Tan-y-Garn, Ynysarwed, Morlais, Lindsay, Cadley Hill and Taff Merthyr. Details of the design and history of these treatment schemes is contained within Chapter 3.

Selected data such as alkalinity and concentrations of major ions are given as measured in the field. Much of the rest of the information in the following figures is the result of geochemical and numerical modelling using the logged values of pH, temperature and dissolved oxygen (DO) that were recorded throughout the experiments. Examples of logged data are included to give an indication as to the volumes of data collected, though the majority of the raw logged data is contained within Appendix 2. The results presented in this chapter are broken down into two main sections; Homogeneous oxidation rates and k_1 and Heterogeneous oxidation rates and k_2. The first section compares the measured changes in Fe(II) concentration during the oxidation experiments to the results generated using a numerical 4^{th} order Runge-Kutta (RK4) method. The RK4 method was used to produce iterative changes in

Fe(II) over time using the rate equation for homogeneous Fe(II) oxidation and values for pH, dissolved oxygen (DO) and temperature logged every 10 seconds throughout the experiments. The fit between the measured Fe(II) concentrations and those produced using the RK4 method were optimised to give values for k_1 the rate constant for homogeneous Fe(II) oxidation. Rates of Fe(II) oxidation were higher in the field than in published laboratory studies. Three possible reasons are considered; heterogeneous autocatalysis, the possibility that secondary oxidants such as H_2O_2 are more important under field conditions than in laboratory studies and the role of bacterial oxidation.

The second section presents the results of the heterogeneous oxidation experiments where HFO solids were added to freshly emerged mine water at the Tan-y-Garn treatment scheme in order to assess their influence on the oxidation rate of Fe(II). The measured changes in Fe(II) concentration are compared to changes predicted for homogenous oxidation by the RK4 method based on the values determined for k_1 during the homogeneous oxidation experiments. Finally, the limitations of the experimental procedure and RK4 method used are discussed and recommendations are made for improvements.

6.1 Homogeneous oxidation rates and k_1

Large quantities of data were logged during the experimental runs used for the measurement of Fe(II) oxidation rates and determination of k_1 the rate constant for homogenous oxidation. Where data logged during the iron oxidation experiments are included this is intended to be indicative of the type and quantity of data collected during these experiments across all sites. A full set of all logged data is contained in Appendix 1. Experiments at each of the sites were conducted in triplicate, however only one set of results for each site is shown within this chapter and is taken to be representative of the entire data set for a particular site. Again the remainder of the data are contained within Appendix 2.

6.1.1 Background Chemistry

In order to carry out meaningful geochemical modelling using the PHREEQCi software it is necessary to know the concentrations of ions that make a significant contribution to the ionic strength of a solution in addition to the species of particular interest. These ions are described here along with pH as comprising the background chemistry of the ferruginous mine waters under investigation. The sites at which the homogeneous oxidation experiments were carried out, together with information about background chemistry and water temperature are listed in Table 6-1. Concentrations are given in mg/L as is the literature convention for much of the published work on ferruginous mine drainage. Anion concentrations were determined by ion chromatography and cation concentrations by ICP-OES as described in Chapter 4, Section 4.4.

The pH values for the freshly emerged waters were all in the range 5.6 - 6.8. Of the sites studied all were net-alkaline apart from Tan-Y-Garn and Ynysarwed which were marginally net-acidic (information provided by the UK Coal Authority). A discussion of the terms net-acid and net-alkaline are given in Chapter 2, Section 2.3. The variation in concentrations of anions and cations other than Fe(II)/(III) across the sites was relatively low, with the exception of Ynysarwed and Cadley Hill. Sulphate concentration was 2-4 times higher at Ynysarwed than at any of the other South Wales

sites. At Cadley Hill concentrations of all ions were markedly higher than at the other sites with concentrations of Na^+ and Cl^- greater by 2 orders of magnitude. Concentrations of chloride and sulphate as well as carbonate have been shown to have an effect on Fe(II) oxidation rate as described previously in Chapter 2, Section 2.2.1 and will be considered further in Section 6.1.6.

All of the measurements presented here for the South Wales site were taken during summer 2009. The experiments at Cadley Hill were carried out in winter 2009. It is important to note that the concentrations of ions and alkalinities reported here may vary from values reported later for the same sites that were revisited for the CO_2 degassing experiments in Chapter 7. These differences reflect the natural variations in ferruginous mine drainage which occur as a result of, for example, rainfall events that alter the rate of water flowing through the abandoned mine workings. All three experimental runs at each of the sites were carried one immediately after the other on the same day as samples were taken for analysis of major anions and cations presented in Table 6-1.

Table 6-1: Concentrations[a] of major cations and anions and background chemistry[10]

Site name	N[o]	Fe^{2+}	Alkalinity[b]	pH[c]	T[d]	SO_4^{2-}	Cl^-	Ca^{2+}	Na^+	K^+	Mg^{2+}
Tan-y-Garn	1	39.6	73	5.65	11.5	212	51.4	39	10	6	29
Ynysarwed	2	76.5	125	5.89	13.5	836	13.9	144	78	18	80
Morlais	3	10.4	283	6.74	14.3	348	18.0	83	89	27	49
Lindsay	4	15.6	251	6.72	15.4	225	13.3	72	64	119	60
Taff Merthyr	5	5.65	238	6.95	12.2	224	12.2	94	14	12	38
Cadley Hill	6	27.2	741	6.77	13.0	1560	5575	434	3800	98	325

[a] mg/L, [b] as $CaCO_3$ equivalent, [c] average initial pH, [d] temperature at start of experiment ^oC

[10] Values presented in this table are for freshly emerged mine water may vary from those in Table 7-3 for the same sites. This reflects the natural variations in the mine water chemistry that occur over time.

6.1.2 Rates of Fe(II) oxidation and k_1

Table 6-2 presents a set of logged data for the first 3 minutes of one of the oxidation runs carried out at the Morlais treatment scheme. Similar data was logged for each of the experimental runs at each of the sites. The pH data were then averaged over the readings of the two logging meters and input into the spreadsheet used in the calculation of k_1 using the RK4 method. Concentrations of DO were converted from ppm to atm. Temperature readings were used in the calculation of $[OH^-]$ since the dissociation constant for water K_w is temperature dependent and in the determination of k_1 which was calculated as a temperature dependent rate constant assuming an activation energy for the Fe(II) oxidation reaction of 96 kJ/mol (Stumm and Morgan 1996) It can be seen that the resulting values for k_1 were averaged over a large number of individual time steps.

Table 6-2 Logged data from an Fe(II) homogenous oxidation experiments at Morlais

Probe Time	Run time (s)	°C	pH	DO ppm	°C	pH	DO ppm
			Meter 1			Meter 2	
15:06:02	0	14.22	6.70	1.59	14.29	6.70	1.47
15:06:12	10	14.23	6.67	1.52	14.29	6.68	1.43
15:06:22	20	14.24	6.65	1.46	14.28	6.66	1.39
15:06:32	30	14.26	6.63	1.38	14.28	6.64	1.34
15:06:42	40	14.31	6.62	1.35	14.27	6.63	1.36
15:06:52	50	14.28	6.59	1.41	14.23	6.60	1.45
15:07:02	60	14.31	6.57	1.54	14.23	6.58	1.56
15:07:12	70	14.32	6.55	1.76	14.26	6.57	2.04
15:07:22	80	14.34	6.54	2.18	14.27	6.56	2.27
15:07:32	90	14.36	6.53	2.29	14.29	6.55	2.40
15:07:42	100	14.37	6.52	2.37	14.31	6.54	2.49
15:07:52	110	14.39	6.51	2.52	14.33	6.53	2.57
15:08:02	120	14.40	6.50	2.67	14.34	6.53	2.71
15:08:12	130	14.41	6.50	2.72	14.35	6.52	2.80
15:08:22	140	14.43	6.49	2.95	14.37	6.52	3.06
15:08:32	150	14.45	6.49	3.23	14.39	6.52	3.16
15:08:42	160	14.46	6.48	3.39	14.41	6.52	3.44
15:08:52	170	14.48	6.48	3.56	14.42	6.51	3.52
15:09:02	180	14.50	6.47	3.75	14.44	6.51	3.77

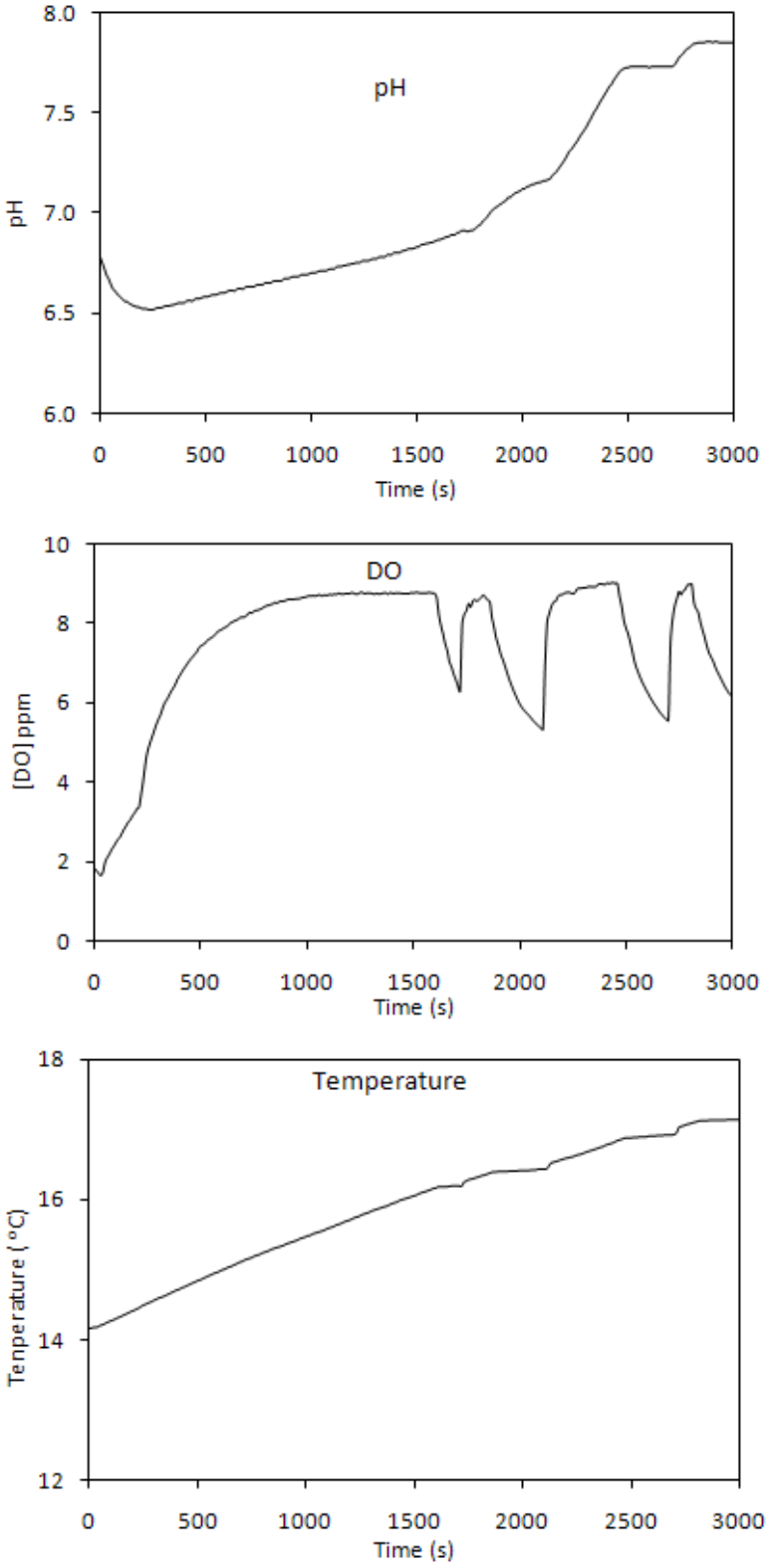

Figure 6-1: Variation in pH, DO and temperature throughout experiment at Morlais

It can be seen from Table 6-2 that none of the parameters measured pH, temperature, DO) remained constant throughout the experiments. In DO, pH and temperature all increased markedly throughout the experiments (as can be seen from Figure 6-1)

something which caused the aerated waters to become visibly turbid more quickly than water that was left to stand without agitation. This difference was most apparent for the net-acid waters where almost no HFO precipitates were visible in the standing waters even after 2 hours. This is clearly illustrated by the example of Tan-y-Garn as shown in Figure 6-2.

(a) (b)

Figure 6-2 Comparison of water at Tan-y-Garn after 2 hours (a) agitated (b) standing

In the case of the net-acid sites (Tan-y-Garn and Ynysarwed) pH began to decrease again after about 15-20 minutes whereas for the rest of the sites it continued rising right up until the end of the experiment. The shapes of the pH curves will be revisited and discussed in detail in Chapter 7. Table 6-3 shows the variations in pH that were observed throughout the experiments.

Table 6-4 gives an example of the type of spreadsheet used in the RK4 calculations. It contains data from the first 3 minutes of the experiment at the Morlais site as shown in Table 6-2. Values of Fe(II) concentration are calculated in Mols.

Table 6-3 Summary of variations in pH throughout the Fe(II) oxidation experiments[11]

Site	Initial pH	Highest pH reached	Final pH
Tan-y-Garn	5.65	6.35	5.75
Ynysarwed	5.89	6.28	5.69
Morlais	6.74	7.85	7.85
Lindsay	6.72	7.95	7.95
Taff Merthyr	6.95	8.13	8.13
Cadley Hill	6.77	7.58	7.58

Figure 6-3 compares measured changes in Fe(II) concentration to changes predicted by the RK4 method for selected experiments at each of the sites studied. The shape of the curve produced by the RK4 method fits well with the data in all cases. The ability of the numerical method to fit the empirical data means that the rate law appears to hold true for the range of conditions tested in this study. As would be expected from the rate equation for Fe(II) oxidation shown in Chapter 2, Section 2.2.1 the rates of Fe(II) oxidation were higher in the net-alkaline waters with the highest pH. The inverse squared dependence of d[Fe(II)]/dt on H^+ ion concentration over the circumneutral pH range and the logarithmic nature of the pH scale means that small increases in pH result in large increases in Fe(II) oxidation rate. An increase in pH of 1 unit should result in a 100 fold increase in oxidation rate.

It can be seen that for all of the net-alkaline sites (where pH was higher) Fe(II) concentration dropped below 1 mg/L in less than 1 hour. For Morlais, Lindsay and Taff Merthyr Fe(II) concentrations dropped below 1 mg/L in less than 30 minutes. Fe(II) concentrations did not reach this level within the 2 hour timescale of the experiment for either of the net-acid sites (where pH was lower).

[11] Highest pH reached is the highest reached over all 3 experimental runs. Final pH is the lowest pH recorded over all 3 experimental runs in the case of the net-acidic sites and the highest recorded for the net-alkaline sites. All pH values are taken as an average of the readings given by the two pH probes used.

Table 6-4: First three minutes of RK4 calculations for Morlais data

°C	pH	DO ppm	DO[a]	[H+]	[OH]^{2b}		RK4[d]				Fe(II)
Mean meter reading			(atm)	(M)	(M)	ϑ [c]	x_1	x_2	x_3	x_4	(M)
14.47	6.57	1.10	0.022	2.72E-07	2.34E-16	4.150	-1.00E-08	-1.00E-08	-1.00E-08	-1.00E-08	1.80E-04
14.47	6.56	1.09	0.022	2.79E-07	2.24E-16	4.150	-9.55E-09	-9.55E-09	-9.55E-09	-9.54E-09	1.80E-04
14.46	6.55	1.10	0.022	2.85E-07	2.14E-16	4.153	-9.14E-09	-9.14E-09	-9.14E-09	-9.14E-09	1.80E-04
14.46	6.55	1.10	0.022	2.85E-07	2.14E-16	4.153	-9.14E-09	-9.13E-09	-9.13E-09	-9.13E-09	1.80E-04
14.43	6.54	1.13	0.023	2.92E-07	2.03E-16	4.171	-8.87E-09	-8.87E-09	-8.87E-09	-8.87E-09	1.80E-04
14.37	6.53	1.26	0.025	2.99E-07	1.92E-16	4.206	-9.30E-09	-9.30E-09	-9.30E-09	-9.30E-09	1.80E-04
14.41	6.52	1.35	0.027	3.06E-07	1.85E-16	4.183	-9.60E-09	-9.60E-09	-9.60E-09	-9.60E-09	1.79E-04
14.44	6.51	1.39	0.028	3.13E-07	1.77E-16	4.168	-9.51E-09	-9.51E-09	-9.51E-09	-9.51E-09	1.79E-04
14.45	6.51	1.42	0.029	3.13E-07	1.77E-16	4.159	-9.76E-09	-9.76E-09	-9.76E-09	-9.76E-09	1.79E-04
14.46	6.51	1.44	0.029	3.13E-07	1.78E-16	4.153	-9.93E-09	-9.92E-09	-9.92E-09	-9.92E-09	1.79E-04
14.48	6.50	1.45	0.029	3.16E-07	1.74E-16	4.145	-9.81E-09	-9.81E-09	-9.81E-09	-9.81E-09	1.79E-04
14.49	6.50	1.48	0.030	3.20E-07	1.71E-16	4.136	-9.83E-09	-9.83E-09	-9.83E-09	-9.82E-09	1.79E-04
14.50	6.50	1.50	0.030	3.20E-07	1.71E-16	4.130	-9.99E-09	-9.99E-09	-9.99E-09	-9.98E-09	1.79E-04
14.51	6.50	1.53	0.031	3.20E-07	1.71E-16	4.124	-1.02E-08	-1.02E-08	-1.02E-08	-1.02E-08	1.79E-04
14.53	6.50	1.55	0.031	3.16E-07	1.76E-16	4.116	-1.06E-08	-1.06E-08	-1.06E-08	-1.06E-08	1.79E-04
14.54	6.51	1.57	0.032	3.13E-07	1.80E-16	4.110	-1.11E-08	-1.11E-08	-1.11E-08	-1.11E-08	1.79E-04
14.55	6.51	1.60	0.032	3.09E-07	1.84E-16	4.104	-1.16E-08	-1.16E-08	-1.16E-08	-1.16E-08	1.78E-04
14.56	6.52	1.62	0.033	3.06E-07	1.89E-16	4.098	-1.20E-08	-1.20E-08	-1.20E-08	-1.20E-08	1.78E-04

[a] From Henry's law, K_H = 769 L atm mol^{-1},(temperature correction factor C = 1500 K)

[b] Calculated using [OH$^-$] = 1 x 10^{-14} x 0.1253 x e$^{-0.0831 \times T}$

[c] From Arrhenius equation using E_a = 96 kJ/mol (Stumm and Morgan 1996)

[d] See Chapter 4, Section 4.5.3 for details of equations

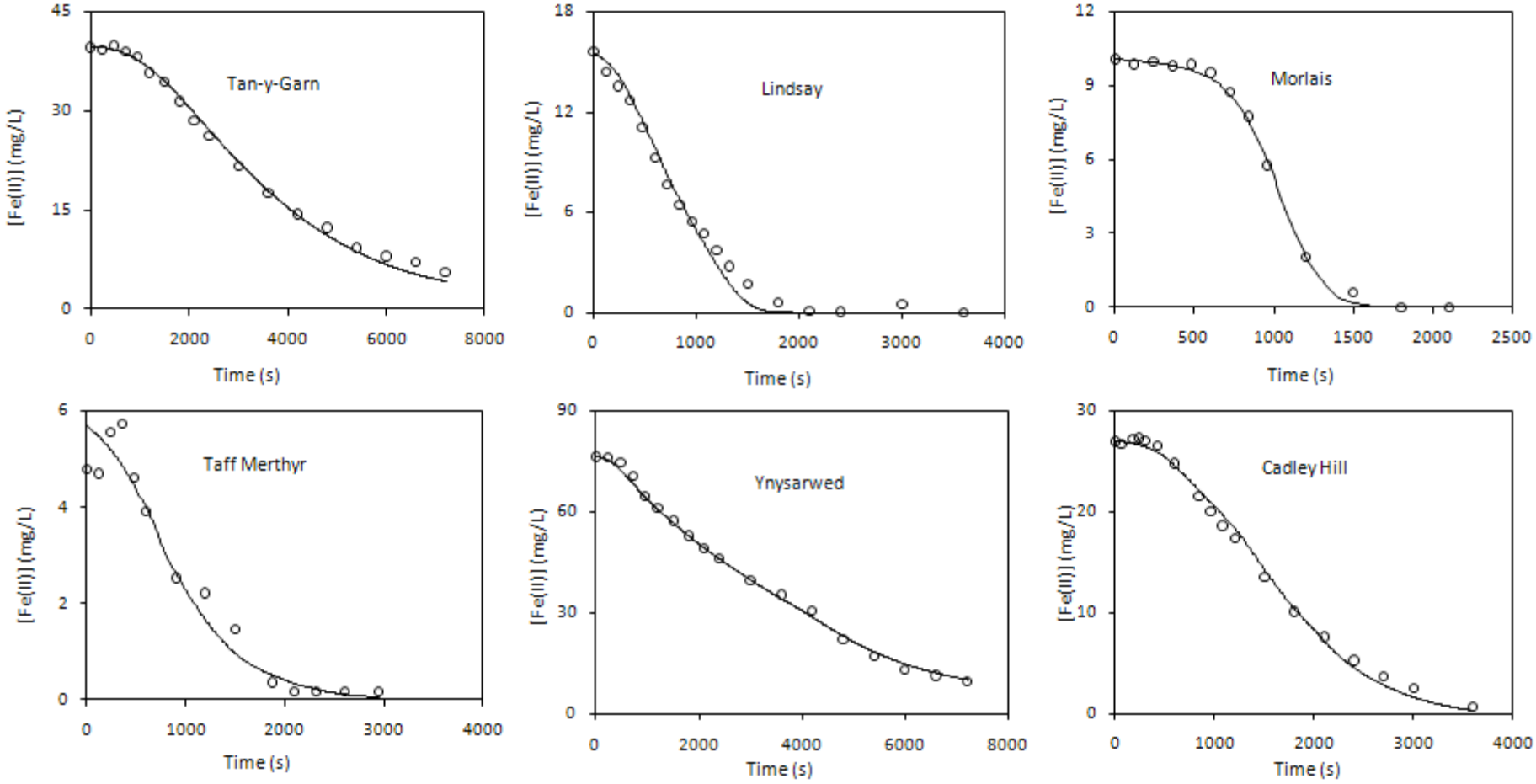

Figure 6-3 Experimental (open symbol) and predicted (unbroken line) changes in Fe(II) concentration during oxidation experiments.

6.1.2.1 Shape of the curve for [Fe(II)] vs time

The vast majority of the work previously published on iron(II) oxidation chemistry has been carried out in systems where the key parameters of pH, DO and temperature were controlled (e.g. Shenk and Webber 1968; Millero 1985; Liang 1993). In the work presented here however these parameters were allowed to vary freely throughout the experiments. The resulting shapes of the curves for d[Fe(II)]/dt are therefore very different from those which would normally be seen in the literature.

Figure 6-4 shows a comparison of real data measured in the field to data modelled for the same site (using the RK4 method) at fixed k_1, pH, temperature and DO with [Fe(II)] the only variable allowed to change. The resulting curve (b) is typical of 1st order chemical kinetics.

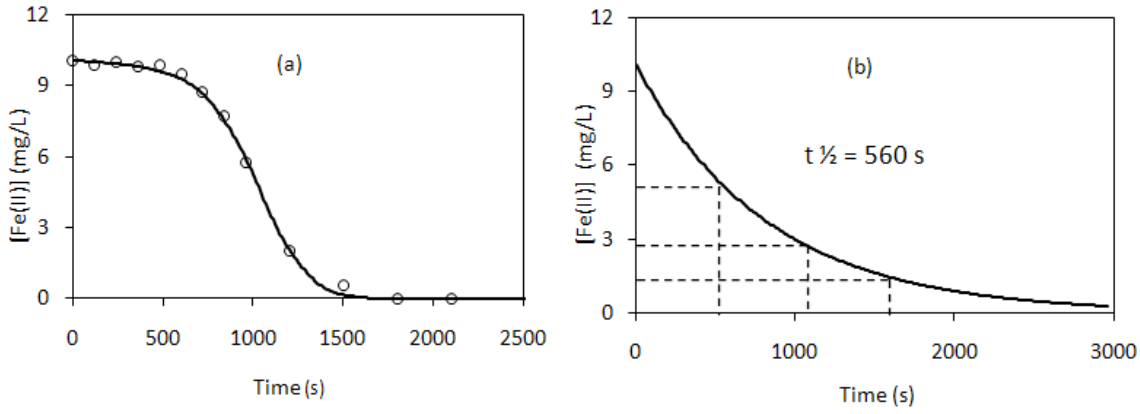

Figure 6-4 Comparison of field determined changes in Fe(II) concentration (a) with changes modelled for constant pH, temperature and DO (b)[12]

The difference between the shapes of the two curves can be explained by the changing pH as well as, to a lesser extent, DO and temperature during the course of the field experiments that produce the s shaped curve (a). In the field experiments (curve (a)) [Fe(II)] initially changes slowly as pH and DO are relatively low. As the experiment proceeds aeration causes not only an increase in DO but also CO_2 degassing (discussed in detail in Chapter 7) which in turn leads to rising pH levels. The 2nd order dependence

[12] Data for (a) taken from an experiment at the Morlais treatment scheme

of d[Fe(II)]/dt on $[H^+]$ (Kirby et al. 1999) means that rising pH causes the rate of Fe(II) oxidation to increases rapidly. The result is that Fe(II) oxidation rate increases during the initial stages of the experiment giving rise to the s shaped curves seen in Figure 6-3. Increasing levels of dissolved oxygen during the first few minutes enhance this effect as does the slight rise in temperature over the course of the reaction. For the net-acidic sites at Tan-y-Garn and Ynysarwed, Fe(II) oxidation rate decreases again towards the end of the experiment as acid generation resulting from the formation of HFO (see Chapter 2, Section 2.2.1) causes pH to decrease.

In the case where all variables (pH, DO, temperature) are held constant apart from [Fe(II)] (curve (b)) the rate of reaction is fastest at the beginning of the experiment where [Fe(II)] is greatest. As Fe(II) is consumed during the experiment the rate of reaction steadily decreases giving a curve with a constant half-life typical of 1^{st} order chemical kinetics. The pH input into the RK4 simulation to produce this curve was 6.8 and Po_2, 0.161 atm. This was the same as the average pH and Po_2 taken over the course of the experiment represented in curve (a).

6.1.2.2 Comparison of k_1 values across the sites studied

The RK4 method was run for each set of experimental data across each of the sites. The rate equation for Fe(II) oxidation as described in Chapter 2 Section 2.2.1 was used to model changes in [Fe(II)] based on logged values of pH, DO and temperature. The curves produced were then optimised with respect to obtaining a curve of best fit to the measured changes in [Fe(II)] by varying the input value for k_1 the rate constant for homogeneous Fe(II) oxidation. The range of values of k_1 calculated for each of the sites is shown in Figure 6-5. The filled circles show the value of k_1 averaged over 3 experimental runs. Each value of k_1 used in calculating these averages was itself determined using pH readings averaged over the two logging pH meters. This averaging over the two sets of pH readings was intended to minimise the error introduced by inaccuracies in pH measurement. In order to show the range of values that can be produced by even small differences in pH measurement the error bars in Figure 6-5 show the values of k_1 calculated using the highest and lowest sets of logged data from each of the two pH meters without averaging. The average values for k_1

ranged from $8.08x10^{14}$ to $1.29x10^{16}$ $M^{-2}atm^{-1}min^{-1}$. These are the temperature dependent values calculated based on an activation energy of 96 kJ/mol (Stumm and Morgan 1996). Temperature independent values were also calculated (effectively assuming an activation energy of zero) to assess the influence of the value chosen for activation energy to the final values of k_1. The temperature independent values of k_1 were found to be in the range $9.12x10^{13}$ – $6.00x10^{15}$ $M^{-2}atm^{-1}min^{-1}$, an order of magnitude smaller at the lower limit and 50% smaller at the upper limit than the temperature dependent values. Both temperature dependent and temperature independent values for k_1 were significantly larger than those published based on laboratory studies as discussed in the following Section (6.1.5).

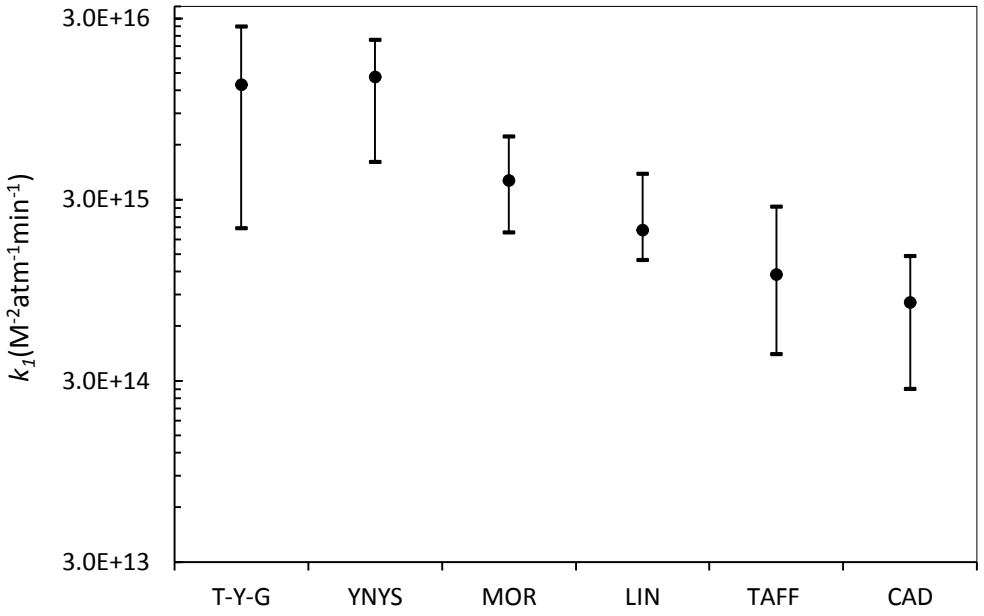

Figure 6-5 Range of values for k_1 across each of the sites[13]

6.1.2.3 Accuracy of pH measurement and implications for k_1

As discussed previously in this thesis (Chapter 2) and by other authors (Davison and Seed 1983) the greatest source of error in calculating values for k_1 is pH measurement. It was for this reason that all pH measurements taken during this study were recorded in duplicate. Over the course of the experiments there was variation between the

[13] Points represent values averaged over 3 experimental runs.

values recorded by the two pH probes despite daily calibration and regular cleaning. Figure 6-5 shows how these differences in recorded pH affect the calculated values of k_1. The maximum range based on the highest and lowest sets of recorded pH values are marked by the error bars. The largest differences between the pH values recorded by the two pH probes were for the Tan-y-Garn experiments and resulted in maximum possible range of k_1 values of just over an order of magnitude. As will be seen in the following section however this does not affect the main findings of this study.

6.1.2.4 Comparison of k_1 with previously published values

The variation in the values calculated for k_1 by the RK4 model was much wider than expected with a range of two orders of magnitude. Given that the experiments were all conducted within the circumneutral pH range over which the chosen rate equation should hold true (see Chapter 2, Section 2.2.1) it was surprising to see how much the field determined values deviated from published laboratory studies. The values for k_1 reported in this thesis are compared to a number of different literature studies reporting on laboratory based experiments in Table 6-5. The table also contains a summary of the most important experimental parameters from each of these reported studies.

Table 6-5 Comparison of results to reported literature values for k_1

Authors	k_1 (M^{-2} atm^{-1} min^{-1})	Comments
Stumm and Lee (1961)	$1.5(\pm 0.5) \times 10^{13}$	pH=6.50-7.24, T=20.5°C, Po_2 variable, $[Fe(II)]_0$<50µM
Shenk and Webber (1968)	$2.1(\pm 0.5) \times 10^{13}$	pH=6.70 ,T=25°C, Po_2=0.21atm, $[Fe(II)]_0$<50µM
Davison and Seed (1983)	$1.5 - 3.2 \times 10^{13}$	pH=7.0, T=25°C, Po_2 variable, $[Fe(II)]_0$>5µM
Millero(1985)	$2.0 - 3.2 \times 10^{13}$	Varies according to ionic strength as $\text{Log } k_1 = 13.82 - 2.805\ \text{I}^{1/2} + 1.82\ \text{I}$ Values quoted for $0.1 \leq I^{1/2} \leq 0.6$
Liang et al (1993)	3.0×10^{13}	pH=6.84, T=25°C, Po_2=0.2, $[Fe(II)]_0$=34.6µM Converted from 1.90×10^{-12} Mmin^{-1} using $k_w=10^{-14}$
Geroni and Sapsford (2011)	$8.1 \times 10^{14} - 1.3 \times 10^{16}$	pH=6.8-7, T=20.5°C, Po_2=0.2atm, $Fe[(II)]_0$= 60-65µM pH=5.65-7.85, Po_2 variable, T= temperature corrected to 25°C, $[Fe(II)]_0$= 100-1370µM (temperature corrected to 25°C)

All of the results quoted from laboratory studies were from experiments carried out within the pH range 6.50 – 7.24 and within the temperature range 20.5 – 25°C.

Concentrations of Fe(II) were within the µM range with [Fe(II)] at the beginning of the experiment ranging from 5 - 65 µM. Stumm and Lee (1961) and Davison and Seed (1983)quoted variable Po_2 values of 0.107 – 0.197 atm and 0.09 – 0.45 atm respectively, all other experiments were carried out at Po_2 = 0.2 atm.

The previously published studies shown in Table 6-1 are in good agreement in terms of their values of k_1 varying by only a factor of 2 between the lowest to the highest values. The difference when compared to the results from the field trials carried out in the current study however is much more significant at 1-3 orders of magnitude for the temperature dependent values and up to 2 orders of magnitude for the temperature independent values. There was nothing immediately apparent in the experimental procedures or the experimental conditions that could account for this difference. It was decided therefore to investigate in more detail the variations in background chemistry as described in the following sections in an attempt to account for the unexpected values (and range of values) obtained for k_1.

6.1.2.5 Effect of background chemistry on k_1

A number of background chemistry parameters have been shown to have an effect on Fe(II) oxidation rate. As discussed in Chapter 2, section 2.2.1 several anions commonly found in ferruginous mine drainage can form ion pairs with dissolved Fe(II) which have the effect of either increasing or decreasing oxidation rates compared to what would be expected were these anions not present. Sung and Morgan (1980) showed marked reductions in Fe(II) oxidation rate in the presence of Cl^- and SO_4^{2-} as a result of the formation of $FeSO_4$ and $FeCl^+$ ion pairs which are slower to react than hydrolysed Fe(II) species. They showed that the half life of Fe(II) in solution (pH 6.5) increased from just over 3 hours with 0.1M NaCl to nearly 23 hours with 0.5M NaCl. By contrast King (1998) showed that in solutions with carbonate concentration higher than 1mM and pH greater than 6 trace concentrations of the fast reacting $Fe(CO_3)_2^{2-}$ complex can dominate the oxidation kinetics, though the mole fraction of Fe(II) carbonate species decreases rapidly below pH 7.

In line with the studies mentioned previously concentrations of Cl^-, SO_4^{2-} and CO_3^{2-} were considered to be the most relevant to the current work as these were present in

concentrations comparable to, or greater than Fe(II) concentration across the sites studied. Values for concentrations of all the major cations and anions as well as pH, alkalinity and temperature were input into PHREEQCi in spreadsheet mode in order to determine the speciation of Fe(II) in each of the waters under investigation. Values for the concentrations of ion pairs most likely to affect the rate of Fe(II) oxidation were compared to k_1 across the sites. If Cl^- and/or SO_4^{2-} were influencing the oxidation rates it was expected to see a negative correlation between the concentrations of these species and k_1. For the purposes of modelling, concentrations of the ionic species were converted from mg/L to mol/L (M) as shown in Table 6-6.

Table 6-6 Concentrations (M) of ions used in PHREEQCi modelling

Site name	Fe^{2+}	CO_3^{2-}	SO_4^{2-}	Cl^-	Ca^{2+}	Na^+	K^+	Mg^{2+}
Tan-y-Garn	7.1E-04	7.3E-04	2.1E-03	1.4E-03	9.8E-04	4.3E-04	1.5E-04	1.2E-03
Ynysarwed	1.4E-03	1.3E-03	8.4E-03	3.9E-04	3.6E-03	3.4E-03	4.6E-04	3.3E-03
Morlais	1.9E-04	2.8E-03	3.5E-03	5.1E-04	2.1E-03	3.9E-03	6.9E-04	2.0E-03
Lindsay	2.8E-04	2.5E-03	2.3E-03	3.7E-04	1.8E-03	2.8E-03	3.1E-03	2.5E-03
Taff Merthyr	1.0E-04	2.4E-03	2.2E-03	3.4E-04	2.4E-03	6.1E-04	3.1E-04	1.6E-03
Cadley Hill	4.9E-04	7.4E-03	1.6E-02	1.6E-01	1.1E-02	1.7E-01	2.5E-03	1.4E-02

Concentrations of $FeSO_4$ and ion pairs are compared to the values obtained for k_1 in Figure 6-6. There appeared to be a positive correlation between the two sets of values in the case of $FeSO_4$ though this was not linear as the R^2 value was 0.53. In the case of $FeCl^+$ it can be seen that at low concentrations there was wide variation in k_1. The outlier on this chart is Cadley Hill where higher $FeCl^+$ could be at least partially responsible for the lower values of k_1. Since there was not a strong correlation in either case and since the general trend that would be expected based on the literature should be negative and not positive it was concluded that $FeSO_4$ and $FeCl^+$ concentrations could not be used to explain the variation in k_1 across the sites studied.

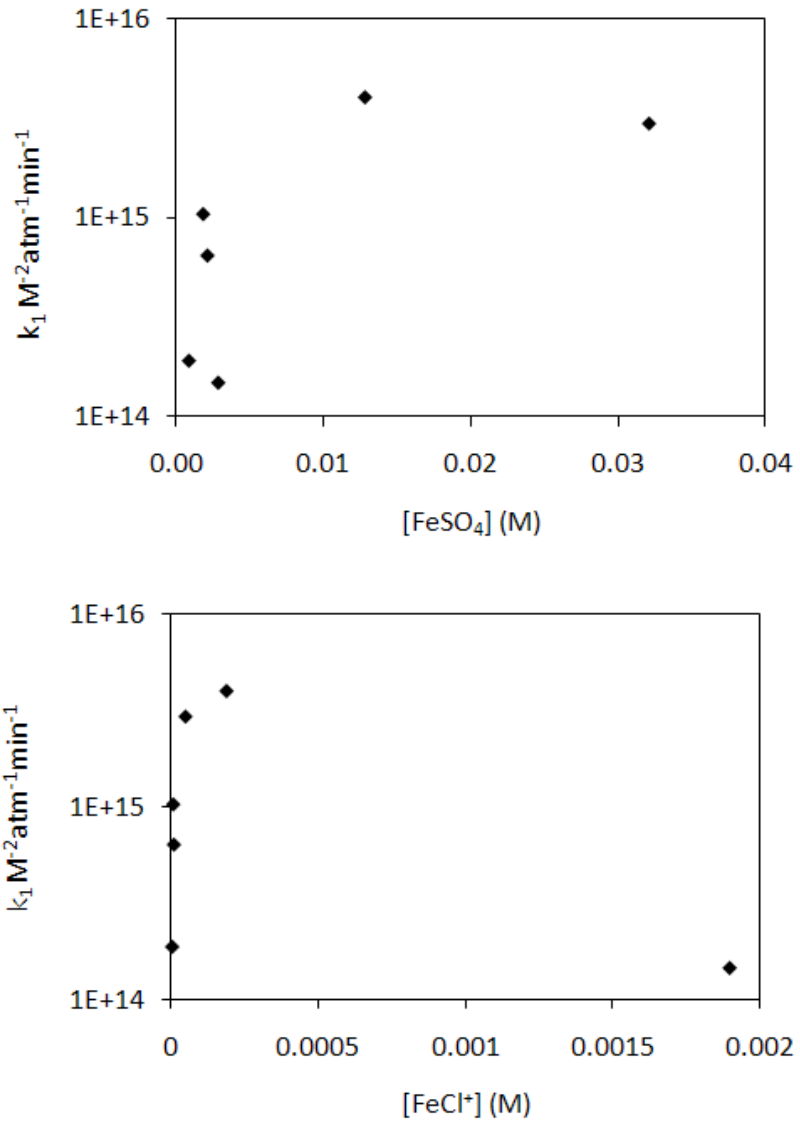

Figure 6-6 Comparison of k_1 with [FeSO4] and [$FeCl^+$]

Much of the previous work looking at the effects of anion concentrations on Fe(II) oxidation rates has been carried out in brines or seawater (e.g. Millero et al (1987) and Santana-Cassiano et al (2004)) The concentrations of Cl^- and SO_4^{2-} in these waters as in the laboratory investigation of Sung and Morgan (1980) give ratio of Fe^{2+}:anion upwards of 1:1250, far higher than at any of the sites investigated here (with the exception of the Cadley Hill) which had Fe^{2+}:anion ratios of the order of 1:1 to 1:10. As a result the concentrations of the slow reacting $FeSO_4$ and $FeCl^+$ ion pairs only made up a small proportion of dissolved Fe(II) and did not greatly influence the oxidation rate. Millero et al (1987) showed k_1 decreasing by a factor of 4 as ionic strength of a saline solution (made up from dilutions of seawater) increased from 9 x 10^{-3} M to 0.723 M.

Since a 3 order of magnitude change in salinity only resulted in a change in k_1 by a factor of 4 in for Millero et al (1987) it seems unlikely that variations in SO_4^{2-} and Cl^- of 1 order of magnitude in the experiments presented here could result in order of magnitude differences in k_1.

At concentrations greater than 1mM alkalinity and pH > 6 the ion pair determined as being dominant in terms of accelerating Fe(II) oxidation rate is $Fe(CO_3)_2^{2-}$ (King 1998). Alkalinity at all of the sites studied was within the mM range. A look at the concentrations of CO_3^{2-} in Table 6-6 however shows that carbonate concentrations were lowest at the sites with the highest values for k_1, Tan-y-Garn and Ynysarwed and highest for the sites with the lowest k_1 value Cadley Hill. Again, this trend goes against what would be expected, and so again it was concluded that the presence of $Fe(CO_3)_2^{2-}$ was unlikely to be responsible for the higher than expected rates of Fe(II) oxidation. This finding can also be explained by the relative concentrations of Fe(II):anion. The study by King (1998) was conducted on lake and sea waters where Fe(II) concentrations were in the range 1-5 µM compared to 100-1400 µM in this study giving the ratio $[Fe(II)]:[CO_3^{2-}]$ in the range 1:7200 and again 1:1 – 1:10 respectively. The proportion of Fe existing as $Fe(CO_3)_2^{2-}$ is therefore likely to be much lower in the ferruginous mine drainage used in the oxidation experiments described in this thesis (and given the lower pH at the net-acidic sites less likely to dominate the reaction kinetics).

Figure 6-7 reproduced from King (1998) shows how speciation of Fe(II) changes with pH over the range pertinent to this thesis. Direct comparison with the work presented here is difficult as the concentrations of NaCl and Na_2SO_4 are much higher than in the mine waters, but it can be seen that below pH 7 concentrations Fe(II) carbonate species drop off rapidly suggesting decreasing Fe(II) oxidation rates as the slow reacting species begin to dominate. Again this is contrary to the high Fe(II) oxidation rates (and correspondingly high k_1 values) measured at the sites with pH < 6 in the current study.

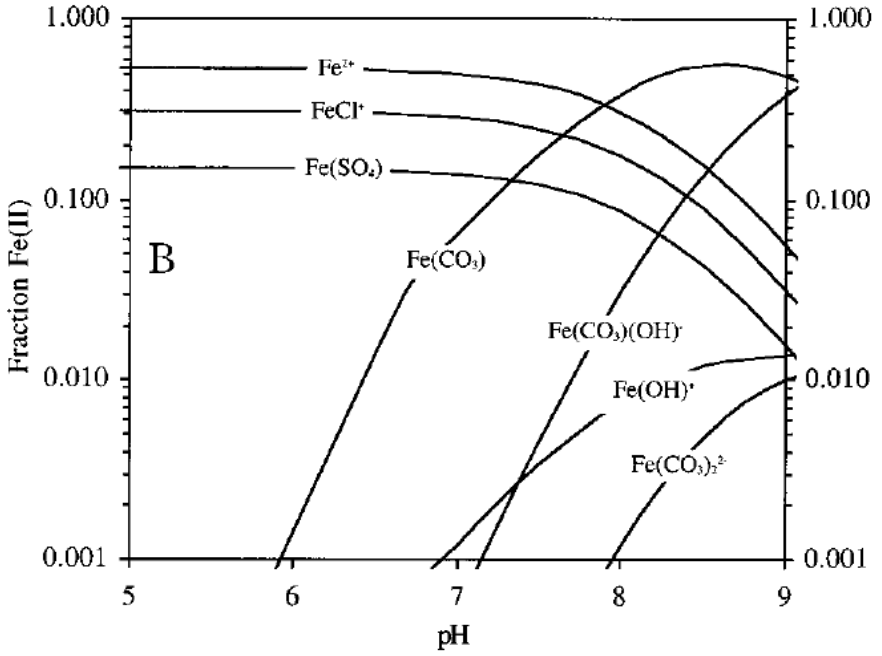

Figure 6-7 Fe(II) speciation in 0.7M NaCl, 0.03M Na_2SO_4, 2.3mM $NaHCO_3$, 0.03 atm Pco_2
Reproduced from King (1998)

6.1.2.6 Effect of pH on k_1

As described in Chapter 4, Section 4.5, pH was logged every 10 seconds throughout the experiments and corresponding values for $[H^+]$ were input into the RK4 method used to calculate k_1. The resulting values for k_1 produced by the RK4 method should therefore have been independent of pH. It was noticed however that the values of k_1 did appear to show a correlation with pH. In order to test the significance of this correlation k_1 was plotted vs $[H^+]$. Figure 6-8 shows a plot of $[H^+]$ values vs k_1 and since pH was not controlled in the experiments values for $[H^+]$ were determined by averaging H^+ ion concentration over each experimental run. It can be seen that there is a strong positive correlation between the two sets of values with $R^2 = 0.98$. This result suggests that iron oxidation reactions occuring in the systems under investigation can not be adequately described by the homogeneous mechanism alone.

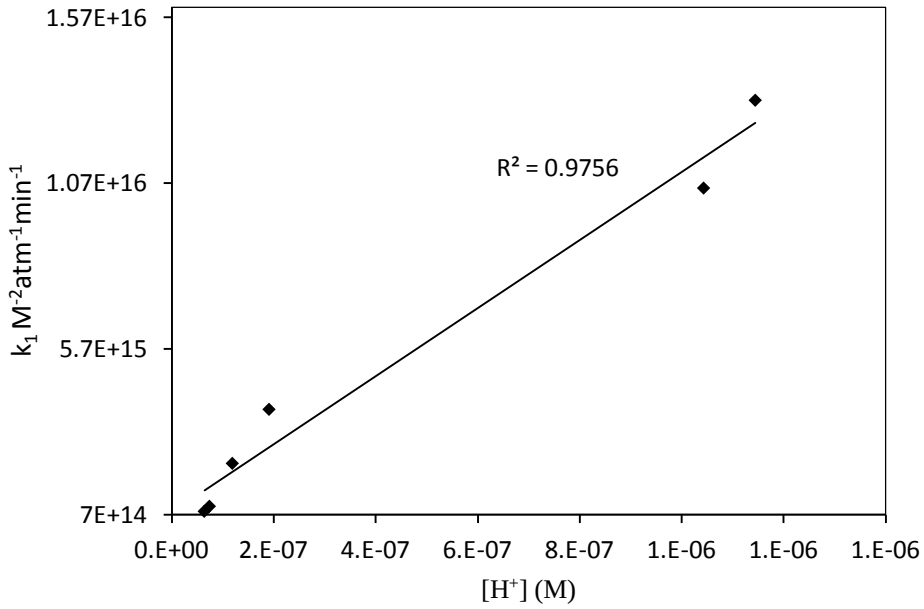

Figure 6-8 Comparison of k_1 values with $[H^+]$ across the sites studied

Three possible mechanisms were considered in an attempt to account for the deviation from the behaviour predicted by the rate equation for homogenous iron oxidation, heterogeneous autocatalysis, the contribution of secondary oxidants such as H_2O_2 to the overall oxidation rate under conditions in the field, and the contribution of bacterial Fe(II) oxidation. These mechanisms are discussed in more detail in the following sections.

6.1.2.7 Potential role of autocatalytic heterogeneous Fe(II) oxidation

Equation 6-1 (from Tamura et al (1976)) describes both the homogeneous and heterogeneous pathways for Fe(II) oxidation with the corresponding rate constants k_1 and k_2. It can be seen from the equation that pH has a greater influence on the rate of homogeneous oxidation compared to heterogeneous oxidation with the two pathways having inverse second and first order dependence on $[H^+]$ respectively. The result is that according to Equation 6-1 heterogeneous oxidation should become increasingly important with respect to homogeneous oxidation as pH decreases. In cases where no additional HFO solids are added to the reaction mixture the heterogeneous pathway can have an autocatalytic effect and increase the overall oxidation rate as a result of Fe(III) produced in-situ (Sung and Morgan, (1980)).

Equation 6-1 $$-\frac{\mathbf{d[Fe(II)]}}{\mathbf{dt}} = (\boldsymbol{k_1}[\mathbf{H^+}]^{-2}\mathbf{P_{O_2}} + \boldsymbol{k_2}[\mathbf{Fe(III)}][\mathbf{H^+}]^{-1}\mathbf{P_{O_2}})[\mathbf{Fe(II)}]$$

Equation 6-2 $$[\mathbf{Fe(II)_{sorb}}]/[\mathbf{Fe(II)}] = \boldsymbol{K}[\mathbf{Fe(III)}]/[\mathbf{H^+}]$$

In their experiments Sung and Morgan (1980) only observed autocatalysis in waters above pH 7. This can be explained in terms of the pH dependence of Fe(II) adsorption onto the surface of HFO solids as shown by Equation 6-2 (Tamura et al (1976)). As pH decreases and $[H^+]$ increases the proportion of sorbed Fe(II) decreases so that at pH<7 the proportion of [Fe(II)] that is sorbed is too low to have a significant influence on the overall oxidation rate. In their experiments Sung and Morgan used concentrations of Fe(II) in the range 34.7-50 µM compared to 100-1400 µM in the mine waters in this study. Over the course of an oxidation experiment this would result in suspended HFO concentrations 2 – 28 times greater in the mine waters than in Sung and Morgan's experiments. This increased solids concentration could result in a greater contribution from the autocatalytic heterogeneous oxidation pathway and has been discussed previously by Tufekci and Sarikaya (1996).

In order to assess the potential contribution of heterogeneous oxidation to the systems under investigation, the measured oxidation rates were compared to previously published rates of heterogeneous oxidation and other field measured rates. The results are shown in Figure 6-9. The broken lines delineate the upper and lower limits for Fe(II) oxidation rate from this study with the solid line denoting homogeneous oxidation rates for k_1= 2.0 x 10^{13} $M^{-2}atm^{-1}min^{-1}$ (from Davison and Seed 1983). The Fe(II) oxidation rates were calculated based on DO of 0.1 atm and [Fe(II)] of 5 mg/L (893 µM). Data points shown for other studies were calculated based on $[Fe(II)]_0$ of 5 mg/L. It should be noted that the temperature of the experiments for the field measured rates of Kirby and Brady (1998) was 11-12 ^oC. If a temperature correction were applied with an activation energy of 96 kJ/mol as used elsewhere in this thesis the oxidation rate would be approximately 1 order of magnitude higher at 25 ^oC. Park and Dempsey (2005) added concentrations of HFO solids an order of magnitude greater than concentrations of Fe(II), but their reaction rates were controlled by low Po_2) 0.002 - 0.0096 atm. Dempsey et al (2001) did not give precise Fe(III) concentrations as their experiment was based on the addition of a slug of HFO

into flowing water taking measurements of Fe(II) concentrations up and down stream of the addition. The example taken from Tufekci and Sarikaya (1996) was based on the addition of 5 mg/L HFO solids.

Discounting the possibility of a contribution from biotic oxidation the main difference between the chemical composition of the waters considered here and those of earlier laboratory studies is the total iron concentration. Table 6-5 shows that the initial concentrations of [Fe(II)] were 1-2 orders of magnitude higher in the mine drainage than in any of the laboratory based work. Given the higher concentrations of catalytic Fe(III) particulates that would therefore be formed in the water column it is likely that the effect of the heterogeneous oxidation is more significant in these natural waters. It has previously been noted by Pham and Waite (2008) that different reaction pathways for Fe(II) oxidation predominate at the micromolar and nanomolar scales and that heterogeneous catalysis could account for higher rates observed at micromolar Fe(II) concentrations.

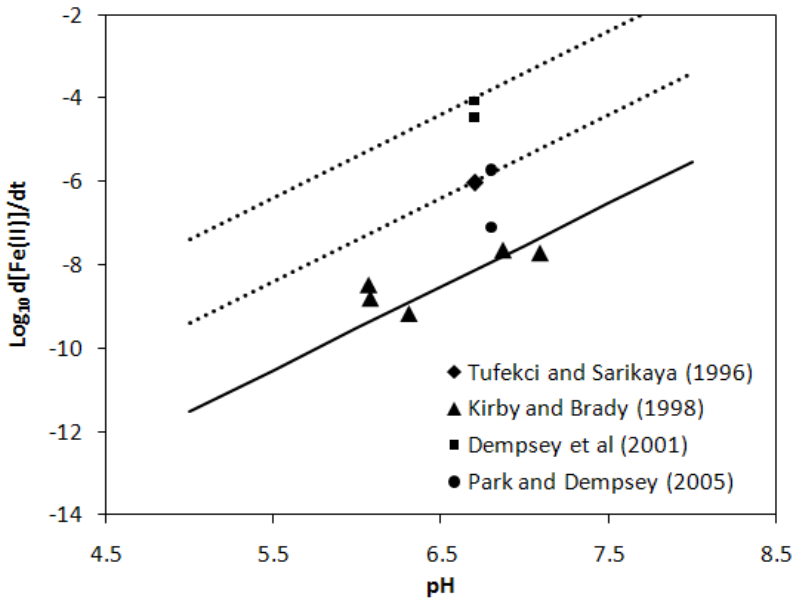

Figure 6-9 Comparison of Fe(II) oxidation rates from this study with previously determined field, and heterogeneous rates[14]

[14] Field oxidation rates (Kirby and Brady 1998), heterogeneous oxidation rates (Tufekci and Sarikaya 1996, Dempsey et al 2001, Park and Dempsey 2005). All values corrected to Ms^{-1}. The solid line represents expected oxidation rates based on $k_1 = 2.0 \times 10^{13}$ $M^{-2}atm^{-1}min^{-1}$ see Table 6-5 for references. Broken lines delineate the upper and lower limits for d[Fe(II)]/dt based on the values of k_1 determined in the current study.

6.1.2.8 Fe(II) oxidation by H_2O_2 in natural waters

As described in Chapter 2 Section 2.2.1 and reproduced in Table 6-7 several oxidising species are produced as a result of the Fe(II) oxidation reaction itself which may contribute to the overall Fe(II) oxidation rate. Both $O_2^{-\bullet}$ and $OH^{\bullet}$ are very fast reacting and may in fact react with species other than Fe(II) in the water column with the overall rate of Fe(II) oxidation usually determined by either reaction 1 or 3 (King et al. 1995).

Table 6-7: Mechanism of homogeneous Fe(II) oxidation

Reaction	No.
$Fe^{2+} + O_2 \rightarrow Fe^{3+} + O_2^{-\bullet}$	1
$Fe^{2+} + O_2^{-\bullet} + 2H^+ \rightarrow Fe^{3+} + H_2O_2$	2
$Fe^{2+} + H_2O_2 \rightarrow Fe^{3+} + OH^{\bullet} + OH^-$	3
$Fe^{2+} + OH^{\bullet} \rightarrow Fe^{3+} + OH^-$	4

Numerous authors have conducted studies to investigate the relative importance of Fe(II) oxidation by O_2 and H_2O_2 in natural systems (e.g. Emmenegger et al. 1998; Rose and Waite 2002; Pham and Waite 2008). Examples of such studies have been discussed in Chapter 2 Section 2.2 (e.g. Millero and Sotolongo 1989; Emmenegger et al. 1998) showing that in lake and sea waters over the pH range 6.5-8 O_2 is the dominant oxidising species. Many of these investigations of natural waters however have been carried out at nanomolar concentrations of Fe(II) where the reaction kinetics differ from those observed at micromolar concentrations (Pham and Waite 2008). This makes interpretation in light of these previous studies, of the oxidation rates and k_1 measured here difficult due to the relatively high concentrations of Fe(II) found in ferruginous mine water. Whilst it is possible that both hydrogen peroxide and the superoxide species generated as a result of Fe(II) oxidation could be contributing to the accelerated rate of reaction there is little discussion of this in the literature for ferruginous mine water.

Aside from the reactions in Table 6-7oxidising species can be generated in Fe bearing waters by the interaction of HFO solids and organic Fe(II)/(III) complexes with UV light. The degradation of organic complexes by UV light can result in the release of organic radicals in addition to the species generated by the Fe(II)/Fe(III) redox processes (though these reactions may also be accompanied by a reduction of Fe(III)/Fe(II)) (Hug et al. 2001). Oxidising radicals are also generated by the photo reductive dissolution of HFO in the presence of UV light (Borer et al. 2009), but again this is accompanied by a regeneration of Fe(II) and so is unlikely to accelerate the overall rate of oxidation. Since no attempt was made to control levels of light reaching the experiments, and the concentrations and speciation of organic carbon in the sample is unknown it is difficult to draw any conclusions about the influence of these reactions on the overall rate of Fe(II) oxidation.

6.1.2.9 Bacterial Fe(II) oxidation in ferruginous mine drainage

It has been widely accepted that in the case of ferruginous mine water bacterial oxidation of Fe(II) has the greatest contribution to the overall oxidation rate within the acidic range (< pH 5) (Kirby et al. 1999). This finding has been confirmed by a number of authors for ferruginous mine drainage scenarios (including Hallberg and Johnson 2003 and Noike et al. 1983) as discussed in Chapter 2, Section 2.2.1. At circumneutral pH the rate of bacterial oxidation of Fe(II) by species such as *Gallionella ferruginea* only becomes competitive with abiotic oxidation under sub-oxic conditions (Sobolev and Roden 2001). Thus for the well aerated circumneutral waters described in this thesis bacterial contribution to the overall rate it is unlikely to be the dominant reason for the high values of k_1.

6.1.3 The need for a revised rate equation

The results presented thus far imply the need for a revised rate equation which provides an additional reaction pathway to that of homogeneous oxidation alone. To that end the RK4 model used in the calculation of k_2 for the heterogenous oxidation experiments (See Chapter 4) was applied to the data from the homogenous oxidation experiments. Precipitation of HFO was assumed to be instantaneous and so the

concentration of Fe(III) particulates was calculated according to Equation 6-3 where $[Fe(II)]_o$ is the concentration at the start of the experiment and $[Fe(II)]_t$ is the concentration at time t.

Equation 6-3 $$[Fe(III)] = [Fe(II)]_o - [Fe(II)]_t$$

For the updated model k_1 was taken to be 2.0 x 10^{13} $M^{-2}atm^{-1}min^{-1}$ as suggested by laboratory studies in the literature (see table 6-5). Values for k_2 were then chosen so as to give the best fit with the measured data and the changes in Fe(II) concentration predicted by the RK4 model. It was hoped that this change to the RK4 model would allow the application of the same k_1 value across all of the sites, with any deviation from the expected oxidation rate accounted for by the heterogeneous part of the rate equation and k_2. It was found however that incorporating the heterogeneous autocatalytic pathway into the predictions for changing Fe(II) concentration resulted in predicted values significantly different to those measured (see Figure 6-10). This was in stark contrast to the values predicted by the RK4 method for homogenous oxidation alone (Figure 6-3). The shapes of the curves produced (shown in Figure 6-10) are typical of what would be expected for an autocatalytic reaction with a lag phase during the initial stages where the low concentration of the catalyst (HFO) is rate limiting. This is followed by a sharp increase in reaction rate as the concentration of HFO increases and finally a decrease in rate as the concentration of Fe(II) rather than HFO becomes rate limiting.

The predictions made by the model using only the homogenous oxidation pathway produce an excellent fit for the data collected in the field. Despite this fact, this form of the rate equation as shown by Equation 2-6 cannot be telling the whole story as the rate constant k_1 should by definition be constant as changes to dFe(II)/dt should be described by changes in the other parameters(Fe(II), H^+ and DO concentration). Since incorporating the heterogenous oxidation pathway into the equation actually makes the correlation between the measured and modelled data worse it suggests that the current accepted form of the rate equation for the Fe(II) oxidation pathway is not applicable to the ferruginous mine waters in this thesis. Therefore there must be

another as yet unaccounted for parameter that is influencing the overall Fe(II) oxidation rate.

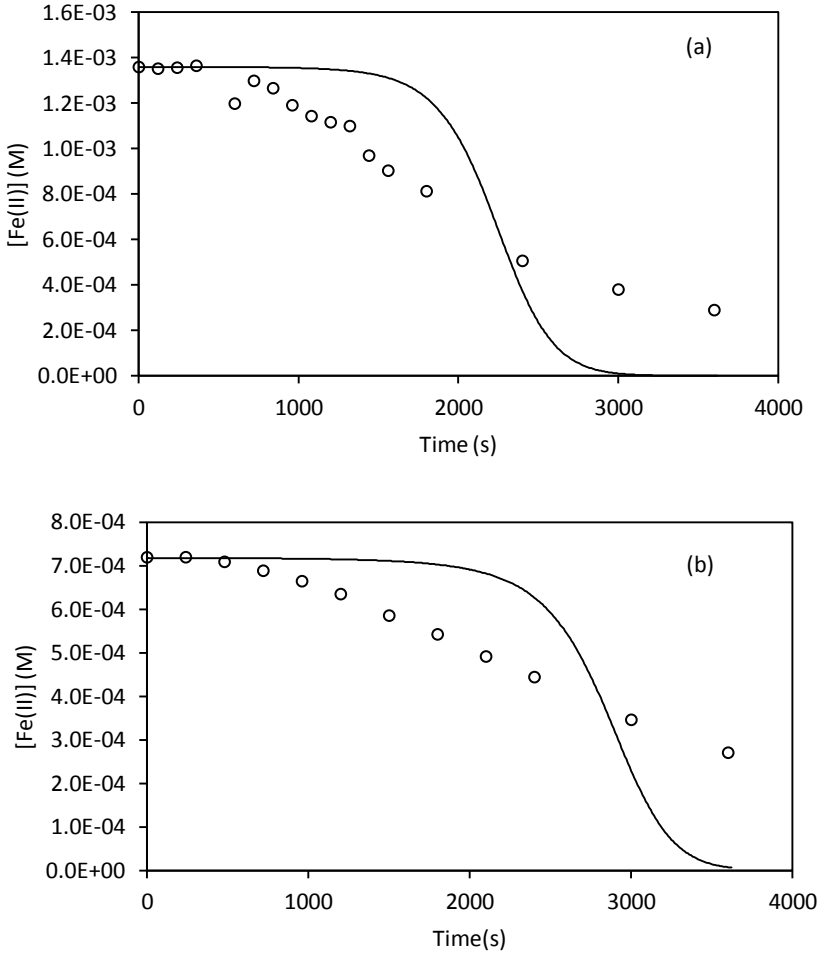

Figure 6-10 Predictions of changes in [Fe(II)] over time using the RK4 include autocatalytic heterogeneous oxidation vs field measured values

Values calculated using RK4 method unbroken line, field measured values as circles. (a) Ynysarwed, $k_2 = 1.8 \times 10^{12}$ $M^{-2}atm^{-1}min^{-1}$ (b) Tan-y-Garn, $k_2 = 4.2 \times 10^{12}$ $M^{-2}atm^{-1}min^{-1}$

6.2 Heterogeneous oxidation rates and k_2

The findings presented here, in line with other studies e.g. Park and Dempsey (2005) and Tamura et al (1976) are the result of addition of HFO solids to ferruginous mine drainage giving Fe(III) concentrations 2 orders of magnitude greater than initial Fe(II) concentrations. All heterogeneous oxidation experiments conducted in the production of this thesis were carried out at the Tan-y-Garn site which had marginally net-acid water and initial pH of 5.6.

Details about the background chemistry of the water are contained in Table 6-1. Changes in Fe(II) concentration upon addition of HFO solids to freshly emerged mine water at Tan-y-Garn were measured according to the methods described in Chapter 4, Section 4.6. Values for k_2 (the rate constant for heterogeneous oxidation) were then calculated using a further development of the RK4 method used in the calculation of k_1 (the rate constant for homogeneous oxidation) as described in Chapter 4, Section 4.6.2. The following Sections present the results of the heterogeneous oxidation experiments. As with the homogenous oxidation experiments there was a large amount of data logged during the experiments. This data is contained within Appendix 1. As with the homogeneous oxidation experiments no attempt was made to control the variables pH, DO and Temperature. Figure 6-11 typical variations in these parameters throughout the heterogeneous oxidation experiments.

6.2.1 Heterogeneous vs homogeneous rates

Two sets of experiments were carried out with concentrations of HFO solids added 1.3 g/L and 3.3 g/L. Data was logged in the same way as for the homogenous oxidation experiments (see Table 6-2). Again the logged data was used along with the RK4 method to try to produce a best fit curve for the measured Fe(II) concentrations over time (see Chapter 4, Section 4.3.5 for details). The results of the experiments and RK4 calculations are shown in Figure 6-12 (a sample of the RK4 spreadsheet is shown in

Table 6-8 6-8). It can be seen that the rate of oxidation increased when the concentration of suspended HFO increased from 1.3 g/L to 3.3 g/L. The reasons for the

deviation of the predicted from the measured values for 1.3 g/L of HFO solids will be discussed in Section 6.4.2.

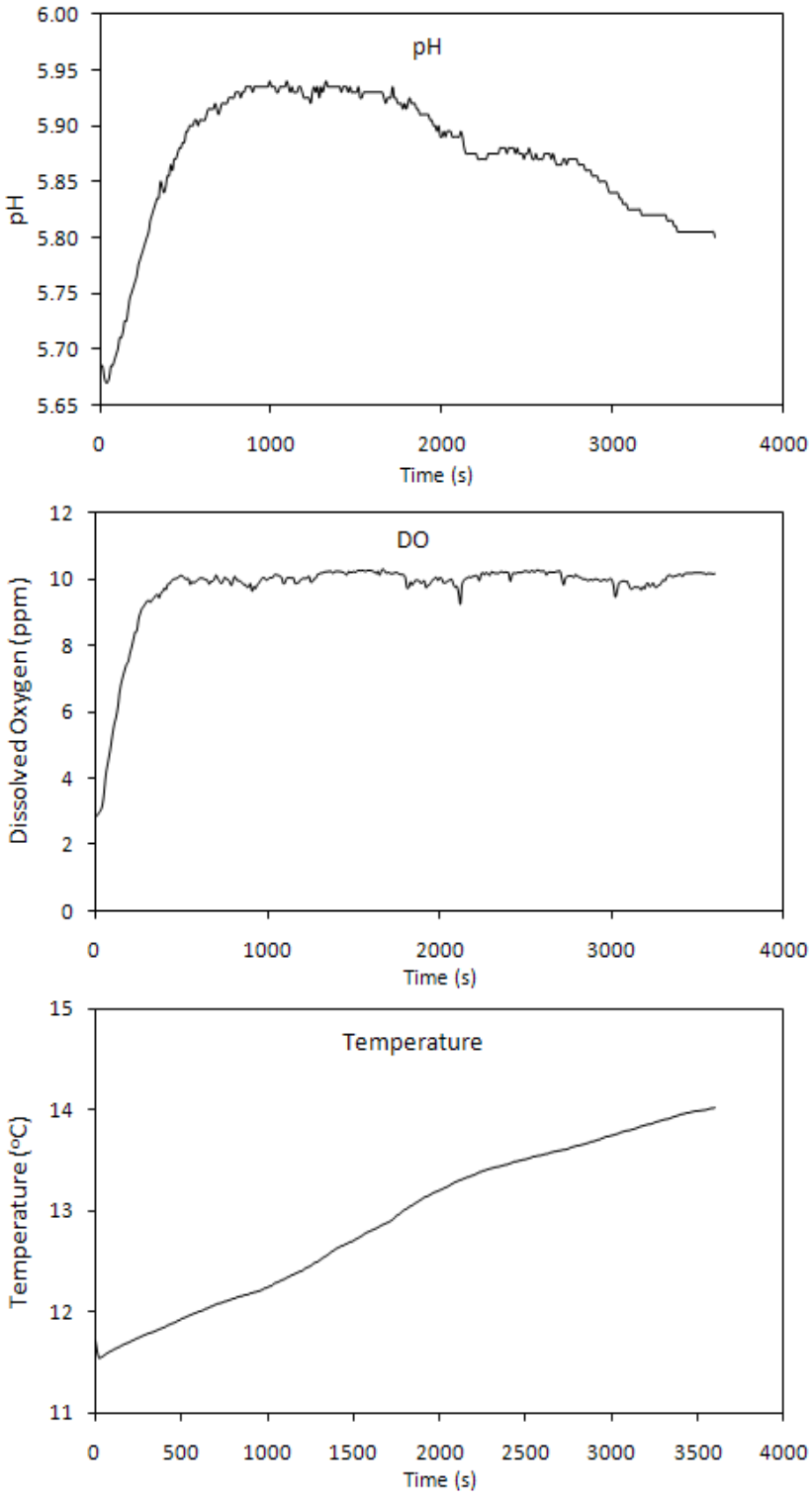

Figure 6-11: Variations in pH, DO and temperature throughout the heterogeneous oxidation experiments

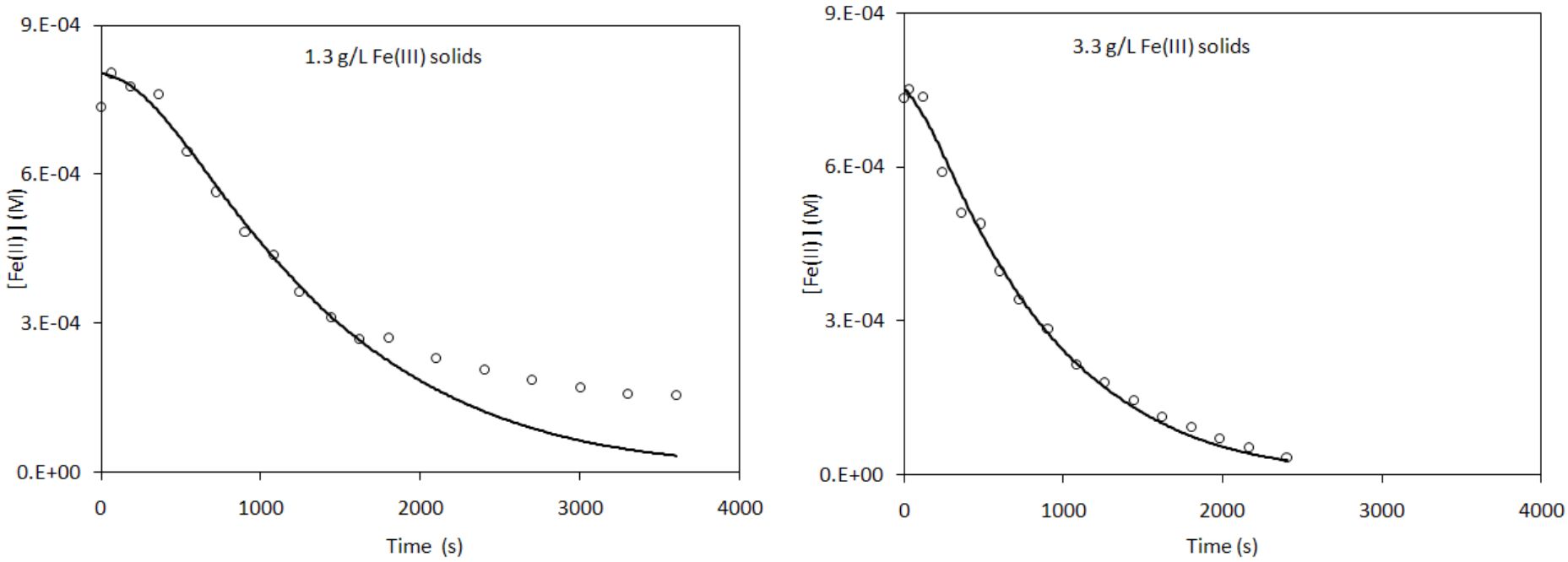

Figure 6-12 Comparison of changes in [Fe(II)] measured during heterogeneous oxidation experiments to those predicted by the RK4 method[15]

[15] Circles, measured values, solid line, predicted values.

Table 6-8: First three minutes of RK4 calculations for heterogeneous oxidation

Mean meter reading						Homogeneous RK4					Heterogeneous RK4					
Time (s)	°C	pH	DO ppm	DO atm	$[HO^-]^2$ (M)	ϑ	x_{1a}	x_{2a}	x_{3a}	x_{4a}	ϑ	x_{1b}	x_{2b}	x_{3b}	x_{4b}	[Fe(II)] (M)
0	14.1	5.94	3.21	0.064	1.22E-17	4.36	-7.59E-08	-7.59E-08	-7.59E-08	-7.58E-08	15.93	-1.76E-07	-1.76E-07	-1.76E-07	-1.75E-07	8.35E-04
10	14.2	5.90	3.54	0.071	1.02E-17	4.32	-7.07E-08	-7.06E-08	-7.06E-08	-7.06E-08	15.41	-3.40E-07	-3.39E-07	-3.39E-07	-3.38E-07	8.32E-04
20	14.0	5.92	4.43	0.089	1.12E-17	4.41	-9.39E-08	-9.39E-08	-9.39E-08	-9.38E-08	16.05	-4.24E-07	-4.23E-07	-4.23E-07	-4.21E-07	8.28E-04
30	14.0	5.90	4.72	0.094	9.94E-18	4.42	-8.84E-08	-8.84E-08	-8.84E-08	-8.83E-08	16.09	-4.22E-07	-4.21E-07	-4.21E-07	-4.20E-07	8.23E-04
40	14.0	5.89	4.86	0.097	9.52E-18	4.41	-8.69E-08	-8.68E-08	-8.68E-08	-8.68E-08	16.03	-4.25E-07	-4.24E-07	-4.24E-07	-4.23E-07	8.18E-04
50	14.0	5.88	5.27	0.105	9.10E-18	4.41	-8.95E-08	-8.95E-08	-8.95E-08	-8.94E-08	16.01	-4.48E-07	-4.47E-07	-4.47E-07	-4.46E-07	8.13E-04
60	14.0	5.88	5.62	0.112	9.11E-18	4.40	-9.51E-08	-9.50E-08	-9.50E-08	-9.49E-08	15.97	-4.76E-07	-4.75E-07	-4.75E-07	-4.73E-07	8.08E-04
70	14.1	5.89	5.75	0.115	9.56E-18	4.40	-1.01E-07	-1.01E-07	-1.01E-07	-1.01E-07	15.93	-4.97E-07	-4.95E-07	-4.95E-07	-4.94E-07	8.02E-04
80	14.1	5.88	5.97	0.120	9.35E-18	4.39	-1.02E-07	-1.02E-07	-1.02E-07	-1.02E-07	15.90	-5.07E-07	-5.06E-07	-5.06E-07	-5.04E-07	7.96E-04
90	14.1	5.89	6.19	0.124	9.58E-18	4.39	-1.08E-07	-1.08E-07	-1.08E-07	-1.08E-07	15.86	-5.30E-07	-5.28E-07	-5.28E-07	-5.26E-07	7.90E-04
100	14.1	5.88	6.47	0.130	9.38E-18	4.38	-1.10E-07	-1.10E-07	-1.10E-07	-1.10E-07	15.82	-5.45E-07	-5.43E-07	-5.43E-07	-5.41E-07	7.84E-04
110	14.1	5.88	6.67	0.134	9.39E-18	4.38	-1.13E-07	-1.13E-07	-1.13E-07	-1.12E-07	15.80	-5.58E-07	-5.56E-07	-5.56E-07	-5.54E-07	7.77E-04
120	14.1	5.88	6.78	0.136	9.40E-18	4.37	-1.14E-07	-1.14E-07	-1.14E-07	-1.14E-07	15.76	-5.64E-07	-5.62E-07	-5.62E-07	-5.60E-07	7.70E-04
130	14.1	5.88	7.02	0.141	9.20E-18	4.37	-1.14E-07	-1.14E-07	-1.14E-07	-1.14E-07	15.717	-5.75E-07	-5.72E-07	-5.72E-07	-5.70E-07	7.64E-04
140	14.1	5.88	7.20	0.144	9.43E-18	4.36	-1.19E-07	-1.19E-07	-1.19E-07	-1.19E-07	15.697	-5.92E-07	-5.90E-07	-5.90E-07	-5.87E-07	7.57E-04
150	14.1	5.88	7.36	0.147	9.43E-18	4.36	-1.21E-07	-1.21E-07	-1.21E-07	-1.21E-07	15.676	-6.01E-07	-5.98E-07	-5.98E-07	-5.96E-07	7.50E-04
160	14.1	5.88	7.60	0.152	9.24E-18	4.35	-1.21E-07	-1.21E-07	-1.21E-07	-1.21E-07	15.614	-6.10E-07	-6.08E-07	-6.08E-07	-6.05E-07	7.42E-04
170	14.1	5.88	7.88	0.158	9.47E-18	4.35	-1.28E-07	-1.28E-07	-1.28E-07	-1.28E-07	15.594	-6.35E-07	-6.33E-07	-6.33E-07	-6.30E-07	7.35E-04
180	14.1	5.89	8.11	0.163	9.70E-18	4.34	-1.34E-07	-1.34E-07	-1.34E-07	-1.34E-07	15.553	-6.57E-07	-6.54E-07	-6.54E-07	-6.51E-07	7.28E-04

In order to determine the effect of adding additional HFO solids to the reaction mixture, the values of Fe(II) measured throughout the heterogeneous oxidation experiments were compared to values predicted by the RK4 method assuming only homogenous Fe(II) oxidation was occurring. Changes in [Fe(II)] over time via the homogenous mechanism were calculated, based on the values of pH, temperature and DO logged throughout the experiments, together with previously determined values for k_1, the rate constant for homogeneous oxidation (see Figure 6-5). Figure 6-13 compares the data output by the RK4 method for homogenous Fe(II) oxidation to measured changes in [Fe(II)] over the course of the experiments. It can be seen that addition of HFO solids resulted in rates of Fe(II) oxidation considerably faster than would be expected for homogeneous oxidation under the same conditions.

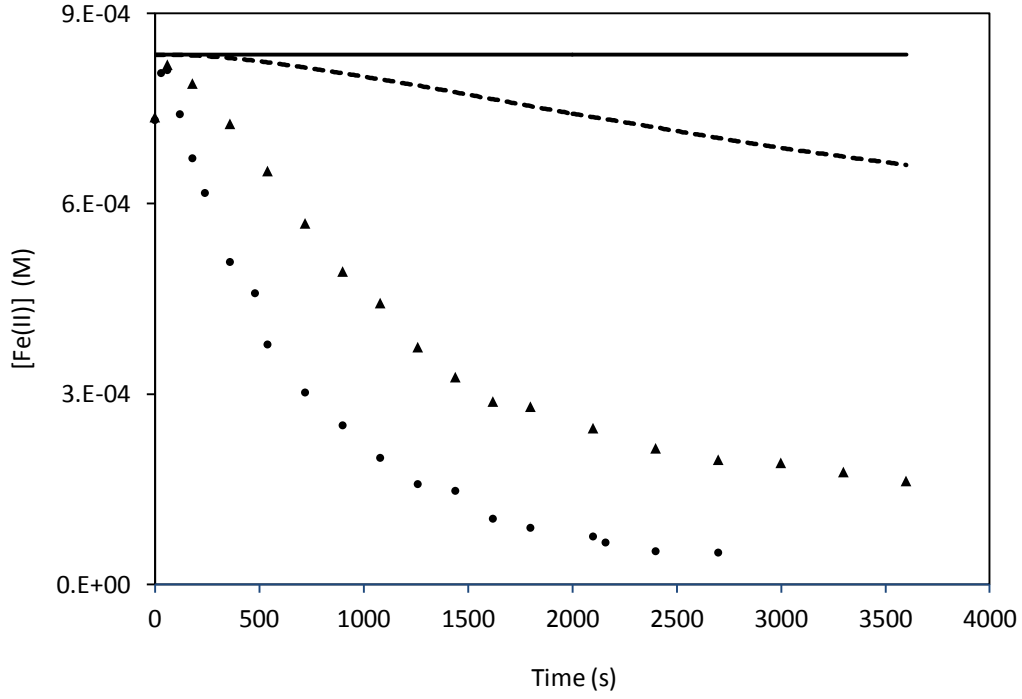

Figure 6-13 Comparison of changes in [Fe(II)] over time measured during heterogeneous oxidation experiments to those predicted by the RK4 method for homogenous oxidation[16].

Predictions of Fe(II) oxidation rate by the homogenous RK4 method over the first 1000 seconds of the experiment ranged from 5.2 x 10^{-12} Ms^{-1} to 6.1 x 10^{-9} Ms^{-1} with k_1 = 2.0 x 10^{13} $M^{-2}atm^{-1}min^{-1}$ and k_1 = 1.3 x 10^{16} $M^{-2}atm^{-1}min^{-1}$ respectively. The range of k_1

[16] Broken line k_1 = 1.3 x 10^{16}, solid line k_1 = 2.0 x 10^{13}, triangles = measured [Fe(II)] with 1.3 g/L solids added, dots = [Fe(II)] with 3.3 g/L solids added

values used reflects the highest value of k_1 obtained over the three repeats of the homogenous oxidation experiment at Tan-y-Garn in the upper limit and the k_1 values determined from laboratory studies (see Table 6-5) in the lower limit. The actual rates of Fe(II) oxidation observed were in the range 3.8 – 9.0 x 10^{-7} Ms^{-1}, showing a 2 – 7 order of magnitude increase compared to predictions based on homogenous oxidation alone. This corresponds to an Fe(II) removal rate in mg/L of 1.3 – 3.0 mg/L/min and is comparable to the rates of Fe(II) removal recorded by Dietz and Dempsey (2002) for a reactor using recirculated HFO sludge at concentrations up to 2 g/L.

6.2.2 Calculation of k_2

Values for k_2 were calculated using a version of the RK4 method adapted to take into account both homogenous and heterogeneous Fe(II) oxidation pathways as described in Chapter 4, Section 4.6.2. Figure 6-12 compares the measured values for [Fe(II)] over time to the data output from the RK4 method. Values calculated for k_2 were consistent within a factor of 3 and were all within the range 7.2 x 10^8 – 2.0 x 10^9 $M^{-2}atm^{-1}s^{-1}$. At the time of writing there are no values for k_2 that have been published using a method such as the one described here which does not require any of the variables (pH, DO, temperature) to be held constant. The values of k_2 are consistent to within a factor of 3 across both sets of experimental runs (1.3 and 3.3 mg/L HFO). These values are however not yet directly comparable to other previously published values for k_2 for reasons that will be discussed in the following sections.

The main value of this set of experiments therefore is the development of an experimental method and numerical analysis that can be used to evaluate rates of Fe(II) oxidation in the field without the need for careful control of experimental conditions. The following Sections give a thorough discussion of further refinements that need to be made to the procedures used in the determination of k_2 for future work. The need for additional analyses of the HFO solids used is also discussed in order to allow meaningful comparisons with the work of other authors.

6.2.3 Equilibration of sorbed Fe(II) and background chemistry effects

The extent of Fe(II) sorption onto HFO solids depends on several factors including length of equilibration time and pH. Jeon et al (2001) studied Fe(II) sorption onto HFO solids in the circumneutral and mildly acidic region. They showed a reduction in sorbed Fe(II) from nearly 100% of available surface sites at pH 7 to less than 20% at pH 5.5. The rate of decline in the proportion of sorbed Fe(II) with pH was heavily influenced by equilibration time, changing on a timescale of days to weeks. They also showed that variations in sulphate concentration have a marked effect on Fe(II) sorption over the mildly acidic pH range.

The HFO used in the experiments presented here was collected from the RAPS at Tan-y-Garn and had had several months (if not years) of equilibration time with the water passing over it. It is likely therefore that the that the amount of sorbed Fe(II) would be significantly different from that observed in laboratory studies where equilibration time was of the order of minutes or hours. In addition to this the presence of naturally occurring sulphate would also have an effect on Fe(II) sorption that would not be seen in laboratory work where sulphate was not added to the reaction mixture.

A detailed analysis of the HFO solids used (which was beyond the scope of this study) would therefore be required in order to determine the density of surface sites available for sorption of Fe(II).

6.2.4 Limitations of the experimental procedure and model for k_2

It has been shown that in addition to the effect of equilibration time, the proportion of sorbed Fe(II) changes depending on the nature of the solids present (Park and Dempsey (2005)). Similarly, Vikesland and Valentine (2002) have shown that the type of iron oxide solid present effects the catalytic activity of the Fe(II)/Fe(III) oxidation reaction in the order magnetite > goethite >> lepidocrocite > haematite >> ferrihydrite. In order to give meaningful values of k_2 that could be applied across different sites there therefore are several key parameters that need to be measured. These are primarily physical characteristics of the HFO solids as described below;

1. Surface area/weight ratio of the solids

The solids collected from the RAPS system were dense, granular and dark red in colour unlike the fluffy orange/brown precipitates that tend to form in the water column at circumneutral pH. For practical purposes the most likely measurement of amount of solid added to a reaction is weight, when the important factor in terms of catalysis is surface area. Thus it is important to be able to convert easily from one parameter to the other.

2. Density of surface sorption sites/proportion of sorbed Fe(II)

To allow an accurate comparison between different systems a knowledge the density of sites suitable for Fe(II) sorption (see Chapter 2, Section 2.2.2) and (depending on the background chemistry of the water under investigation) what proportion of these sites are actually available for Fe(II) sorption is also necessary. Whilst it is possible to predict how the proportion of sorbed Fe(II) might change in response to changing pH, the interaction with other species such as sulphate and phosphate would also need to be taken into account.

Aside from the need for a thorough characterisation of the HFO solids being used there are also considerations relating to the experimental procedure (which is not as straight forward as for the determination of k_1) that need to be addressed. Figure 6-14 shows a typical comparison between measured values of Fe(II) for the system under investigation and those predicted by the model. It can be seen that towards the end of the experimental run there was in increasing discrepancy between the measured and predicted values for Fe(II). This observation can be attributed to the experimental procedure used and in line with several other studies (Barnes 2008, and references therein) provides evidence for the presence of sorbed recalcitrant (unoxidised) Fe(II).

Park and Dempsey (2005) recognised that a portion of the sorbed iron remains unoxidised and concluded that the ratio of sorbed Fe(II):Fe(III) does not change during the oxidation reaction with only the proportion of dissolved Fe(II) diminishing. This can be explained in terms of two distinct types of surface adsorption site for Fe(II) (Dzomback 1990) where the more strongly sorbed Fe(II) does not oxidise.

The sampling method used in this study required quenching aliquots of the reaction mixture by adding them directly to the 2’2-bipyridyl/acetate buffer. This method was

chosen as the concentrations of HFO solids present made filtration through a 0.2µm filter very slow and it was thought that the build up of a filter cake might further accelerate Fe(II) oxidation.

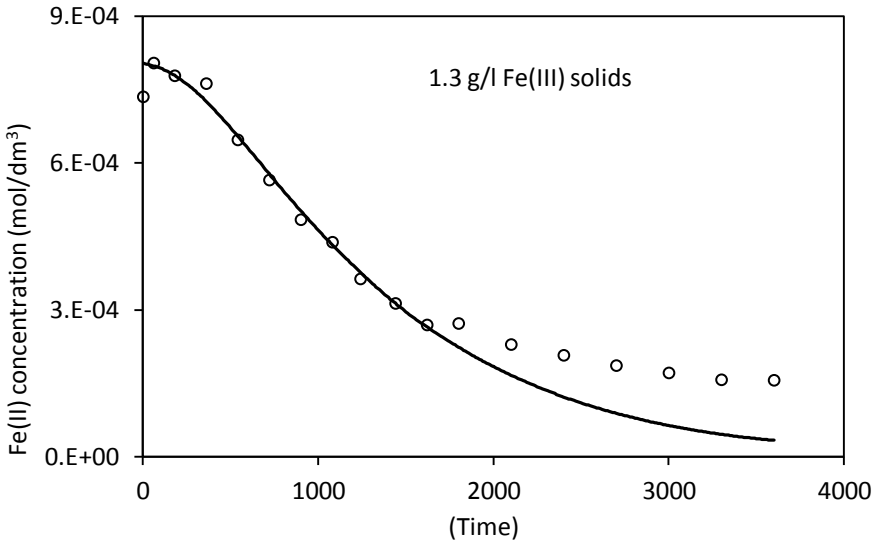

Figure 6-14 Comparison between measured (dots) and modelled (unbroken line) changes in Fe(II) concentration for the heterogeneous oxidation experiments

Complexation of Fe(II) by 2'2-bipyridyl halted oxidation without dissolving the HFO solids. Subsequent filtration of the samples allowed determination of Fe(II) without concerns about interference from high background Fe(III) concentrations. The problem with this method (which was only discovered after analysis of several experimental runs) is that the 2'2-bipyridyl appears to strip the sorbed Fe(II) from the solids which interferes with the determination of dissolved Fe(II) concentrations. This can be illustrated by Figure 6-10. On the day that the 3.3 mg/L experiment was carried out there were two people on site (one sampling and one filtering the samples immediately afterwards) allowing for a shorter time between sampling and filtering compared to the 1.3 mg/L experiment which the author conducted alone. It can be seen that the measured values of [Fe(II)] fit much better with the RK4 values throughout the experiment when the time between sampling and filtering was shorter. It may therefore be better in future to make every effort to filter samples taken from the reaction mixture prior to quenching with either acid, or the complexing agent. Unfortunately it was not possible to test this methodology due to time constraints on the project.

6.3 Implications for the treatment of ferruginous mine water

As a result of the increasing cost of land in the UK the decision about whether to build a new active or passive mine drainage treatment facility often comes down to a trade off between the short term expense of a large area of land (for a passive system) and the longer term expense of chemical dosing and plant maintenance (for an active system). The results presented here have increased the understanding of the behaviour of circumneutral mine drainage and have implications for the way in which mine waters might be assessed and systems designed in the future.

The finding that Fe(II) oxidation rates in waters where dissolved iron concentrations are of the order of 10s – 100s of mg/L can be up to 3 orders of magnitude higher than previously published will have an impact on the sizing of passive systems. As noted by Sapsford and Watson (2011) the removal of iron from waters contaminated by dissolved Fe(II) is a two step process (Equation 6-4) where k_1 and k_s are the first order rate constants for Fe(II) oxidation and particulate settling respectively.

Equation 6-4

$$\mathbf{Fe(II)_{(aq)} \xrightarrow{k_1} Fe(III)_{(s)} \xrightarrow{k_s} Settled\ Fe(III)}$$

Where iron oxidation rates are low the first step will be rate limiting, but as oxidation rates rise, the rate of settling becomes the limiting factor. The high values of k_1 shown here mean that for systems where residence times were previously calculated based on lower rates of iron oxidation in the future such systems could be made smaller and optimised for particulate settling instead.

6.4 Summary

Iron (II) oxidation rates were studied in the field at a number of mine water treatment schemes across the UK. Batch-wise experiments were conducted to investigate the rate of Fe(II) oxidation by both the homogenous and heterogeneous oxidation mechanism. A numerical 4th order Runge-Kutta (RK4) method was used to determine values for k_1, the rate constant for homogeneous oxidation and k_2 the rate constant for heterogeneous oxidation. The chapter can be summarised as follows:

- Values determined for k_1 were 1-3 orders of magnitude higher than those previously published from laboratory studies. The values were found to have a linear correlation with [H^+] suggesting that the homogenous mechanism alone is insufficient to describe Fe(II) oxidation in these systems.
- The influence of bacterial oxidation and various background chemistry parameters were considered in relation to the elevated oxidation rates. It was concluded that the most likely explanation was an increased initial iron concentration compared to much of the work in the literature, leading to a contribution from heterogeneous autocatalysis.
- The form of the Fe(II) oxidation rate equation reported in the literature including both homogeneous and heterogeneous oxidation pathways was found to be unsuitable for describing the ferruginous mine water.
- The methodology developed during the heterogeneous oxidation experiments was found to require further refinement in order to produce values of k_2 comparable to those already in the literature. The results produced in this study were however consistent with changing HFO solids concentration and highlight the potential of the RK4 method to produce values of k_2 independent of pH and Po_2.
- The elevated values for iron oxidation rates in ferruginous mine drainage compared to what would be predicted from laboratory studies could lead to a reduction in the footprint of passive treatment systems in the future, with residence times optimised for particulate settling as this becomes the rate limiting step.

7 Results and Discussion: CO_2 degassing

This chapter presents the results of the work carried out on CO_2 degassing. Aeration and degassing experiments were carried out at a number of different mine water treatment schemes across the UK. The effectiveness of both aeration cascades and batch-wise forced aeration/degassing are discussed with particular emphasis on the changes in pH that accompany decreasing concentrations of dissolved CO_2. The work discussed in this chapter has been split into five main sections, aeration cascade testing, batch-wise CO_2 degassing and implications for the treatment of AMD.

All aeration cascade testing work was carried out at the Strafford mine water treatment site in the North of England. The effect of aeration cascade design on CO_2 degassing and the corresponding changes in pH are discussed. The potential benefits of inclusion of aeration cascades for the purpose of CO_2 degassing at both net-acid and net-alkaline mine water treatment sites are also considered.

Batch-wise CO_2 degassing experiments were conducted at Dawdon and Blenkinsopp in the North of England and Ynysarwed, Tan-y-Garn and Six Bells in South Wales. The results can be divided into two main sections; experimental results, and modelling results. Experimental data are presented in Section 7.2.1 with further reworking and

analysis of the data using numerical and geochemical models shown in Sections 7.2.2 to 7.2.4.

The ability of the numerical 4^{th} order Runge Kutta (RK4) method (as described in Chapter 4, Section 4.6.2) and the PHREEQCi geochemical modelling software to model the Fe oxidation/CO_2 degassing system is discussed, paying particular attention to the sensitivity of the models to changes in alkalinity. The effect of experimental design and assumptions made by the models are also discussed with respect to variations in the constants k_1, the rate constant for homogeneous Fe oxidation and k_La, the mass transfer coefficient for CO_2 degassing.

7.1 Aeration cascade testing

The design of the aeration cascades at the Strafford site has been described previously in detail in Chapter 4 Section 4.7. The cascades consist of two sets of steps (one containing three steps and the other two steps) above a distribution channel. The total drop in height was identical for each of the configurations. The entire flow was diverted down one or other of the sets of steps at a time with changes made regarding the inclusion (or not) of weir boards at the edges of the steps that resulted in the formation of shallow plunge pools (10 cm deep). Configuration (a) consisted of one long drop into a plunge pool so that it resembled a small waterfall. Flow rates were monitored continuously by equipment on site in the pumping house and were within the range 29-30 L/s throughout the experiments. It was expected that the configurations that contained plunge pools (a, d & e) would show the greatest changes in dissolved CO_2 concentration and hence pH due to the increased residence time in the plunge pools which were well mixed with the entrainment of a large number of air bubbles (Figure 7-1). Calculation of residence times in the plunge pools based on a flow rate of 30 L/s were in the range 5 to 9 s which although not a long period of time in itself should be a significant increase relative to the situation where no plunge pools are present.

Figure 7-1 Example of plunge pools created during the aeration cascade trials

The changes in pH across the aeration cascades, and the corresponding changes in dissolved CO_2, calculated using PHREEQCi (see Chapter 4, Section 4.2) by inputting values for alkalinity and pH are shown in Table 7-1. The pH was measured using 4 pH probes, two at the top and two at the bottom of the cascades. The probes were swapped over half way through the day so that each probe logged pH at both the top and bottom of the cascades. The values in Table 7-1 are a result of averaging over readings from all 4 pH probes, more than 4000 logged data points. All of the logged data is contained within Appendix 3.

Table 7-1 pH values measured at the top and bottom of the aeration cascades at Strafford and calculated values for dissolved CO_2

	pH			CO_2 (mg/L)		
Cascade design	**Top of cascade**	**Bottom of cascade**	**Increase**	**Top of cascade**	**Bottom of cascade**	**Decrease**
a	6.7	7.0	0.3	252	126	126
b	6.6	6.8	0.2	317	200	117
c	6.6	6.8	0.2	317	200	117
d	6.7	7.0	0.3	252	126	126
e	6.8	7.0	0.2	200	126	74

Monitoring pH was considered to be a suitable method for the determination of dissolved CO_2 as the bicarbonate buffer system is well understood and the equilibrium constants for the relationships between $CO_{2(aq)}$, H_2CO_3, HCO_3^- and CO_3^{2-} have long been established (Stumm and Morgan, 1996, Langelier 1997 and references therein). In the CO_2/bicarbonate buffered system the pH is determined by the relative concentrations of the weak acid present, in this case H_2CO_3*(≈CO_2) and its conjugate base in this case HCO_3^-. The relationship between pH and the concentrations of the species that comprise the buffer is governed by Equation 7-1, the Henderson-Hasselbalch equation (Pratt and Cornely, 2005) where pK_a is the acid dissociation constant for H_2CO_3.

Equation 7-1

$$\mathbf{pH = pK_a + \log {[HCO_3^-]}/{[CO_2]}}$$

Figure 7-2 shows how the pH of a bicarbonate buffered system changes as the ratio of $[HCO_3^-]$:$[CO_2]$ changes. It can be seen that even within the well buffered region between pH 6 and 7 changes in the concentrations of these species still result in small

changes in pH. Therefore measurement of pH and alkalinity (which is effectively comprised of only HCO_3^- at pH 6-7) allows the concentration of dissolved CO_2 to be calculated since all of the required equilibrium constants are known.

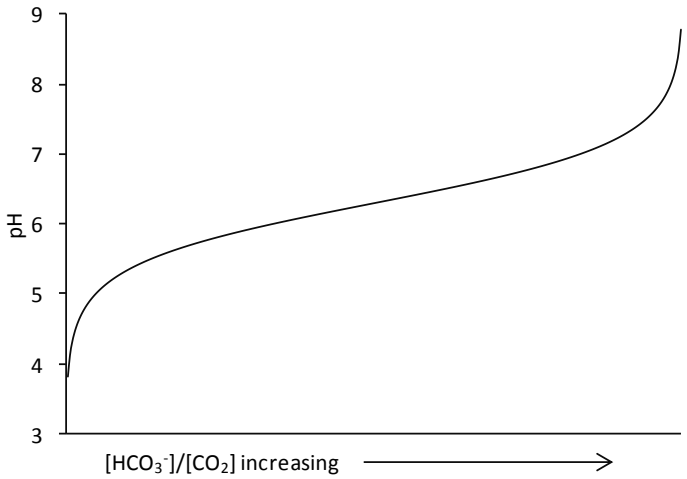

Figure 7-2 Henderson-Hasselbalch graph showing how the pH of a bicarbonate buffered solution changes as the ratio $[HCO_3^-]$:$[CO_2]$ is altered

The change in pH between the top and bottom of the cascades was no more than 0.3 pH points for any of the configurations studied. Increased residence time in plunge pools did not appear to increase CO_2 degassing. This result is not surprising given that the emerging water had initial pH within the well buffered region shown in figure 7-2. The changes in dissolved CO_2 were of the order of 100 mg/L of CO_2 degassed for a pH change of 0.2 points and it was interesting to note that even these small changes in pH were a result of relatively large changes in the concentration of dissolved CO_2.

An alternative way to describe the apparently large changes in dissolved CO_2 with only small changes in pH can be explained in terms of the relationship between the concentrations of dissolved CO_2 and $[H^+]$ and the logarithmic nature of the pH scale. In any solution containing dissolved carbon dioxide the following equilibrium is established (Equation 7-2) (Stumm and Morgan 1996).

Equation 7-2
$$\frac{[\mathbf{H^+}][\mathbf{HCO_3^-}]}{[\mathbf{H_2CO_3^*}]} = \mathbf{K_1} = \mathbf{10^{-6.3}}$$

Since $[CO_{2(aq)}] >> [H_2CO_3]$ then the approximation that $[H_2CO_3^*]=[CO_{2(aq)}]$ can be made and since $[H+] \cong [HCO_3^-]$ at circumneutral pH this gives Equation 7-3 (Lower 2011).

Equation 7-3 $$\frac{[H^+]^2}{[CO_2]} \cong 10^{-6.3}$$

Since $\mathrm{pH} = -\log[\mathrm{H}^+]$, in the case of solutions containing dissolved CO_2 (in pure water in the absence of other solutes) Equation 7-4 should hold true (Lower 2011).

Equation 7-4 $$pH \cong -\log\frac{1}{2}[CO_2] \times 10^{-6.3}$$

Thus in order to produce an increase in pH of one unit, the concentration of dissolved CO_2 must decrease by two orders of magnitude. In practice this means that there was probably insufficient residence time over the aeration cascades at Strafford to degass enough CO_2 (several hundred mg/L) to produce large changes in pH.

Table 7-2 Summary of iron concentrations measured across the Strafford site

Cascade design	1			2			3		
	Fe(II)	Fe(III)	Fe_{tot}	Fe(II)	Fe(III)	Fe_{tot}	Fe(II)	Fe(III)	Fe_{tot}
a	3.3	1.1	4.4	3.2	1.0	4.1	0.1	2.8	2.9
b	3.4	0.9	4.3	3.4	1.1	4.6	0.9	2.5	3.4
c	3.3	1.0	4.4	3.6	1.0	4.6	0.6	2.7	3.3
d	3.6	1.3	4.9	3.7	1.6	5.3	0.7	3.1	3.8
e	3.7	0.8	4.5	3.9	0.8	4.7	0.8	2.6	3.4

Numbers 1,2 and 3 correspond to sampling sites as described in Chapter 4, Figure 4-11. Sample point 1, top of aeration cascades, point 2, bottom of aeration cascades, point 3 end of 1st settling lagoon. Samples taken after 24 hours of new cascade design running.

In addition to the pH measurements taken at the cascades Fe concentrations were also measured at the top and bottom of the cascades and at the end of the first settling lagoon to investigate the effect of cascade design on Fe removal. Data recorded for iron concentrations across the site are shown in Table 7-2. As with the pH changes, it can be seen that there was no significant difference in the Fe concentrations measured for any of the cascade designs. The variation in the measurements mostly lies within the +/- 10% error associated with measurements by ICP-OES.

Proportions of Fe(II)/(III) at the outlet to the first lagoon are shown in Figure 7-2. Fe(II) concentrations were < 1mg/L for all of the cascades by the end of the first settling lagoon, though total Fe remained in the range 3-4 mg/L suggesting that the rate of HFO settling was at least partially limiting in terms of Fe removal. It can also be seen that there was little difference in total iron removal between the different configurations. Given the similarities in the pH changes observed with the different cascade designs this outcome is not surprising.

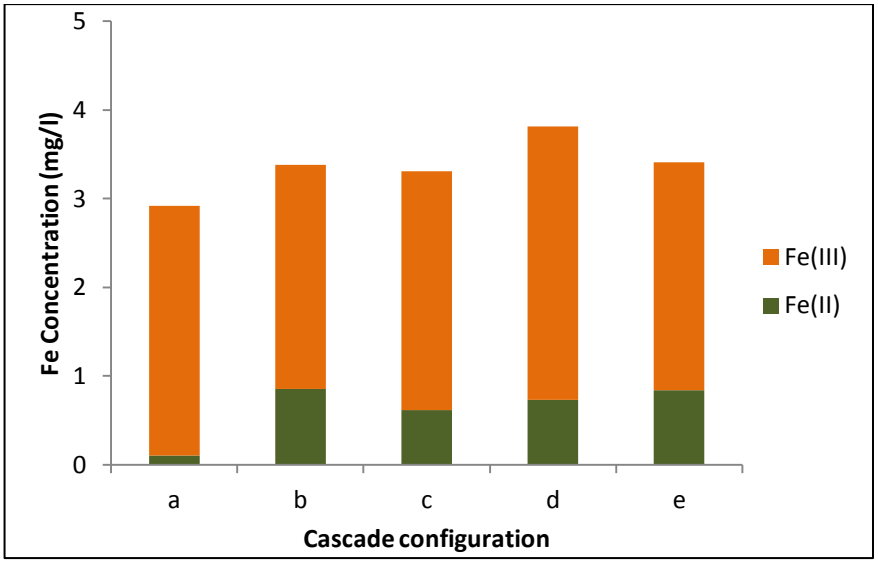

Figure 7-3 Variations in iron concentration at outlet of first lagoon (sample point 3)

Alkalinity measurements were also taken at various points across the site throughout the experimental period. These measurements showed very little variation across the site during the study period averaging 520mg/l $CaCO_3$ equivalent. Due to the low influent Fe(II) concentrations, the changes in alkalinity brought about by iron oxidation would only be of the order of 4-5mg/l and so would be within the range of experimental error for this kind of field measurement.

Contrary to expectations, the variations in cascade design did not seem to have a measureable effect on either pH changes or Fe removal rates at the Strafford site. A logical next step would therefore be to test cascades of different total heights in an attempt to further increase the quantities of CO_2 degassed. Since at many treatment sites water is already pumped tens of meters up from underground sumps an additional 5 meters (for example) in height at the top of an aeration cascade may not

significantly increase pumping costs. Any increase in cost could in any case be offset by reduced treatment area/chemical dosing cost further down the line.

Despite the acceptance that elevated dissolved CO_2 levels can hinder the treatment of mine drainage by both passive and active means (Younger et al. 2002) there have been few published studies dealing with aeration cascades (or other methods) specifically in relation to CO_2 stripping. Levels of dissolved CO_2 are more often discussed with respect to carbonate solubility in anoxic limestone drains or reducing alkalinity producing systems (e.g. Watzlaf et al. 2003). More commonly published are methods for CO_2 stripping in other industries e.g. paper milling (Kim et al. 2003) or intensive aquaculture (Summerfelt et al. 2000) though these are unlikely to be suitable for the treatment of mine drainage due to the high flow rates and volumes of water concerned and the rate at which pipe work and pumps could become fouled with HFO or other precipitates.

One of the largest areas of research relating to CO_2 degassing at aeration cascade or waterfall type structures is relating to water softening or $CaCO_3$ (tufa) deposits at natural waterfalls (Dandurand et al. 1982; Zaihua et al. 1995; Zhang et al. 2000), though the focus of these studies is usually on the rates of calcite deposition. Zhang et al (2000) explain the degassing of excess CO_2 at waterfall sites in three ways;

1. The aeration effect where eddies and falling water trap and suck large air bubbles into the flowing water increasing the air water interface.

2. The jet flow effect where fast flowing or falling water is separated into individual droplets which again increases the air water interface.

3. The low pressure effect where the falling flow has a lower water pressure according to the Bernoulli effect and the dissolved gases in the water can be released as low pressure gas bubbles.

In addition to these three effects they point out that turbulence reduces the thickness of the boundary layer at the air water interface again increasing the rate of gas transfer. Points 1 to 3 above may explain why the cascades at Strafford with plunge pools did not show any major differences in CO_2 degassing compared to those without

plunge pools. If these are the most important mechanisms for CO_2 transfer and they are occurring within the falling water rather than the plunge pools (which although well mixed will not have such a high air water interface area as the falling water) then the additional residence times in the plunge pools may not be contributing greatly to the overall CO_2 loss. These mechanisms for CO_2 degassing also add weight to the argument for testing cascades with a greater overall height as this will increase the timescale over which the effects described above can operate.

One published trial of a system (for the removal of metals from circumneutral mine drainage) that included several aeration/degassing steps with plunge pools was carried out by Trumm et al (2009). In their study the plunge pools were relatively large compared to the ones included at Strafford and they found that pH could be increased in such a system, but that surprisingly pH fell during the initial stages of aeration/degassing where the rate of CO_2 degassing should have been highest. One possible explanation is that the rate of acid production by the Fe(II) oxidation/precipitation reaction was actually greater than the rate of loss of acidity as of CO_2 degassed. The initial decrease in pH measured by Trumm et al (2009) is in disagreement with all of results presented throughout this chapter and highlights the difficulties involved in producing a one size fits all solution for mine waters with different chemistries.

Despite the quantity of data gathered it is worth noting that Strafford is not perhaps the ideal site for this kind of trial. The high alkalinity coupled with low inlet Fe concentrations means that the water should be easy to treat and thus it might be difficult to see variations in Fe removal efficiency compared to a site with higher inlet Fe concentrations and lower alkalinity. The small changes in pH over the aeration cascades mean that an inaccuracy in measurement of just 0.1 units will have a large impact on the calculated quantities of CO_2 degassed and improvements in Fe(II) or total Fe removal might be a better way of assessing the impact of changing cascade design.

7.1.1 Degassing over cascades compared to lagoons and wetlands

For highly net alkaline waters the inclusion of an aeration cascade for the purposes of raising pH likely to be unnecessary as pH will increase naturally throughout the system as CO_2 degasses since the alkalinity in such systems is high enough to buffer acidity generated by the formation of HFO. In these cases the primary function of cascades will be to encourage saturation with respect to DO rather than CO_2 degassing. Examples of this kind of system (the majority of which have been described elsewhere in this thesis) can be seen in Sapsford and Pugh (2010). For Lindsay pH was shown to increase by 0.8 points across the first settling lagoon, for Taff Merthyr by 0.5 points and for Moralis the pH increased by 0.7 points between the first distribution weir and the end of the first settling lagoon. As a result the majority of Fe(II) had oxidised by the end of the first settling lagoon in each case with the remainder of treatment system providing the required residence time for particulate settling. By contrast, for two other sites Coal Authority sites, Glyncastle and Blaenavon, not discussed in detail in this study the change in pH over the first settling lagoons was negligible. Rates of iron oxidation were correspondingly much lower at these two sites with Fe(II) persisting much longer within the treatment system. At these sites improved CO_2 degassing up front of the settling lagoons should result in increased Fe(II) oxidation rates and improved system performance.

7.2 Batch-wise CO_2 degassing studies

All batch-wise CO_2 degassing experiments were carried out in the field on fresh mine water samples as described in Chapter 4 Section 4.8. The logged data for each of the experiments in contained within Appendix 3.The method used and data collected were similar to that of Cravotta (2007) used in the evaluation of a circumneutral mine water in Pennsylvania USA. This data was used in predictions of Fe(II) oxidation rate by the RK4 method and in the geochemical modelling software PHREEQCi to determine changes in the chemistry of the waters over time.

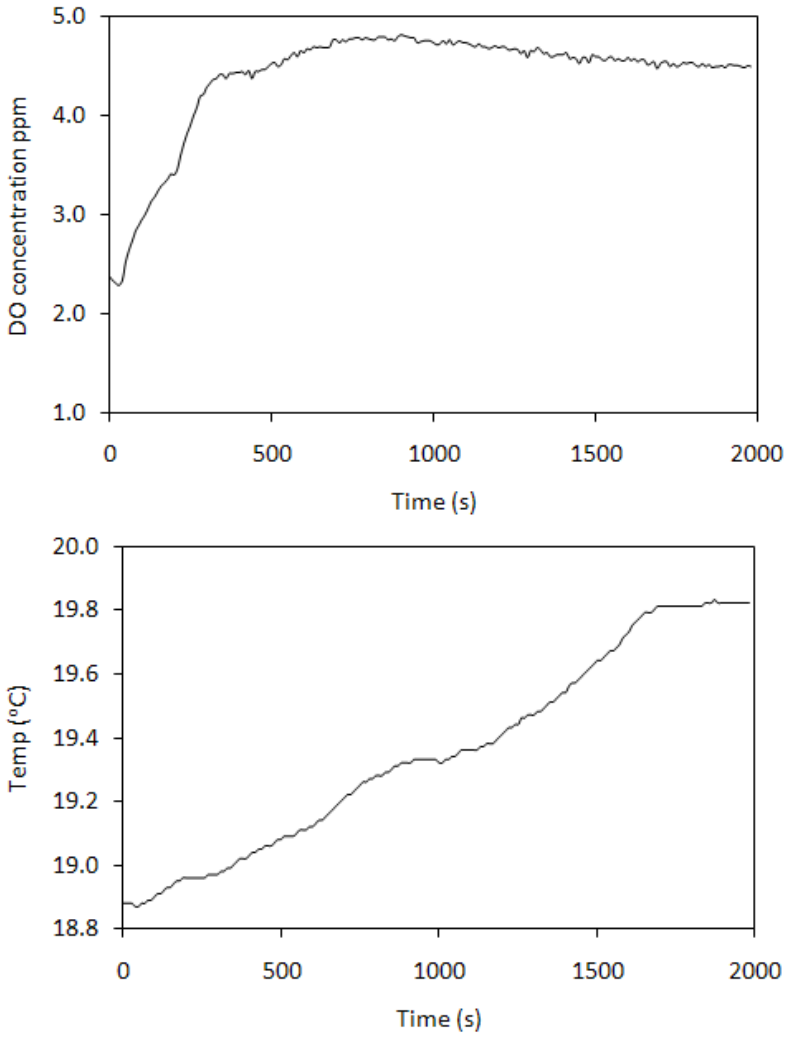

Figure 7-4 Typical shapes of curves for DO concentration and temperature change throughout CO_2 degassing experiments

Example of Six Bells shown for illustrative purposes

Details of both the RK4 method and the PHREEQCi software are contained within Chapter 4 Section 4.8. By far the most important of the logged parameters was pH (having such as large influence on Fe(II) oxidation rates and being directly related to dissolved CO_2 concentration). Curves for logged pH data at each of the sites are shown in Figure 7-5. The drift downwards in O_2 measurement over the course of the experiment has been noted other authors (Kirby et al. 2009) and can be attributed to fouling of the membrane of the DO probe by HFO over the course of the experiment.

7.2.1 Acidity, alkalinity and pH changes

In order to better understand the effect of dissolved CO_2 on the acidity and pH of the waters under investigation, acidity and alkalinity were measured at each of the sites before and after CO_2 degassing. Two different methods were used in the determination of acidity and alkalinity. Cold titrations were carried out on the freshly emerged water as well as a hot titration that required the addition of hydrogen peroxide followed by boiling for several minutes to ensure that all Fe(II) was oxidised and all CO_2 was degassed. Briefly, alkalinity was determined by titration of the minewater with H_2SO_4 to an endpoint determined by a colour change from green to pink using a bromocresol green-methyl red indicator. Acidity was determined by titration with NaOH to pH 8.4. Further details of the methods for determination of acidity and alkalinity are contained within Chapter 4, Section 4.4. The results of the hot titration were used directly to classify the sites as net-acid or net-alkaline (see Chapter 2 for a more detailed discussion of acidity and alkalinity). The results of the acidity and alkalinity titrations are given in Table 7-3. The range of values measured for alkalinity and particularly acidity at a number the sites illustrates the difficulties inherent in accurate determination of these parameters in the field.

The variations in recorded alkalinity pre-aeration were largely due to the subjective nature of the determination of the end point of the titration. Post aeration they were most likely due to slight differences in the rates of reaction and exact chemical composition of the water at the end of each different experimental run. The range of values for acidity however is a direct result of both the fact that CO_2 is degassed on the

timescale of the titrations, and that the addition of alkali causes the rapid oxidation of Fe(II) to Fe(III) and the sudden precipitation of both Fe(II) and Fe(III) hydroxides.

Both the oxidation and precipitation steps change the acidity of the sample as described in Chapter 2, Section 2.2. Depending upon how quickly the titration is carried out the sample may turn predominantly dark green indicating the presence of Fe(II) hydroxide precipitates or orange/brown indicating the presence of Fe(III) precipitates. Thus the hot peroxide titration which ensures that all CO_2 has been degassed and that all Fe(II) has oxidised gives the most reliable indication about the balance between acidity and alkalinity in the system.

Table 7-3 Acidity, alkalinity and [Fe(II)] measurements pre and post aeration, compared to the hot peroxide titration[a]

Site	Pre aeration (mg/L)			Post aeration (mg/L)			Hot peroxide (mg/L)
	Acidity	Alkalinity	Fe(II)	Acidity	Alkalinity	Fe(II)	
Blenkinsopp	423-476	264	137	23-21	34-38	5.75	33-55 net-acid
Tan-y-Garn	177-186	57-58	41	16-19	1	4.3	22-16 net-acid
Ynysarwed	259-280	143-146	93.7	45-51	5-7	2.79	29-33 net-acid
Dawdon	472-485	422-428	66.3	133-109[b]	286-265	0.06	191-199 net-alkaline
Six Bells	208-222	746-752	19	0	618-631	0.05	615 net-alkaline

[a]Values presented in this table may vary from those in Table 6-1 for the same sites and reflect the natural variations in the mine water chemistry that occur over time.
[b]On the day of the Dawdon trial there were problems with the battery used to drive the aeration pump. The relatively high remaining acidity is a result of incomplete CO_2 degassing

To further highlight the problems with relying on the cold acidity and alkalinity titrations Table 7-4 summarises the average values for acidity and alkalinity pre and post aeration at each of the sites together with a classification of net-acid or net-alkaline based on these values. It can be seen that at both Blenkinsopp and Dawdon the classification changed between the pre and post aeration samples. While these findings are not necessarily surprising they do underline the importance of the method chosen for determination of net-acidity or alkalinity at a site.

Table 7-4 Determination of waters as net-acid or net-alkaline based on cold acidity and alkalinity titrations[b]

Site	Pre aeration			Post aeration		
	Acid	Alk	Difference	Acid	Alk	Difference
Blenkinsopp	449	264	185 net-acid	22	36	14 net-alkaline
Tan-y-Garn	181	57	124 net-acid	17	1	16 net-acid
Ynysarwed	270	145	125 net-acid	48	6	42 net-acid
Dawdon	479	425	54 net-acid	121[a]	276	153 net-alkaline
Six Bells	251	749	498 net-alkaline	0	625	625 net-alkaline

[b]Average values for acidity, alkalinity measurements pre and post aeration (mg/L $CaCO_3$ equivalent)

Using the results presented in Table 7-3 for the hot peroxide titrations, the waters at Blenkinsopp, Tan-y-Garn and Ynysarwed are classified as net-acidic, while Dawdon and particularly Six Bells are highly net-alkaline. In addition to the results of the titrations, the measurements for Fe(II) concentration taken at the end of the degassing experiments (see Table 7-3) also give a useful indication as to the potential Fe removal that could be achieved without chemical dosing. With sufficient up front aeration and CO_2 degassing most of the Fe(II) could be removed from all of these waters extending the lifetime of later treatment stages such as a RAPS by reducing clogging with HFO precipitates.

The classification of the waters as net-acid or net-alkaline has implications beyond simply deciding whether or not an alkalinity generating step is required during the treatment process. Changes brought about in pH with mechanical aeration were monitored throughout the experiments and are presented in Figure 7-5. It can be seen that the net-acidic sites all have a similar characteristic shape to the curve for pH vs time with an initial sharp increase in pH and peak at around 1000 s followed by a steady decrease in pH. In contrast, the two net-alkaline sites show pH increasing throughout the experiments. Experiments at the net-acid sites were carried out over a longer time scale than at the net-alkaline sites. This is because the aim of these experiments was to increase d[Fe(II)]/dt by CO_2 degassing and at net-alkaline sites the time taken to reach concentration Fe(II) < 1 mg/L is less than at net-acid sites. The unusual shape of the pH curve at the Dawdon site is a result of inconsistent aeration

because the battery powering the pump started to run down during the experiment. The following descriptions highlight the reasons for the observed changes in pH in each case.

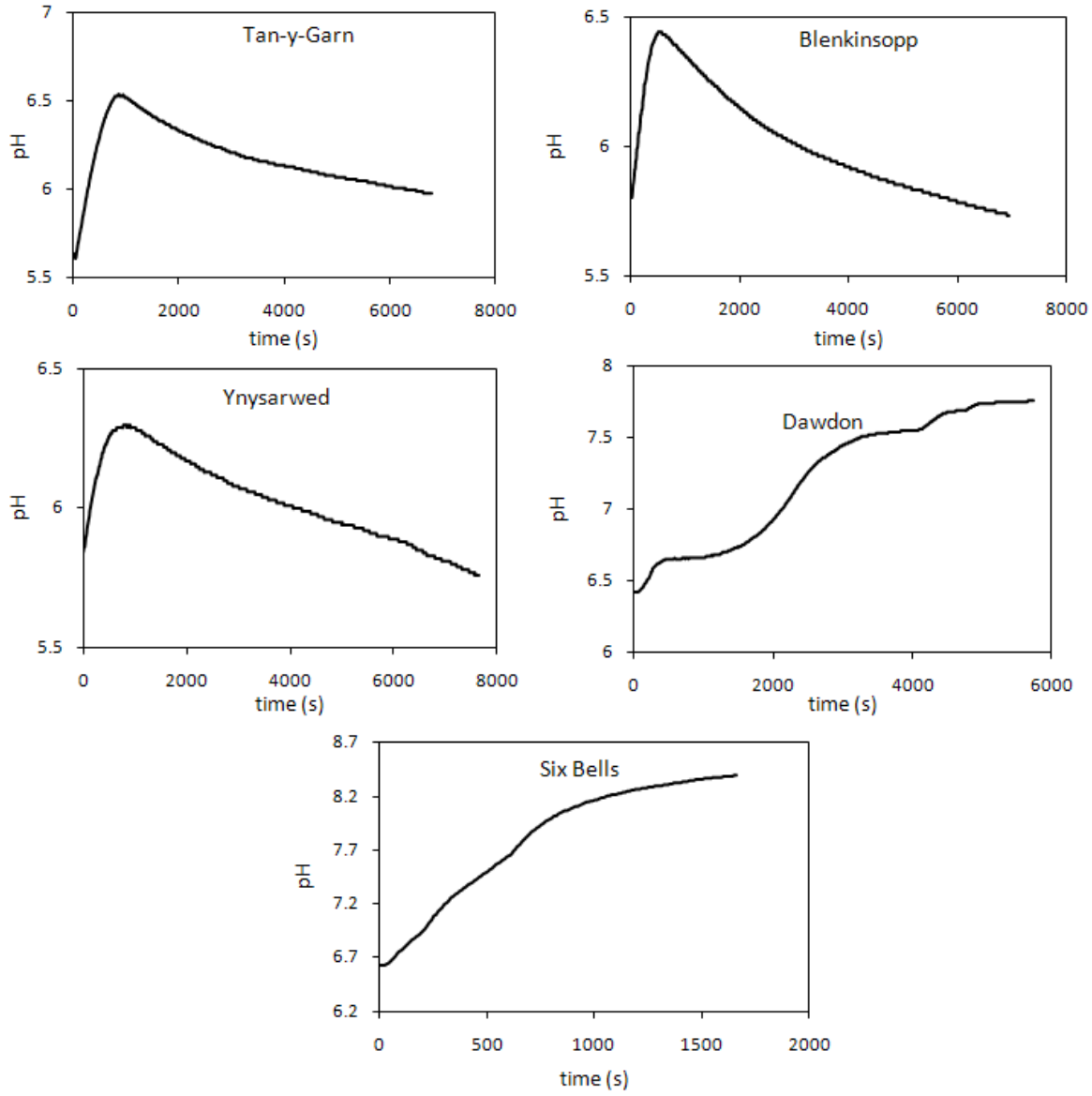

Figure 7-5 Comparison of pH curves observed on CO_2 degassing at net-acid and net-alkaline sites

Net-acid sites Blenkinsopp, Tan-y-Garn and Ynysarwed. Net-alkaline sites Dawdon and Six Bells

Net-acid and borderline net-acid sites

For all of the sites that were net (or borderline) acid the initial pH values were below pH 6. It can be seen that pH rose quickly within the first 10 minutes of aeration indicating the degassing of dissolved CO_2. The pH peaked at all three sites between 6.3

- 6.5 before decreasing again. The characteristic shapes of the curves can be explained by the changing chemistry of the system over time.

1. Initial increase in pH corresponds to rapid CO_2 degassing.
2. As rate of CO_2 degassing slows rate of increase of pH also slows.
3. Rising pH causes increasingly rapid Fe oxidation and precipitation which consumes alkalinity and causes pH to fall again.

Net-alkaline sites

It can be seen that the shapes of the curves for pH change in net-alkaline waters (Figure 7-5) are very different to those observed for net-acid waters. The pH rises continuously throughout the experiment with CO_2 degassing as there is sufficient alkalinity present to neutralise any acidity generated by the formation of Fe(III) hydroxides.

The fact that the pattern of the pH changes observed remains consistent across a number of different sites implies that this method of aeration with pH monitoring can serve as a useful guide in the assessment of new mine water discharges. As has been noted previously, measurements of acidity and alkalinity can vary widely and the accuracy of the measurements is highly dependent on the skill and experience of the individual carrying out the work. By contrast, provided that the pH meter used is working correctly the degassing method with pH logging is a very straightforward way in which to assess a discharge with far less likelyhood of the introduction of operator error.

7.2.2 Excel RK4 modelling for Fe oxidation and alkalinity consumption

In order to determine the rates of CO_2 degassing occurring during in the batch-wise experiments it was necessary to calculate the rate of change of alkalinity. As described in Chapter 4 it was assumed that alkalinity consumption was stoichiometrically linked to Fe(II) oxidation. The numerical 4^{th} order Runge-Kutta (RK4) method described in Chapter 4 Section 4.5.3 was used to calculate changes in [Fe(II)] over time based on the logged values for pH, DO and temperature as well as initial Fe(II) concentration.

The RK 4 method performs iterative calculations based on the rate equation for a chemical reaction to predict the changes in the concentration of the reactant of interest over time. Since the waters in this study had similar chemistry (and in some cases were exactly the same) as those described in Chapter 6 values for k_1 (the rate constant for homogeneous Fe(II) oxidation) chosen based on those calculated in Chapter 6 Section 6.1.4. The RK 4 method was run using these k_1 values which were verified by confirming that the final measured concentration of Fe(II) at the end of each experiment was matched by that predicted using the RK4 method. These values are given in Table 7-5.

Table 7-5 k_1 values used in RK4 model for CO_2 degassing experiments

Site	k_1 ($M^{-2}atm^{-1}s^{-1}$)
Blenkinsopp	8.50×10^{13}
Tan-y-Garn	2.90×10^{13}
Ynysarwed	1.33×10^{14}
Dawdon	1.58×10^{13}
6 Bells	4.5×10^{12}

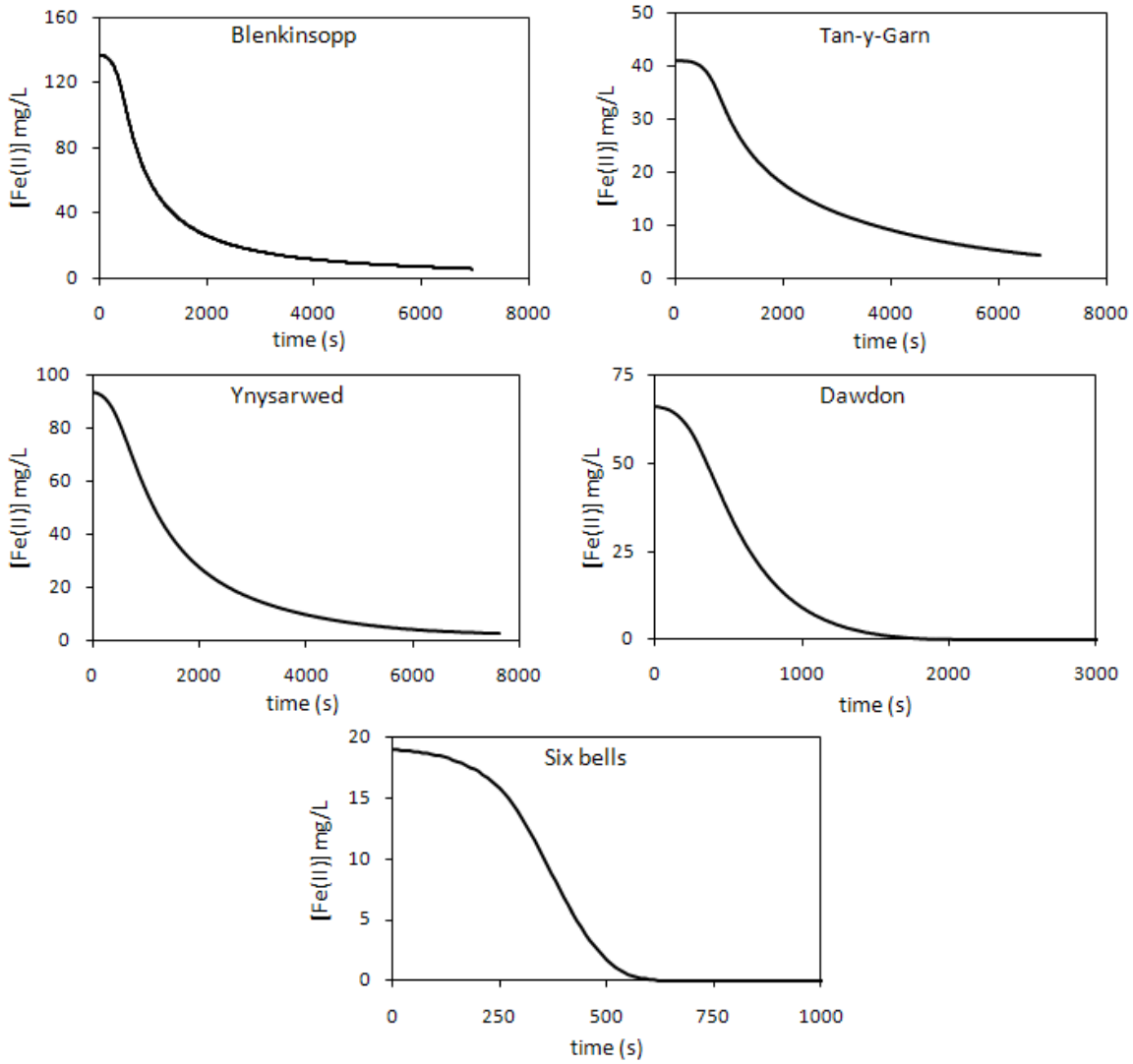

Figure 7-6 Fe oxidation curves produced from CO_2 degassing experiments

The results of the Fe(II) oxidation curves produced by the RK4 method are shown in Figure 7-6. It can be seen that Fe oxidation occurred much more rapidly at the net-alkaline sites than at the net-acid sites. As would be expected from earlier experiments Fe(II) concentrations at the two net-alkaline sites Dawdon and 6 Bells dropped to < 1 mg/L in under 30 minutes. The changes measured in Fe(II) concentration during the degassing experiments were very similar (again expectedly) to those observed previously during the work carried out on Fe oxidation rates.

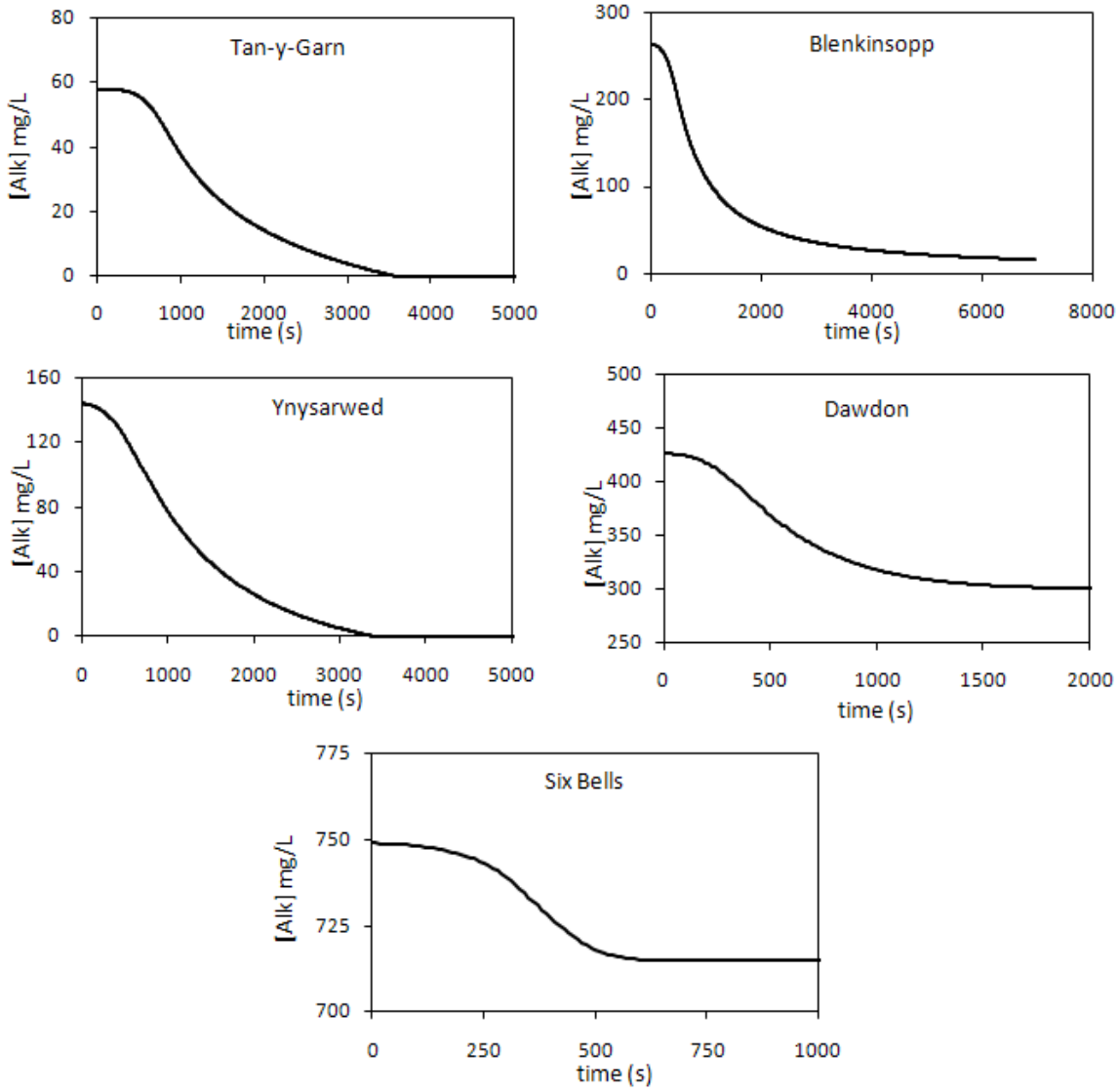

Figure 7-7 Calculated changes in Alkalinity (mg/L $CaCO_3$ equivalent)

The changes in Fe(II) concentration were then used to calculate changes in alkalinity over time in the waters under investigation. It was assumed for the purposes of these calculations that once Fe(II) had oxidised to Fe(III) the precipitation of Fe(III) hydroxides was instantaneous. As a result, changes in Fe(II) concentration could be directly related to changes in Alkalinity concentrations as described in Chapter 4, Section 4.8.1. Curves were produced for changes in alkalinity at each of the sites calculated using the changes in Fe(II) concentration over time shown in Figure 7-7.

It can be seen that for the net-acid sites the alkalinity is predicted to drop to zero or approach zero towards the end of the experiment, whereas for the net-alkaline sites

the alkalinity remains high at the end of the experiment. These outcomes were expected based on the way in which alkalinity consumption was calculated. It is highly unlikely that alkalinity actually dropped to zero at the net-acid sites as this would imply that total dissolved inorganic carbon was zero since the whole system is in equilibrium. This highlights that this method of calculation is over simplified. These results do however provide a useful guide as to the changes that could be expected over the initial stages of the experiments.

7.2.3 Using PHREEQCi to calculate concentrations of dissolved carbonate species

The geochemical modelling software PHREEQCi can be used in a number of different ways in order to produce information about the concentrations of dissolved species in an aqueous environment. In spreadsheet mode lists of known parameters such as pH, alkalinity etc can be input and the software will produce a list of the species present in solution for each line of the input spreadsheet.

In order to determine the concentrations of dissolved CO_2 and other carbonate species in the waters studied here the logged values for pH, DO and temperature together with the calculated values for Fe(II) and Alkalinity concentrations were input into PHREEQCi in spreadsheet mode. The values output by the model for dissolved CO_2, total dissolved inorganic carbon (TDIC), HCO_3^- and CO_3^{2-} are shown in Figure 7-8.

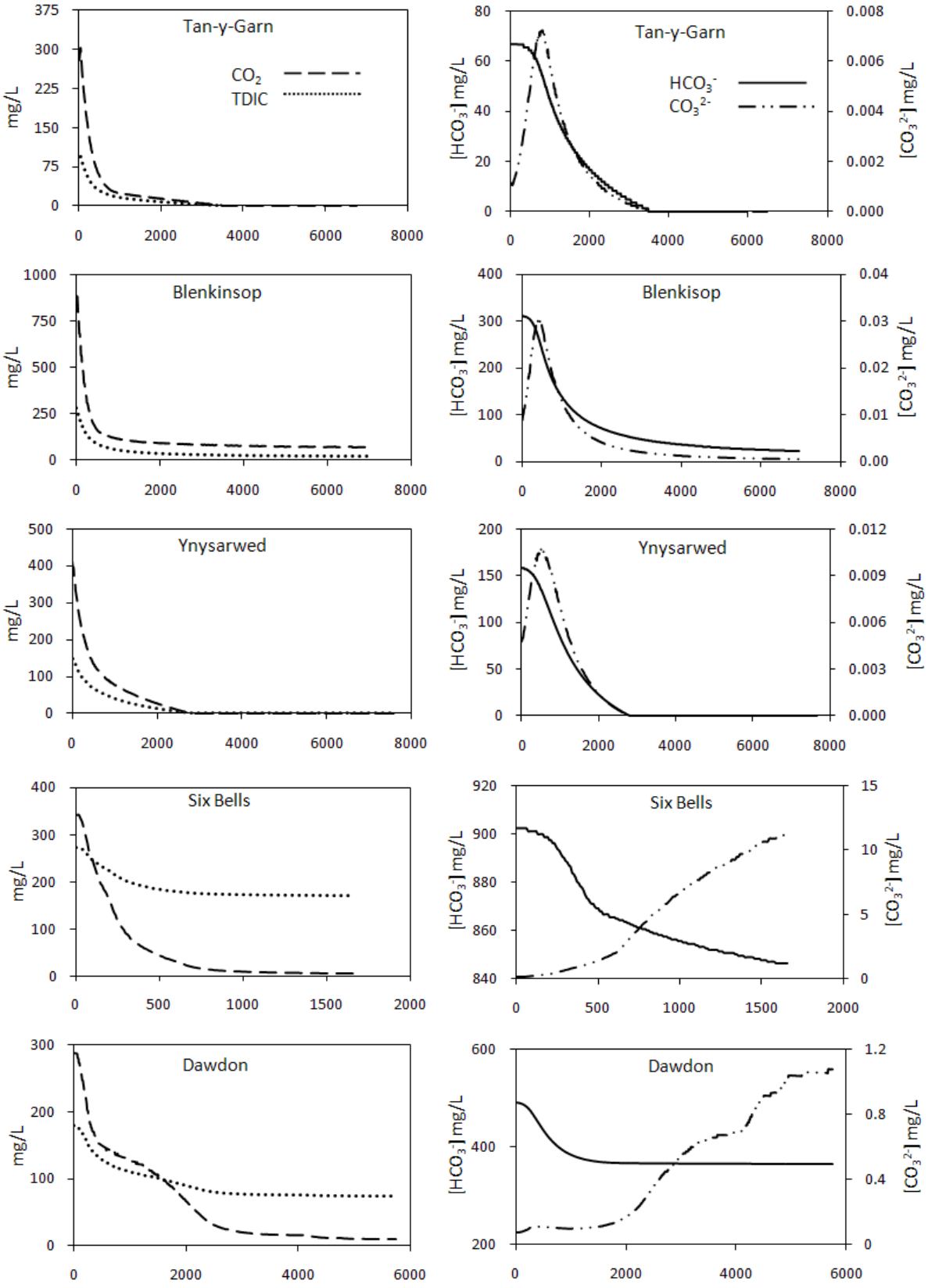

Figure 7-8 Calculated concentrations of carbonate species with CO_2 degassing

Time along the x axis in seconds

It can be seen that in all cases the calculated concentration of dissolved CO_2 drops off rapidly at first and then much more slowly towards the end of the experiment. In the case of Ynysarwed and Tan-y-Garn, the model predicts that TDIC drops off to zero by the end of the reaction. For the net-acidic sites CO_3^{2-} initially rises in line with increasing pH before decreasing again as alkalinity is consumed. For the net-alkaline sites, the proportion of TDIC represented by CO_3^{2-} was shown to increase throughout the experiments. Changes in HCO_3^- are a direct result of alkalinity consumption by the formation of Fe(III) oxyhydroxide (HFO) precipitates. Whilst percentage changes in CO_3^{2-} (tracking closely changes in pH) might appear large, in reality the concentration of this species compared to all of the others under investigation is actually very low.

Initial and final values for dissolved CO_2 along with equilibrium concentration with respect to the atmosphere are shown in Table 7-6. Atmospheric CO_2 concentration was taken to be 387 ppm (NOAA 2011). It can be seen that the model did not show any of the sites reaching atmospheric equilibrium by the end of the experiments. In the case of the net-acid sites this is because dissolved CO_2 is predicted to drop to zero. The failure of such CO_2 degassing experiments to result in atmospheric equilibrium has previously been noted in similar studies of circumneutral mine drainage (Cravotta 2007, Kirby et al 2009) though it has not been explained.

Table 7-6 Comparison of initial and final values for dissolved CO_2 concentration produced by PHREEQCi to concentration of dissolved CO_2 at atmospheric equilibrium

Site	Initial [CO_2] (M)	Final [CO_2] (M)	Equilibrium [CO_2] (M)
Tan-y -Garn	6.7×10^{-3}	0	1.6×10^{-5}
Blenkinsopp	1.8×10^{-2}	1.5×10^{-3}	1.6×10^{-5}
Ynysarwed	9.4×10^{-3}	0	1.6×10^{-5}
6 Bells	7.8×10^{-3}	1.2×10^{-4}	1.5×10^{-5}
Dawdon	6.5×10^{-3}	2.3×10^{-4}	1.4×10^{-5}

Differences in equilibrium [CO_2](calculated using Henry's law) are a result of different water temperatures at the sites

Broadly speaking the changes in carbonate species predicted by PHREEQCi based on pH and alkalinity were to be expected. In the case of the net-acid sites, the fact that the concentrations of all carbonate species (including dissolved CO_2) drop to zero arises as when used in spreadsheet mode the PHREEQCi software cannot bring the

species in the reaction mixture into atmospheric equilibrium. According to the equations for carbonate equilibria (as described in Chapter 2, Table 2-2) used by the PHREEQCi software if the concentration of one carbonate species is input as zero then all others must correspondingly be zero. The main drawback of this simplistic modelling therefore is that in truly net-acid conditions the calculated consumption of all available alkalinity results in the prediction of the complete removal of dissolved inorganic carbon from the system over the course of the experiment.

It was necessary therefore to find a different way of modelling the carbonate speciation of the system that could account for both rate CO_2 degassing and Fe(II) oxidation/alkalinity consumption simultaneously. It was decided to use a PHREEQCi model previously developed by Cravotta (2007) and described in Chapter 4, Section 4.8 to couple the rate equations for d[Fe(II)]/dt and d[CO_2]/dt (the two main reactions that control pH in ferruginous mine waters).

The form of the rate equation for Fe(II) oxidation is well known and has been discussed in Chapters 2 and 6 with values for k_1 (the rate constant for homogenous oxidation) calculated for ferruginous mine drainage in the field. There was still work to be done however in determining the form of the rate equation and values for the rate constant k_La (the liquid film coefficient) for the CO_2 degassing reaction. A detailed description of the methods employed in calculating k_La values and establishing the form of the rate equation are explained more fully in Chapter 4, Section 4.8.1.

It was shown that CO_2 degassing was best described by the second order form of the rate equation (see Chapter 4, Section 4.8.1). This was then taken in its integrated form (Equation 7-5) and [1/(Cs-Ct)+1/(Cs-Co)] was plotted vs time where C_s is the equilibrium concentration of CO_2, C_o is the initial concentration and C_t is the concentration at time t. Values of k_La were taken to be the gradient of the line produced.

Equation 7-5

$$\mathbf{k_L a \times t = \frac{1}{(C_s - C_t)} + \frac{1}{(C_s - C_0)}}$$

Values of k_La were then verified by comparing plots of logPco_2 calculated from pH and alkalinity plots logPco_2 calculated using the 2nd order rate equation. These charts are shown in Figure 7-9. The values for k_La input into the rate equation were taken as the

gradient of the line of [1/(Cs-Ct)+1/(Cs-Co)] vs time plotted over the first 10 minutes of the experiment . Further explanation of (and reasons for) this method of calculation are given in Chapter 4 Section 4.8. Values calculated for k_La are shown in Table 7-7.

Table 7-7 Comparison of k_La values for CO_2 degassing across the sites studied

Site Name	Alkalinity (mg/L)	k_La ($atm^{-1}s^{-1}$)
Blenkinsopp	264	3.66×10^{-4}
Blenkinsopp	240*	4.12×10^{-4}
6 Bells	749	1.31×10^{-3}
Tan-y-Garn	58	7.31×10^{-4}
Tan-y-Garn	65*	6.70×10^{-4}
Ynysarwed	144	2.36×10^{-4}
Ynysarwed	160*	2.41×10^{-4}

*values adjusted to improve fit of modelled data to measured data

As would be expected there was some variation in k_La (up to a factor of 6) across the sites studied. This can be accounted for by several factors, one of which is the difficulty in replicating the exact same experimental conditions across a variety of different sites in the field. It can be seen from Chapter 4, Figure 4-2 (the experimental set up was the same for homogenous oxidation and CO_2 degassing experiments) that the precise position of the pump within the bucket used during the experiments can easily be varied resulting in slight differences in the way the water is circulated inside the bucket. In addition to this, the 12V car battery that was used to power the pump began to run down towards the end of some of the experiments resulting in small reductions in the rate of mixing over the course of some of the experiments. Therefore, despite every effort to replicate the same conditions small variations in the experimental set up could have occurred to alter the A/V (surface area/volume) ratio that is incorporated into k_La in this work. Additionally, the proportion of TDIC that exists as CO_2 (and hence the driving force for CO_2 degassing) is dependent on pH. Since the pH changes observed in these systems are not just a function of concentration of dissolved CO_2, but also Fe oxidation and alkalinity consumption, the variation in k_1

observed across the sites (and hence rate of alkalinity consumption) is also likely to contribute to some extent to the differences in k_La.

It can be seen from Table 7-7 that for three of the sites more than one value of k_La and alkalinity are given. This was a result of adjustments made after the initial runs using PHREEQCi. The PHREEQCi model described in Chapter 4 was found to be highly sensitive to changes in alkalinity. As a result of this sensitivity and the uncertainties inherent in the measurement of alkalinity in the field it was decided to adjust this parameter in order to give the best fit between the measured values of pH and the values predicted by PHREEQCi. Adjustments to alkalinity had a knock on effect in terms k_La as in order to maintain the same initial pH conditions any changes to alkalinity must be compensated for by a change in dissolved CO_2 concentrations which will in turn have an effect on the rate of CO_2 degassing. Thus k_La was recalculated for each of the different values for alkalinity.

The data for Six Bells were not used further in the PHREEQCi model as due the highly net-alkaline nature of the water TDIC was not predicted to approach zero and so the results shown in Section 7.2.3 were taken to give a realistic representation of the system. As a result of the problems experienced with the aeration pump at Dawdon it was not possible to produce a meaningful value of k_La at this site and so again there will be no further discussion of the conditions at this site.

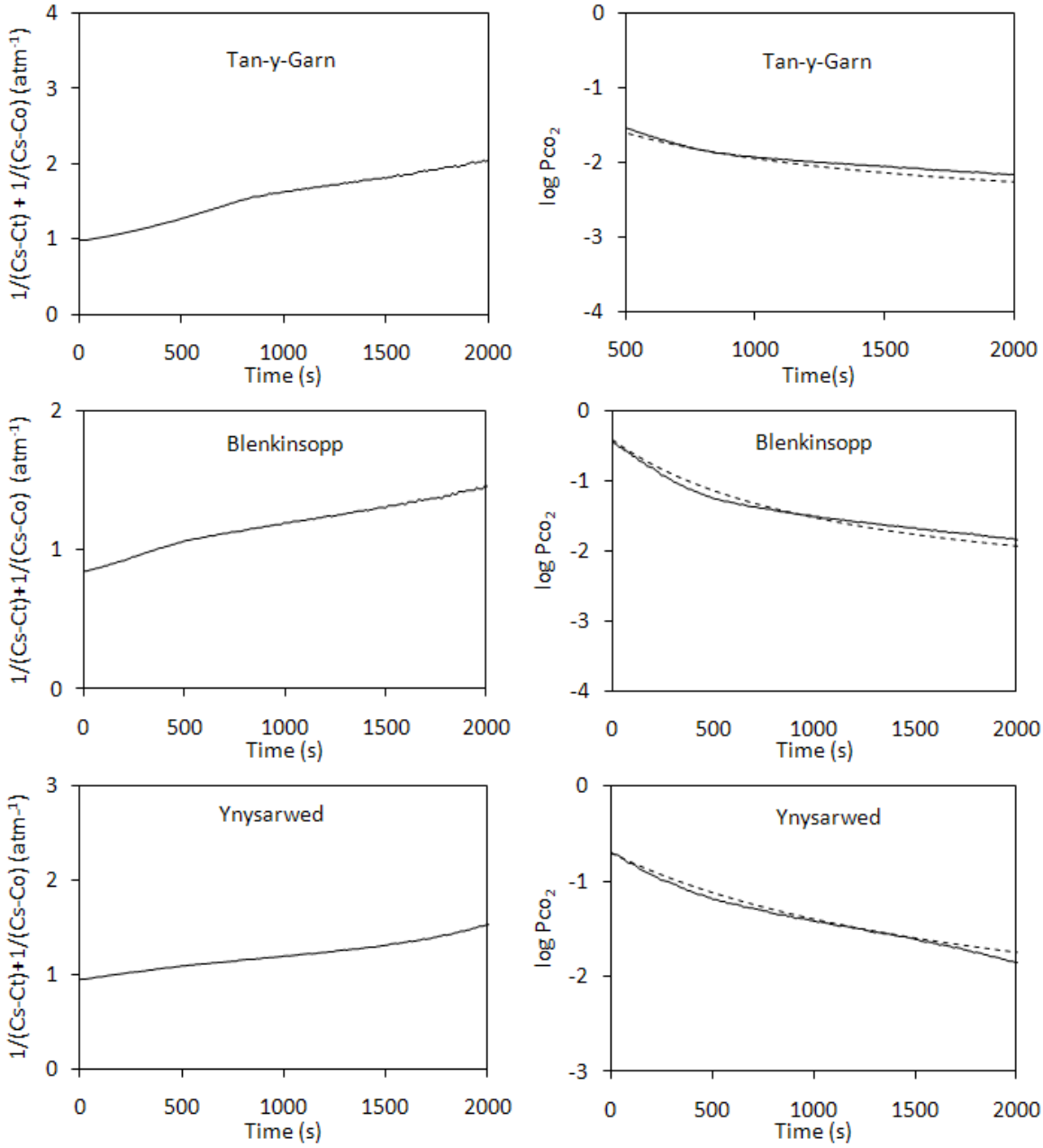

Figure 7-9 Plots of integrated 2nd order rate equation for CO_2 degassing and corresponding plots of log Pco_2

Predicted values of logPco_2 calculated using k_La (broken line) logPco_2 calculated from pH and alkalinity data (solid line)

7.2.4 PHREEQCi modelling of Fe oxidation and CO_2 degassing based on k_1 and k_La

The purpose of further refining the model of CO_2 degassing was to determine whether the pH changes in the mine waters under investigation could be adequately accounted

for by loss of acidity via CO_2 stripping and acidity generation resulting from Fe(II) oxidation. Coupling of the rate equation for CO_2 degassing to the rate equation for Fe(II) oxidation in PHREEQCi would give several pieces of information if the pH changes predicted by the model matched those measured in the field. Firstly it would confirm the validity of the rate equation for CO_2 degassing in these waters, secondly it would allow a good approximation of the changes in chemical composition of the mine water over time to be generated, and thirdly it would further validate the range of values calculated for k_1 during the homogeneous oxidation experiments presented previously (see Chapter 6).

The PHREEQCi model used in this section can be summarised as follows:

- Rate equation for CO_2 degassing as used previously by Cravotta (2007) was input into the model
- Rate equation Fe(II) oxidation was also input into the model
- Values for the rate constants k_1 and k_La were input
- Other values for equilibrium constants for various aqueous species including Fe species were taken from example 9 in the PHREEQCi manual (Parkhurst and Appelo 1999) as suggested by Cravotta (2011)
- Values for alkalinity were input
- The model was run with time steps of 10 s such that the rate of CO_2 degassing and Fe(II) oxidation was adjusted every 10 seconds as the chemical composition and pH of the solution changed.

Further details about the PHREEQCi model (combining the rate equations for CO_2 loss and Fe(II) oxidation) are contained within Chapter 4, Section 4.8 and Appendix 3. Values of k_1 were chosen that gave the best correlation with the Fe(II) oxidation curves produced by the RK4 method and were within the range previously determined during the Fe oxidation experiments (Chapter 6, Section 6.1).

Curves for alkalinity, dissolved Fe(II) and dissolved CO_2 were compared to those calculated previously and shown in Section 7.2.3. The pH curves produced by the model were compared to those measured directly during the degassing experiments. The results are shown in Figure 7-10 to 7-14. It can be seen that by using this method

to model the system neither alkalinity nor dissolved CO_2 are predicted to drop to zero. A more detailed discussion of the results for each of the sites studied is given below. Where two different values for alkalinity were input into the PHREEQCi model, the first was the value measured on site (the average of at least 2 titrations), the second (adjusted) value was chosen to give a better fit between the model and the measured pH data.

Ynysarwed

It can be seen from Figure 7-10 that the initial attempt to model the system using the alkalinity as measured on site produced quite large differences between the outputs from PHREEQCi and the measured changes in pH and Fe(II) concentration. The pH did not rise as quickly in the model as the measured pH and started to decrease again sooner and more sharply. This lower predicted pH caused a lower rate of Fe(II) oxidation which caused Fe(II) concentration to increasingly deviate from that obtained experimentally. At the end of the experiment empirical and modelled values for pH and Fe(II) concentration were 5.78 vs 5.52 and 3.1 mg/L vs 14.5 mg/L respectively. Adjustment of the input alkalinity from 144 to 160 mg/L brought the modelled and measured values into much better agreement particularly with respect to pH (Figure 7-11) now 5.78 vs 5.82 (empirical vs modelled) at the end of the experiment. Increasing the alkalinity affected the model by allowing for an initial rapid degassing of a greater quantity of CO_2 that resulted the larger initial increase in pH. The higher pH produced a corresponding increase in the rate of Fe(II) oxidation giving a final Fe(II) concentration of 7.3 mg/L closer to that obtained experimentally, though still not within the 10 % error associated with the ICP-OES analysis.

Blenkinsopp

At this site input of the measured alkalinity of 264 mg/L resulted in non-convergence of the PHREEQCi model and so no meaningful outputs could be obtained, thus only the results for the adjusted alkalinity (240 mg/L) are shown (Figure 7-12). At this site the agreement between the changes in Fe(II) concentration as measured on site and predicted by the model was excellent, as was the agreement for the pH curve over the initial stages of the experiment. In this example final pH and Fe(II) concentrations were

5.74 vs 5.76 and 6.0 mg/L vs 5.8 mg/L for modelled vs measured values respectively. Given the errors associated with measurements of pH the 10 % error for ICP-OES measurements discussed in Chapter 4 Section 4.1 the values produced by the model are within the range of experimental/analytical error of the field measured values in this case.

Tan-y-Garn

As with the results for Ynysarwed, adjustment of the input alkalinity from the measured values of 58 mg/L to 65 mg/L produced much better agreement between the measured and modelled values for changes in Fe(II) and pH at this site (see Figure 7-13 and 7-14) Measured final values for pH and Fe(II) were 5.98 and 4.4 mg/L. Increasing the alkalinity increased the modelled pH at the end of the experiment from 5.74 to 5.93 and reduced Fe(II) concentration from 9.6 to 5.9 mg/L.

The results produced by the PHREEQCi model for changes in pH and dissolved Fe(II) correlated well with the measured values across the three sites studied. This correlation gives confidence in the values of k_La and k_1 calculated for each of the waters under investigation and adds weight to the previous conclusions (see Chapter 6) that rates of Fe oxidation in the field are often several orders of magnitude higher than those observed in the laboratory.

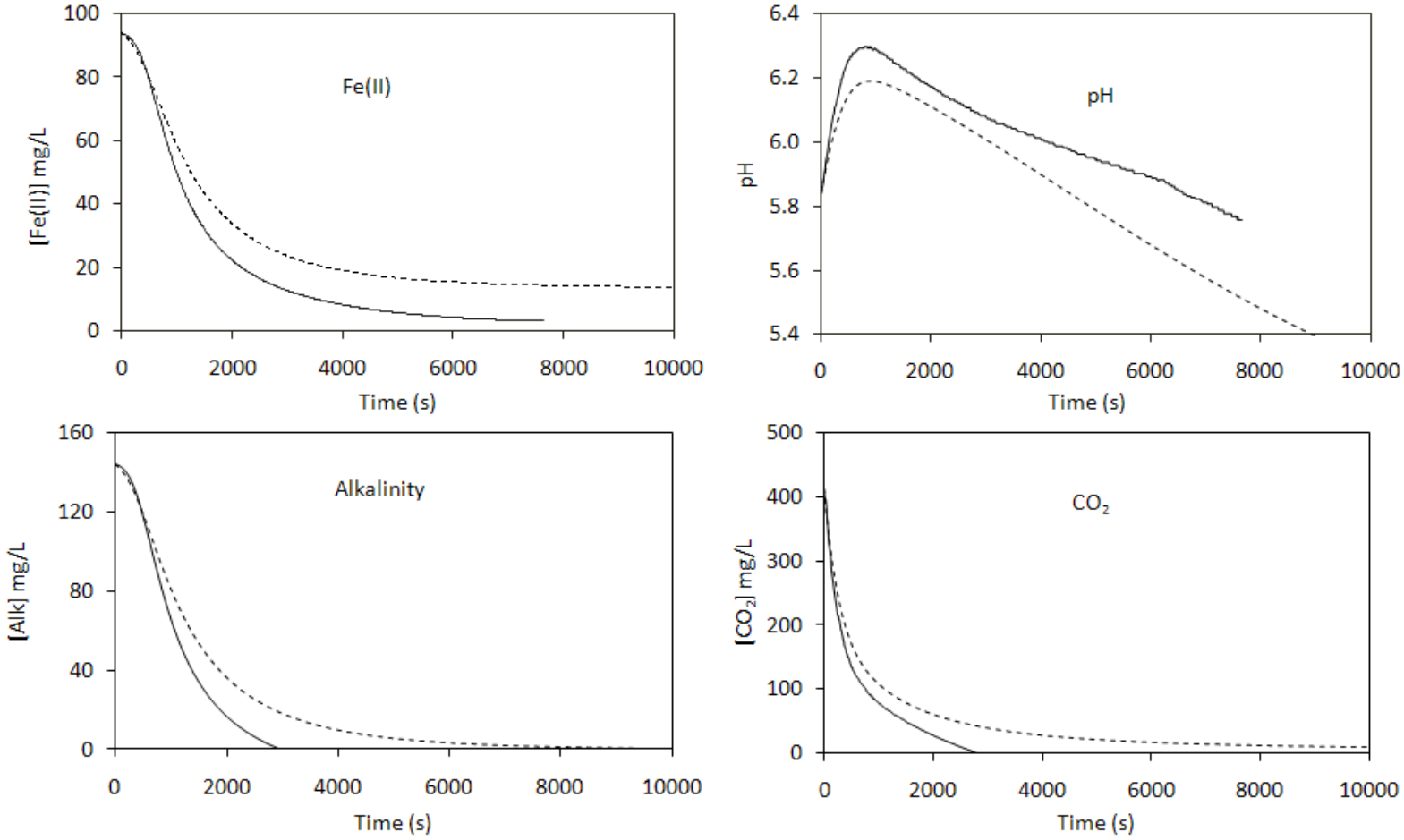

Figure 7-10 Comparison of PHREEQCi modelled values to measured pH and RK4 predicted values for Fe(II), Alkalinity and CO_2concentration at Ynysarwed

PHREEQCi values broken line, measured (pH) and RK4 values solid line. $k_1 = 7.30 \times 10^{13}\ M^{-2}atm^{-1}s^{-1}$, A=alkalinity = 144 mg/L

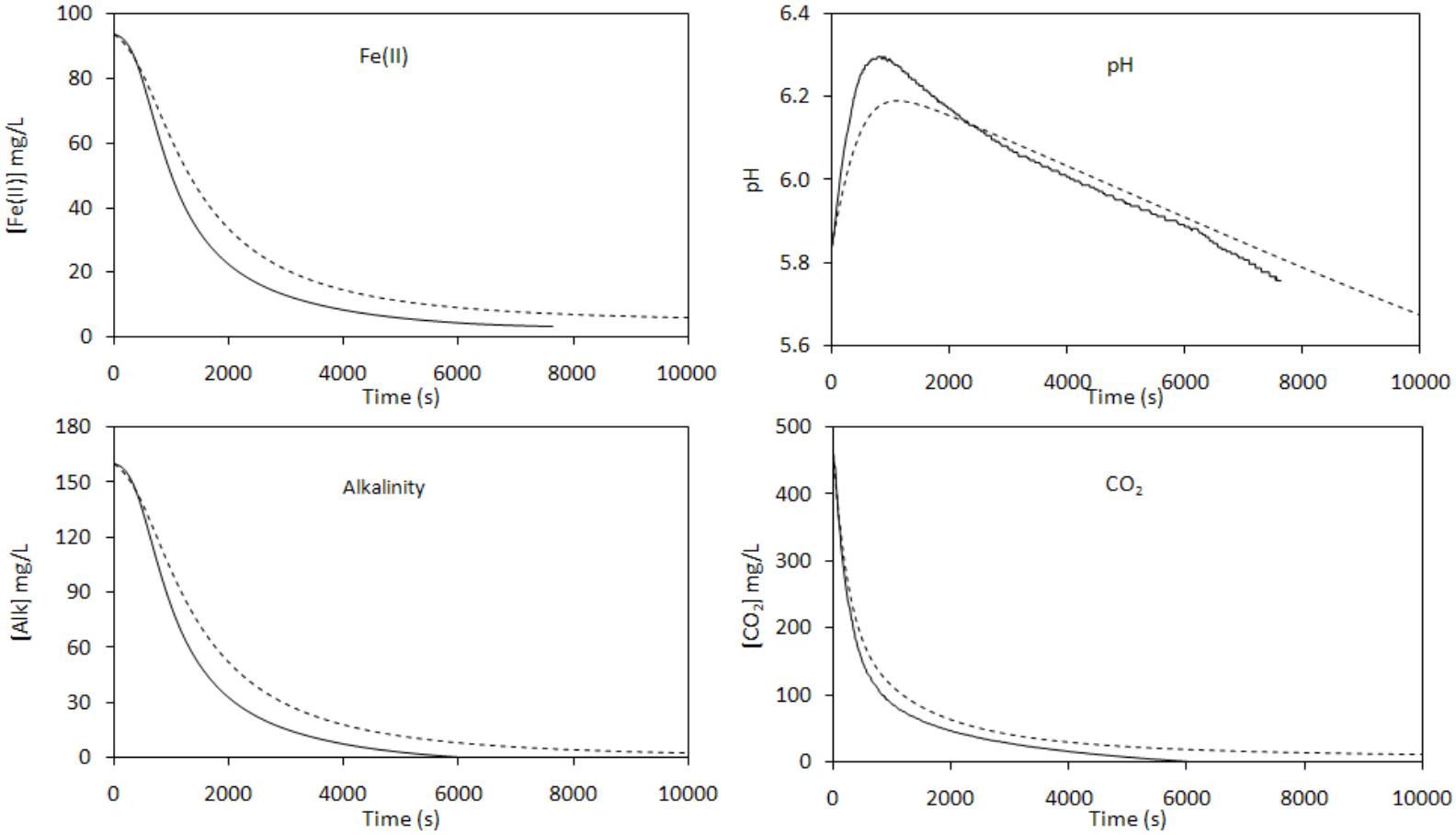

Figure 7-11 Comparison of PHREEQCi modelled values to measured pH and RK4 predicted values for Fe(II) alkalinity and CO_2concentration at Ynysarwed
PHREEQCi values broken line, measured (pH) and RK4 values solid line. k_1 = 7.30 x 10^{13} $M^{-2}atm^{-1}s^{-1}$, alkalinity = 160 mg/L

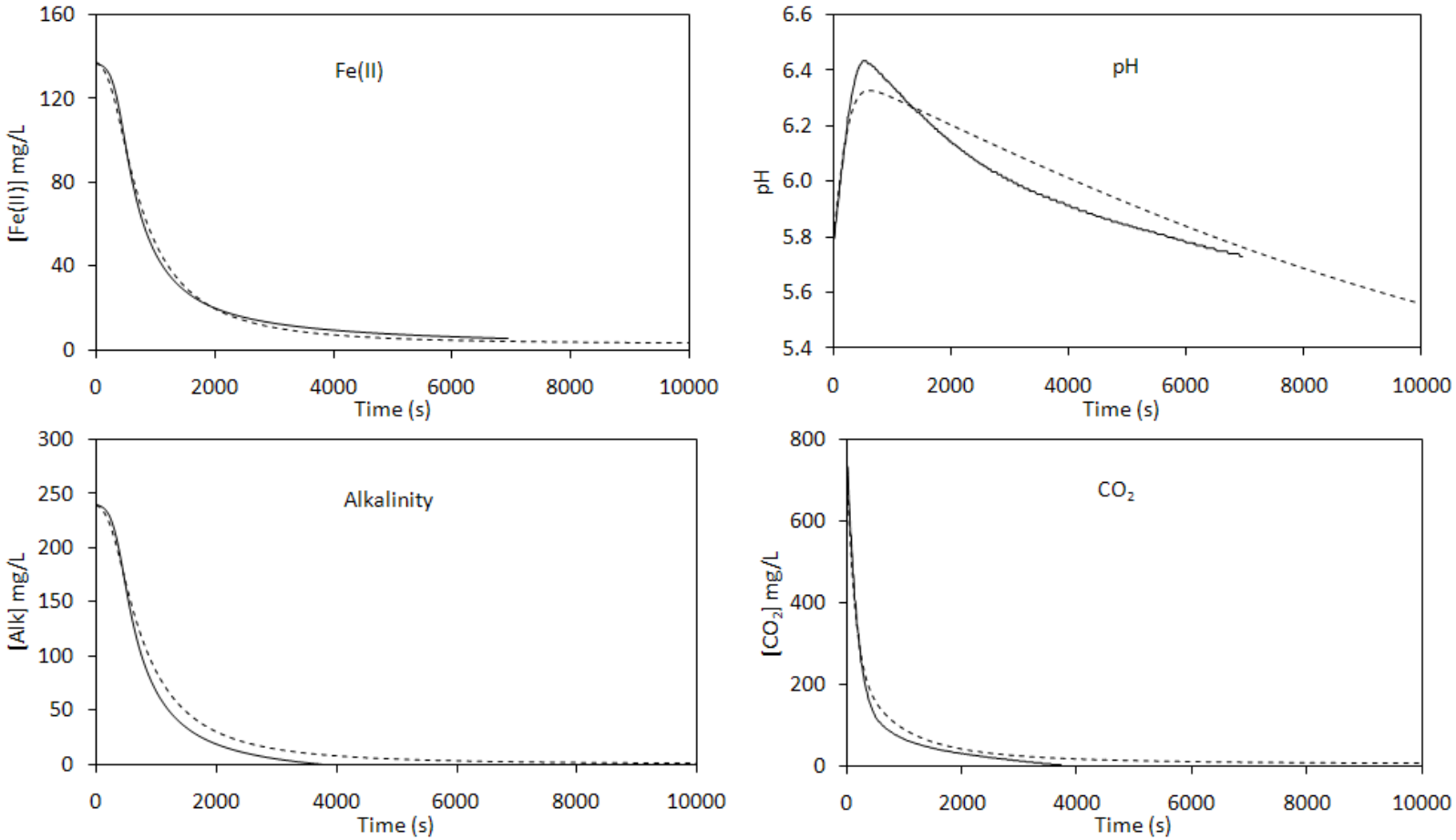

Figure 7-12 Comparison of PHREEQCi modelled values to measured pH and RK4 predicted values for Fe(II), Alkalinity and CO_2concentration at Blenkinsopp

PHREEQCi values broken line, measured (pH) and RK4 values solid line. k_1 = 7.89 x 10^{13} $M^{-2}atm^{-1}s^{-1}$, Alkalinity = 240 mg/L

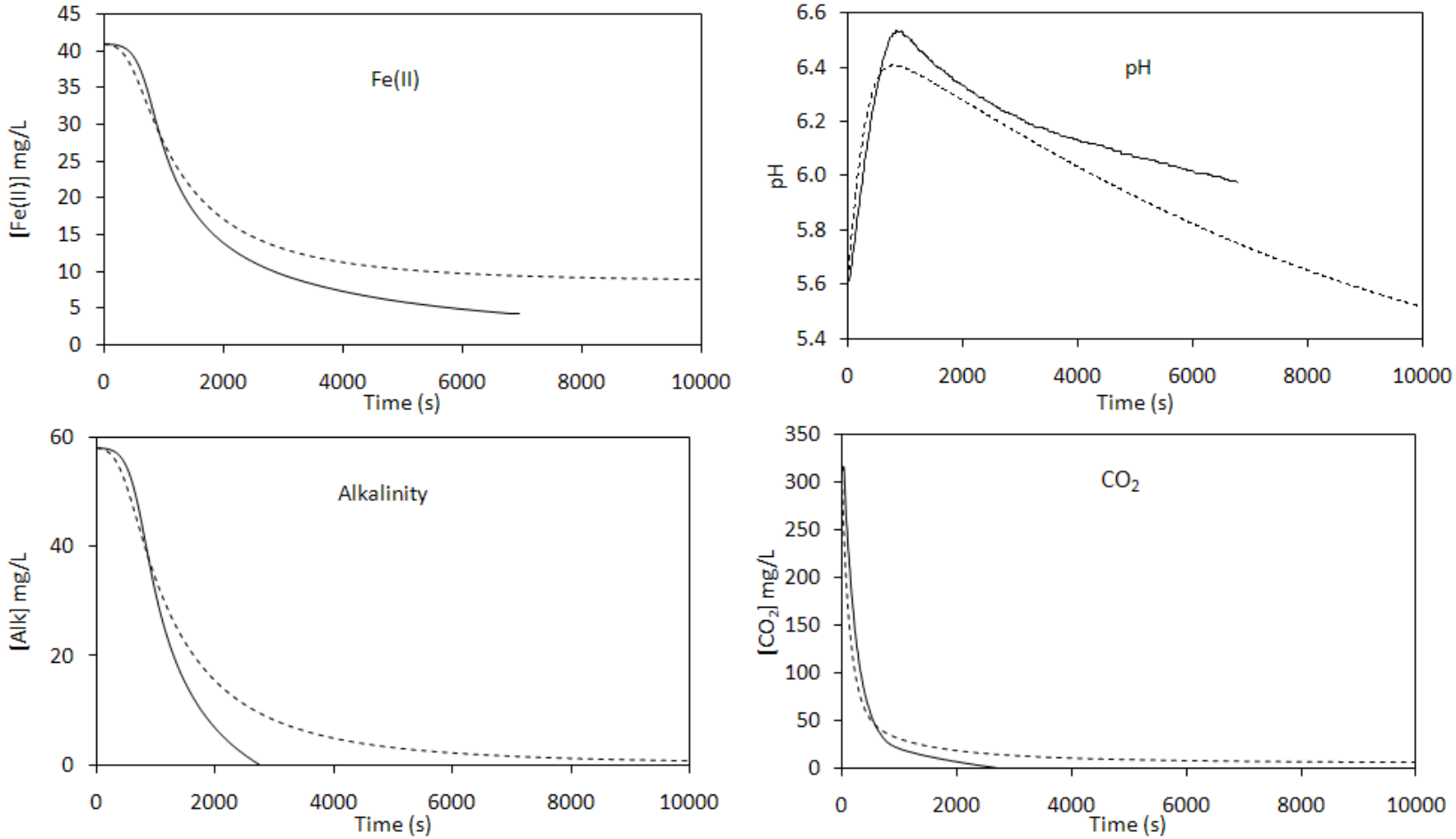

Figure 7-13 Comparison of PHREEQCi modelled values to measured pH and RK4 predicted values for Fe(II), Alkalinity and CO_2concentration at Tan-y-Garn

PHREEQCi values broken line, measured (pH) and RK4 values solid line. $k_1 = 2.66 \times 10^{13}\ M^{-2}atm^{-1}s^{-1}$*, Alkalinity = 58 mg/L*

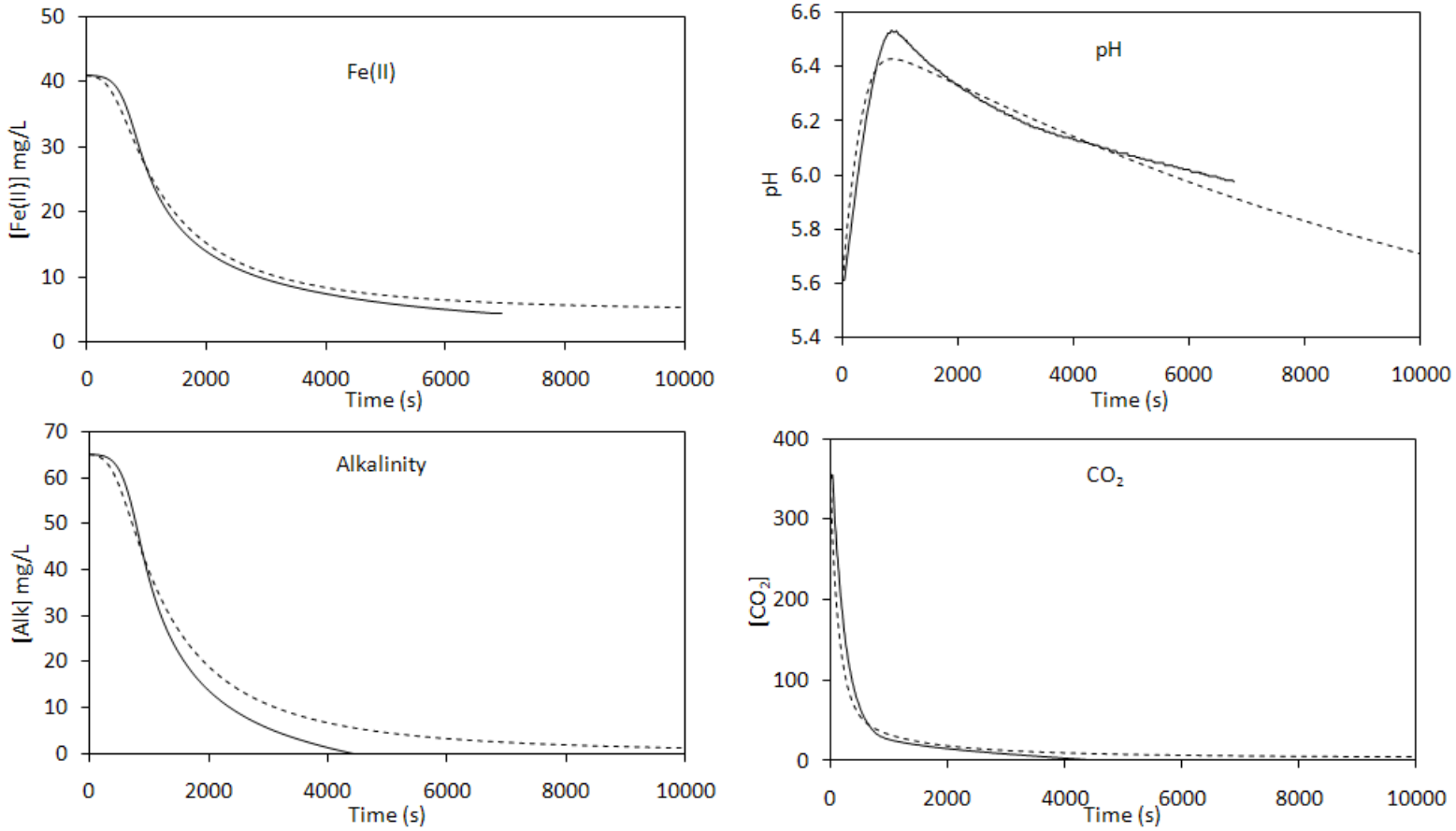

Figure 7-14 Comparison of PHREEQCi modelled values to measured pH and RK4 predicted values of Fe(II), Alkalinity and CO_2concentration at Tan-y-Garn
PHREEQCi values broken line, measured (pH) and RK4 values solid line. k_1 = 2.66 x 10^{13} $M^{-2}atm^{-1}s^{-1}$, Alkalinity = 65 mg/L

Differences between the shapes of the measured and modelled pH curves are difficult to explain in simple terms. The reason why the model does not give the same maximum pH as that which was measured experimentally is not clear. It would seem logical that making incremental adjustments to the input alkalinity and (hence rate/quantity of CO_2 degassing) would raise the maximum pH attained by the model. Looking at the examples of Ynysarwed and Tan-y-Garn however it can be seen that in reality changing the alkalinity concentration has little effect on the highest pH value reached by the model, though it clearly increases the rate of Fe(II) oxidation. It appears that there may be other factors in the field experiments that are causing the pH to vary that cannot be explained simply by the rate equations used in the PHREEQCi model. This observation was also made by Cravotta (2007) in his attempts to model a net-alkaline ferruginous mine drainage who also found that the PHREEQCi model was highly sensitive to changes in alkalinity and also equilibrium Pco_2.

Kirby et al (2009) used a different software (Stella™, a graphical interface differential equation solver) to model changes in the carbonate and Fe speciation in ferruginous mine drainage. As with the PHREEQCi model used in this study (and previously by Cravotta (2007)) input parameters were initial alkalinity, pH, DO and Fe(II) concentration in as well as initial Pco_2 (calculated using PHREEQCi). The model then calculated changes in all of these parameters over time based on governing rate equations as detailed in Kirby et al's paper (2009). As with the PHREEQCi model the Kirby et al's Stella™ model showed a good correlation between measured and modelled Fe concentrations throughout the experiment, but the correlation of the model outputs with measured pH over the initial stages of the experiment was less good. Whereas the PHREEQCi model for net-alkaline waters under predicts pH change the Stella™ model over predicted pH change in the net-acid waters (though it did reach the same final steady state concentration).

Differences between the measured and modelled values shown in Figure 7-10 to 7-12 (and possibly in the other studies discussed above) could however at least in part be accounted for by factors that were uncontrolled in the experimental work but that were held constant by the PHREEQCi model throughout each set of calculations. The two most important factors were;

1. Dissolved oxygen: The model assumed oxygen saturation throughout the experiment. Concentrations of dissolved oxygen varied considerably in the field, particularly over the first few minutes of the experiment as was shown in Figure 7-4.
2. Temperature: The temperature varied by around 4^{o}C between the beginning and the end of the experiment across each of the sites studied while the PHREEQCi model held the temperature constant (this was taken to be the temperature at the start of each degassing run.)

The fact that the data produced by PHREEQCi shows increasing deviation from the measured pH and calculated values for Fe(II) concentration over time is therefore not surprising, though this still does not account for the variation between measured and modelled pH in the initial stages of the experiment. The RK4 method originally used to determine changes in Fe(II) concentration accounts for the changes in all parameters that influence the rate equation with adjustments to the oxidation rate as a result of changing DO or temperature made automatically. In the case of the PHREEQCi model however, the fixed nature of these input parameters is likely to cause increasing (although minor) deviations as the reaction proceeds.

Regarding rates of CO_2 degassing it can be seen that the majority of the dissolved CO_2 (>75%) is removed within the first 10-20 minutes of aeration with the rate of CO_2 removal dropping off rapidly after this point as would be expected for a rate law with 2nd order dependence on the reacting (in this case degassing) species (Langmuir 1997). The rates of CO_2 degassing over the first 5 minutes of the experiments are shown in Table 7-8.

Table 7-8 Comparison of CO_2 degassing rates at net-acid sites

Site name	Degassing rate (mg/L/min)
Blenkinsopp	163
Ynysarwed	134
Tan-y-Garn	70

A comparison of these degassing rates to observations made during the aeration cascade testing where around 100 mg/L of CO_2 was degassed over several seconds highlights the efficiency of these hydraulic structures relative to the mechanical

degassing technique used in this study. It is therefore clear that where recirculation of AMD over an aeration cascade is possible this would be preferable to mechanical degassing in terms of CO_2 stripping efficiency.

7.3 Implications for the treatment of mine drainage

7.3.1 Aeration cascade testing

The results presented here are in line with the results of a previous study carried out on aeration cascades at several mine water treatment sites in south Wales (Sapsford and Pugh 2010). In their report Sapsford and Pugh investigated pH changes across several different designs of aeration cascades of varying step height, length and total difference in head. None of the cascades produced a pH change greater than 0.3 points; in some instances a change of less than 0.1 points was recorded.

The ability of aeration cascades to increase the efficiency of passive treatment systems by increasing pH may well therefore be limited without a major rethink about the size and way in which they are incorporated into the treatment schemes. With regards to active treatment systems however, where lime dosing is required to raise pH, an aeration cascade that can remove 50% of the dissolved CO_2 (as seen at the Strafford site) would have a significant impact on the quantity of lime consumed in order to raise pH to the desired level. A change in dissolved CO_2 of 120 mg/L corresponds to a reduction in the quantity of lime required to neutralise the associated carbonic acid of 202 mg/L. At a treatment site where the flow rate is 50 L/s this gives a reduction of 864 kg of lime per day. Not only is there an obvious benefit in economic terms as a reduction in the up-front purchase cost of the lime, but a lower concentration of dissolved $CaCO_3$ will result in less lime scale formation reducing maintenance costs and a reduced mass of sludge sent to landfill.

7.3.2 Mechanical CO_2 degassing

The results of the CO_2 degassing trials could play an important role in the design of semi-passive treatment systems. As with the inclusion of an aeration cascade the inclusion of any mechanical degassing step up front of an active treatment plant for net-acid water will reduce the rate of lime consumption which is likely to have a significant cost benefit in the long term as the cost of transport and raw materials increases. In all of the sites investigated here (which are typical of coal mine drainage

in the UK) an efficient aeration tank with sufficient residence time could completely eliminate the need for chemical dosing from marginally net-acidic sites. In the case of net-alkaline sites, several minutes aeration (whether in a reaction vessel or by recirculation over an aeration cascade) could increase pH to a point where HFO settling rather than Fe(II) oxidation rate quickly becomes the rate determining step for Fe removal.

The modelling work conducted here has given an increased understanding about the rates of CO_2 degassing that could be expected for AMD (and other CO_2 rich ground waters). This new understanding could prove useful in the design and costing of future treatment schemes where predictions about the quantities of lime required to raise alkalinity, or pH for estimation of Fe(II) oxidation rates are needed.

7.3.3 Other options for CO_2 stripping

Aside from the two methods of CO_2 stripping used in this study there are a number of other methods that have been used in water treatment in a different industries. Some are not applicable to the treatment of ferruginous mine drainage as they would quickly become fouled with HFO. The remainder of this section discusses an alternative that would not be hindered by HFO accumulation.

Summerfelt et al (2000) discuss the problems associated with high dissolved CO_2 levels in intensive aquaculture systems and the various options for CO_2 stripping (as opposed to aeration for increasing DO). In this industry air-stripping columns are preferred where air is blow upwards counter current to the downwards flow of water. Whilst this method is clearly not practical in a mine drainage scenario, Summerfelt et al (2000) highlight that it is the dispersion of water into fine droplets in these that provides the key to efficient gas transfer something which is also common to tray aerators used in the treatment of municipal waters. This method for the stripping of CO_2 from drinking water supplies as a means of controlling corrosion of distribution pipes has been investigated by a number of authors including LaMotta and Chinthakuntla (1996). They used a tray aerator, where water was pumped to the top of a tower and allowed to cascade down through a number of perforated trays to develop a formula for CO_2

degassing that related the number of trays to the amount of changes in pH and the amount of CO_2 degassed. They found that when designed correctly these aerators were highly efficient in CO_2 removal. The tray aerators investigated by LaMotta and Chinthakuntla (1996) are conceptually similar to SCOOFI reactors designed for the treatment of mine drainage as described by Jarvis and Younger (2001). The focus in trials carried out on these systems has previously been their efficiency in removing Fe and Mn by accretion on the high surface area media, but they have the potential to be optimised for CO_2 stripping and could be trialled as an alternative to aeration cascades where there is either a sufficient drop in head across a site, or pumping costs are not prohibitive.

7.4 Summary

The data presented in this chapter are the result of CO_2 degassing trials carried out at aeration cascades and during batch experiments at a number of mine water treatment schemes across the UK. Both empirical and modelled data have been compared and discussed along with the implications for CO_2 degassing as a means to increase the efficiency of mine water treatment. The main findings can be summarised as follows:

- Aeration cascades can be highly efficient at degassing CO_2. The relatively short residence time of these hydraulic structures however means that the change in pH measured between the top and bottom of the cascades at the site studied was small at 0.2-0.3 units.
- The design of an aeration cascade does not appear to have a significant influence on its ability to degass CO_2. The inclusion (or not) of plunge pools or different step heights had no measurable difference on the amount of CO_2 degassed or the Fe removal efficiency of the associated settling ponds.
- The incorporation of aeration cascades with a larger drop in height (or recirculation of water) at mine water treatment schemes would be likely to result in a larger increase in pH and could reduce the need for chemicals dosing at active treatment plants.
- Measurements of acidity and alkalinity in the field can be difficult to perform accurately. Batch-wise aeration and CO_2 stripping with pH logging throughout could be a useful alternative in the determination of a mine water as net-acid or net-alkaline.
- CO_2 stripping by forced aeration can be used to manipulate the pH of a mine water without the addition of chemicals. In the case of net-alkaline sites pH can be raised to a point where Fe(II) oxidation is so fast that the rate determining step in the Fe removal process becomes particulate settling. In the case of net-acid sites, CO_2 stripping can dramatically reduce the quantities of lime required to raise pH and accelerate Fe(II) oxidation rates.
- Coupling of the rate equation for CO_2 degassing to the homogeneous rate equation for Fe(II) oxidation using the PHREEQCi geochemical modelling

software allowed predictions to be made about the changing concentrations of carbonate species in the mine waters over time. The results output from the PHREEQCi model for pH and Fe(II) concentration matched closely those measured in the field giving confidence in the predictions about carbonate speciation.

- The PHREEQCi modelling confirmed that the two main factors controlling pH in mine water scenarios are Fe(II) oxidation and CO_2 degassing and validated the earlier conclusion (see Chapter 6) that rates of Fe(II) oxidation in the field can be several orders of magnitude higher those previously measured in laboratory studies.

8 Conclusions and Further Work

The following sections summarise the main findings of this thesis. As with previous sections and chapters they have been split into three parts.

8.1 The Vertical Flow Reactor

i. The VFR at Taff Merthyr could not be run so that the predominant Fe removal mechanism was HFO accretion over the long term. The water chemistry at the site favoured Fe(II) oxidation and precipitation within the water column with subsequent filtration of the HFO particulates.

ii. The maximum Fe removal rate that was achieved was 60 g/m^2/day though this rapidly declined to around 30 g/m^2/day for around 100 days before finally settling at approximately 10 g/m^2/day.

iii. Sampling of Mn at the inflow and outflow of the VFR showed that Mn removal was only occurring within the VFR bed and not within the water column. Water overflowing from the VFR without passing through the bed showed no reduction in Mn concentration.

iv. The distribution of Mn bands throughout the VFR sludge as reported by Barnes (2008) was confirmed and suggests autocatalytic Mn oxidation and precipitation. The chemical conditions associated with the bands of Mn oxides encourage the removal of a number of other trace elements from the mine water including Ba, Tl, Cr, Co and Ni.

v. Trials of a VFR system at the Ynysarwed site showed that there is the potential to at least partially treat net-acid waters, though considerable further work is required in this area.

8.2 Iron(II) Oxidation Rates

i. Methodology developed in the experimental and numerical modelling phases of this work proved to be successful in establishing values for the rate constant for homogenous Fe(II) oxidation k_1 without the need to hold any of the variables pH, temperature, dissolved O_2 constant.

ii. Published rates of homogeneous iron(II) oxidation as measured in the laboratory do not give a good approximation as to what is occurring in the mine waters investigated in the current study.

iii. Calculated values for k_1 the homogenous rate constant for Fe(II) oxidation were up to 3 orders of magnitude higher than for previously published laboratory studies. It is suggested that heterogenous autocatalysis makes a greater contribution to the overall oxidation rates in mine waters as a result of higher total Fe concentrations compared to those used in the laboratory studies.

iv. The methodology developed during the heterogeneous oxidation experiments was found to require further refinement in order to produce values of k_2 comparable to those already in the literature.

8.3 Carbon Dioxide Degassing

i. Aeration cascades can be used to remove a large proportion of the excess dissolved CO_2 present in freshly emerged mine water, though this does not necessarily correspond to a large increase in pH.

ii. Comparison of a number of aeration cascades of the same height showed that the design of the aeration cascade does not appear to have an effect on the amount of CO_2 degassed from a mine water.

iii. Changing the design of an aeration cascade (assuming on change in total height) up front of a treatment scheme did not influence the overall iron removal efficiency at the site investigated.

iv. Geochemical modelling based on the rate equations for CO_2 degassing and Fe(II) oxidation showed that changes in pH occurring in a mine water over time could be successfully accounted for by these two sets of reactions alone.

v. The different methods available for measuring acidity and alkalinity in the field can produce widely varying results. Monitoring pH whilst aerating and degassing a mine water will give a reliable indication as to whether the water is net-acid or net-alkaline with much lower risk of the introduction of operator error compared to acidity and alkalinity titrations.

8.4 Recommendations for further work

- The trial of the VFR at Ynysarwed should be restarted in order gather more data to assess the effectiveness of this type of system in treating net-acid mine waters. Initial results indicated that Fe(II) removal rates could be significantly higher in this system than in a settling lagoon or wetland with similar residence time. Ideally a new pilot scale reactor would be at least 1 m^3 in volume in order to allow the system to be run over a longer period of time than was achieved for the small VFR trial used at Ynysarwed in this study. Aeration of the water feeding the pilot scale VFR should be kept to a minimum in order to keep Fe(II) oxidation rates within the water column as low as possible. Monitoring of flow rate and residence time would allow a comparison between expected iron removal in a well aerated system (as presented in this thesis) to Fe removal within the VFR. It should then be possible to determine the contribution to total Fe removal arising from heterogeneous catalysis and accretion within the HFO bed. Monitoring of total iron removal and changes in bed permeability over time would also allow predictions to be made about the expected useful lifetimes of these systems treating net-acid waters.

- Further analysis of the RAPS sludge at Tan-y-Garn as detailed in Chapter 6 Section 6.4.2 could be carried out in order to allow a better comparison of the heterogenous oxidation rates and the rate constant k_2 to literature values. In order to assess the catalytic effect of an Fe(III) solid on Fe(II) oxidation it is necessary to know the number of surface sites per unit volume available for Fe(II) sorption. It is also desirous to know if the Fe(III) solid is present as a well defined crystalline phase or is truly amorphous, as different forms of hydrated

ferric oxides have been shown to have varying degrees of catalytic activity with respect to Fe(II) oxidation. In addition to determining the structure, surface area and density of sorption sites for Fe(II) there is also scope for increasing knowledge and understanding about the effect of other aqueous species such as Cl^- and SO_4^{2-} on the ability of HFO to adsorb Fe(II). Since the concentration of these species can vary by orders of magnitude between different mine waters their influence on heterogenous catalysis of Fe(II) oxidation in mine water scenarios particularly with respect to the VFR requires further investigation.

- A trial of aeration cascades of different heights could provide data for the definition of a relationship between drop in height and CO_2 degassed/pH change for mine waters. As waterfalls it accelerates and increasingly disperses in to a spray of fine droplets with greater entrainment of air bubbles within the flow. It would make sense therefore that as the total drop in height increases so does the opportunity for the degassing of excess CO_2. Since the work on described in this thesis began an aeration cascade has been installed at the Blenkinsopp site resulting in a 50% decrease in the lime dose required for effective treatment of the water. Development of a greater understanding of the relationship between cascade height and CO_2 degassed should allow even greater reductions in the lime dose required at this site as evidenced by the reduction of Fe(II) from 140 to 5mg/L during the batchwise experiment. In addition to the net-acid waters which would undoubtedly benefit from optimised aeration cascade design carefully designed trials at net alkaline sites such as Six Bells should completely remove the need for chemicals dosing.
- Further development of the PHREEQCi model used to couple the rate equation for CO_2 degassing to the rate equation for Fe(II) oxidation should be carried out in order to elucidate the process by which k_1 is ostensibly elevated in the waters in this study. Additional modelling work including heterogeneous autocatalysis suggested that this is not the mechanism responsible for the elevated oxidation rates. The acceleration of oxidation rates was constant throughout each experimental run and not dependent on increasing concentrations of Fe(II) solids within the system. The apparent relationship k_1

and pH suggests that the rate equation needs to be reworked for these waters since the rate constant should by definition be a constant with changes in rate accounted for by the concentrations of reactants and other species present.

References

Amos, P. W., Younger, P. B. 2003. Substrate characterisation for a subsurface reactive barrier to treat colliery spoil leachate. *Water Research* 37, pp. 108-120.

American Water Works Association 1999. *Standard Methods for the Examination of Water and Wastewater*.

Atkins. 2006a. Blenkinsopp & Byrons Drift – Treatment of Abandoned Mine Discharge. 1-3. Operations Manual for the Coal Authority.

Atkins 2006b. Blenkinsopp & Byrons Drift – Treatment of Abandoned Mine Discharge. Health and Safety Manual for the Coal Authority.

Atkins. 2006c. Tan-y-Garn mine water treatment scheme. Operations Manual for the Coal Authority.

Atkins 2006d. Tan-y-Garn mine water treatment scheme. Health and Safety Manual for the Coal Authority.

Barnes, A. 2008. *Rates and mechanisms of Fe(II) oxidation in a passive vertical flow reactor for the treatment of ferruginous mine water. PhD Thesis.* Cardiff Universtiy.

Barnes, A., Sapsford, A. J., Dey, M., Williams K. P. 2009. Heterogeneous Fe(II) oxidation and zeta potential. *Journal of Geochemical Exploration* 100, pp. 192-198.

Batty, L. C., Younger, P. L. 2002. Critical role of macrophytes in achieving low iron concentrations in minewater treatment wetlands. 36(3997-4002).

Baylar, A., Bagatur, T., Emiroglu, E.2007. Aeration efficiency with nappe flow over stepped cascades. *Proceedings of the Institution of Civil Engineers: Water Management 160* WM1, pp. 43-50.

Best, G. A., Aikman D. I. 1983. The treatment of ferruginous groundwater from an abandoned colliery. 82(537-566).

Borer, P. Sulzberger, B., Hug, S. J., Kraemer, S. M., Kretzschmar, R., 2009. Photoreductive Dissolution of Iron(III) (Hydr)oxides in the Absence and Presence of Organic Ligands: Experimental Studies and Kinetic Modeling. *Environmental Science & Technology* 43(6), pp. 1864-1870.

CEC, Council of the European Communities, 2000. Council dorective of 23 October establishing a framework for the community action in the field of water policy (the EU Water Framework Directive) (2000/60/EC). Official *Journal of the European Communities*. L.327

Coulton, R., Bullen, C., Hallett, C. 2003. The design and optimisation of active mine water treatment plants. *Land contamination and reclamation* 11(2), pp. 273-279.

Cravotta III, C. A., Brady, K. B. C., Rose, A. W., Douds, J. B. 1999. Frequency distribution of the pH of coal-mine drainage in Pennsylvania. D.W. Morganwalp (Ed.), In U.S. Geological Survey

Toxic Substances Hydrology Program-Proc. Technical Meeting, U.S. Geological Survey, Water-Resources Investigation. pp. 313–324 Report 99–4018A

Cravotta III, C. A. 2007. Passive aerobic treatment of net-alkaline, iron-laden drainage from a flooded underground anthracite mine, Pennsylvania, USA. *Minewater and the Environment* 26, pp. 128-149.

Cravotta III, C. A. 2011. Personal communication.

Dandurand, D. L., Grout, R., Hoefs, J., Menschel, G., Schott, J., Usdowski, E., 1982. Kinetically controlled variations of major components and carbon and oxygen isotopes in a calcite-precipitating spring. *Chemical Geology* 36, pp. 299-315.

Davison, W., Seed, G. 1983. The kinetics of the oxidation of ferrous iron in synthetic and natural waters. *Geochimica et Cosmochimica Acta* 47(1), pp. 67-79.

Dempsey, B. A., Dietz, J., Jeon, B. H., Roscoe, H. C., Ames, R. ed. 2002. *Heterogeneous oxidation of ferrous iron for treatment of mine drainage*. National Meeting of the American Society of Mining and Reclamation, Lexington KY. ASMR, 3134 Montavesta Rd., Lexington, KY 40502.

DeNicola, D. M., Stapleton, M. G. 2002. Impact of acid mine drainage on benthic communities in streams: the relative roles of substratum vs. aqueous effects. *Environmental Pollution* 119(3), pp. 303-315.

Dey, M. Williams, K., Coulton, R. 2009. Treatment of arsenic rich waters by the HDS process. *Journal of Geochemical Exploration* 100(2-3), pp. 160-162.

Dietz, J. M., Dempsey, B. A. 2002. Innovative treatment of alkaline mine drainage using recirulated iron oxides in a complete mix reactor. *National Meeting of the American Society of Mining and Reclamation* Lexington, KY, June 9-13.

Dills, G., Rogers Jr., D. T. 1974, Macroinvertibrate community structure as an indicator of acid mine pollution. *Environmental Pollution*. 6, pp. 239-262

Dudeney, A. W. L., Ball, S., Monhemius, A. J., 1994, Treatment Processes for Ferruginous Discharges from Disused Coal Workings. The National Rivers Authority, R&D Note 243.

Dzomback, D. A., Morel F. M. M. 1990. *Surface complexation modelling: hydrous ferric oxide*. Wiley Inter-Science.

Emiroglu, M. E., Baylar, A. 2006. Self-aeration in smooth and stepped chutes. *International Journal of Science & Technology* 1(2), pp. 105-133.

Emmenegger, L., King, D. W., Sigg, L., Sulzberger, B. 1998. Oxidation Kinetics of Fe(II) in a Eutrophic Swiss Lake. *Environmental Science & Technology* 32(19), pp. 2990-2996.

Epstein, I. R., Kustin, K., Warshaw, L. J. 1980. A kinetics study of the oxidation of iron(II) by nitric acid. Journal of the American Chemical Society 102(11), pp. 3751-3758.

Felmy, A., Girvin, D., Jenne, E. 1984. MINTEQ--A COMPUTER PROGRAM FOR CALCULATING AQUEOUS GEOCHEMICAL EQUILIBRIA. U.S. Environmental Protection Agency, Washington, D.C., EPA/600/3-84/032

Ghosh, MM. 1974. Oxygenation of Ferrous Iron in Highly Buffered Waters, In: Aqueous Environmental Chemistry of Metals. (Ed. Rubin, A. J.), pp. 193-217. Ann Arbor Science, Michigan.

Gonçalves, M. A., 2005. Geochemical Models, in: Water Encyclopedia: Ground Water (Eds. Lehr, J. H., Keely, J.) Wiley Interscience, pp. 138-140

Gray, N. F. 1998. Acid mine drainage composition and the implications for its impact on lotic systems. *Water Research* 32(7), pp. 2122-2134.

Grundle, T., Delwiche, J. 1993. Kinetics of ferric oxyhydroxide precipitation. 14(1, 71-97).

Hallberg, K. B., Johnson, D. B. 2003. Novel acidophiles isolated from moderately acidic mine drainage waters. *Hydrometallurgy* 71(1-2), pp. 139-148.

Hem, J. D. 1977. Reactions of metal ions at surfaces of hydrous iron oxide. *Geochimica et Cosmochimica Acta* 41(4), pp. 527-538.

Heaney, S. I., Davison, W. 1977. The determination of ferrous iron in natural waters with 2,2' - bipyridyl. *Limnology and Oceanography* 22(4), pp. 753-760.

Hindmarsh, W. E., Leighfield, K. G., Pentreath, J., Thomas, R., Martin, C., Mills, M., Gregory, P., Jones, A., Roderick, P. 1992. Water pollution from abandoned coal mines. In: Houses of Commons Welsh Affais Committee Minutes of Evidence. Wed. 11th March 1992, pp 1-36

Howe, K. J., Lawler, D. F. 1989. Acid-base reactions in gas transfer: A mathematical approach. *Journal of the American Water Works Association* 81, pp. 61-66.

Hug, S. J., Canonica, L., Wegelin, M., Gechter, D., von Gunten, U. 2001. Solar Oxidation and Removal of Arsenic at Circumneutral pH in iron containing waters. Environmental Science and Technology. 35, pp. 2114-2121.

Huisman, W. E. , Wood, L. 1974. Slow sand filtration. ISBN 92 4 154037 0.

Jarvis, A. P., Younger, P. L. 2001. Passive treatment of ferruginous mine waters by high surface area media. *Water Research* 35(3643-3648).

Jarvis, A. P., England, A., Mee, S. 2003. Mine water treatment at Six Bells colliery, South Wales: problems and solutions, from conception to completion. *Land Contamination & Reclamation*, 11 (2) pp. 153-160

Jeon, B. H., Dempsey, B. A., Burgos, W. D., Royer, R. A. 2001. Reactions of ferrous iron with hematite. *Colloids and Surfaces A: Physicochemical and Engineering Aspects* 191(1-2), pp. 41-55.

Johnson, D. B., Hallberg, K. B. 2005. Acid mine drainage remediation options: A review. *Science of the Total Environment*. 338(1-2), pp. 3-14.

Kester, D. R., Byrne, R. H., Liang, Y. 1975. Redox Reactions and Solution Complexes of Iron in Marine Systems. In: Marine Chemistry of the Coastal Environment (Ed. T. M. Church), pp. 56-79. American Chemical Society

Kim, Y., Han, K., Lee, W. 2003. Removal of organics and calcium hardness in liner paper wastewater using UASB and CO2 stripping system. *Process Biochemistry* 38(6), pp. 925-931.

King, D. W. 1998. Role of Carbonate Speciation on the Oxidation Rate of Fe(II) in Aquatic Systems. *Environmental Science & Technology* 32(19), pp. 2997-3003.

King, D. W. Lounsbury, H. A., Millero, F. J. 1995. Rates and Mechanism of Fe(II) Oxidation at Nanomolar Total Iron Concentrations. *Environmental Science & Technology* 29(3), pp. 818-824.

Kirby, C. S., Brady, J. A. E. 1998. Field determination of Fe^{2+} oxidation rates in acid mine drainage using a continuously-stirred tank reactor. *Applied Geochemistry* 13(4,), pp. 509-520.

Kirby, C. S. Thomas, H. M., Southam, G., Donald, R. 1999. Relative contributions of abiotic and biological factors in Fe(II) oxidation in mine drainage. *Applied Geochemistry* 14(4), pp. 511-530.

Kirby, C. S., Cravotta, C. A. 2005a. Net alkalinity and net acidity 1: theoretical considerations. *Applied Geochemistry* 20(10), pp. 1920-1940.

Kirby, C. S., Cravotta, C. A. 2005b. Net alkalinity and net acidity 2: practical considerations. *Applied Geochemistry* 20(10), pp. 1941-1964.

Kirby, C. S., Dennis, A., Kahler, A. 2009. Aeration to degas CO2, increase pH, and increase iron oxidation rates for efficient treatment of net alkaline mine drainage. *Applied Geochemistry* 24(7), pp. 1175-1184.

Kleinmann, R. L. P., Hedin, R. S., Nairn, R. W. 1998. Treatment of mine drainage by anoxic limestone drains and constructed wetlands. Acidic Mining Lakes: Acid Mine Drainage, Limnology and Reclamation, pp. 303–319 (Eds. Geller, A., Klapper, H., Salomons, W.) Springer, Berlin

Koenig, R. A., Johnson, C. R. 1941. Spectrophotometric determination of iron (II). Use of 2,2 bipyridine. *Jounal of Biological Chemistry* 143, pp. 159-163.

Laine, D. M., Jarvis, A. P. 2002. Engineering design aspects of passive in situ remediation of mining effluents, *Proceedings of the National Conference: Mine Water Treatment: A decade of progress*. 11-13 November 2002(25-40).

LaMotta, E. J., Chinthakuntla, S. 1996. Corrosion control of drinking water using tray aerators. *Journal of Environmental Engineering-Asce* 122(7), pp. 640-648.

Langmuir, D. 1997. Aqueous Environmental Geochemistry. *Prentice Hall, New Jersey, USA* ISBN 0203674121.

Li, X., Thornton, I. 1993. Multi-element contamination of soils and plants in old mining areas, U.K. *Applied Geochemistry* 8(Supplement 2), pp. 51-56.

Liang, L., McNabb, A. J., Paulk, J. M., Gu, B., McCarthy, J. F. 1993. Kinetics of Fe(II) Oxygenation at Low Partial Pressure of Oxygen in the Presence of Natural Organic Matter. *Environmental Science and Techonolgy* 27, pp. 1864-1870.

Liger, E., Charlet, L., Van Cappellen, P. 1999. Surface catalysis of uranium(VI) reduction by iron(II). *Geochimica et Cosmochimica Acta* 63(19-20), pp. 2939-2955.

Lower, S. 2011: http://www.chem1.com/acad/webtext/virtualtextbook.html. chem1 virtual text book: A reference text for General Chemistry. *Simon Fraser University*.

Maeder, M., Neuhold, Y. M. 2007. *Practical data analysis in chemistry*. 1st ed. Elsevier.

Matter-Müller, C., Gujer, W., Giger, W. 1981. Transfer of volatile substances from water to the atmosphere. *Water Research*. 15(11) pp. 1271-1279

Merck Chemicals. 2011. www.merck-chemicals.com/photometry. Instruction manual for Iron Cell Test 1.14896.0001.

Miles, C. J., Brezonik, P. L. 1981. Oxygen consumption in humic-colored waters by a photochemical ferrous-ferric catalytic cycle. *Environmental Science & Technology* 15(9), pp. 1089-1095.

Millero, F. J. 1985. The effect of ionic interactions on the oxidation of metals in natural waters. *Geochimica et Cosmochimica Acta* 49(2), pp. 547-553.

Millero, F. J., Sotolongo, S. 1989. The oxidation of Fe(II) with H_2O_2 in seawater. *Geochimica et Cosmochimica Acta* 53(8), pp. 1867-1873.

Millero, F. J., Sotolongo, S., Izaguirre, M. 1987. The oxidation kinetics of Fe(II) in seawater. *Geochimica et Cosmochimica Acta* 51(4), pp. 793-801.

Moses, C. O., Nordstrom, K, D. ,Herman, J, S., Mills, A, L. 1987. Aqueous pyrite oxidation by dissolved oxygen and by ferric iron. *Geochimica et Cosmochimica Acta* 51(6), pp. 1561-1571.

Mott MacDonald. 2009a. Dawdon – Minewater treatment scheme operations manual. Report to the Coal Authority

Mott MacDonald. 2009b. Dawdon - Minewater treatment scheme health and safety manual. Report to the Coal Authority

NOAA. 2011. [Online]. Available at: http://www.esrl.noaa.gov/gmd/ccgg/trends/ [Accessed: 16/03/2011].

Noike, T. Nakamura K., Matsumoto, J. 1983. Oxidation of ferrous iron by acidophilic iron-oxidising bacteria from a stream receiving acid mine drainage. *Water Research* 17, pp. 21-27.

Nordstrom, D., K. 1985. The rate of ferrous iron oxidation in a stream receiving acid mine effluent. *U.S.G.S. Water Supply Paper, 2270* 133-199.

Nordstrom, D., K., Ball, J. W. 2001. *Users manual for WateQ4F, with revised thermodynamic data base and test cases for calcualting speciation of major, trace, and redox elements in natural waters*. U.S. Geological Survey, Open-File Report 91-183

Nordstrom, D. K., Alpers, C. N., Ptacek, C. J., Blowes, D. W. 1999. Negative pH and Extremely Acidic Mine Waters from Iron Mountain, California. *Environmental Science & Technology* 34(2), pp. 254-258.

Novak, P., Avery, S. 1978. Oxygen transfer at hydraulic structures. *Journal of the Hydraulics Division, ASCE*. 104(11), pp. 1521–1540

Novak, P. 1994. Improvement of water quality in rivers by aeration at hydraulic structures. In: Water Quality Control (Ed. Hino, M.) pp. 147-168

Park, B., Dempsey, B. 2005. Heterogeneous Oxidation of Fe(II) on Ferric Oxide at Neutral pH and a Low Partial Pressure of O_2. *Environmental Science and Technology* 39, pp. 6494-6500.

Parker, K. 2003. Minewater management on a national scale - experiences from the Coal Authority. *Land contamination and reclamation* 11 (2)(181-190).

Parkhurst, D. L., Appelo, C. A. J. 1999. *User's guide to PHREEQC (Version 2)--a computer program for speciation, batch-reaction, one-dimensional transport, and inverse geochemical calculations*.

Parsons Brinkerhoff. 2004a. Lindsay – Treatment of an Abandoned Mine Discharge. Operations manual for the Coal Authority.

Parsons Brinkerhoff. 2004b. Morlais – Treatment of an Abandoned Mine Discharge. Operations manual for the Coal Authority.

Perry, R. H. 1997. Perry's Chemical Engineers' Handbook. 7th Edition (Ed. Green, D. W.) McGraw Hill. 6

Pham, A. N., Rose, A. L., Feitz, A. J., Waite, T. D. 2006. Kinetics of Fe(III) precipitation in aqueous solutions at pH 6.0-9.5 and 25 °C. *Geochimica et Cosmochimica Acta* 70(3), pp. 640-650.

Pham, A. N., Waite, T. D. 2008. Oxygenation of Fe(II) in natural waters revisited: Kinetic modeling approaches, rate constant estimation and the importance of various reaction pathways. *Geochimica et Cosmochimica Acta* 72(15), pp. 3616-3630.

PIRAMID. 2003. *Engineering guidlines for the passive rememdiation of acidic and/or metalliferous mine drainage and similar wastewaters*. ISBN 0-9543827-1-4: University of Newcastle Upon Tyne.

Rose, A. L., Waite, T. D. 2002. Kinetic model for Fe(II) oxidation in seawater in the absence and presence of natural organic matter. *Environmental Science & Technology* 36, pp. 433-444.

Pratt, C., W., Cornely, K. 2005. Essential Biochemistry, John Wiley & Sons. ISBN 0471393878

Santana-Casiano, J. M. González-Dávila, M., Millero, F. J. 2004. The oxidation of Fe(II) in NaCl-HCO3- and seawater solutions in the presence of phthalate and salicylate ions: a kinetic model. Marine Chemistry 85(1-2), pp. 27-40.

Santana-Casiano, J. M. González-Dávila, M., Millero, F. J. 2005. Oxidation of Nanomolar Levels of Fe(II) with Oxygen in Natural Waters. *Environmental Science & Technology* 39(7), pp. 2073-2079.

Santana-Casiano, J. M. González-Dávila, M., Millero, F. J. 2010. Comment on "Oxygenation of Fe(II) in natural waters revisited: Kinetic modelling approaches, rate constant estimation and the importance of various reaction pathways" by Pham and Waite (2008). *Geochimica et Cosmochimica Acta* 74(17), pp. 5150-5153.

Sapsford, D. J., Pugh, D. 2010. Evaluation of physicochemical processes occurring in mine water treatment systems in South Wales, UK. *Technical Report to Coal Authority* Cardiff School of Engineering Report No: 3200.

Sapsford, D. J., Williams, K. P. 2009. Sizing criteria for a low footprint passive mine water treatment system. *Water Research* 43(2), pp. 423-432.

Sapsford, D. J., Watson, I. 2011. A process-orientated design and performance assessment methodology for passive mine water treatment systems. *Ecological Engineering* 37(6), pp. 970-975.

Scott Wilson. 2003a. Taff Merthyr – Treatment of abandonned mine discharge. Health and Safety report to the Coal Authority.

Scott Wilson. 2003b. Taff Merthyr – Treatment of abandonned mine discharge. Operations nd Maintenance report to the Coal Authority.

Scott Wilson. 2004a. Lindsay – Treament of an Abandonned Mine Discharge. Health and Safety report to the Coal Authority.

Scott Wilson. 2004b. Morlais – Treament of an Abandonned Mine Discharge. Operations and maintenance report to the Coal Authority.

Shenk, J. E., Webber, W. J. 1968. Chemical interactions of dissolved silica with iron II and iron III. *Journal of the American Water Works Association.* 60, pp. 199-212.

Singer, P. C., Stumm, W., 1970. Acidic mine drainage: The rate determining step. *Science.* 167(3921), pp. 1121-1123

Sobolev, D., Roden, E. E. 2001. Suboxic Deposition of Ferric Iron by Bacteria in Opposing Gradients of Fe(II) and Oxygen at Circumneutral pH. *Applied Environmental Microbiology* 67(3), pp. 1328-1334.

Sogaard, E. G., Medenwaldt, R., Abraham-Peskir, J. V. 2000. Conditions and rates of biotic and abiotic iron precipitation in selected Danish freshwater plants and microscopic analysis of precipitate morphology. *Water Research* 34 (10), pp. 2675-2682.

Spotts, E., Dollhopf, D. J. 1992. *Evaluation of phosphate materials for control of acid production in pyritic mine overburden*. Journal of Environmental Quality, 21, pp. 627-634

Stumm, W. 1992. *Chemistry of the solid-water interface: Processes at the mineral-water and particle-water interface in natural systems*. New York NY: John Wiley & Sons.

Stumm, W., Lee, G. F. 1961. Oxygenation of Ferrous Iron. *Industrial and Engineering Chemistry* 53, pp. 143-146.

Stumm, W., Morgan, J. J. 1996. *Aquatic Chemistry, Chemical Equilibria and Rates in Natural Waters*. 3rd ed. Wiley Interscience.

Summerfelt, S. T. Vinci, B. J., Piedrahita, R. H. 2000. Oxygenation and carbon dioxide control in water reuse systems. Aquacultural Engineering 22(1-2), pp. 87-108.

Sung, W., Morgan, J. J. 1980. Kinetics and Product of Ferrous Iron Oxygenation in Aqueous Systems. *Environmental Science and Technology* 14(5), pp. 561-568.

Sung, W., Morgan, J. J. 1981. Oxidative removal of Mn(II) from solution catalysed by the [gamma]-FeOOH (lepidocrocite) surface. *Geochimica et Cosmochimica Acta* 45(12), pp. 2377-2383.

Tamura, H., Goto, K., Nagayama, M. 1976. The effect of ferric hydroxide on the oxygenation of ferrous ions in neutral solutions. *Corrosion Science.* 16, pp. 197-207.

Tamura, H., Kawamura, S., Hagayama, M., 1980. Accelleration of the oxidation of Fe^{2+} ions by Fe(III)-oxyhydroxides. *Corrosion Science*. 20(8-9), pp. 963-971.

Tebbutt, T. H. Y., 1972. Some studies on reaeration cascades. *Water Research*. 6(3) 297-298

Theis, T. L., Singer, P. C. 1974. Complexation of iron(II) by organic matter and its effect on iron(II) oxygenation. *Environmental Science & Technology* 8(6), pp. 569-573.

Toombes, L., Chanson, H. 2000. Air-water flow gas transfer at aeration cascades: a comparative study of smooth and stepped chutes. *Proceedings of the International Workshop on Hydraulics of Stepped Spillways*, pp. 77-84.

Trapp, J. M., Millero, F. J. 2007. The Oxidation of Iron(II) with Oxygen in NaCl Brines. *Journal of Solution Chemistry* 36, pp. 1479-1493.

Trumm, D. Pope, J.,Newman, N. 2009. Passive treatment of neutral mine drainage at a metal mine in New Zealand, using an oxidising system and slag leaching bed. Proceeding of the International Conference on Acid Rock Drainage, Skelleftea, Sweden.

Tufekci, N., Sarikaya, H. Z. 1996. Catalytic effects of high Fe(II) concentrations on Fe(II) oxidation. *Water Science and Technology* 34,(7-8), pp. 389-396.

UNEP report. 1991. Environmental aspects of Selected Non-Ferrous Metals Ore Mining. UNEP Technical Guide, pp. 32-44

United States Geological Survey. 2009
http://wwwbrr.cr.usgs.gov/projects/GWC_coupled/phreeqc/.

Vikesland, P. J., Valentine, R. L. 2002. Iron Oxide Surface-Catalyzed Oxidation of Ferrous Iron by Monochloramine: Implications of Oxide Type and Carbonate on Reactivity. *Environmental Science & Technology* 36(3), pp. 512-519.

Watzlaf, G. R., Schroeder, C. T., Kleinmann, R. L. P., Kairies, C. L., Nairn, R. W. 2003. The Passive Treatment of Coal Mine Drainage. National Energy Technology Laboratory, U.S. Department of Energy, School of Civil Engineering and Environmental Science, University of Oklahoma USA.

Weiss, J. 1935. Electron transition process in the mechanism of oxidation and reduction reactions in solutions. *Naturwissenschaften* 23, pp. 64-69.

Wherli, B. 1990. Redox reactions of metal ions at mineral surfaces. In: Stumm, W. ed. Chichester: John Wiley and Sons.

Wiseman, I. M., Edwards, P. J. 2004. Constricted wetlands for mine water treatment: Performance and sustainability. *Water and Environment Journal* 18(3), pp. 127-132.

Wolthoorn, A., Temminghoff, E. J. M., Weng, L., van Riemsdijk, W. H. 2004 Colloid formation in groundwater: effect of phosphate, manganese, silicate and dissolved organic matter on the dynamic heterogeneous oxidation of ferrous iron. *Applied Geochemistry* 19, pp.611-622.

Younger, P. L., Banwart, S. A., Hedin, A. S. 2002. Minewater: Hydrology, Pollution, Remediation. Springer ISBN 10: 140200138X.

Zaihua, L. Svensson, U., Dreybrodt, W., Daoxian, Y., Buhmann, D. 1995. Hydrodynamic control of inorganic calcite precipitation in Huanglong Ravine, China: Field measurements and theoretical prediction of deposition rates. *Geochimica et Cosmochimica Acta* 59(15), pp. 3087-3097.

Zhang, D. D., Peart, M., Zhang, Y., Zhu, A., Cheng, X. 2000. Natural water softening processes by waterfall effects in karst areas. Desalination 129(3), pp. 247-259.

Ziemkiewicz, P. F., Skousen, J. G., Brant, D. L., Sterner, P. L., Lovett , R.J., 1997. Acid Mine Drainage Treatment with Armored Limestone in Open Limestone Channels. Journal of Environmental Quality 26, pp. 1017-1024.

Appendix 1: Published Work

Journal paper

J.N. Geroni, D.J. Sapsford, Kinetics of iron (II) oxidation determined in the field, *Applied Geochemistry*, 2011, 26 (8), pp 1452-1457

Conference papers

Jennifer N. Geroni, Devin J. Sapsford, Kay Florence, CO_2 degassing: implications for treatment of circumneutral mine drainage, *International Mine Water Conference,* September 4-11, 2011, Aachen, Germany

Jennifer N. Geroni, Devin J. Sapsford, Ian Watson, The potential for semi-passive mine water treatment by CO_2 stripping at Ynysarwed, S.Wales, *International Mine Water Conference*, September 5-9, 2010, Sydney, Nova Scotia, Canada

J. N. Geroni, D. J. Sapsford, A. Barnes, I. A. Watson, K. P. Williams, Current Performance of Passive Treatment Systems in South Wales, UK, *International Mine Water Conference*, October 19-23, 2009, Pretoria, South Africa

Applied Geochemistry 26 (2011) 1452–1457

Contents lists available at ScienceDirect

Applied Geochemistry

journal homepage: www.elsevier.com/locate/apgeochem

Kinetics of iron (II) oxidation determined in the field

Jennifer N. Geroni *, Devin J. Sapsford

Cardiff School of Engineering, Cardiff University, Queen's Buildings, The Parade, Cardiff CF243AA, UK

ARTICLE INFO

Article history:
Received 12 October 2010
Accepted 25 May 2011
Available online 12 June 2011
Editorial handling by R.R. Seal

ABSTRACT

This paper presents the results of extensive field trials measuring rates of Fe(II) oxidation at a number of Fe-bearing mine drainage discharges in the UK. Batch experiments were carried out with samples taken at regular intervals and Fe(II) concentration determined spectrophotometrically using 2′2-bipyridyl as the complexing agent. Initial concentrations for Fe(II) were 5.65–76.5 mg/L. Temperature, pH and dissolved O_2 (DO) were logged every 10 s, with pH at the start of the experiments in the range 5.64–6.95 and alkalinity ranging from 73 to 741 mg/L $CaCO_3$ equivalent. A numerical model based on a fourth order Runge–Kutta method was developed to calculate values for k_1, the rate constant for homogeneous oxidation, from the experimental data. The measured values of pH, temperature, [Fe(II)] and DO were input into the model with resulting values for k_1 found to be in the range 2.7×10^{14}–2.7×10^{16} M^{-2} atm^{-1} min^{-1}. These values for k_1 are 1–3 orders of magnitude higher than previously reported for laboratory studies at a similar pH. Comparison of the observed Fe(II) oxidation rates to data published by other authors show a good correlation with heterogenous oxidation rates and may indicate the importance of autocatalysis in these systems. These higher than expected rates of Fe oxidation could have a significant impact on the design of treatment schemes for the remediation of mine drainage and other Fe-bearing ground waters in the future.

1. Introduction

1.1. Iron redox chemistry

Iron is by far the most abundant transition element found on Earth comprising nearly 5.6% by mass of the crust (Lide, 1996). The redox cycling of this metal plays a major role in a variety of biogeochemical processes including mineral solubility, acid-rock drainage and the catalysis of aqueous oxidation reactions (King et al., 1995). As a result, the presence of aqueous Fe(II)/(III) and oxides of Fe influence the speciation, mobility and bioavailability of numerous contaminants including As (Chakravarty et al., 2002), U (Liger et al., 1999), and many other elements.

Iron(II) sorbed onto the surface of hydrous ferric oxide precipitates (HFO) and Fe oxide minerals is a stronger reducing agent than dissolved Fe(II) alone (Stumm and Sulzberger, 1992; Liger et al., 1999). This redox system has been used in the remediation of waste waters and contaminated ground waters for the removal of both organic and inorganic species (Charlet et al., 1998; Buerge and Hug, 1999; Karschunke and Jekel, 2002). In addition to industrial applications, the low toxicity and low cost of Fe salts and HFO solids make them ideal for water treatment in remote rural settings, for applications such as As removal from groundwater (Meng et al., 2001).

Abiotic Fe oxidation in natural systems occurs via two competing pathways, homogeneous and heterogeneous. Numerous studies of these mechanisms have been carried out under controlled laboratory conditions (e.g. Davison and Seed, 1983; Stumm and Lee, 1961; Sung and Morgan, 1980). The rate equation for homogenous oxidation can be described by Eq. (1) (Kirby et al., 2009; valid between pH 4–9) and shows a second order relationship with H^+ activity making the reaction highly pH dependent.

$$-\frac{d[\mathrm{Fe(II)}]}{dt} = k_1[\mathrm{Fe(II)}]P_{O_2}(a_{H^+})^{-2} \quad (1)$$

In recent years a number of authors have preferred to reduce the mixed rate expression shown here to one which considers individually the major reactive Fe(II) species known to have the greatest effect on measured oxidation rates. Detailed studies of the effect of different ion pairs have been used to develop composite rate laws where each individual species can be given its own rate constant (e.g. King, 1998). The overall Fe oxidation rate can then be explained as a weighted sum of the oxidation rates of individual Fe(II) species, with the individual rate constants for fast reacting species being greater than for slow reacting species.

1.2. This study

The aim of this study was to determine whether the rate equation and previously published composite values for k_1 the rate constant for homogeneous Fe oxidation hold true in Fe-bearing

* Corresponding author.
E-mail address: geronijn@cf.ac.uk (J.N. Geroni).

0883-2927/$ - see front matter © 2011 Elsevier Ltd. All rights reserved.
doi:10.1016/j.apgeochem.2011.05.018

discharges. With this in mind all data were collected solely from field experiments as the authors considered that any laboratory based study is unlikely to give an accurate reflection of the chemistry occurring in freshly collected samples due to changes that occur in transit such as degassing of CO_2. The authors also consider it unlikely that where synthetic samples are prepared in the laboratory the conditions occurring in the field will be accurately replicated. Despite the difficulties inherent in working on Fe oxidation rates the methods used here are shown to provide a robust approach to the study of these reactions in the field. A good discussion of the sources of inaccuracy affecting determination of Fe oxidation rates can be found in Davison and Seed (1983).

The authors have chosen to use the mixed form of the rate equation in this work rather than calculating k for individual species as it is intended to give a straightforward and practical guide to Fe oxidation rates which can be applied directly in the remediation of contaminated waters. For the purposes of the numerical model the rate equation was recast in the form of Eq. (2) in order that the k_1 values produced would have units of $M^{-2}\,atm^{-1}\,min^{-1}$ for comparison to earlier works (e.g. Stumm and Lee, 1961; Millero, 1985).

$$-\frac{d[\mathrm{Fe(II)}]}{dt} = k_1[\mathrm{Fe(II)}]P_{o_2}[\mathrm{OH}^-]^2 \quad (2)$$

2. Methods

There have been a number of studies conducted on field oxidation rates of Fe(II) in acidic mine waters. Many of these studies including Nordstrom (1985), Noike et al. (1983) and Sánchez España et al. (2007) deal with waters below pH 3.5 where bacterial oxidation has a major role. All of the sites discussed here have waters with pH between 5.5 and 7, over which range it has been shown that biotic oxidation rates are low compared to abiotic oxidation rates, and so all Fe oxidation was assumed to be abiotic (Kirby et al., 1999).

2.1. Site descriptions

In total the results of experimentation at six sites are presented, of which five are located in Wales and one in the north of England. All six sites are current or potential UK Coal Authority treatment schemes for mine drainage. The map in Fig. 1 shows the locations of the sites with details of their chemistries shown in Table 1.

2.1.1. Tan-y-Garn

This site comprises a gravity fed Reducing Alkalinity Producing System (RAPS) to treat the net acidic water followed by two reed beds. Water was taken from a manhole built to access the water entering the RAPS by placing a bucket into the flow.

2.1.2. Ynysarwed

This treatment scheme was designed to comprise both active and passive components as it is marginally net acidic; though at the time of this study the addition of floc blocks to a distribution chamber ahead of the site's two reed beds was the only chemical dosing underway. The water emerges from an adit and is pumped 0.5 km from a collection chamber to the reed beds. Water was taken from the adit using a peristaltic pump.

2.1.3. Morlais

Mine water discharges by gravity from a shaft, the collar of which has been raised to enable an aeration cascade to be constructed. The cascade feeds into a 50 m long channel which then feeds into two settling lagoons in series. The water flows out of the second lagoon into two parallel wetlands and finally through a third wetland before discharge to a River. Water was collected as it emerged ahead of the aeration cascade.

2.1.4. Lindsay

Mine water is collected in a sump and pumped up to a distribution chamber above an aeration cascade leading to two parallel lagoons. The water then flows through a series of three reed beds prior to discharge. Water was collected from the distribution chamber.

2.1.5. Taff Merthyr

Mine water is collected in a sump and pumped up to a distribution chamber. In total there are four settlement lagoons with preceding aeration cascades and 16 wetlands which eventually discharge into a River. Water was collected from the distribution chamber prior to aeration.

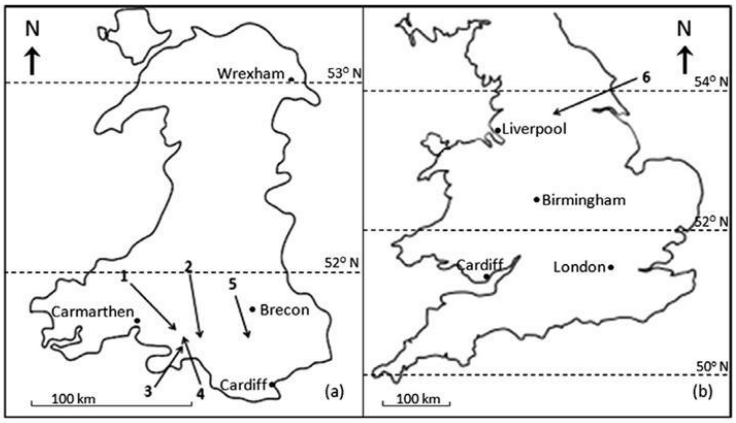

Fig. 1. Map showing the locations of the sites under investigation. On the left is an enlarged map of Wales (a) and on the right a map of England and Wales, UK (b). Numbers on the maps correspond to the numbers shown in Table 1.

Table 1
Concentrations[a] of key solutes and background chemistry.

Site name	N°	Fe^{2+}	Alkalinity[b]	pH[c]	T[d]	SO_4^{2-}	Cl^-	Ca^{2+}	Na^+	K^+	Mg^{2+}
Tan-y-Garn	1	39.6	73	5.65	11.5	212	51.4	39	10	6	29
Ynysarwed	2	76.5	125	5.89	13.5	836	13.9	144	78	18	80
Morlais	3	10.4	283	6.74	14.3	348	18.0	83	89	27	49
Lindsay	4	15.6	251	6.72	15.4	225	13.3	72	64	119	60
Taff Merthyr	5	5.65	238	6.95	12.2	224	12.2	94	14	12	38
Cadley Hill	6	27.2	741	6.77	13.0	1560	5575	434	3800	98	325

[a] mg/L.
[b] As $CaCO_3$ equivalent.
[c] Average initial pH.
[d] Temperature at start of experiment.

2.1.6. Cadley Hill

At the time of this study a pumping test was underway at Cadley Hill in Derbyshire, England. All water was treated with flocculent and H_2O_2 upfront of a temporary settling lagoon. The test was carried out as part of a feasibility study to determine future treatment options that would prevent contamination of a nearby aquifer. As a result of local geology the water at this site is relatively high in NaCl compared to other inland mine waters in the UK. All water was collected prior to any chemical dosing via a sampling point in the main pipeline feeding the settling lagoon.

2.2. Chemicals

All chemicals, 2′2-bipyridyl, acetic acid, ammonium acetate, HCl, H_2SO_4, HNO_3, $K_2Cr_2O_7$, $FeSO_4.7H_2O$, were analytical grade from Fisher Scientific and were used as received. High purity 18 MΩ deionised water was used for the preparation of solutions in the laboratory.

2.3. Field methods

At each site approximately 8 L of freshly emerged mine water was taken in a bucket and stirred and aerated using a battery powered pump. The pH, temperature and DO were measured and logged every 10 s using two hand held Hanna combination meters HI-9828. The two meters were used together to better define the accuracy of pH measurement and were calibrated daily according to manufacturer's instructions on site prior to experimentation.

2.3.1. Homogeneous oxidation experiments

During the experiment 15 mL samples of the mine water were taken at regular intervals and immediately filtered through 0.8/0.2 μm Acrodisc PF syringe filters with Supor membrane and acidified with four drops of 10% HNO_3 to quench the oxidation reaction. Preliminary experimentation along with consideration of reaction kinetics (Epstein et al., 1980) had shown that the resulting concentration of HNO_3 in the sample was too low to result in noticeable Fe(II) oxidation between sampling and analysis. Where possible all samples were analyzed the same day. Where this was not possible samples were stored over night at 5 °C and analyzed the following day.

2.4. Fe(II) analysis

Iron(II) was measured spectrophotometrically using 2′2-bipyridyl as the complexing agent. A solution of 2′2-bipyridyl was prepared by dissolving 2 g of the solid in 100 mL of 0.2 M HCl. A 2 mL aliquot of aqueous Fe(II) (acidified as described previously) was added to 5 mL of ammonium acetate buffer (prepared according to APHA et al. (1999)) containing two drops of the 2′2-bipyridyl solution. The absorbance at 520 nm was measured using a Hitachi U1900 spectrophotometer previously calibrated using an aqueous $FeSO_4$ standard. The $FeSO_4$ solution was standardized using a method adapted from a chemical oxygen demand test in APHA et al. (1999) as used by Park and Dempsey (2005). Beer's Law was obeyed with Fe(II) concentrations in the range 1–50 mg/L.

2.5. Determination of background chemistry

Fresh mine-water samples were collected for determination of total concentrations of Cl^-, SO_4^{2-}, Ca^{2+}, Mg^{2+}, Na^+ and K^+. Samples were filtered using 0.8/0.2 μm syringe filters prior to analysis. Anion concentrations were determined using a Dionex ICS-2000 Ion Chromatography System. Cation concentrations were determined using a Perkin Elmer Optima 2100DV ICP-OES. Alkalinity was determined using a Hach digital titrator with a 1.6 N H_2SO_4 cartridge according to manufacturer's instructions within 15 min of sampling.

2.6. Iron oxidation model

Numerical modeling was carried out in Microsoft Excel. Values for k_1 were determined using a fourth order Runge–Kutta (RK4) method which can be described mathematically by Eqs. (3)–(7) below. This numerical method is often used to solve simple differential equations and is employed in its fifth and sixth order form to solve rate equations in PHREEQCi (Parkhurst and Appelo, 1999). All Runge–Kutta methods generate successive values for the concentration of the species under investigation over time. The ability of the method to accurately model the changes in a system depends on the length of the chosen time step between C_i and C_{i+1}. A more detailed discussion of the RK4 method and its application to chemical kinetics is given in Maeder and Neuhold (2007). Incremental changes in [Fe(II)] were calculated using Eq. (4), where C_i = [Fe(II)] and h = time interval between t_i and t_{i+1} (in this case 10 s). The values for c_1–c_4 were calculated by plugging the field measured values of temperature, pH and DO into Eqs. (4)–(7). By using measurements logged every 10 s it was possible to keep the individual time steps small relative to the overall length of the experiment and allowed an averaging out of k_1 over a large number of iterations. The temperature correction factor ϑ is described by Eq. (8) where Tm = measured temperature, R = the gas constant and E_a = the activation energy for the oxidation reaction, 96 kJ/mol (23 kcal) taken from Stumm and Morgan (1996) and previously used by Kirby et al. (1999, 2009).

$$C_{i+1} = C_i + \left[\frac{1}{6}(c_1 + 2c_2 + 2c_3 + c_4)\right]h \tag{3}$$

$$c_1 = (k_1/\vartheta)[\mathrm{Fe(II)}]P_{o_2}[OH^-]^2 \tag{4}$$

$$c_2 = (k_1/\vartheta)([\mathrm{Fe(II)}] + (5c_1))P_{o_2}[OH^-]^2 \tag{5}$$

$$c_3 = (k_1/\vartheta)([\mathrm{Fe(II)}] + (5c_2))\mathrm{P}_{o_2}[\mathrm{OH}^-]^2 \quad (6)$$

$$c_4 = (k_1/\vartheta)([\mathrm{Fe(II)}] + (10c_3))\mathrm{P}_{o_2}[\mathrm{OH}^-]^2 \quad (7)$$

$$\vartheta = e^{[(1/Tm)-(1/298)](E_a/R)} \quad (8)$$

The fit between the field-measured values of [Fe(II)] and the predicted values of [Fe(II)] from the RK4 method were optimized with an iterative least squares fit using the Solver tool in Microsoft Excel. The final values of k_1 chosen gave the best fit between the measured and predicted values of [Fe(II)].

2.7. PHREEQCI simulations

PHREEQCI (Parkhurst and Appelo, 1999) was used to determine concentrations of Fe(II) species $FeCl^+$, $FeSO_4$ in the waters under investigation. Input parameters were initial concentrations for alkalinity and Fe(II) as well as concentrations of Ca^{2+}, Mg^{2+}, Na^+, K^+, Cl^-, SO_4^{2-}, DO, pH and temperature. The phreeqc.dat database was used in all calculations.

3. Results and discussion

3.1. Rate constant for Fe(II) oxidation

Across all experiments aeration initially caused pH to increase as a result of CO_2 degassing as observed previously by Kirby et al. (2009). This caused a marked increase in the rate at which the waters became visibly turbid compared to water that was left to stand without aeration. In the case of the net acid sites (Tan-y-Garn and Ynysarwed) pH began to decrease again after about 15–20 min whereas for the rest of the sites it continued rising right up until the end of the experiment. These changes in pH can be used to explain the shapes of the curves for [Fe(II)] vs. time shown in Fig. 2. Initially [Fe(II)] changes slowly as pH is relatively low. The second order dependence on $[H^+]$ means that as pH rises the rate of Fe(II) oxidation increases rapidly giving rise to the s shaped curves below which are very different from those that are produced when pH is held constant. For the net acidic sites at Tan-y-Garn and Ynysarwed, Fe(II) oxidation rate drops off again towards the end of the experiment as pH decreases.

It can be seen from Fig. 2 that the values for [Fe(II)] produced by the model compared well to the measured values across all sites. The shapes of the curves produced based on the logged data for pH, temperature and DO fit well with the empirical data in all cases giving R^2 values in the range 0.94–1. The temperature independent values of k_1 were found to be within the range 1.52×10^{12}–$1.00 \times 10^{14}\ \mathrm{M^{-2}\,atm^{-1}\,s^{-1}}$. Temperature dependent values for k_1 were also calculated using an activation energy of 96 kJ/mol as temperature was not held constant throughout the experiments (varying by up to 8 °C). Table 2 compares the values derived for k_1 using the numerical methods described above to published values from laboratory and field work.

3.2. Background chemistry effects

As a result of the range of values for k_1 across the sites it was decided to investigate the influence of a number of Fe(II) ion pairs in relation to Fe(II) oxidation rate. Values for alkalinity, pH and temperature as well as major cations and anions were input into PHREEQCi (Parkhurst and Appelo, 1999) in order to determine the concentrations of Fe(II) species thought most likely to effect the rate of Fe(II) oxidation.

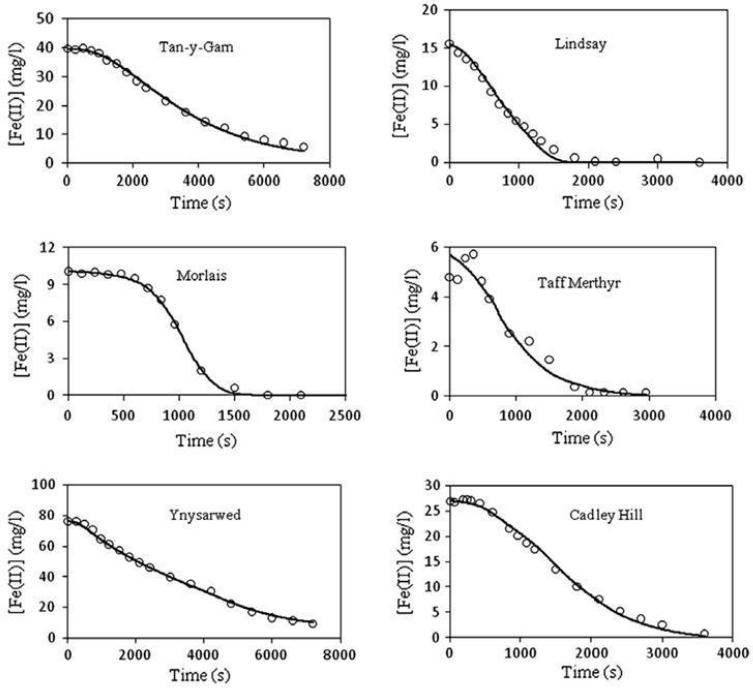

Fig. 2. Experimental (open symbol) and modeled (unbroken line) changes in Fe(II) concentration during oxidation experiments.

Table 2
Comparison of results to reported literature values for k_1.[a]

Authors	k_1	Comments
Stumm and Lee (1961)	$1.5(\pm0.5) \times 10^{13}$	pH = 6.5–7.24, T = 20.5 °C, pO_2 variable, $[Fe(II)]_0 < 50$ μM
Shenk and Webber (1968)	$2.1(\pm0.5) \times 10^{13}$	pH = 6.70, T = 25 °C, pO_2 = 0.21 atm, $[Fe(II)]_0 < 50$ μM
Davison and Seed (1983)	$1.5–3.2 \times 10^{13}$	pH = 7.0, T = 25 °C, pO_2 variable, $[Fe(II)]_0 > 5$ μM
Millero (1985)	$2.0–3.2 \times 10^{13}$	Varies according to ionic strength as $\text{Log}k_1 = 13.82 - 2.805I^{\frac{1}{2}} + 1.82I$ Values quoted for $0.1 \leqslant I^{\frac{1}{2}} \leqslant 0.6$
Liang et al. (1993)	3.0×10^{13}	pH = 6.84, T = 25 °C, pO_2 = 0.2, $[Fe(II)]0$ = 34.6 μM Converted from 1.90×10^{-12} M min^{-1} using $k_w = 10^{-14}$
This paper	$2.7 \times 10^{14}–2.7 \times 10^{16}$	pH = 6.8–7, T = 20.5 °C, pO_2 = 0.2 atm, $Fe[(II)]_0$ = 60–65 μM pH = 5.65–7.85, pO_2 variable, T = temperature corrected to 25 °C, $[Fe(II)]_0$ = 100–1370 μM (temperature corrected to 25 °C)

[a] All values for k_1 given as M^{-2} atm^{-1} min^{-1}.

Concentrations of $FeSO_4$ and $FeCl^+$ were compared to the values obtained for k_1. There was no correlation with either background concentrations of ions or ion pairs. Sung and Morgan (1980) showed marked reductions in Fe oxidation rate in the presence of Cl^- and SO_4^{2-} but in their study the ratio Fe^{2+}:anion was 1:1250 and upwards. With the exception of the Cadley Hill site, the relative concentrations of the anions in the examples presented here are low. As a result the concentrations of $FeSO_4$ and $FeCl^+$ only make up a relatively small proportion of dissolved Fe(II) and hence (being slower to react than hydrolyzed Fe(II) species) do not greatly influence the oxidation rate. King et al. (1995) showed that in solutions with carbonate concentration higher than 1 mM and pH greater than 6, trace concentrations of the fast reacting $Fe(CO_3)_2^{2-}$ complex can dominate the oxidation kinetics. As with SO_4^{2-} and Cl^+, however, no relationship was found between CO_3^{2-} concentration and Fe oxidation rate in this study. Variations in the activity coefficient γ of Fe(II) were also compared to k_1 to determine the influence of a primary kinetic electrolyte effect (primary salt effect as described by Millero, 1985, and references therein). Again there was no apparent correlation across the sites studied.

3.3. Effect of pH

As described previously the pH was measured throughout the experiments and corresponding values for $[H^+]$ were incorporated into the model for k_1. The resulting values for k_1 produced by the model should, therefore, be independent of pH. It was noticed, however, that the values of k_1 did show a correlation with pH. In order to test the significance of this correlation k_1 was plotted vs. $[H^+]$. Because pH was not controlled in the experiments values for $[H^+]$ were determined by averaging over each experimental run. Fig. 3 shows a plot of these mean $[H^+]$ values vs. k_1. It can be seen that there is a positive correlation between the two sets of values with $R^2 = 0.96$ indicating a gradient significantly different from zero. The rate constant k_1 is not independent of pH across the sites studied here suggesting that the rates of Fe(II) oxidation cannot be described by the homogeneous mechanism alone.

Eq. (9) (from Tamura and Nagayama, 1976) describes both the homogeneous and heterogeneous pathways for Fe(II) oxidation with the corresponding rate constants k_1 and k_2. It can be seen from the equation that pH has a greater influence on the rate of homogeneous oxidation compared to heterogeneous oxidation with the two pathways having inverse second and first order dependence on $[H^+]$ respectively. The result is that according to Eq. (9) heterogeneous oxidation should become increasingly important with respect to homogeneous oxidation as pH decreases. In cases where no additional Fe(III) solids are added to the reaction mixture the heterogeneous pathway can have an autocatalytic effect and increase the overall oxidation rate as a result of Fe(III) produced *in situ* (Sung and Morgan, 1980).

$$-\frac{d[Fe(II)]}{dt} = \left(k_1[H^+]^{-2}P_{O_2} + k_2[Fe(III)][H^+]^{-1}P_{O_2}\right)[Fe(II)] \quad (9)$$

In their experiments Sung and Morgan (1980) only observed autocatalysis in waters above pH 7. This can be explained in terms of the pH dependence of Fe(II) adsorption onto the surface of Fe(III) solids (Eq. (10) from Tamura and Nagayama (1976). The unexpectedly high values for k_1 reported here suggest, however, that contrary to the results of these previous studies autocatalytic heterogeneous oxidation may be contributing to the overall rate of Fe(II) oxidation in natural waters at pH levels as low as 5.6.

$$[Fe(II)_{sorb}]/[Fe(II)] = \frac{K[Fe(III)]}{[H^+]} \quad (10)$$

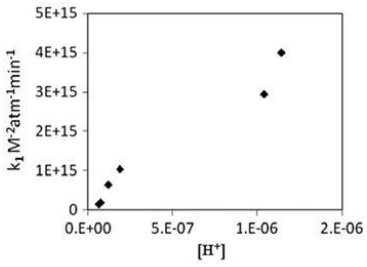

Fig. 3. Comparison of calculated values for k_1 with average values for $[H^+]$ across all of the sites.

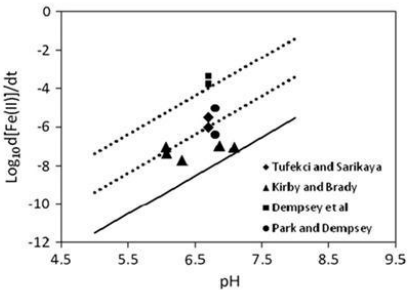

Fig. 4. Comparison of field Fe(II) oxidation rates in this study with previously determined field oxidation rates (Kirby and Brady, 1998), and heterogeneous oxidation rates (Tufekci and Sarikaya, 1996; Dempsey et al., 2001; Park and Dempsey, 2005). All values corrected to ms^{-1}.

3.4. Comparison with heterogeneous oxidation rates and other field trials

In order to assess the potential contribution of heterogeneous oxidation to the systems under investigation, the measured oxidation rates were compared to previously published rates of heterogeneous oxidation and other field measured rates. The results are shown in Fig. 4. The broken lines delineate the upper and lower limits for Fe(II) oxidation rate from this study with the solid line denoting homogeneous oxidation rates for $k_1 = 2.0 \times 10^{13}$ $M^{-2}\,atm^{-1}\,min^{-1}$. It can be seen that the heterogeneous rates fit well with oxidation rates observed in the field experiments. It is also worth noting that the field measured rates of Kirby and Brady (1998) were higher than would have been predicted by homogeneous oxidation alone.

Discounting the possibility of a contribution from abiotic oxidation the main difference between the chemical composition of the waters considered here and those of earlier laboratory studies is the concentration of Fe(II). Table 2 shows that the initial concentrations of Fe(II) were 1–2 orders of magnitude higher in this study than in any of the laboratory based work. Given the higher concentrations of Fe(III) particulates that would, therefore, be formed in the water column it is likely that the effect of the heterogeneous oxidation is more significant in these natural waters.

3.5. Significance of results

It has been shown that over the pH range 5.6–7.5 Fe oxidation rates in the field are often higher than would be predicted from the results of laboratory studies. The higher than expected values for k_1 are possibly due to heterogeneous autocatalysis occurring as a result of higher total Fe concentrations and hence higher concentrations of Fe(III) particulates compared to previously published laboratory studies. Iron oxidation rates for pH < 6 were up to three orders of magnitude greater than previously published a fact that is likely to be a significant factor in the future design of treatment schemes for Fe-rich waters.

Acknowledgements

The authors would like to thank the UK Coal Authority, Cardiff University and EPSRC for their financial support.

Appendix A. Supplementary material

Supplementary data associated with this article can be found, in the online version, at doi:10.1016/j.apgeochem.2011.05.018.

References

APHA (American Public Health Association), AWWA (American Water Works Association), WEF (Water Environment Federation), 1999. Standard Methods for the Examination of Water and Wastewater.

Buerge, I.J., Hug, S.J., 1999. Influence of mineral surfaces on chromium(VI) reduction by iron (II). Environ. Sci. Technol. 33, 4285–4291.

Chakravarty, S., Dureja, V., Bhattacharrya, G., Maity, S., Bhattacharjee, S., 2002. Removal of arsenic from groundwater using low cost ferruginous manganese ore. Water Res. 36, 625–632.

Charlet, L., Liger, E., Gerasimo, P., 1998. Decontamination of TCE- and U-rich waters by granular iron: role of sorbed Fe(II). J. Environ. Eng. 124, 25–30.

Davison, W., Seed, G., 1983. The kinetics of the oxidation of ferrous iron in synthetic and natural waters. Geochim. Cosmochim. Acta 47, 67–79.

Dempsey, B.A., Roscoe, H.C., Ames, R., Hedin, R., Jeon, B.H., 2001. Ferrous oxidation chemistry in passive abiotic systems for the treatment of mine drainage. Geochem. Explor. Environ. Anal. 1, 81–88.

Epstein, I.R., Kustin, K., Warshaw, L.J., 1980. A kinetics study of the oxidation of iron (II) by nitric acid. J. Am. Chem. Soc. 102, 3751–3758.

Karschunke, K., Jekel, M., 2002. Arsenic removal by iron hydroxides, produced by enhanced corrosion of iron. Water Sci. Technol.: Water Supply 2, 237–245.

King, D.W., 1998. Role of carbonate speciation on the oxidation rate of Fe(II) in aquatic systems. Environ. Sci. Technol. 32, 2997–3003.

King, D.W., Lounsbury, H.A., Millero, F.J., 1995. Rates and mechanism of Fe(II) oxidation at nanomolar total iron concentrations. Environ. Sci. Technol. 29, 818–824.

Kirby, C.S., Brady, J.A.E., 1998. Field determination of Fe2+ oxidation rates in acid mine drainage using a continuously-stirred tank reactor. Appl. Geochem. 13, 509–520.

Kirby, C.S., Dennis, A., Kahler, A., 2009. Aeration to degas CO2, increase pH, and increase iron oxidation rates for efficient treatment of net alkaline mine drainage. Appl. Geochem. 24, 1175–1184.

Kirby, C.S., Thomas, H.M., Southam, G., Donald, R., 1999. Relative contributions of abiotic and biological factors in Fe(II) oxidation in mine drainage. Appl. Geochem. 14, 511–530.

Liang, L., McNabb, A.J., Paulk, J.M., Gu, B., McCarthy, J.F., 1993. Kinetics of Fe(II) Oxygenation at low partial pressure of oxygen in the presence of natural organic. Matter. Environ. Sci. Technol. 27, 1864–1870.

Lide, D.R., 1996. CRC Handbook of Chemistry and Physics: Special Student Edition, 77th ed. CRC Press.

Liger, E., Charlet, L., Van Cappellen, P., 1999. Surface catalysis of uranium(VI) reduction by iron (II). Geochim. Cosmochim. Acta 63, 2939–2955.

Maeder, M., Neuhold, Y.M., 2007. Practical Data Analysis in Chemistry, first ed. Elsevier.

Meng, X., Korfiatis, G.P., Christodoulatos, C., Bang, S., 2001. Treatment of arsenic in Bangladesh well water using a household co-precipitation and filtration system. Water Res. 35, 2805–2810.

Millero, F.J., 1985. The effect of ionic interactions on the oxidation of metals in natural waters. Geochim. Cosmochim. Acta 49, 547–553.

Noike, T., Nakamura, K., Matsumoto, J., 1983. Oxidation of ferrous iron by acidophilic iron-oxidising bacteria from a stream receiving acid mine drainage. Water Res. 17, 21–27.

Nordstrom, D.K., 1985. The rate of ferrous iron oxidation in a stream receiving acid mine effluent. U.S. Geol. Surv. Water Supply Paper 2270, 133–199.

Park, B., Dempsey, B., 2005. Heterogeneous oxidation of Fe(II) on ferric oxide at neutral pH and a low partial pressure of O2. Environ. Sci. Technol. 39, 6494–6500.

Parkhurst, D.L., Appelo, C.A.J., 1999. User's guide to PHREEQC (Version 2)–a computer program for speciation, batch-reaction, one-dimensional transport, and inverse geochemical calculations. U.S. Geol. Surv. Water-Resour. Invest. Rep., 99–4259.

Sánchez España, J., López Pamo, E., Santofimia Pastor, E., 2007. The oxidation of ferrous iron in acidic mine effluents from the Iberian Pyrite Belt (Odiel Basin, Huelva, Spain): field and laboratory rates. J. Geochem. Explor. 92, 120–132.

Shenk, J.E., Webber, W.J., 1968. Chemical interactions of dissolved silica with iron II and iron III. J. Am. Water Woks Assoc. 60, 199–212.

Stumm, W., Lee, G.F., 1961. Oxygenation of ferrous iron. Ind. Eng. Chem. 53, 143–146.

Stumm, W., Morgan, J.J., 1996. Aquatic Chemistry,, .. Chemical Equilibria and Rates in Natural Waters, third ed. Wiley Interscience.

Stumm, W., Sulzberger, B., 1992. The cycling of iron in natural environments: considerations based on laboratory studies of heterogeneous redox processes. Geochim. Cosmochim. Acta 56, 3233–3257.

Sung, W., Morgan, J.J., 1980. Kinetics and product of ferrous iron oxygenation in aqueous systems. Environ. Sci. Technol. 14, 561–568.

Tamura, H.G.K., Nagayama, M., 1976. The effect of ferric hydroxide on the oxygenation of ferrous ions in neutral solutions. Corros. Sci. 16, 197–207.

Tufekci, N., Sarikaya, H.Z., 1996. Catalytic effects of high Fe(II) concentrations on Fe(II) oxidation. Water Sci. Technol. 34, 389–396.

CO_2 degassing: implications for treatment of circumneutral mine drainage

Jennifer N. Geroni*, Devin J. Sapsford, Kay Florence

*Cardiff School of Engineering, Cardiff University, Queen's Buildings, The Parade, Cardiff, CF24 3AA UK.*geronijn@cf.ac.uk*

Abstract

This paper presents the results of investigation of the effects of CO_2 degassing on the chemistry of both net acid and net alkaline circumneutral mine drainage. Batch studies were carried out to mechanically aerate and degas the waters at a number of sites across the UK which resulted in large changes in alkalinity, dissolved CO_2, pH and concentrations of dissolved Iron. In the case of the net alkaline waters pH was raised by nearly 2 points over the course of the experiment. A simplistic model for CO_2 degassing was constructed in order to assess $d[CO_2]/dt$ over the initial stages of degassing. CO_2 concentrations were shown to decrease sharply over the first few minutes of the experiments. The results of this study have implications for the design of both passive and active mine water treatment schemes. The highly pH dependent nature of iron oxidation rates means that stripping CO_2 and thereby raising (or stabilising) pH can reduce residence times needed for Fe(II) oxidation and also reduce the cost of chemical dosing where it is required.

Key words: alkalinity, acidity, CO_2 degassing, pH

Introduction

It is widely accepted that control of pH is critical in the remediation of ferrous mine drainage since rate of Fe(II) oxidation is highly pH dependent, with an increase in pH of one unit resulting in a 100 fold increase in oxidation rate (Equations 1 and 2)(Liang 1993). Raising pH can therefore reduce the residence time required for iron oxidation in a treatment system from days or weeks to just a few minutes.

$$-\frac{\mathbf{d}[\mathbf{Fe^{2+}}]}{\mathbf{dt}} = \frac{\mathbf{k_1}[\mathbf{Fe^{2+}}]\mathbf{P_{O_2}}}{[\mathbf{H^+}]^{\mathbf{2}}} \qquad \textit{Equation 1}$$

$$\mathbf{pH} = -\mathbf{log_{10}}[\mathbf{H}]^{+} \qquad \textit{Equation 2}$$

Circumneutral mine drainage, whether net acid or net alkaline often contains significant amounts of dissolved CO_2, far in excess of concentrations that would be observed at atmospheric equilibrium. These high CO_2 concentrations contribute to the acidity and hence reduce the pH of the water by the presence of carbonic acid. Dissolved CO_2 concentrations can be reduced by mechanical aeration and degassing to produce measureable changes in pH in the waters in question (Kirby et al 2009).

Treatment of net alkaline waters often includes an aeration cascade to increase dissolved oxygen followed by a filtration step, settling lagoon or wetland. For net acid sites pH is often raised by the addition of chemicals such as calcium or sodium hydroxide or by the inclusion of an alkalinity generating step such as a limestone drain prior to removal of Fe(III) hydroxide precipitates. As far as the authors are aware it is uncommon to find aeration cascades or mechanical aeration steps included in such treatment schemes specifically designed for the stripping of excess CO_2 from the water prior to any additional chemical dosing that might still be required. The reduction in the acidity of a mine water brought about by CO_2 stripping could have a large impact on the chemical consumption of an active treatment plant.

Methods

Experimental procedure: Analytical grade HNO_3 from Fisher Scientific was used as received. High purity 18MΩ deionised water was used for the preparation of solutions in the laboratory. All syringe filters used were 0.8/0.2µm Acrodisc PF with Supor membrane. A submersible Whale® Water Systems self venting pump powered by a 12 V car battery was used for aeration and CO_2 degassing (as in Figure 1). Approximately 10 L of fresh mine-water was collected and aerated with pH, temperature, and dissolved oxygen (DO) measured and logged every 10 seconds throughout using two hand held Hanna combination meters HI-9828. Both meters were calibrated according to manufacturer's instructions prior to experimentation.

Two 15 mL samples of the mine water were taken at the beginning and end of each experiment and acidified with 4 drops of 20% HNO_3. One of the samples was passed through a syringe filter prior to acidification to remove Fe(III) particulates and was taken to be representative of dissolved Fe(II). All Fe samples were then analysed by a Perkin Elmer Optima 2100DV ICP-OES previously calibrated using standard solutions according to manufacturer's instructions.

Alkalinity was determined using a Hach digital titator with a 1.6 N H_2SO_4 cartridge according to manufacturer's instructions. 100 mL samples of fresh mine water were titrated using a bromocresol green methyl red indicator. The end point was determined as a colour change from green to pink. Titrations were carried out in duplicate and in triplicate where the first two readings differed by more than 5 mg/L $CaCO_3$ equivalent.

Cold acidity titrations were also carried out using a Hach digital titator with 1.6 N NaOH cartridge according to manufacturer's instructions. Samples were titrated to an end point of pH 8.4 measured using the pH module on a Hanna combination meter HI-9828. It should be noted that it was very difficult to get agreement between different titrations as both CO_2 degassing and iron oxidation and precipitation occur on the same timescale as the titration.

In order to overcome the difficulties encountered with the cold acidity titration an additional "hot titration" was carried out as described by AWWA (1999) to determine net acidity/alkalinity. Initially 100 mL of fresh mine water was taken and titrated to pH 4 using a Hach digital titator with a 1.6 N H_2SO_4 cartridge. Three drops of 30% H_2O_2 were then added. The sample was heated to boiling point and boiled for 2 minutes using a camping stove. The sample was then allowed to cool before titration to pH 8.4 again using the Hach digital titrator with a 1.6 N NaOH cartridge. Net acidity or alkalinity was then determined according to the difference between the quantities of acid and alkali consumed during the procedure.

Site descriptions

The sites investigated are located across the UK. Blenkinsop and Dawdon are situated in the north of England while Tan-y-Garn and Six Bells are located in south Wales.

Blenkinsop: The treatment scheme at Blenkinsop was designed as a preventative measure upon closure of the mine in 2002. Prior to the commissioning of the treatment scheme in 2005 predictions of iron concentrations of around 100 mg/L were expected for up to 11 years before settling down to 10-20 mg/l. In fact the first flush saw levels of 1000 mg/L of iron which to date have reduced to around 140mg/l. The water which was originally highly net acid is now borderline acid with mineral acidity and carbonate alkalinity almost perfectly balanced. The water is pumped from 20m below the shaft top and passed initially through a Newton aerator to begin the oxidation process. The flow of water then is split between two parallel settling ponds before flowing through two reed beds in series. Due to the higher than expected levels of iron encountered, a lime dosing system has been employed to treat the minewater.

Tan-y-Garn: The experimental Tan-y-Garn treatment scheme was commissioned in January 2006, using a reducing alkalinity producing system (RAPS) which was the first of its kind to be used by the UK Coal Authority in the treatment of mine water. The scheme is entirely passive

being gravity fed and comprising a series of three settling ponds and one wetland for the removal of Fe(III) precipitates after the RAPS. The flow rate on site is low being only 3 L/s and varying considerably with high rainfall and drought events. Influent iron concentration has remained fairly constant since the site was commissioned at around 50 mg/L

Dawdon: The primary objective for developing this active treatment plant (commissioned in 2009) was to prevent contamination of the East Durham Aquifer in the North of England, which provides drinking water to a number of nearby towns. The water being treated is highly saline as much of the flooding of the old workings is a result of the ingress of water from the North Sea. The contaminated mine water is pumped to control levels within the old workings to some depth below sea level. Water is then transferred from the mine shaft to the treatment plant via an 850m pipeline. The heavy contamination and salinity of the mine water required a bespoke process design to be developed. Initially there is an aeration stage followed by lime dosing. Recirculation of hydrated ferric oxide (HFO) solids between the treatment tanks results in the formation of high density sludge and further increases iron removal efficiency. Finally, the water is passed through a clarifier with the overall process reducing the iron levels in the water from 160 mg/L to less than 1mg/L. The treated effluent is eventually discharged out to sea via twin directionally drilled outfalls.

Six Bells: Mine water is extracted via a borehole driven 216m into the ground at a point where an underground roadway intercepts the disused mine workings. Despite relatively low influent Fe concentrations and high alkalinity it was decided to install an active treatment plant at this site due to sizing constraints. The water is initially pumped into a hydrogen peroxide aeration system before flowing into two parallel settlement lagoons measuring 1540m^2 each. The water then flows into a wetland area before being released into a nearby river. Pumping commenced in January 2002, the fisrt flush of water found to contain 250 mg/L iron, which was treated by increased caustic soda dosing. After a period of four months the Fe concentration in the water had reduced to 45mg/L with further reduction to 20mg/L by 2010 and final effluent in the order of 1 mg/L.

Figure 1 *experimental setup for batch-wise mechanical aeration*

Results and discussion

The sites studied using mechanical aeration and degassing can be split into two groups in terms of their behaviour regarding changing pH and concentrations of dissolved carbonate species. These groups are characterised by their determination as net acid (or borderline net acid) and net alkaline. Values of alkalinity and acidity were determined using several different techniques the results of which are shown in Table 1. Measurements were taken pre and post

aeration and it can be seen that the differences between these measurements was significant (up to 427 mg/L $CaCO_3$ equivalent). The final classification of a site as net acid or net alkaline was based on the results of hot peroxide titrations which ensured that all CO_2 had been removed and all iron oxidised. It can be seen that the results of cold acidity and alkalinity measurements made after 2 hours of aeration fit much more closely with the results from the hot peroxide titrations highlighting the effect of large quantities of dissolved CO_2 on the acidity present in the water.

Table 1 *Average values for acidity, alkalinity measurements pre and post aeration, compared to the hot peroxide titration (mg/L $CaCO_3$ equivalent) with post aeration Fe(II) (mg/L)*

	Pre aeration			Post aeration				
Site	**Acid**	**Alk**	**Difference**	**Acid**	**Alk**	**Difference**	**Fe(II)**	**Hot peroxide**
Blenkinsop	449	264	185 net acid	22	36	14 net alk	5.75	44 net acid
Tan-y-Garn	181	57	124 net acid	17	1	16 net acid	4.3	19 net acid
Dawdon	479	425	54 net acid	121[a]	276	153 net alk	0.06	195 net alk
Six Bells	251	749	498 net alk	0	625	625 net alk	0.05	615 net alk

[a]On the day of the Dawdon trial there were problems with the battery used to drive the aeration pump. The relatively high remaining acidity is a result of incomplete CO_2 degassing.

The main impact of the high concentrations of dissolved CO_2 is the reduction in pH of the emerging mine water compared to samples with the same alkalinity at atmospheric equilibrium. Figure 2 shows the changes in pH measured at two of the sites over the course of the degassing experiments as CO_2 concentration decreases. The shapes of these curves are characteristic of the changes in pH observed at net acid and net alkaline sites and are explained in detail below.

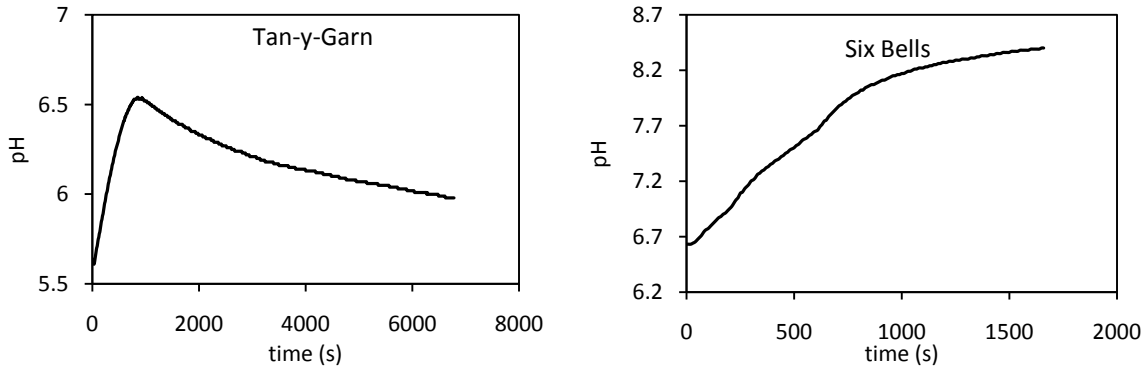

Figure 2 *Typical changes in pH recorded during batch-wise mechanical aeration experiments*

Net acid and borderline net acid sites

For all of the sites that were net (or borderline) acid the initial pH values were below pH 6. It can be seen that pH rose quickly within the first 10 minutes of aeration indicating the degassing of dissolved CO_2. The pH peaked at all net acid sites between 6.3 - 6.5 before decreasing again. The characteristic shapes of the curves can be explained by the changing chemistry of the system over time.

4. Initial increase in pH corresponds to rapid CO_2 degassing.
5. As rate of CO_2 degassing slows rate of increase of pH also slows.
6. Rising pH causes increasingly rapid iron oxidation and precipitation which consumes alkalinity and causes pH to fall again.

Net alkaline sites

The shapes of the curves for pH change in net alkaline waters are very different to those observed for net acid waters. The pH rises continuously throughout the experiment with CO_2 degassing as there is sufficient alkalinity present to neutralise any acidity generated by the formation of Fe(III) hydroxides. It is worth noting the final pH at Six Bells of 8.3 which would give near instantaneous Fe(II) oxidation.

The fact that the pattern of the pH changes observed remains consistent across different sites with similar chemistry implies that this method of aeration with pH monitoring can serve as a useful guide in the assessment of mine water discharges. As has been noted above, measurements of acidity and alkalinity can vary widely and the accuracy of the measurements is highly dependent on the skill and experience of the individual carrying out the work. By contrast, provided that the pH meter used is working correctly the degassing method with pH logging is a very straightforward way in which to assess a discharge, with far less likely hood of the introduction of operator error. The measurements for Fe(II) concentration taken at the end of the degassing experiments also give a useful indication as to the potential iron removal efficiencies that could be achieved without chemical dosing. It can be seen that for these circumneutral net acid waters final iron concentrations can be brought close to 5 mg/L with 2 hours aeration alone.

Having observed such significant changes in pH it was decided to attempt to model CO_2 degassing in these systems. A simple model was constructed based on changes in Fe(II) concentration and pH over time. The model assumed that after oxidation, precipitation of Fe(III) hydroxides was instantaneous and that alkalinity was consumed stoichiometrically according to Equation 3. This method has been used previously by Kirby et al (2009).

$$Fe^{2+} + CO_3^{2-} + 2\tfrac{1}{2}H_2O + \tfrac{1}{4}O_2 \rightarrow Fe(OH)_3 + H_2CO_3 \quad \textbf{\textit{Equation 3}}$$

Changes in Fe(II) concentration over time were calculated (at 10 second intervals) using a 4th order Runge Kutta (RK4) method and values of k_1 (the rate constant for homogeneous iron oxidation) as described by Geroni and Sapsford (2011). The corresponding changes in alkalinity were then calculated at 10 second time intervals. Concentrations of Fe(II) and alkalinity, together with logged values for pH, temperature and DO were then input into PHREEQCi in spreadsheet mode to produce the values for dissolved CO_2. Examples of the outputs typical of net acid and net alkaline sites are shown in Figure 3.

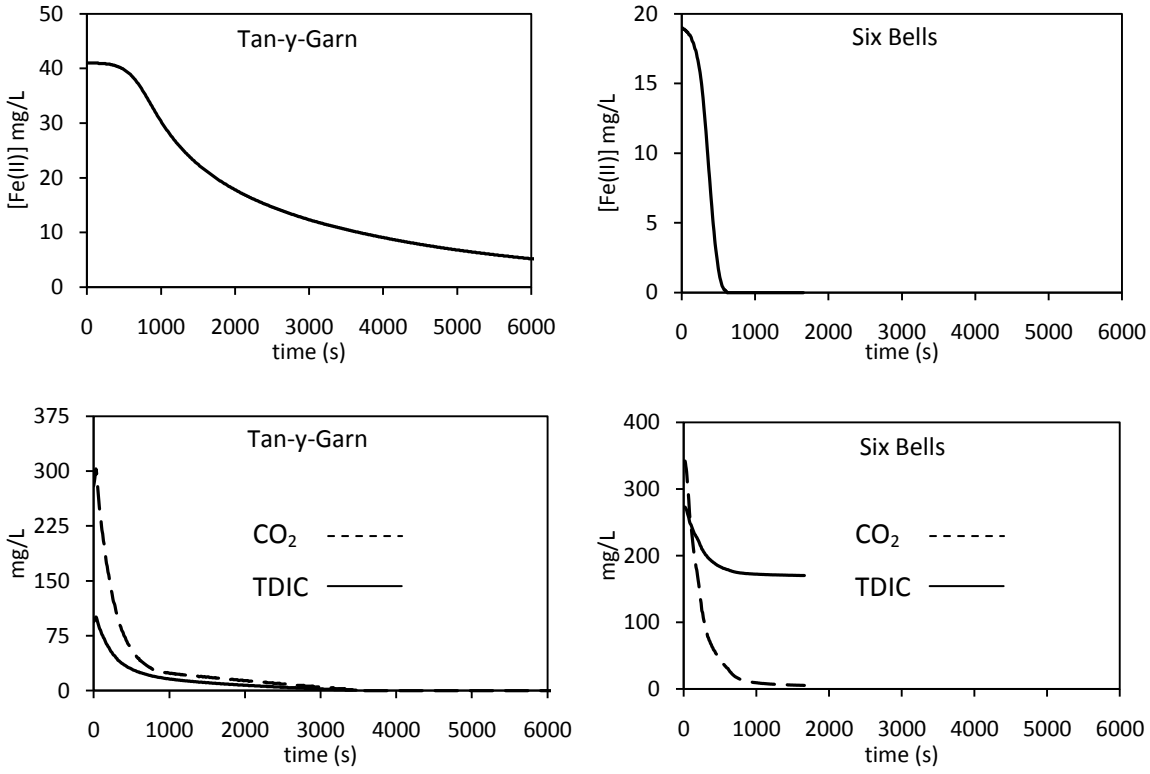

Figure 3 *Typical changes in concentration of Fe(II) and carbonate species with CO_2 degassing. Tan-y-Garn is representative of net acid sites with Six Bells showing net alkaline behaviour.*

The data highlights the differences in iron oxidation rates between the different sites, with near complete iron oxidation in around 10 minutes at Six Bells compared to around 8 mg/L Fe(II) remaining after 100 mins at Tan-y-Garn. The TDIC output from PHREEQCi follows closely changes in alkalinity and it can also be seen that this is completely consumed for the net acid site whereas (as expected) it remains high for net alkaline conditions. The only real similarity between the two types of sites was in the rate of CO_2 degassing. In all cases it was rapid over the first 5-10 minutes, after which point the rate slowed significantly. This corresponds with the peak in pH observed under net acid conditions between 10-15 minutes after aeration commenced. As the experiment proceeded, for net acid sites, where alkalinity was predicted to go to zero the concentration of dissolved CO_2 also dropped to zero as when used in spreadsheet mode PHREEQCi cannot bring the species in the reaction mixture into atmospheric equilibrium. For the net alkaline systems dissolved CO_2 did not reach equilibrium with the atmosphere over the time scale of the experiments for any of the waters investigated suggesting that further degassing would have led to even greater increases in pH.

The reduction of TDIC and dissolved CO2 to zero under net acid conditions underlines the oversimplification of the system by the assumptions made in this way of modelling. However the model does provide a useful guide as to the changes that could be expected in similar systems over the initial stages of aeration and degassing.

The results of these CO_2 degassing trials could play an important role in the design of semi-passive treatment systems. The inclusion of any aeration/degassing step up front of an active treatment plant for circumneutral water will reduce the rate of lime consumption which is likely to have a large cost benefit in the long term as the cost of transport and raw materials increases. In all of the sites investigated here (which are typical of coal mine drainage in the UK) an efficient aeration tank with sufficient residence time could completely eliminate the need for chemical dosing from marginally net acidic sites. In the case where only a few

minutes residence time was available it would still be possible to remove between 30-50% of excess CO_2. A change in dissolved CO_2 of 120 mg/L corresponds to a reduction in the quantity of lime required to neutralise the associated carbonic acid of 202 mg/L. At a treatment site where the flow rate is 50 L/s this gives a reduction of 864 kg of lime per day. Not only is there an obvious benefit in economic terms as a reduction in the up-front purchase cost of the lime, but a lower concentration of dissolved $CaCO_3$ will result in less lime scale formation reducing maintenance costs and a reduced mass of sludge sent to landfill.

In the case of net alkaline sites, several minutes aeration (whether in a reaction vessel or by recirculation over an aeration cascade) could increase pH to a point where HFO settling rather than Fe(II) oxidation rate becomes the rate determining step for iron removal. This point is particularly important with relation to the Six Bells site discussed in this study. The current treatment system with hydrogen peroxide dosing could be completely replaced by a large aeration cascade that would increase pH above 7 meaning that the relatively small settling ponds would have sufficient residence time for Fe(II) oxidation.

Acknowledgements

The authors would like to thank the UK Coal Authority, EPSRC and Cardiff University for their financial support.

References

1999. *Standard Methods for the Examination of Water and Wastewater*. American Water Works Association.

Geroni, J. N. and Sapsford, D. J. Kinetics of iron (II) oxidation determined in the field. *Applied Geochemistry* In Press, DOI.10.1016/j.apgeochem.2011.05.018.

Kirby, C. S., Dennis, A., Kahler, A. 2009. Aeration to degas CO2, increase pH, and increase iron oxidation rates for efficient treatment of net alkaline mine drainage. *Applied Geochemistry* 24(7), pp. 1175-1184.

Liang, L., McCarthy, John F., Jolley, Louwanda W., McNabb, J. Andrew, Mehlhorn, Tonia L. 1993. Iron dynamics: Transformation of Fe(II)/Fe(III) during injection of natural organic matter in a sandy aquifer. *Geochimica et Cosmochimica Acta* 57(9), pp. 1987-1999.

Potential for semi-passive mine water treatment by CO_2 stripping at Ynysarwed South Wales

Jennifer N. Geroni[1*], Devin J. Sapsford[1], Ian Watson[2]

[1]*Cardiff School of Engineering, Cardiff University, Queen's Buildings, The Parade, Cardiff, CF24 3AA UK.*geronijn@cf.ac.uk*
[2]*The Coal Authority, 200 Lichfield Lane, Mansfield, Nottinghamshire, NG18 4RG, UK*

Abstract

In the Spring the of 1993 the Ynysarwed mine water discharge in South Wales became a serious problem affecting a 12km length of the Neath Canal. As a result of the severity of the discharge, pH 3.5, 400mg/l Fe, a combination of active and passive treatment steps were installed. Chemical dosing was stopped in 2009 as conditions had improved pH>5, 100mg/l Fe. The existing mine water treatment scheme is in the process of being reviewed. Different treatment options are being considered including stripping dissolved CO_2 from the mine water, thereby maintaining mildly acidic pH and accelerating Fe(II) oxidation rates.

Key words: oxidation rate, CO_2 degassing, aeration, active treatment.

Introduction

What's next for the Ynysarwed Minewater discharge? After many years of low flow the Ynysarwed minewater discharge near Neath in South Wales became a serious problem in the Spring of 1993 affecting a 12km length of the Neath Canal. The severity of this discharge (400mg/l Fe, pH 3.5) and sensitivity of the affected water body resulted in the deployment of a combination of active and passive treatment steps, comprising mechanical aeration with calcium/magnesium hydroxide addition and flocculent dosing/lamellae plate clarification followed by a constructed wetland to provide final polishing. It was envisaged that active treatment would only be required for a decade at which point the iron concentration would be sufficiently low as to be treatable by passive means alone. Chemical dosing was stopped in 2009 with all water being discharged directly into the reed beds. Despite the reduced influent iron concentration of <100mg/l and pH>5 the site sometimes struggles to meet target effluent iron concentrations. Thus the existing mine water treatment scheme is in the process of being reviewed. Different treatment options are being considered including innovative approaches. This paper provides a snapshot of current system performance and demonstrates the potential for treating this water by stripping dissolved CO_2 stabilising the pH in the mildly acidic region and thereby increasing Fe(II) oxidation rates.

Methods

CO_2 degassing experiements. Fresh minewater was collected from the adit and returned to the lab for degassing experiments. The pH, temperature, and dissolved oxygen (DO) were measured (only selected data presented here) using two hand held Hanna combination meters HI-9828 while 8l of the water was aerated and degassed using a compressed air line. Both meters were calibrated according to manufacturer's instructions prior to experimentation. Measurements were logged every 10 seconds. Two 15ml samples of the mine water were taken at the beginning and end of the experiment and acidified with 4 drops of 20% nitric acid. One of the samples was passed through a 0.8/0.2µm Acrodisc PF syringe filter prior to acidification to remove Fe(III) particulates and was taken to be representative of dissolved Fe(II) concentration. All Fe samples were then analysed by ICP-OES. Acidity and Alkalinity were determined using Hach digital titrators with cartridges containing 1.6N NaOH and H_2SO_4 respectively. Acidity titrations were carried out to an end point of pH 10.4 to determine total acidity as described by Stumm and Morgan (1996). This end point was chosen as a pH of 10.4 ensured that all Fe(II) was oxidized on the timescale of the titration and so a true comparison of the acidity generated at the beginning and end of the experiment could be made. Alkalinity titrations were carried out using a bromcresol green methyl red indicator and were titrated until the colour change from green to pink was observed.

Site Survey: A survey was conducted of the reed beds and distribution channels at the Ynysarwed site. Dissolved oxygen (DO), pH, and conductivity were determined using two Hanna HI-9828 multi-parameter data logging probes which were deployed in unison, and programmed to log a reading every 10 seconds. After sampling for 10-15 minutes at each point, logging was discontinued and average values across the time period determined. On the day that the site survey was carried out 0.6 l/sraw mine water was being treated by a pilot scale plant for the production of high density sludge (HDS) before being recirculated into the main influent stream to the reed beds. Blocks containing flocculent and magnesium hydroxide were also being added periodically at the distribution weir just ahead of the reed beds. Acidity, alkalinity and iron concentrations were determined in the same way as for the CO_2 degassing experiments.

Results and Discussion

A schematic outline of the passive part of the Ynysarwed treatment scheme is shown in Figure 15. The influent water is pumped from an adit 0.5km to the North East of the site. 0.6l/s of the flow is then diverted through the HDS plant before being returned to the bulk flow and

pumped into a distribution chamber where the flow splits, with half going through the smaller wetland (a) to the left and half through the larger wetland (b) to the right. The pump transferring the water from the adit to the wetland is cycled on and off throughout the day with peaks in flow of 15-16 l/s through each of the wetlands giving an average flow of 8.4 l/s (16.8 l/s total).

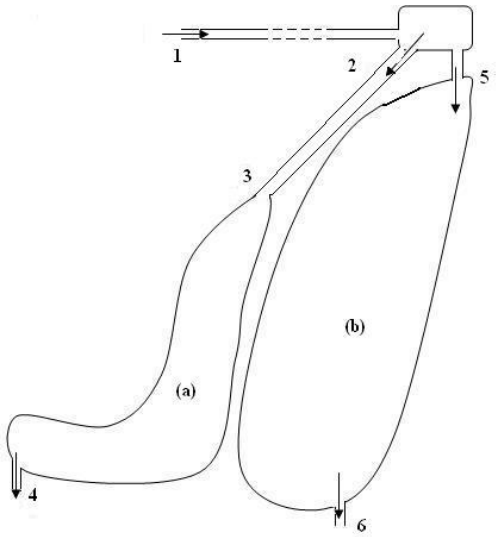

Figure 15 *Schematic outline of Ynysarwed wetlands. Small lagoon (a) 3080m^2, Large lagoon (b) 6800m.^{2}HDS plant located between sample points 1 and 2*

Figure 2 shows changes in concentration of Fe(II) and Fe(III) across the site. The initial sample was taken at point (1) as the water emerges from the adit. The drop in total iron between the adit (1) and the start of the wetlands (2) and (5) can be accounted for by the partial diversion of 0.6 l/s through the HDS pilot plant and ochre accretion in the transfer pipe. In the HDS plant the water is aerated and the pH increased to accelerate iron oxidation before being returned to the main pipe. This also accounts for the increase in pH between the adit and sample points (2) and (5).

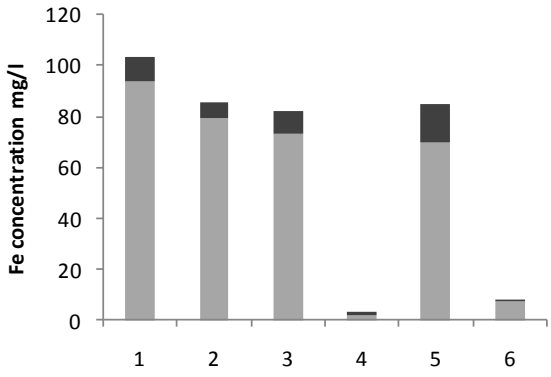

Figure 2 *Variation in Fe concentration across the site, Fe(II) light gray, Fe(III) dark grey*

Contrary to initial expectations total iron removal is higher across the smaller wetland than across the larger one. Historic data from the site shows that this is consistently the case, though the reasons for this are not clear. One possible explanation would be better hydraulics e.g. less short cutting in the small wetland.

Table 1 shows changes in pH, acidity and alkalinity across the site. It can be seen that large changes in alkalinity correlate with large changes in acidity. This is to be expected because as iron oxidises the acidity generated is consumed by the available alkalinity resulting in an overall reduction of both. In addition to this CO_2 degassing across the site will also account for a proportion of the reduction in acidity.

Table 1 *Comparison of total iron concentration, pH and alkalinity (mg/l $CaCO_3$ equivalent) across the site*

Survey point	Total Fe (mg/l)	pH	Alkalinity	Acidity
1	103.5	5.77	132	400
2	85.4	6.32	119	321
3	82.2	6.59	109	319
4	3.0	6.64	11.0	84
5	84.5	6.60	139	334
6	8.1	6.28	17.5	102

Numerous definitions of alkalinity and acidity have been suggested by a variety of authors ((Kirby and Cravotta 2005) and references therein) and are applied depending on the pH of the water being tested and the end usage for which the data is required. Decisions taken about whether or not to treat a minewater discharge actively or passively are often based on

calculations of net acidity or net alkalinity as defined by (Hedin *et al* 1994) where:Net acidity (meq/l) = Total permanent(metal + proton) acidity – total alkalinity

In these cases, acidity is generally measured by titration in the field and so has considerable contribution from dissolved CO_2 which cannot be considered to be permanent acidity (Kirby *et al.* 2009). A number of recent publications have highlighted the importance of this difference in accurately determining the potential of a minewater to be treated without chemical dosing including McAllan *et al* (2009).

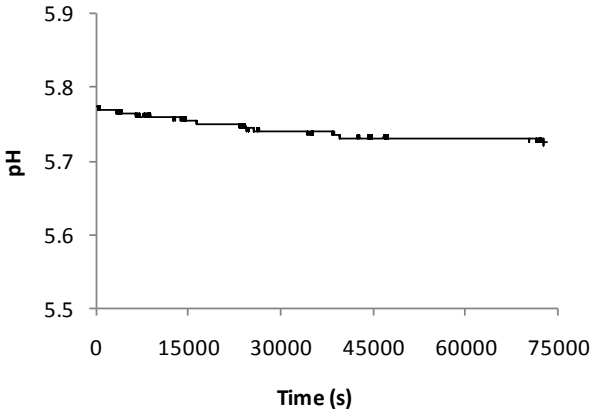

Figure 3 *Change in pH with aeration and CO_2 degassing*

Figure 3 shows the change in pH of the mine water over a 20h period with continuous aeration. Previous experiments conducted by the authors suggest that the majority of oxidation takes place within the first 2h with dissolved CO_2 dropping from 0.286 to 0.0142mg/l (modelled using PHREEQCi (Parkhurst and Apello 1999) with the phreeq.dat database) over that time. Both the acidity and alkalinity decreased as expected from 400 to 51, and 132 to 7 respectively. The pH dropped from an initial value of 5.78 to 5.72 and Fe(II) dropped from 93.7 to 2.79.

The magnitude of the reduction in Fe(II) over the timescale of this reaction is surprising given the pH conditions. The half life for homogeneous Fe(II) oxidation in a well aerated solution can be calculated using published rate constants to be of the order of days at pH 5.8. The most likely explanation for the observed oxidation rate is accelerated oxidation via the heterogeneous mechanism with Fe(II) adsorbing onto the surface of the newly formed hydrous ferric oxide (HFO) precipitates. This was an unexpected outcome given the results of Sung and Morgan (1980) who stated that autocatalytic iron oxidation is not important below pH 7.

Conclusions

The results of the site survey show that the effluent water at Ynysarwed is currently meeting the discharge consent for Fe(II) concentration. Comparison with the degassing studies of fresh minewater suggests that this is likely to be because of the slightly elevated pH resulting from the HDS trial plant. The results presented here show that 97% iron removal can be achieved and the mine water can be brought within the discharge limit for iron by aeration and degassing alone. Previous work carried out by the authors at this site shows that iron concentrations can be reduced to acceptable levels for discharge in around 2 hours (assuming that the same gas transfer efficiencies can be achieved at larger scale). With current flow rates a 60m^3 tank would provide a 2 hour residence time for iron oxidation. Continuous agitation and circulation of the HFO precipitates would ensure maximum oxidation rate by including the heterogenous as well as the homogeneous oxidation pathway.

Acknowledgements

The authors thank the UK Coal Authority and the EPSRC for funding the project and Mr Daniel Pugh for his invaluable assistance with the field work.

References

Hedin, R. S., Nairn, R., Kleinmann R. (1994) Passive Treatment of Coal Mine Drainage, US Bureau of Mines IC 9389, Dept of the Interior, Washington DC

Kirby, C. S., Cravotta, C. A. (2005) Net alkalinity and net acidity 1: Theoretical considerations. Applied Geochemistry 20(10): 1920-1940

Kirby, C. S., Dennis, A., Kahler, A. (2009) Aeration to degas CO_2, increase pH, and increase iron oxidation rates for efficient treatment of net alkaline mine drainage. Applied Geochemistry 24(7): 1175-1184

McAllan, J., Banks, D., Beyer, N., Watson, I. (2009) Alkalinity, temporaty (CO2) and permanent acidity: an empirical assessment of the significance of field and laboratory determinations on mine waters. Geochemistry: Exploration, Environment Analysis 9: 299-312

Parkhurst, D. L., Appelo, C. A. J. (1999) User's guide to PHREEQC (Version 2)--a computer program for speciation, batch-reaction, one-dimensional transport, and inverse geochemical calculations. U.S. Geological Survey Water-Resources Investigations. 99-4259

Stumm, W., Morgan J. J. (1996) Aquatic Chemistry, Chemical Equilibria and Rates in Natural Waters, Wiley Interscience

Sung, W. Morgan., J. J. (1980) Kinetics and Product of Ferrous Iron Oxygenation in Aqueous Systems. Environmental Science and Technology 14(5): 561-568

CURRENT PERFORMANCE OF PASSIVE TREATMENT SYSTEMS IN SOUTH WALES, UK

J. N. Geroni[1*], D. J. Sapsford[1], A. Barnes[2], I. A. Watson[3], K. P. Williams[1]

[1] Cardiff School of Engineering, Cardiff University, Cardiff, CF24 3AA, UK, email:geronijn@cf.ac.uk*

[2]SRK Consulting (UK), Cardiff, CF10 2HH

[3]The Coal Authority, Mansfield, NG18 4RG, UK

Abstract

This study presents the results of the chemical and hydraulic characterisation of a number of passive mine water treatment sites across South Wales. Various measures of system hydraulic efficiency are presented in conjunction with influent and effluent iron chemistry to give a snapshot of system performance. The effectiveness of both settlement lagoons and wetlands are discussed with respect to rates of iron removal and the relative importance of different iron removal mechanisms. It is suggested that where significant accumulations of ochre sludge occur in settlement lagoons reductive dissolution of Fe(III) may lead to remobilisation of iron as Fe(II) into the surrounding water. The role of aeration cascade design in increasing dissolved oxygen and increasing pH via CO_2 degassing is also considered for a number of the sites investigated. The sites studied include four systems comprising settling lagoons and wetlands. Influent iron concentration, pH and alkalinity varied considerably between sites with 5.67- 48.2 mg/L Fe, pH 2.20-7.22 and 120-251 mg/L as $CaCO_3$ alkalinity. Settling lagoons were found to work more efficiently at higher influent iron concentrations though all of the systems met their targets for effluent water quality. The data collected are used to critically evaluate current international guidelines for the sizing of passive treatment systems and inform recommendations for future system design.

Introduction

Settling lagoons and constructed wetlands have been widely deployed in the UK for the passive treatment of net-alkaline mine waters. The UK Coal Authority has built and now operates more than 50 passive treatment sites across the country for the remediation of coal mine drainage. South Wales has historically been the site of a large number of coal mines and today has numerous major mine water discharges. 14 treatment systems are currently in operation across the South Wales coal field, mostly dealing with well buffered ferruginous waters that can be treated using a combination of settling lagoons and aerobic wetlands. The

incorporation of lagoons as a first stage in the treatment process is important as it ensures that much of the iron is removed prior to the wetlands, increasing their lifespan and reducing the maintenance costs associated with the site (lagoons being much easier to "de-sludge" than reed beds).

The removal of dissolved iron from mine water discharges occurs in two stages; firstly the oxidation of Fe(II) as it emerges from below ground, followed by the rapid hydrolysis of Fe(III) and secondly the coagulation and settling of the resulting Fe(III) precipitates. The overall success of any treatment system is therefore affected not only by properties of the influent water (temperature, pH, alkalinity, dissolved O_2 and CO_2 etc) but also by the residence time and rates of gas transfer taking place, both of which can be optimized by careful system design. Many of the passive mine water treatment schemes built to date have been sized according to rules of thumb such as those listed in the PIRAMID (2003) guidelines, e.g. 48h retention time or 10 g/m^2/d/, though these criteria often lead to quite different estimates for system size.

The simplest way of ensuring maximum iron removal is to increase residence time for Fe(II) oxidation and provide a larger area over which the settling of precipitates can take place. This of course requires the use of a larger area of land, something that especially in the UK comes increasingly at a premium. In order to reduce the area required for treatment it is necessary to gain a greater understanding of both the chemical and physical processes taking place within it. This paper aims to provide a greater insight into the influence of system design on Fe(II) removal using data gathered during the course of a large study of a number of passive treatment facilities in South Wales. This study aims to stand out from many of those already in the literature by incorporating data for both ferrous and ferric iron, pH, flow rates and the effect of aeration cascades on dissolved O_2 and CO_2 (seen as increasing pH). It is hoped that this paper will add to the insight gained through case studies previously published by Sapsford *et al* (2009).

Sites Studied

Glyncastle

This site is situated close to the town of Resolven, South Wales. Water discharges by gravity out of two directionally drilled, sub-horizontal boreholes into the scheme (Watson, 2007). The scheme is unusual in that it features two triangular settling lagoons, instead of the usual rectangular design. Water flows out of the settling lagoons into a series of three reed beds

prior to discharge. A schematic plan of the site, and the other study sites described below, is shown in Figure 1.

Morlais

This site is situated near to the town of Llangennech in South Wales. Mine water discharges by gravity from a shaft, the collar of which was raised to enable an aeration cascade to be constructed. The cascade feeds into a 50m long channel which then feeds into two settling lagoons in series. The water flows out of the second lagoon into two parallel wetlands and finally through a third wetland before discharge to a nearby river. At the time of this study lagoon L1 was not in use. All water was directed to L2 via a diversion channel.

Taff Merthyr

Situated in the Taff Bargoed valley near Merthyr Tydfil, mine water is collected in a sump and pumped up to a distribution chamber. In total there are 4 settlement lagoons with preceding aeration cascades and 16 wetlands. Two of the lagoons run in parallel and feed three independent series of wetlands, whereas the other two unconnected lagoons feed two chains of wetlands that combine before the mine water is discharged into the Taff Bargoed river. On the day of sampling at this site the pumps were not working and all flow was directed through lagoon L4 and onwards through wetlands E1 – F2.

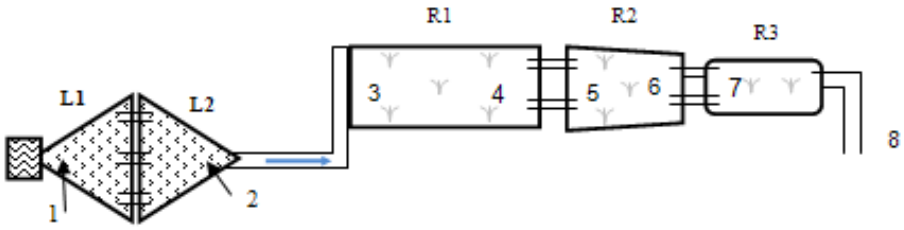

Glyncastle flow rate = 20.41 l/s, Fe_{TOT}in= 24.53 mg/l, Fe_{TOT}out= 1.25 mg/l, pH= 6.2-6.8†, lagoon area L1= 1766 m², L2 = 1005 m², reedbed area R1 = 1958 m², R2 = 532 m², R3 = 271 m², total area = 4532m², hydraulic loading, L1 = 1.00 m/d, L2 = 1.75m/d

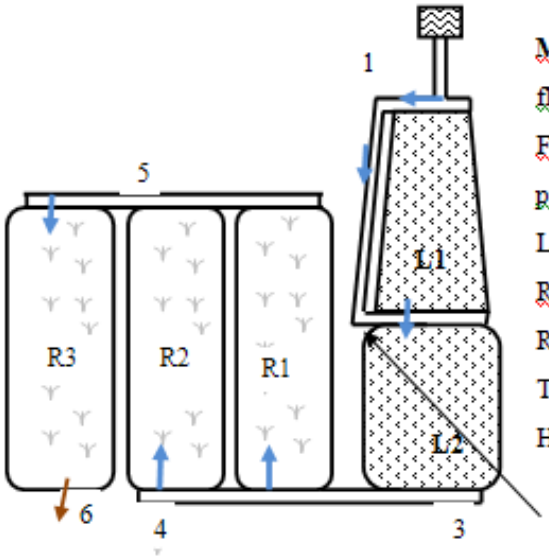

Morlais

flow rate = 120 l/s Fe_{TOT}in= 20.53 mg/l

Fe_{TOT}out= 1.25 mg/l

pH= 6.4-7.1

Lagoon area L1= 5640 m², L2 = 5680 m²,

Reedbed area R1 = 8816 m², R2 = 9582 m²,

R3 = N/A

Total area(L1-R2) = 30,718 m²,

Hydraulic loading, L1 = 1.84 m/d, L2 = 1.89m/d

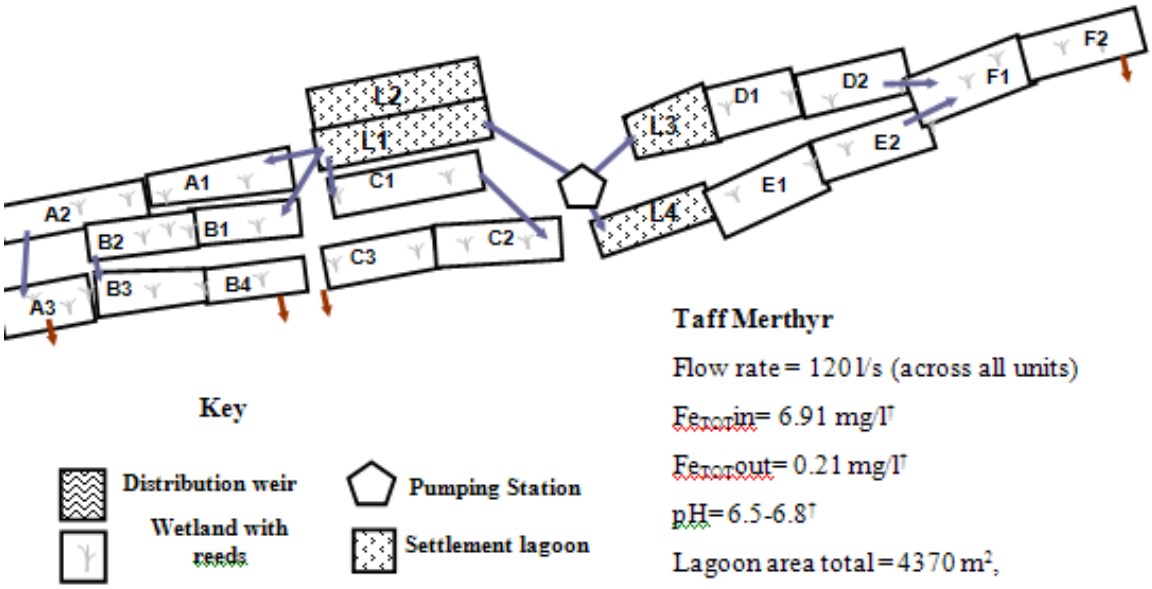

Taff Merthyr

Flow rate = 120 l/s (across all units)

Fe_{TOT}in= 6.91 mg/l†

Fe_{TOT}out= 0.21 mg/l†

pH= 6.5-6.8†

Lagoon area total = 4370 m²,

Reedbed area A1&A2 = 1250 m²

Total area ~ 32,500m²

Figure 1. Schematics of the studied mine water treatment sites. Reported data are mean data from Coal Authority data base. † Data collected in study 08/2008. (Diagrams not to scale)

Lindsay

This site is located close to Capel Hendre, Carmarthenshire, South Wales. Mine water is collected in a sump and pumped up to a distribution chamber above the aeration cascades leading to the two parallel lagoons. The site was originally designed for the treatment of mine waters with Fe(II) concentrations up to 98 mg/l. Observations at site indicate that considerable accumulations of ochre have occurred within the aeration and distribution channels as well as the lagoon. A detailed site survey and discussion of the overall performance at this site have been presented previously by Sapsford *et al* (2009). A description of the design and performance of the aeration cascades are presented here.

Methods

Water quality

Site surveys were conducted at the water treatment sites detailed above. pH, dissolved oxygen (DO), and conductivity were initially determined using a range of field meters (only selected data shown). After 07-08-2008 two Hanna HI-9828 multi-parameter data logging probes were used. The probes were, where possible, employed in unison, and programmed to take a reading every 5 seconds. After sampling for 10-15 minutes at each point, logging was discontinued and average values across the time period determined. Concentrations of Fe were determined using ICP-OES. Both total and filtered (0.45µm) samples were taken and fixed prior to analysis, the filtered iron analysis is taken to represent dissolved Fe(II). An alternative method was also employed to provide a comparable value of Fe(II). Spectrophotometric determinations (using a portable HACH DR-890 colorimeter or laboratory spectrophotometer) of Fe(II) were made after addition of 1-10 phenanthroline as per standard methods (e.g. APHA *et al*, 2005).

Aeration cascades

In the case of aeration cascades initial analysis was performed using the data logging multi-parameter probes for 1 hour of sampling, logging every 5 seconds. After on site calibration, the probes were positioned at the top and bottom of the cascade and logging initiated.

Results and Discussion

Iron Removal Data

Glyncastle

At Glyncastle the pH of the influent at 6.23 is the lowest of all the sites discussed in this study. The pH is in fact closer to that at Tan y Garn (Watson *et al*, 2009, Sapsford *et al*, 2009) where a Reducing Alkalinity Producing System (RAPS) has been installed to treat the marginally net acidic water. However, Glyncastle mine water is net-alkaline, so does not require a RAPS. Only 57% of the Fe(II) is oxidised by the end of the lagoons (in comparison to almost 94% at Morlais) with an iron removal rate of around 6.61 $g/m^2/day$. Despite the relatively low pH there is sufficient alkalinity, 121 mg/l as $CaCO_3$ (at the inlet) in the system to ensure that the remaining iron is oxidised in the reed beds. Concentrations of Fe(II) and Fe(III) across the site are shown in Figure 2 for the sample points identified in Figure 1.

On the day this survey was undertaken the discharge consent (1 mg L^{-1}) had been met with total iron concentration of 0.82 mg L^{-1} exiting the system. However, previous studies of the site conducted during early 2008 reported a discharge total iron concentration in excess of 1 mg L^{-1}. During the early 2008 winter visits the last reed bed was very sparsely vegetated, but at the time of the survey during summer 2008 was densely vegetated.

Morlais

The flow rate through lagoon L2 is the highest flow rate through any single lagoon in a passive treatment system on the Coal Authority database. The area of the lagoon however is also one of the largest on the database and despite the closure of lagoon L1 still allows for a relatively low hydraulic loading (2.93 m/d) that on the day of testing gave a reduction in Fe(II) concentration of just less than 94% from 21.5 to 1.3mg/L with iron removal rate of approximately 22 $g/m^2/d$. A small portion of the iron is removed prior to the lagoon, and is observed as an ochre coating in the distribution channel. Unlike the Glyncastle site, the reed beds at Morlais serve mainly to polish the effluent prior to discharge rather than removing large quantities of iron themselves.

Taff Merthyr

On the day of sampling the pump at the site was not operational. All flow was directed through lagoon L4 and exited the site via reed bed F2. Unsurprisingly performance of the lagoon was reduced in terms of %Fe removed as a result of the higher flow rate (hence reduced residence time) compared to times of normal operation, though the iron removal efficiency ($g/m^2/d$) actually increased. Overall it was observed that despite a 6 fold (approximate) increase in hydraulic loading through from L4 to F2 there was very little effect on the quality of the

effluent water. It is not clear if this apparent improved performance would be sustained in the long term, or if it was a temporary effect due to the pumps having recently turned off.

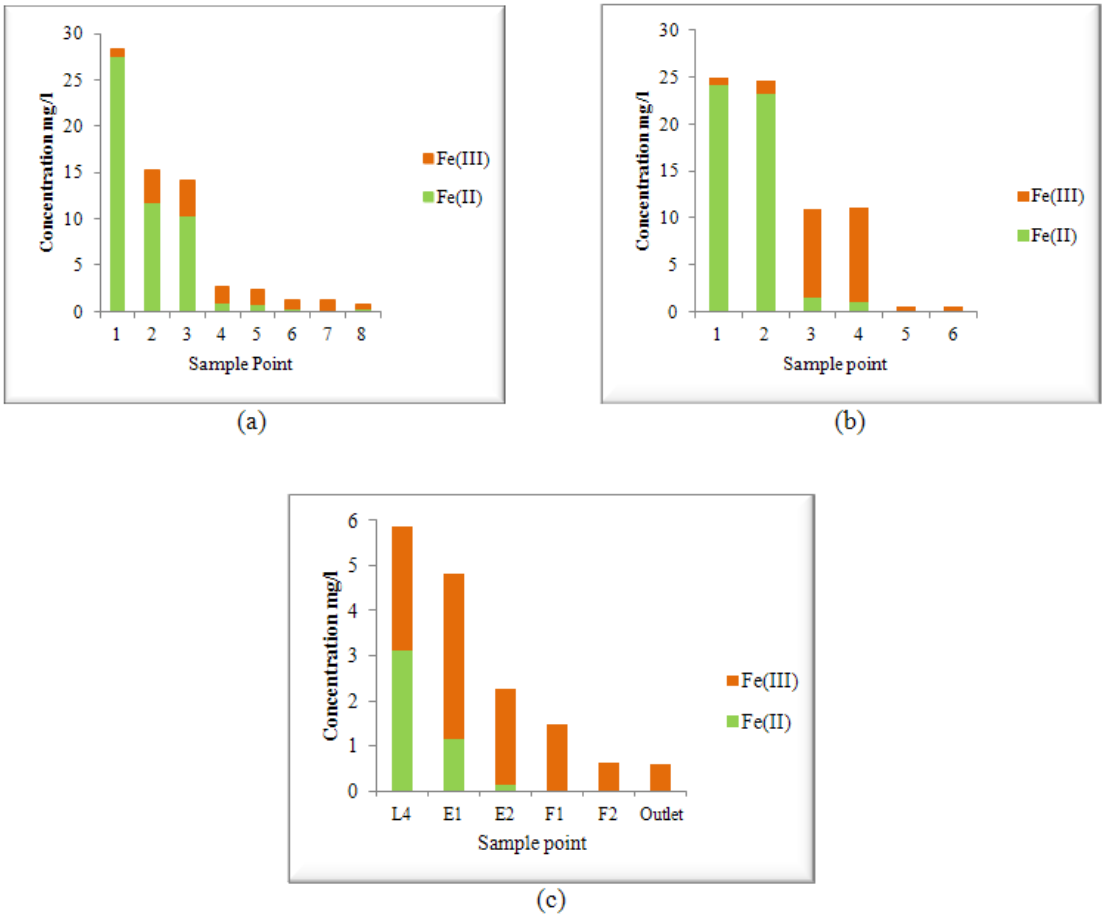

Figure 2. Concentrations of Fe(II) and Fe(III) across the sites studied (a) Glyncastle, (b) Morlais, (c) Taff Merthyr (sample locations given in Figure 1.)

Aeration cascades

The performance of aeration cascades is a continuing area of research interest because achieving the maximum possible gas transfer (increasing dissolved O_2 and degassing of CO_2) is desirable in order to improve Fe(II) oxidation rates. Dissolved oxygen is clearly vital in the system if iron is to be removed via oxidation. It is for this reason that many aeration cascades have been designed and built as part of the overall treatment process at passive treatment schemes. Equally (if not more) important however is the degassing of CO_2 which ultimately leads to an increase in pH. An increase in dissolved O_2 from 4.0 to 8.0 mg/l (a realistic target for an aeration cascade) should double the rate of Fe(II) oxidation as shown by Equation 1

(Stumm and Lee, 1961). However, at circumneutral pH the second order dependence on OH^- means that even small changes of 0.2 or 0.3 pH points can produce large changes in Fe(II) oxidation rate. Further explanation of the pH dependence of Fe(II) oxidation is given by Morgan and Lahav (2007).

$$\frac{\mathbf{dFe(II)}}{\mathbf{dt}} = -\mathbf{k}[\mathbf{Fe(II)}][\mathbf{O_2}][\mathbf{OH^-}]^{\mathbf{2}}$$

Equation 1. Rate equation for Fe(II) oxidation at circumneutral pH

Lindsay

Data for dissolved oxygen (DO) and pH at the top and bottom of the cascade are shown in Figure 3. A schematic of the cascade is shown in Figure 4. The DO is relatively high at the top of the cascade; this is believed to be due to entrainment of oxygen as the mine water falls into the sump. Thus the oxidation process begins in the sump, and the rising main pipes require regular jetting to prevent rapid blockage. The Coal Authority now seeks to design sumps which do not entrain oxygen, thus minimising this maintenance issue. Fluctuations in the data are an artefact of the on/off water pumping cycles at the site. Unfortunately flow rates were not measured at the same time as pH and DO so rates of gas transfer cannot be calculated, although if required estimates could be made using the site flow data. Aside from the aqueous chemistry it is worth noting the build up of ochre behind each of the steps in the cascade. This is not the fluffy ochre seen in the lagoons, but dense hard flecks of solid and is discussed further at the end of this section.

Taff Merthyr

The aeration cascade that feeds lagoon L2 was studied. A schematic of the cascade is provided in Figure 4. The change in pH between the top and bottom of the cascade is plotted in Figure 3 along with the change in DO. Like Lindsay, the mine water is partly pre-aerated at the pumping sump, with pH increasing down the cascade (though the pH increase here is somewhat greater), suggesting CO_2 degassing.

The dissolved oxygen results also show a similar trend to that observed in the Lindsay data, fluctuating with the pumping cycles. The rise in DO is much greater at Taff Merthyr, approximately 3-4 mg/l, compared to just 1-2 mg/l at Lindsay, showing this cascade to be more

necessary. The final level of DO reached in both cases is very similar, as it is approaching saturation in both cases. While this shows that both cascades are successful in increasing DO their efficiency with regards to CO_2 degassing requires further study.

Morlais

The cascade at Morlais differs from those at Lindsay and Taff Merthyr in that the channel narrows over the length of the cascade as shown in Figure 4 rather than remaining of a fixed width. Observations suggest that this narrowing increases the turbulence and entrainment of air bubbles, though a more detailed study of the cascade would be required to confirm this in terms of rates of gas transfer.

It has been suggested that the use of a series of plunge pools in place of a simple cascade will increase the gas transfer (PIRAMID, 2003) over a cascade. The narrowing of the cascade at Morlais creates areas of deeper water where mixing can take place so perhaps it is not surprising that the greatest change in pH of 0.28 occurred here compared to 0.06 and 0.13 and Lindsay and Taff Merthyr respectively (average values). Due to technical difficulties at the time of monitoring no DO data are available for Morlais.

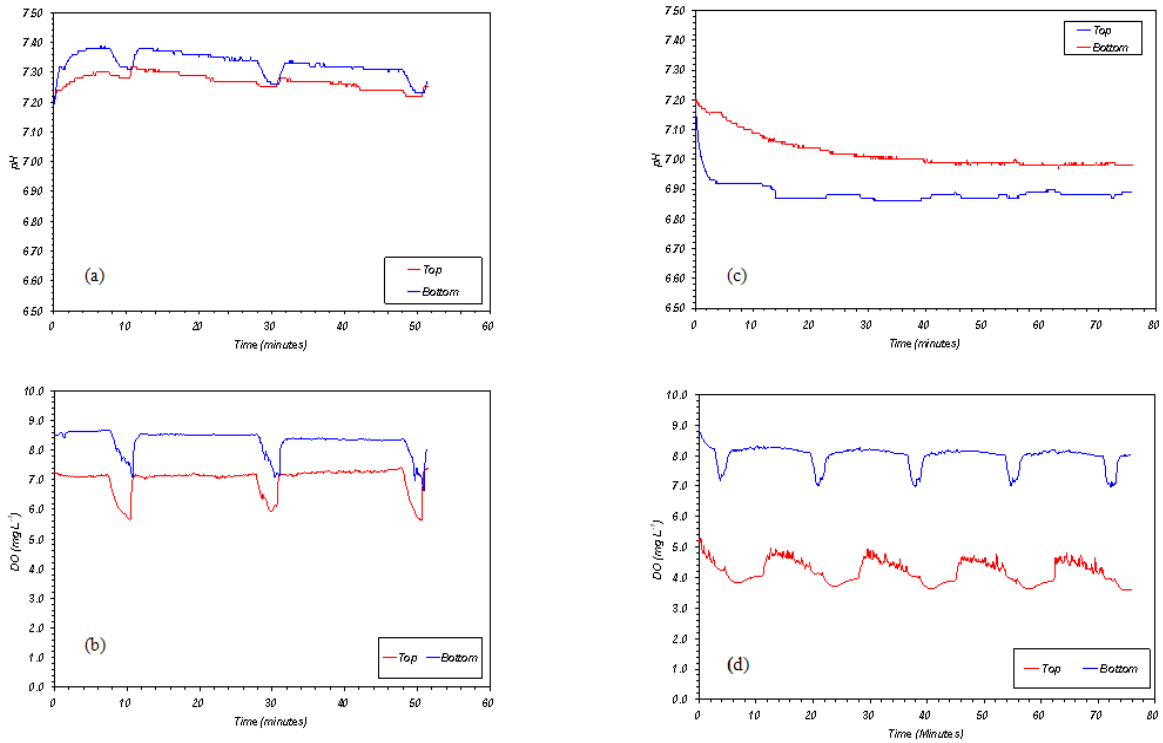

Figure 3. pH and dissolved oxygen data for aeration cascades at Lindsay (a) & (b) and Taff Merthyr (c) & (d)

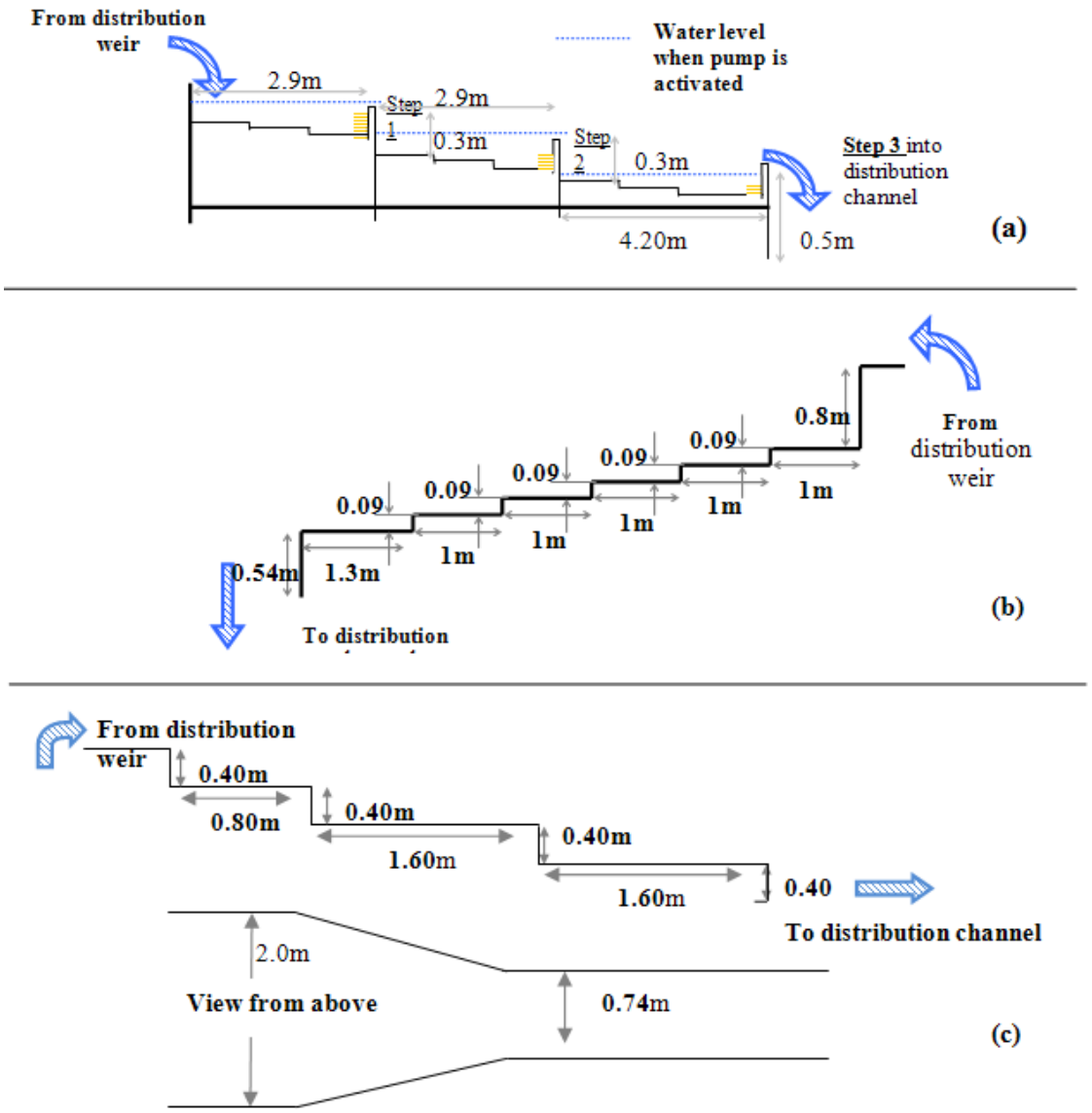

Figure 4. Schematic diagrams of aeration cascades at (a) Lindsay and (b) Taff Merthyr (c) Morlais (Not to scale)

General observations

In addition to the data presented above other more qualitative observations and measurements were made during the study and are briefly outlined below. Scoop sampling of the sludge accumulated in the Taff Merthyr lagoons revealed that at depth the samples were olive green rather than the orange colour seen from the surface. The green colouration is indicative of Fe(II) hydroxide possibly formed by the bioreduction of Fe(III) as P_{O2} decreases with depth. The bioreduction of Fe(III)(hydroxy)oxide and formation of green rust is

documented in O'Loughlin *et al* (2007) and is a potential mechanism for the remobilisation of Fe(II) into the system.

It was noticed that ochre formations at the outlet of the distribution weir at the Lindsay site were hard, brittle and thinly layered with a black substance that was almost glassy in appearance. These deposits were formed where falling water impacted on a hard surface and so were not the result of accumulations of settled ochre flocs. Flecks of this solid had built up behind the steps in the aeration cascade and were also responsible for fouling of the aeration channel. XRD analysis of the samples showed the brittle solid to be goethite.

Conclusions

1. All of the sites studied were meeting their discharge consent at the time of monitoring.
2. Site surveys of existing treatment schemes provide a wealth of data that can be used to inform more effective designs for future systems.
3. Maximising gas transfer over aeration cascades is important not only in terms of increasing dissolved oxygen, but possibly more importantly raising pH by maximising CO_2 degassing.

As land for passive mine water treatment schemes becomes increasingly scarce and increasingly costly it is necessary to find ways to maximise the iron removal efficiency of such systems and hence reduce their required footprint. Increasing understanding of the mechanisms of iron removal in lagoons and maximizing their efficacy is important in ensuring that systems are no longer oversized as has happened in the past. One way to allow for a reduction in the size of lagoons is to increase the Fe(II) oxidation rate, something that can be achieved by optimising gas transfer through careful aeration cascade design.

References

American Public Health Association (APHA), American Water Works Association (AWWA) & Water Environment Federation (WEF) (2005), *Standard Methods for the Examination of Water and Wastewater*.

Morgan, B., Lahav, O., (2007) "The effect of pH on the kinetics of spontaneous Fe(II) oxidation by O_2 in aqueous solution – basic principles and simple heuristic description". *Chemosphere*, 68, 11, 2080-2084

O'Loughlin, E. J., Larese-Casanova, P., Scherer, M. Cook, R. (2007) "Green rust formation from the reduction of gamma-FeOOH (lepidocrocite): Comparison of several Shewanella species". *Geomicrobiology Journal,* 24, 211-230

PIRAMID consortium, (2003) “Engineering guidelines for the passive remediation of acidic and/or metalliferous mine drainage and similar waste waters”. *University of Newcastle Upon Tyne, ISBN 0-9543827-1-4*

Sapsford, D. J., Watson, I., Williams K. P., (2009) “Chemical and Hydraulic Characterisation of Passive Mine Water Treatment Systems in S. Wales”. *Proceedings of Securing the Future and 8th ICARD* June 22-26, Skellefteå, Sweden.

Stumm, W., Lee, G. F., (1961) “Oxygenation of Ferrous Iron”. *Industrial and Engineering Chemistry*, 53, 2, 143-146

Watson, I.A. (2007) ”Managing Minewater In Abandoned Coalfields Using Engineered Gravity Discharges*”. Proceedings of IMWA Symposium 2007,* May 27-31, Cagliari, Sardinia

Watson, I.A., Taylor, K., Sapsford, D.J., Banks, D. (2009) “Tracer Testing to Investigate Hydraulic Performance of a RAPS Treating Mine Water in South Wales” *Proceedings of Securing the Future and 8th ICARD* June 22-26, Skellefteå, Sweden.